118

0-315-16027-6

National Library of Canada — Bibliothèque nationale du Canada

Canadian Theses Division — Division des thèses canadiennes

Ottawa, Canada
K1A 0N4

63936

PERMISSION TO MICROFILM — AUTORISATION DE MICROFILMER

• Please print or type — Écrire en lettres moulées ou dactylographier

Full Name of Author — Nom complet de l'auteur

ROBERT HAROLD SWANSON

Date of Birth — Date de naissance	Country of Birth — Lieu de naissance
15 FEBRUARY 1933	USA

Permanent Address — Résidence fixe

10908-38 AVE
EDMONTON, ALBERTA
T6J 0K7

Title of Thesis — Titre de la thèse

Numerical and experimental analyses of implanted-probe heat pulse velocity theory

University — Université

The University of Alberta

Degree for which thesis was presented — Grade pour lequel cette thèse fut présentée

Ph.D. Plant Physiology

Year this degree conferred — Année d'obtention de ce grade	Name of Supervisor — Nom du directeur de thèse
1983	Dr. James M. Mayo

Date	Signature
4 MARCH 1983	Robert Harold Swanson

NL-91 (4/77)

THE UNIVERSITY OF ALBERTA

NUMERICAL AND EXPERIMENTAL ANALYSES OF IMPLANTED-PROBE HEAT PULSE VELOCITY THEORY

by

(C) ROBERT H. SWANSON

A THESIS

SUBMITTED TO THE FACULTY OF GRADUATE STUDIES AND RESEARCH

IN PARTIAL FULFILMENT OF THE REQUIREMENTS FOR THE DEGREE

OF DOCTOR OF PHILOSOPHY

IN PLANT PHYSIOLOGY

DEPARTMENT OF BOTANY

EDMONTON, ALBERTA

SPRING, 1983

THE UNIVERSITY OF ALBERTA

RELEASE FORM

NAME OF AUTHOR: Robert Harold Swanson

TITLE OF THESIS: NUMERICAL AND EXPERIMENTAL ANALYSES OF IMPLANTED-PROBE HEAT PULSE VELOCITY THEORY

DEGREE FOR WHICH THESIS WAS PRESENTED: DOCTOR OF PHILOSOPHY

YEAR THIS DEGREE GRANTED: SPRING 1983

(Signed) Robert Harold Swanson

PERMANENT ADDRESS:

10908 - 38th avenue

Edmonton, Alberta

CANADA T6J 0K7

DATED: March 4,1983

THE UNIVERSITY OF ALBERTA

FACULTY OF GRADUATE STUDIES AND RESEARCH

The undersigned certify that they have read, and recommend to the Faculty of Graduate Studies and Research, for acceptance, a thesis entitled "Numerical and Experimental Analyses of Implanted-Probe Heat Pulse Velocity Theory", submitted by Robert H. Swanson in partial fulfilment for the degree of Doctor of Philosophy in Plant Physiology.

James M. Mayo
Supervisor

David D. Cass

Kenneth Higginbotham

Walter Moser

K. R. Knoerr
External Examiner

Date 25 February 1983

To my wife, Joanna, my son Karl and daughter Kay, from whom I have stolen so much time during the course of this work.

ABSTRACT

The main purpose of this study was to develop practical heat pulse velocity (HPV) theory and techniques to measure xylem sapflow (transpiration) of forest trees without resort to empirical calibration or coefficients. It was determined that idealized heat transfer theory, describing the velocity of a heat pulse as propagated through sapwood by conduction through the wood and sap substance and convection by moving sap streams, can not be directly applied to measurement of sap flux in coniferous or diffuse porous woods because it does not account for the effect of nonconvecting wood (wound, W) in the plane of the implanted probes that necessarily results from the interruption of flow elements. Nor can it account for the effects of probe materials with thermal properties different from anisotropic wood, or normal variation in wood thermal properties that exists at bark/sapwood and sapwood/heartwood borders.

The partial differential equation for heat transfer by coupled conduction and convection was solved numerically for specific stem tissue and heat pulse probe implant situations. A finite difference numerical model of a section of sapwood in the tangential-longitudinal plane was used to simulate the effect of wounded material from 0.04 to 0.52 cm wide in the plane of sensors. Significant departure from the idealized case occured at 0.04 cm and calculated values of HPV were approximately 50% of those imposed on the model at the 0.16 cm width of practically-sized heat pulse probes. A second model in

the radial-longitudinal plane was used to simulate the effects of bark/sapwood and sapwood/heartwood in radial cross sections of stems with sapwoods of 1, 2 and 3 cm wide. These simulations indicated that both symmetrically and asymmetrically spaced two sensor measurement and analysis techniques were usable at positions in the sapwood greater than 0.5 cm from the bark/ sapwood border and greater than 1 cm from the sapwood/heartwood border.

Experimental results verified that wound in the plane of implanted probes was the major source of departure of practice from idealized theory. In a _Pinus radiata_, calculated transpiration from idealized theory was 49% of actual (by lysimetery), but 103% of actual with the numerically derived equation for a wound width of 0.20 cm. In a diffuse porous hardwood (_Nothofagus solandri_ var _cliffortioides_), calculated transpiration from idealized theory was 26% of actual (by cuvette), but 110% of actual with the numerically derived equation at the measured wound width of 0.48 cm. Similiar results were obtained in _Pinus halepensis_, _Picea glauca_, _Populus tremuloides_ and _Betula papyrifera_.

Heat pulse velocities determined within 1 cm of the sapwood heartwood border are underestimates on the sapwood side, overestimates on the heartwood side. Rod-shaped high thermal conductivity sensors tend to integrate HPV across the sapwood/heartwood border and over a greater area of xylem than bead-shaped sensors.

Wood moisture content may be dynamically and nondestructively determined from longitudinal thermal diffusivity measurements and basic wood density. A limited test of the feasibility and accuracy of such determinations indicated that calculated and actual moisture contents over the range 12 to 150%, oven dry weight basis, were closely correlated, $R^2 = 0.81$, with a standard error of estimate of 16%.

The numerical and experimental results indicate that solutions to the heat transport equation, specific to heat pulse probes and stem cross section, are necessary to achieve accurate results with the implanted line source heat pulse method. Solutions are given for two, 0.16 cm diameter glass or brass sensors, spaced 1 cm up and downstream from a similiar diameter brass heater. These solutions are adequate for measuring heat pulse velocities in most coniferous and diffuse porous hardwood tree species with sapwood radii greater than 1 to 1.5 cm.

ACKNOWLEDGEMENTS

I am grateful to M. D. Hoover, my former supervisor at the Rocky Mountain Forest and Range Experiment Station, Fort Collins, Colorado, who, in 1958, suggested that I "look at an article by D. C. Marshall in Plant Physiology" as a possible technique to use to estimate transpiration. Little did I know then the lifetime of work this suggestion would entail. His suggestion has resulted in periodic "bursts" of activity on my part toward realizing the potential of Marshall's heat pulse method, culminating in this present work.

I am also grateful to Dr. D. C. Marshall, Department of Industrial and Scientific Research, Auckland, New Zealand, and Dr. D. W. A. Whitfield, formerly with the Department of Botany, The University of Alberta, Edmonton, for suggesting the numerical approach used in this study. I am particularily grateful to D. Whitfield for shepherding me through the initial pitfalls of the numerical analyses techniques used in this study.

Dr. J. M. Mayo, my thesis supervisor, has been a constant source of encouragement and advice. I am indebted to Dr. D. D. Cass, Ms. Joyce Kurie and the Department of Botany, The University of Alberta, for the generous allotment of computer time, environmental chamber space and the other laboratory facilities that were so essential to the conduct of this study. I am also indebted to Mr. P. A. Hurdle of the Northern Forest Research Centre, for his willingness to carry my instrumentation ideas through to fruition.

Lastly, I am very grateful to my employer, the Northern Forest Research Centre, Canadian Forestry Service, for allowing me full use of all of its facilities and the freedom to rearrange my normal research activities as needed, in order to carry out this study.

TABLE OF CONTENTS

CHAPTER I 1

INTRODUCTION 1

Transpiration 1

Methods of measuring transpiration 1

Sap flow and transpiration 3

Sap flow calculations 4

Anatomical considerations in sap flow measurement 5

Stem structure 5
Nonporous woods 7
Porous woods 8
Location of flow in sapwood 8

Thermal-sapflow measurement methods 9

General flowmetering analogy 9
Huber method 10
Marshall method 11
Differences between Huber and Marshall methods 11

Confusion in the thermometric flow literature 13

Thesis objectives 14

CHAPTER II 16

ANALYTICAL HEAT PULSE VELOCITY THEORY 16

Description of the physical problem 16

Idealized heat transport theory 17

Partial differential equation (PDE) in 3-dimensions 17
Definition of heat pulse velocity 18
Analytical solution to PDE, idealized case 19

Equations to extract HPV's from time-temperature data 19

Single sensor, fixed time, HPVM 19
Single sensor, fixed time, thermal diffusivity, D 21
Two sensor symmetrical configuration, HPVS 21
Single sensor, time of peak temperature, HPVP 21

Two sensor, asymmetric, time of null temperature, HPVT.................................. 22
Two sensor, asymmetric, fixed times, HPVA........ 22

Auxiliary equations.................................. 23

Sap flux.. 23
Thermal conductivity of wood....................... 24
Wood moisture content from thermal diffusivity and basic density.................... 25

Conditions for application.......................... 27

CHAPTER III.. 33

IDEALIZED HEAT PULSE VELOCITY PRACTICE.................... 33

Introduction... 33

Representative applications of Marshall's method...... 34

HPVM.. 34
HPVP.. 35
HPV?.. 37
HPVT.. 38

Applications of idealized theory to specific problems.. 40

Detection of moisture stress....................... 40
Effects of defoliation.............................. 41
Correlation between environmental parameters and transpiration....................... 41
Simple correlations with sap flow or transpiration.................................. 42
Direct calculations of transpiration............ 44
Loss of sensor sensitivity with extended implantation time...................... 46
Incompatibility of data from differing sensor configurations................. 49

Sources of problems in applications.................. 49

CHATPER IV.. 54

NUMERICAL ANALYSIS OF HEAT PULSE VELOCITY THEORY........... 54

Introduction... 54

The finite difference method.......................... 55

Numerical models of 3-dimensional system.............. 57

Tangential longitudinal model (TLM)........................62

Radial longitudinal model (RLM)........................ 65

Numerical solutions of general cases.................. 67

General cases simulated........................... 68

General case results.............................. 69

Case 1, theoretical verification,
no wound, no sensor material,
TLM and RLM............................... 69
Case 2, wound alone, TLM.................. 73
Case 3, W = 0.20 cm, several
sensor configurations, TLM................ 80
Case 4, effect of glass and
brass sensor materials, TLM and RLM......... 83
Case 5, TLM, combined effects
of wound, glass sensor materials,
brass heater at four sensor
configurations............................ 86
Case 6, effect of stem
tissue borders, RLM only.................. 90

Case 6a, 0.32 cm bark, 3.68 cm
sapwood, no heartwood................. 91
Case 6b, no bark, 3.32 cm
sapwood, 0.68cm heartwood............. 91
Case 6c, 0.32 cm bark, 3.0 cm
sapwood, 0.68 cm heartwood.............102
Case 6d, 0.32 cm bark, 2.0 cm
sapwood, 0.90 cm heartwood.............102
Case 6e, 0.32 cm bark, 1.0 cm
sapwood, 1.1 cm heartwood..............109

Case 7, 0.32 cm bark, 3.0 cm
alternate early-latewood,
0.68 cm heartwood.........................109

General conclusions from Case 6...............113

Summary and conclusions from
the general simulations.........................115

CHAPTER V..117

APPLICATION OF NUMERICAL ANALYSES RESULTS....................117

Introduction...117

HPV instrumentation..119

Situations and results to be examined........................120

EXAMINATION OF INSTRUMENTATION AND PRACTICE..................121

Heat pulse duration..121

Sensor configuration...124

Effect of wounding...127

Xylem flow structure and sapwood thickness...................128

Smoothing effect of sensor materials in radial profile.......131

HPVM's at low HPV's..135

Accuracy of the HPVA and HPVS sensing configurations at zero flow..138

Moisture content from longitudinal diffusivities.............141

QUANTITATIVE RESULTS IN SEMI-IDEALIZED SITUATIONS............143

Introduction...143

Quantitative comparisons.....................................146

1. Aleppo pine on a lysimeter (PH1)..........................146
2. Monterey pine of load cell (PR1)..........................150
3. New Zealand mountain beech -- climatized cuvette (NS1)....154

QUANTITATIVE RESULTS IN MARGINAL SITUATIONS..................156

Introduction...156

Quantitative comparisons.....................................159

1. White spruce lysimeters (PG1, PG2, PG3, PG4).159
2. Hardwood potometers (BP1, BP2, PT1, PT2).....168
Potometer BP1.................................172
Potometer BP2.................................172
Potometer PT1.................................175
Potometer PT2.................................175
Cavitation.......................................175

DISCUSSION OF APPLICATION RESULTS...........................178

Wound...178

Radial variation in stem anatomy.......................181

Sapwood area...183

Sapwood moisture content...............................183

Sampling...187

CHAPTER VI...190

GENERAL DISCUSSION...190

Idealized heat pulse velocity theory....................190

Practical theory based on numerical modeling..........191

Numerical models of HPV probes and tree stems.....191
Macroscopic anatomical considerations.............193
Microscopic anatomical assumptions................194
Future developments.................................195
Precautions..195

Practical sap flow measurement considerations..........196

Wounding upon HPV probe implantation..............196
Analysis method and probe configuration...........198
Analysis method and sensor location...............202
Thermal diffusivity and moisture content..........204
Heat pulse probes.....................................205
Indicating or recording instruments...............207
Sap conducting xylem area..........................210
Sapwood moisture content...........................211

RECOMMENDED PRACTICE....................212

Applicability....................213

Heat pulse instrumentation....................213

Sensor configuration....................213
Analysis technique....................214
Sensor materials....................214
Recorder-controller....................214

Sap conducting area....................217

Moisture content....................217

HPV sampling guidelines....................218

SUMMARY AND CONCLUSIONS....................220

Theoretical....................220

Experimental....................221

LITERATURE CITED....................224

APPENDICES....................236

A PLANE HEAT SOURCE GEOMETRY EQUATIONS....................236

B ENVIRONMENTAL CHAMBERS, UNIVERSITY OF ALBERTA....................238

C WHITE SPRUCE LYSIMETER EXPERIMENTS....................239

Lysimeter construction....................240
Lysimeter calibration....................241
Evaporation from container....................241
Schedule of events....................242
Instrumentation by tree....................244
Sample data each tree....................246

D BIRCH AND POPLAR POTOMETER EXPERIMENTS....................250

Potometer construction....................250
Schedule of events....................251
Instrumentation by tree....................253
Sample data each tree....................257

E HEAT PULSE VELOCITY INSTRUMENTATION....................261

Sensor and heater construction and thermal properties....................261
Heat pulse velocity indicating or recording instrumentation....................264

F COMPUTER PROGRAMS FOR TANGENTIAL AND RADIAL MODELS....................269

Program, Tangential-Longitudinal model....................271
Modifications for Radial-Longitudinal model....................283
Program for subroutine SOLVER....................284
File CPRB....................288
File IPRB, for TLM with sensor, heater materials....................290
File IPRB for RLM without sensor materials, sapwood/heartwood border at node 37, no bark....................292
HPV's imposed at each column....................294
Temperature matrix at t = 60 s....................295
Temperature matrix at t = 120 s....................296
Temperature matrix at t = 180 s....................297
D and HPV's at sensor nodes, @ t = 60, 120 and 180 s....................298

LIST OF TABLES

1. Theoretical results tangential longitudinal model, all sapwood. No sensor-heater materials or wound..............70

2. Theoretical results radial longitudinal model, all sapwood. No sensor-heater materials or wound................71

3. Influence of changing the times at which temperatures or temperature ratios are measured on HPV solutions at wound = 0.20 cm with no sensor or heater materials, TLM..77

4. Influence of wound from 0.00 to 0.24 cm and time at which temperatures are measured on calculated longitudinal thermal diffusivity....................................78

5. Influence of sensor spacing on HPVS, HPVM, HPVP and D at wound = 0.20 cm, TLM. No sensor or heater materials......82

6. Influence of glass or brass sensors and brass heater materials on solutions in sapwood, tangential longitudinal simulation..84

7. Influence of glass or brass sensors and brass heater materials on solutions in sapwood, no wound or heat loss at radial borders, radial longitudinal simulation.........85

8. Influence of glass sensor, brass heater material and 0.20 cm wound on HPVA, HPVM and longitudinal diffusivities with asymmetrical sensors configured (-0.48, 0.0.96 cm) and (-0.96,0.0.96 cm)...............................87

9. Influence of glass sensor, brass heater material and 0.20 cm wound on HPVS, HPVM and longitudinal diffusivities with symmetrical sensors configured (-0.96,0, 0.96 cm) and (-1.44,0,1.44 cm)..................................88

10. Influence of sensor position with respect to the sapwood heartwood border, and time interval used, on the solutions to the equations HPVA, HPVM, HPVS and longitudinal diffusivity. Solutions obtained from temperatures at 60 s intervals, i.e., 60, 120 and 180 s from initiation of heat pulse...99

11. Influence of sensor position with respect to the sapwood heartwood border, and time interval used, on the solutions to the equations HPVA, HPVM, HPVS and longitudinal diffusivity. Solutions obtained from temperatures at 30 s intervals, i.e., 30, 60, and 90 s from initiation of heat pulse..100

12. Influence of sensor position with respect to the sapwood heartwood border on HPVT values, which are obtained at times dependent on the speed of HPVI, are given here for comparison with the fixed time solutions given in Tables 10 and 11..101

13. Influence of heat pulse duration on HPVA, HPVM, HPVP, HPVS, HPVT and D^I at wound = 0.20 cm, TLM simulations..........122

14. Accuracy of HPVA and HPVS configurations at zero sap movement..140

15. Quantitative comparison of transpiration as measured by weight loss and as calculated from heat pulse velocity data in white spruce, tree PG1...............................162

16. Quantitative comparison of transpiration as measured by weight loss and as calculated from heat pulse velocity data in white spruce, tree PG2...............................163

17. Quantitative comparison of transpiration as measured by weight loss and as calculated from heat pulse velocity data in white spruce, trees PG3 and PG4....................164

18. Theoretical temperature rise at a sensor 0.96 or 1.44 cm upstream 120 s after a heat pulse of 1 to 4 s duration in dry sapwood...201

19. Coefficients for calculating imposed HPV's with glass, brass or Teflon sensors spaced (-1.0,0,1.0 cm) calculated using Equation 6...215

20. Coefficients for calculating imposed HPV's from those calculated using Equation 8 (p. 22), HPVT, or Equation 9 (p. 23), HPVA, at t = 60 and 120 s with glass or brass sensors spaced (-0.5,0,1.0 cm)..........................216

22. Evaporation from lysimeter container alone, no tree, all HPV probe leads removed......................................241

23. Schedule of events white spruce lysimeter experiments. Lights on 0900 - 2100, chamber dark 2100 - 0900................242

24. Twelve hour reading schedule....................................243

25. HPV instrumentation installed in white spruce tree PG1...244

26. HPV instrumentation installed in white spruce tree PG2...244

27. HPV instrumentation installed in white spruce tree PG3....245

28. HPV instrumentation installed in white spruce tree PG4....245

29. Sample raw and corrected HPVT data, white spruce tree PG1....246

30. Sample raw and corrected HPVT data, white spruce tree PG2....247

31. Sample raw and corrected HPVT data, white spruce tree PG3....248

32. Sample raw and corrected HPVT data, white spruce tree PG4....249

33. Schedule of events, hardwood potometers....251

34. HPV instrumentation installed in birch potometer tree BP1....253

35. HPV instrumentation installed in birch potometer tree BP2....254

36. HPV instrumentation installed in poplar potometer tree PT1....255

37. HPV instrumentation installed in poplar potometer tree PT2....256

38. Sample data tree BP1, sensor 2103, at 0.8 cm depth, W = 0.40 cm....257

39. Sample data tree BP2, sensor 2203, at 0.8 cm depth, W = 0.40 cm....258

40. Sample data tree PT1, sensor 1107, at 0.3 cm depth, W = 0.22 cm....259

41. Sample data tree PT2, sensor 1207, at 0.6 cm depth, W = 0.28 cm....260

42. Thermal properties of materials used in simulating the sensor materials....261

LIST OF FIGURES

1. Idealized stem cross section illustrating the tissues of importance in xylem sap flow measurement....................6

2. Plots of temperature rise versus time for the various solutions of Equation 3 with HPV = 5 cm/h.....................20

3. Theoretical plotting of sap flow through a constant sapwood area versus heat pulse velocities at Mgw's of (A) 1.5, (B) 1.0, (C) 0.5....................................31

4. Diagrammatic sketch of the asymmetrical, two sensor, HPVT sampling scheme..39

5. Decline in sensitivity with length of time that sensors have been installed....................................47

6. Least squares fitting of relationship between HPVT data obtained from sensors spaced -0.5,0,0.75 cm and those from sensors spaced -0.5,0,1.0 cm...........................50

7. Stem cross sections simulated with numerical models. (a) Tangential-longitudinal. (b) Radial-longitudinal..........58

8. Heat pulse function, Q(0,0,t), used in tangential-longitudinal simulations and Q(0,y,t) used in radial-longitudinal numerical simulations.................................63

9. Influence of wound on two sensor configurations, no sensor materials, tangential longitudinal model. HPVA's or HPVS's measured at (-0.48,0,0.96 cm) or at (-0.96,0,0.96 cm)..74

10. Influence of wound on one sensor configurations, no sensor materials, tangential longitudinal model. HPVM's measured at (0,0.96 cm) or at (0,1.44 cm)..............75

11. Influence of sensors placed at various spacings. Wound = 0.20 cm, no sensor material, tangential longitudinal model...81

12. Influence of stem tissue borders on heat pulse calculations of longitudinal diffusivity, HPVM and HPVA at HPVI = 0. Radial-longitudinal model with 0.32 cm bark, 3.68 cm sapwood, no heartwood....................................92

13. Influence of stem tissue borders on HPVM calculations. Radial-longitudinal model with 0.32 cm bark, 3.68 cm sapwood, no heartwood...93

14. Influence of stem tissue borders on HPVA, HPVS and HPVT calculations. Radial-longitudinal model with 0.32 cm bark, 3.68 cm sapwood, no heartwood........................94

15. Influence of stem tissue borders on heat pulse calculations of longitudinal diffusivity, HPVM and HPVA at HPVI = 0. Radial-longitudinal model with no bark, 3.32 cm sapwood, 0.68 cm heartwood....................................95

16. Influence of stem tissue borders on HPVM calculations. Radial-longitudinal model with no cm bark, 3.32 cm sapwood, 0.68 cm heartwood..96

17. Influence of stem tissue borders on HPVA, HPVS and HPVT calculations. Radial-longitudinal model with no bark, 3.32 cm sapwood, 0.68 cm heartwood.......................97

18. Influence of stem tissue borders on heat pulse calculations of longitudinal diffusivity, HPVM and HPVA at HPVI = 0. Radial-longitudinal model with 0.32 cm bark, 3.00 cm sapwood, 0.68 cm heartwood...........................103

19. Influence of stem tissue borders on HPVM calculations. Radial-longitudinal model with 0.32 cm bark, 3.00 cm sapwood, 0.68 cm heartwood.......................................104

20. Influence of stem tissue borders on HPVA, HPVS and HPVT calculations. Radial-longitudinal model with 0.32 cm bark, 3.00 cm sapwood, 0.68 cm heartwood...................105

21. Influence of stem tissue borders on heat pulse calculations of longitudinal diffusivity, HPVM and HPVA at HPVI = 0. Radial-longitudinal model with 0.32 cm bark, 2.00 cm sapwood, 0.90 cm heartwood...........................106

22. Influence of stem tissue borders on HPVM calculations. Radial-longitudinal model with 0.32 cm bark, 2.00 cm sapwood, 0.90 cm heartwood.......................................107

23. Influence of stem tissue borders on HPVA, HPVS and HPVT calculations. Radial-longitudinal model with 0.32 cm bark, 2.00 cm sapwood, 0.90 cm heartwood...................108

24. Influence of stem tissue borders on heat pulse calculations of longitudinal diffusivity, HPVM and HPVA at HPVI = 0. Radial-longitudinal model with 0.32 cm bark, 1.00 cm sapwood, 1.10 cm heartwood...........................110

25. Influence of stem tissue borders on HPVM calculations. Radial-longitudinal model with 0.32 cm bark, 1.00 cm sapwood, 1.10 cm heartwood.......................................111

26. Influence of stem tissue borders on HPVA, HPVS and HPVT calculations. Radial-longitudinal model with 0.32 cm bark, 1.00 cm sapwood, 1.10 cm heartwood....................112

27. Schematic representation of the toroidal area and initial and subsequent wound widths associated with each heat pulse velocity probe installation..........................118

28. Tangential longitudinal simulation of HPV probes: effect of spacing 0.16 cm diameter glass rod thermister sensors up and downstream from the heater, both plottings at = 0.20 cm...125

29. Corrections of Figure 28 applied to experimental data from sensors spaced (-0.5,0,1.0 cm) and (-0.5,0,0.72 cm)...126

30. Radial depth profiles of experimental and RLM simulated HPV values obtained with 0.16 cm diameter brass point sensors located at various depths in a stem....................129

31. Experimental data obtained with (A) low thermal conductivity Teflon sensors in _Populus tremuloides_, (B) high thermal conductivity glass in _Picea glauca_ and (C) brass rod sensors in _Pinus banksiana_.............................132

32. Radial longitudinal model simulations with several sensor materials...134

33. Simulated (RLM) and experimental results with the HPVM one-sensor configuration at zero sap movement.............137

34. Experimental results using the single sensor HPVM configuration at several sapwood depths where the sap movement was greater than zero...................................139

35. Actual wood moisture content (Mgw) versus that calculated from longitudinal diffusivities and basic wood density...144

36. Transpiration of _Pinus halepensis_ as determined by weighing lysimetry and calculated from heat pulse velocities...149

37. Transpiration of _Pinus radiata_ as determined by weight loss and calculated from heat pulse velocities..........153

38. Transpiration of _Nothofagus solandri_ var. _cliffortiodes_ as estimated from a climatized cuvette and heat pulse velocity measurements..157

39. Transpiration of four *Picea glauca* trees as determined by weight loss and calculated from heat pulse velocities measured within one week to ten days of sensor installation....166

40. Transpiration of *Betula papyrifera*, tree BP1, as determined by potometry and calculated from heat pulse velocities measured with 0.16 cm diameter Teflon-encased thermistor bead sensors....173

41. Transpiration of *B. papyrifera*, tree BP2, as determined by potometry and calculated from heat pulse velocities measured with 0.16 cm diameter Teflon-encased thermistor bead sensors....174

42. Transpiration of *Populus tremuloides*, tree PT1, as determined by potometry and calculated from heat pulse velocities measured with 0.16 cm diameter Teflon-encased thermistor bead sensors....176

43. Transpiration of *P. tremuloides*, tree PT2, as determined by potometry and calculated from heat pulse velocities measured with 0.16 cm diameter Teflon-encased thermistor bead sensors....177

44. Heat pulse velocities in *P. tremuloides*, trees PT1 and PT2, at several positions in the sapwood before and after a stem freezing treatment....179

45. Time trend of Mgw(D^1,Pb) and XPP in *P. tremuloides*, tree PT2, before and after the stem freezing treatment....186

46. "Lysimeter" construction details....240

47. Lysimeter calibration curve....241

48. Sketch of potometer; physical placement of HPV probes and means of determining water uptake....250

49. Construction details of thermistor sensors....262

50. Heater construction details....263

51. Thermistor bridge arrangements for HPVT and HPVA, HPVS, HPVM or D measurement....266

52. Manual instrument for measuring HPVT....267

53. Semi-manual 4-channel HPVT recorder....267

54. Sixteen channel HPVA, HPVS, HPVM or D logger....268

LIST OF FREQUENTLY USED SYMBOLS

Upper case symbols	Definition
A	Area, cm^2
Ann	Area associated with a sensor at depth nn, cm^2
BP	Pre-dawn xylem pressure potential, MPa
B/S	Bark/sapwood interface
C	Specific heat, cal g^{-1} $^{o}C^{-1}$
Cdw	Specific heat of dry wood
Cgw	Specific heat of green wood
Cs	Specific heat of sap (water)
CWA	Counterweight added to spruce lysimeters, g
D	Thermal diffusivity, cm^2 s^{-1}
D^l	Thermal diffusivity in the longitudinal direction
D^r	Thermal diffusivity in the radial direction
D^t	Thermal diffusivity in the tangential direction
Ddw	Thermal diffusivity of oven dry wood
Dwa	Thermal diffusivity of water
HPV	Heat pulse velocity, cm h^{-1}
HPVA	HPV measured with two asymmetrically spaced sensors, temperatures taken at fixed time intervals.
HPVC	HPV corrected in accordance with simulation results
HPVI	HPV imposed on numerical models
HPVM	HPV measured with single sensor, temperatures taken at fixed time intervals
HPVP	HPV measured with single sensor at time of maximum temperature rise, tp
HPVS	HPV measured with two symmetrically spaced sensors, temperatures taken at fixed time intervals
HPVT	HPV measured with two asymmetrically spaced sensors at time of null temperature difference, tz

K	Thermal conductivity, cal s^{-1} cm^{-1} $^oC^{-1}$
K^l	Thermal conductivity in the longitudinal direction
K^r	Thermal conductivity in the radial direction
K^t	Thermal conductivity in the tangential direction
Kdw	Thermal conductivity of dry wood
Kgw	Thermal conductivity of green wood
Kwa	Thermal conductivity of water
L	Thickness of nonconvective layer, cm
LI	Light intensity in environmental chamber (PhAR), W m^{-2}
M	Moisture content, fraction dry weight, i.e., grams of water per grams of dry material
Mdw	Moisture content of dry wood
Mgw	Moisture content of green wood
P	Density of a substance, g cm^{-3}
Pb	Basic density of wood, (oven dry weight)/(green volume)
Ps	Density of sap (water)
PDE	Partial differential equation
RL	Stomatal resistance, s cm^{-1}
Q	Quantity of heat liberated, cal cm^{-3} s^{-1}
RLM	Numerical simulation model of 2-dimensional section of stem lying in the radial-longitudinal plane
S/H	Sapwood/heartwood interface
SWT	Sapwood thickness, i.e., B/S to S/H, cm
T	Temperature, ^oC
Td	Temperature measured at downstream sensor
Tu	Temperature measured at upstream sensor

TLM	Numerical simulation model of 2-dimensional section of sapwood lying in the tangential-longitudinal plane
TR	Transpiration
TR(nn)	Transpiration calculated from heat pulse velocities at wound width nn, (nn in mm)
TR(nnP)	Transpiration calculated from heat pulse velocities at wound nn, plus a correction for position of the sensor tips with respect to the S/H interface
TR(WL)	Transpiration as indicated by weight loss
Va	Volume of air in wood (void volume)
Vgw	Volume of water in green wood, fraction green volume
W	Wound width, cm
X	Distance from origin to a point on the "x" axis, cm
Xd	Distance from heater at the origin to a sensor downstream
Xu	Distance from heater at the origin to a sensor upstream
XPP	Xylem pressure potential, Scholander bomb, MPa
Y	Distance from origin to a point on the "y" axis, cm
Z	Distance from origin to a point on the "z" axis, cm

Lower case symbols

d	Depth of sensor tip measured from B/S interface
dbh	Diameter, outside bark, at breast height (1.4 m), cm
dib	Diameter inside bark, cm
dob	Diameter outside bark, cm
dwb	Dry weight basis, $g\ g^{-1}$
exp	The exponential function, $e^{()}$

ln	Logarithm to the base e
odw	Oven dry weight
t	Time, seconds
te	Time for temperature equilibrium with surroundings, s
tp	Time of maximum temperature rise, HPVP solution
tz	Time of null temperature difference, HPVT solution
u	Sap speed, cm s^{-1}

Miscellaneous

F(X,Y)	Functional notation: F is a function of the variables X and Y, e.g. Mgw(D^1,Pb)

CHAPTER I

INTRODUCTION

Transpiration

Transpiration is an evaporative process at the surfaces of a plant whereby water is lost from the soil via a plant's water conducting system (Slatyer 1967, Salisbury and Ross 1978). In forests, transpiration averages 60% of the annual amount of water lost by evapotranspiration (Baumgartner 1967). The amount of water transpired can, in some instances, exceed the annual precipitation (Larcher 1975). From a hydrologist's point of view, transpiration is loss from a watershed, reducing streamflow (Colman 1953).

Most of the water of transpiration escapes to the surrounding air via stomatal openings, but some loss occurs through the cuticle of leaves and bark and through lenticils in the bark of some plants (Crafts 1968, Zimmerman and Brown 1971, Kramer and Kozlowski 1979). The "openness" of the stomata controls both the inward flow of carbon dioxide used in photosynthesis and the outward flow of water vapor. Thus, measures of transpiration provide the plant physiologist some basis for quantifying carbon dioxide uptake (Brix 1962, Larcher 1975, Salisbury and Ross 1978) and the hydrologist with an estimate of the water lost from potential streamflow (Colman 1953, Baumgartner 1967).

Methods of measuring transpiration

Transpiration occurs as a continuum from soil to plant to atmosphere (Phillip 1966) and it may be measured (estimated) as moisture loss from the soil, liquid flow through the plant or vapour loss to the surrounding atmosphere. The five most commonly used methods are (Kramer and Kozlowski 1979):

1) Lysimetry, that is the weight loss through time from a plant growing in a water tight container (e.g. Fritschen, Hsia and Doraiswamy 1977).

2) Cut shoot or quick weigh, that is the weight loss from an excised twig or branch over a short time interval (e.g. Rutter 1968).

3) Potometry, that is the volumetric uptake by an excised shoot, branch or a whole tree (e.g. Ladefoged 1960, Roberts 1977).

4) Vapour loss into a plastic container from either a branch or an entire tree (e.g. Decker, Gaylor and Cole 1967; Greenwood and Beresford 1979,1980).

5) Sap flow, that is the rate of upward movement of the xylem sap stream (e.g. Huber 1932; Dixon 1937; Ladefoged 1963; Owston, Smith and Halverson 1972; Kline and others 1976; Luvall and Murphy 1982).

Each method has its proponents and critics. The first four will be discussed briefly. The last is the topic of this study.

The cut shoot and potometer methods are simple and relatively easy to apply but cause obvious physiological problems if the measurements are to be continued over extended time. The vapour tent method was severely criticized by Lee (1966) because of the artifical transpiration environment and the uncertainty in interpretation of measurements from trees of differing size or form. The lysimeter method (van Bavel and Myers 1962) is generally conceded to be the most accurate, but also the most expensive. Lysimeters, potometers and vapour tents have been used as controls for evaluating transpiration data obtained by other methods (Ladefoged 1963; Decker and Skau 1964; Lassoie, Scott and Fritchen 1977). Interpretation and physiological questions aside, the above methods of estimating transpiration are of limited use in forests because of the sheer physical size of trees and the differing microclimates that exist in various regions of the canopy (Leyton 1970).

Sap flow and transpiration

Techniques based on the measurement of xylem sap flow appear to be the most promising approach to the difficult problem of measuring transpiration from large trees (Leyton 1970). The transpiration stream has been described as a catena (van den Honert 1948), a chain where water from the soil passes through living root cells, xylem vessels or tracheids, living leaf cells, the intercellular spaces of the leaves, the stomatal openings and into the air layer around the leaves. In a woody plant such as a tree, most of the stem consists of xylem, the principal water conducting tissue (Esau 1977). The stem of a tree, is therefore, a place where the water of transpiration is concentrated. Near the ground is a physically convenient place to measure the flow in it.

About 95 to 99% of the water taken up by plants is eventually lost as transpiration (Salisbury and Ross 1978, Kramer and Kozlowski 1979). Therefore, sap flow through any cross section of a stem below the live crown, and transpiration from the crown are approximately equal in magnitude if one allows for phase shift caused by temporary change in storage of water in plant tissues (Kramer 1962, Swanson and Lee 1966, Doley 1967, Leyton 1970, Swanson 1972, Waring and Running 1978, Waring and Roberts 1979). I will thus use the terms "transpiration" and "sap flow" as being fully equivalent throughout the remainder of this thesis.

Sap flow calculations

Xylem sap movement occurs primarily through the lumen of vessels in porous woods; in total through the lumen of tracheids in nonporous woods (Zimmerman and Brown 1971). Sap flow ($cm^3\ s^{-1}$) can be calculated from some measure of sap speed ($cm\ s^{-1}$) times functioning lumen area (cm^2) or from sap flux (unit area sap flow, $cm^3\ cm^{-2}\ s^{-1}$) times the xylem area (cm^2) over which it applies. Sap speed or flux is generally determined with some trace material that is introduced into the sap stream. To determine transpiration, four things must be considered in addition to the speed or flux measurement: 1) the position or depth in the stem to which movement takes place; 2) the order of magnitude of sap speeds that may be encountered; 3) the cross-sectional area of the conducting tissue that is currently functioning; and 4) how to introduce and detect the trace materials without disturbing normal flow patterns (Marshall 1958, Leyton 1970). Heat has a decided advantage over other trace "materials" in that it can enter and be detected in the sap stream by thermal conduction through the wood structure without causing disturbance to the normal flow patterns, Marshall (1958). The first three are anatomical considerations which will be discussed briefly in the next section. A heat transport method is the subject of this study and it will be discussed in detail in the chapters that follow.

Anatomical considerations in sap flow measurement

Stem structure

In nontechnical terms, a cross section of a tree consists of bark on the outside, xylem or wood in the center, with a thin growing area of vascular cambium between them (Fig. 1) (Esau 1977, Kramer and Kozlowski 1979). All of the cells of xylem, with the exception of the longitudinal and radial parenchyma, and those still differentiating within about 1 mm of the cambium, are dead (Stewart 1966). Thus xylem sap flow occurs through dead cells.

As new increments of xylem are formed at the cambium, metabolic waste products, that are toxic or inhibitory to live cells, are translocated toward the center of the tree where they accumulate to discolour the wood and cause the death of parenchyma cells to form heartwood (Stewart 1966). (There are dissenters to this concept of heartwood formation, e.g. Bamber 1976.) The portion of xylem, which lies between the cambium and the heartwood, which contains tracheary elements and living parenchyma cells is called sapwood (Fig. 1) (Panshin and de Zeeuw 1970, Esau 1979). Sap flow does not occur in the heartwood (Whitehead and Jarvis 1981). Neither does sap flow occur in the transition zone (variously called dry zone, intermediate zone) between sapwood and heartwood in *Pinus radiata* D. Don (Booker and Kinninmonth 1977)

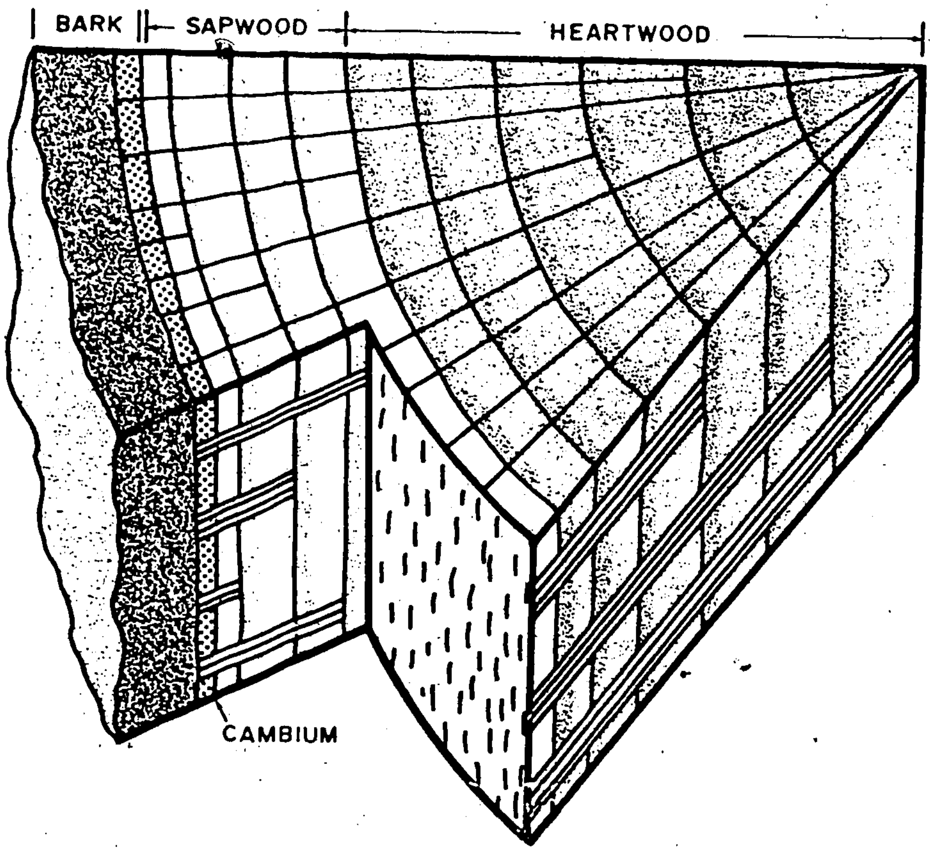

Figure 1. Idealized stem cross section illustrating the tissues of importance in xylem sap flow measurement.

even though living parenchyma cells are metabolically active in this zone (Whitehead and Jarvis 1981).

Not all trees form heartwood, e.g. Alnus spp., Betula spp. (Stewart 1966, Panshin and de Zeuuw 1970). Where it is formed, the presence of heartwood delimits the possible extent of sap conducting xylem, i.e. it must be contained within the sapwood. Within the sapwood, the anatomical features of importance in measuring sap flow are; 1) the type of tracheary elements, 2) the diameter of individual tracheary elements, 3) the spatial distribution of functioning tracheary elements within a given growth ring, and 4) the total number of growth rings containing currently functioning tracheary elements.

Nonporous woods

In nonporous woods (softwoods, conifers), the tracheary elements are tracheids which form the bulk of the xylem tissue (Esau 1977). They range from 15 to 80 micrometers in diameter (Panshin and de Zeuuw 1970) with peak sap speeds ranging from 75 to 200 cm h^{-1} (Hinckley, Lassoie and Running 1978). Tracheids formed in the spring (earlywood) are larger than those formed in the summer (latewood) (Kramer and Kozlowski 1979). Only the earlywood tracheids conduct sap (Whitehead and Jarvis 1981). Therefore, coniferous sapwood may contain concentric bands of non-sap conducting latewood which occupy up to one-half the width of a growth ring (based on saturated longitudinal permeability measurements and variation in intraring density, see Cown and Parker 1978, Booker and Swanson 1979).

Porous woods

In porous woods (hardwoods, angiosperms), the tracheary elements include specialized conducting elements called vessels which in cross sections appear as pores in the wood (Esau 1977, Kramer and Kozlowski 1979). Vessels range from 20 to 800 micrometers in diameter (Kramer and Kozlowski 1979). In ring porous species (e.g. Ulmus, Quercus) the vessels formed in the spring (200-350 micrometers diameter) are much larger than those formed later (Brown, Panshin and Forsaith 1949), and sap movement is confined to the outer 1 or 2 growth rings (Kozlowski and Winget 1963). Peak sap speeds in ring porous woods range from 1550 to 6000 cm h^{-1} (Hinckley, Lassoie and Running 1978). In diffuse porous species (e.g. Populus, Betula), the size of the vessels is fairly uniform (60-120 micrometers diameter), they are distributed evenly throughout each growth ring (Brown, Panshin and Forsaith 1949), and sap movement can occur through many rings (Kozlowski and Winget 1963). Peak sap speeds in diffuse porous woods range from 120 to 625 cm h^{-1} (Hinckley, Lassoie and Running 1978). The variation in vessel size within a ring follows approximately the same pattern that Cown and Parker (1978) show for intra-ring density in ring and diffuse porous woods. The wood of some species (e.g. Juglans spp., Diospyros virginiana L.), have vessel arrangements and sap speeds intermediate to ring or diffuse porous trees. These are termed semi-ring or semi-diffuse porous (Panshin and de Zeeuw 1970).

Location of flow in the sapwood

Aside from the general assertion that sap moves within the sapwood, the actual area of the sapwood through which flow occurs in any given instance, is poorly known. The staining patterns resulting from the uptake of various dyes, have been used to indicate the currently-functioning conducting tissue (Vitè 1959, Vitè and Rudinsky 1959). However Kozlowski and Winget (1964), indicated that more rings were stained, when dye was taken up from a cut across the sapwood, than when dye was taken up by the roots. This casts some doubt on the use of dye techniques to indicate sap flow pathways. Zimmerman and Brown (1971) suggest that the emptying (cavitation) of vessels or tracheids (of water) is irreversible and that once emptied, they cannot be refilled to become a part of the conducting system. However, Waring and Running (1978) consider cavitation (at least in conifers), to be reversible so that the conducting area may recede or expand depending upon plant water status. If the cavitation of tracheary elements is irreversible, then a measure of the volume of air in any portion of sapwood may indicate its permeability (Puritch 1971), i.e., its capability to function in sap conduction. Proven techniques to delineate the portion of sapwood that is functioning at any given time are lacking and this is an area in need of further study.

Thermal-sapflow measurement methods

General flowmetering analogy

There are two ways to use tracers to measure fluid flows which are useful analogies to thermometric methods.

1) By determining the speed of tracer transport from one point to another (Østrem 1964). Flow is calculated from flow geometry, cross sectional area and speed (Venard 1957).

2) By determining the concentration or rate of change in concentration at either the point of injection or some point downstream. The change, or rate of change, in concentration is an indicator of mass flux (Church and Kellerhals 1970).

Heat has been used as a "trace material" in sap flow experiments in both ways, that is both as an indicator of sap speed (Huber 1932, Huber and Schmidt 1937) and as an indicator of flow density or flux (Marshall 1958). It is in connection with the application of these two differing measures that sapwood anatomy becomes important.

Huber method

In the Huber (1932) method, the surface of a 4 mm diameter stem was heated for 1 to 5 s. The time from heat application to the first indication of temperature rise at 6 to 31 cm downstream (usually 6 cm) was noted. The distance between heater and thermocouple was divided by this time to obtain sap speed. According to Huber (1932), this technique is suitable for sap speeds greater than 60 cm h^{-1}, i.e. it is fully applicable in ring porous woods, and marginally applicable in diffuse porous woods.

Huber and Schmidt (1937) recognized that heat conduction through the wood substance interfered with the heat pulse carried by the sap stream at low sap speeds. They proposed a sensing configuration in which one temperature sensor was placed 2 cm downstream, a second 1.6 cm upstream, to compensate for thermal conduction. The time of peak warming of the upstream temperature sensor compared to the one downstream, was used to arrive at a convective velocity, free of thermal conduction interference, and equivalent to that obtained with the one-sensor method. They state that this method is usable in conifer or diffuse porous woods to zero sap speed with an accuracy of $\pm$ 5 cm h^{-1}.

Marshall method

In the Marshall (1958) method, the heater and temperature sensor are implanted 1.5 cm apart into the sapwood. The heater is activated for 1 to 2 s and the rate of temperature rise through time is noted at 1 minute intervals for 3 to 7 minutes. Heat pulse velocity (HPV), which is defined as the weighted average speed of the moving sap and the nonmoving wood moving together, is determined from an analytical solution to the thermal diffusion equation for heat transfer by coupled convection (sap movement) and conduction. The HPV value is averaged over a 1.5 to 2.0 cm diameter area centered on the temperature sensor (Marshall 1958). An assumption of homogeneity of flow throughout this area is implicit to the use of the analytical solution. Thus the heat pulse velocity method of Marshall (1958) is applicable only in woods where there is a reasonably uniform spatial distribution of functioning tracheary elements over a sapwood width of 1.5 cm or more.

Differences between the Huber and Marshall methods

A significant difference between the Huber approach (Huber 1932, Huber and Schmidt 1937) and that of Marshall (1958), is the measure of velocity that is obtained. Because Huber's approach involves only the time of travel of the pulse of heat, the velocity obtained is closely related to actual sap speed. The Marshall approach considers both the time of travel and the magnitude of the pulse. Since heat is lost from the sap while it moves through the stationary wood, the heat pulse is both delayed and reduced in magnitude at the point of measurement, either up or downstream. (The effect of this time delay is present in Huber's approach too so that it does not yield true sap speed. The problem that I have outlined here, is not the only difference between the Huber and Marshall methods.) According to Heine and Farr (1973), the velocities obtained by these two approaches differ on the average by a factor of 20; that is, Huber's method yields a convection velocity that is 20 times larger than Marshall's heat pulse velocity.

With either the Huber or Marshall methods, sap speed or heat pulse velocity are only partial components of total sap flow. To obtain sap flow, sap speed must be integrated over functional lumen area or heat pulse velocity must be combined with sapwood density and specific heat (which are functions of sapwood moisture content), and integrated over the functional sapwood area.

Many researchers, myself included, have not fully appreciated the fundamentally different approaches of Huber and Marshall. A basic problem has been misinterpretation of the values measured, i.e., sap speed is not heat pulse velocity. The literature contains several "heat pulse velocity" methods and the term "heat pulse velocity" has not retained the precise meaning that Marshall (1958) stated, i.e., "the stationary wood and the moving sap act like a single medium moving at a speed defined by V." For example (see Table 5 in Hinckley, Lassoie and Running 1978), heat pulse velocity may refer to peak sap speed, average sap speed, some unknown index to sap speed or to an average of conducted plus convected heat pulse speed depending upon the technique used to obtain the temperature data and the equation(s) used to operate on that data. In addition, other types of thermometric methods, neither based solely on sap speed nor on heat flux but considered by others as equivalent to the heat pulse method (e.g. Kramer 1969, Kramer and Kozlowski 1979), have been published.

Confusion in the thermometric flow literature

There is a confusing body of literature containing accounts of attempts to use some form of thermal technique to study sap movement. These fit into three broad categories.

1) Those using the sap speed approach of Huber and cohorts (Huber 1932; Huber and Schmidt 1936,1937; Dixon 1937; Bloodworth, Page and Cowley 1955; Ladefoged 1960; McNabb and Hart 1962).

2) Those using (and in some instances misusing) some form of Marshall's (1958) heat pulse velocity (heat flux) analysis (this technique will be covered in much greater detail in the next chapter) (Closs 1958; Swanson 1962; Doley and Greive 1966; Wendt, Runkles and Hass 1967; Morikawa 1972; Stone and Shirazi 1975; Balek and Pavlik 1977; Miller, Vavrina and Christensen 1980; Cohen, Fuchs and Green 1981).

3) Miscellaneous thermal budgeting and exotic heating techniques (Vieweg and Ziegler 1960; Daum 1967; Leyton

1967; Ittner 1968; Redshaw and Meidner 1970; Pickard and Puccia 1972; Cermak, Deml and Penka 1973; Pickard 1973; Sakuratani 1982).

Several of the techniques in the citations above should be exploitable for sap flow measurements. Marshall's (1958) implanted line heater method has been widely used; it is the simplest and perhaps the only technique applicable in wide sap-wooded coniferous or diffuse porous trees, which approximate the thermally homogeneous conditions stated by him. Daum's (1967) thermal budget of an entire stem and the applied-heat budget described by Cermak and others (1973) are two methods that appear particularly promising for use in ring porous trees. Sakurtani (1982) used an approach similiar to Daum (1967), and Cermak and others (1973), to determine sap flow in rice and soybean stems. The temperature ratio methods of Leyton (1967) and Ittner (1968) offer the possibility of continuous recording after being calibrated for a particular situation. And certainly the "first onset" technique (Huber 1932, Huber and Schmidt 1936) and the "compensations method" (Huber and Schmidt 1937) may be empirically calibrated for specific instances to provide useful measures of water movement.

Thesis objectives

In spite of the amount of work done using thermal methods for estimating sap flow, no method has been successfully applied in direct, quantitative calculations of transpiration against measured controls. The number of reported attempts are few (Doley and Greive 1966; Cohen, Fuchs and Green 1981; Swanson 1974a) and in these instances, the calculated quantities were in the range 0.45 to 0.65 of that actually measured. There appears to be no theoretical reason why heat transport methods should not work. It is likely that some of the theoretical conditions are not being met in practice. My principal concern remains to investigate transpiration in large trees without recourse to empirical coefficients or calibrations. The most advanced and promising theory for this application is that of Marshall (1958). My objective in this study was to examine the implanted point sensor, line heat source, heat pulse velocity method as described by Marshall (1958), in its application to the measurement of sap flow in the sapwood of conifer and diffuse porous trees. My goals were:

1) To conduct a theoretical analysis of the physical heat conduction and convection system that will account for normal thermal property discontinuities that exist in nonporous and diffuse porous woods and those caused by the implanting of sensing probes.
2) To verify experimentally any new theory or instrumentation techniques that evolve from this analysis.
3) To propose practical instrumentation and analyses techniques and the conditions under which they are valid for measuring sap flow in conifers and diffuse porous trees.

CHAPTER II

ANALYTICAL HEAT PULSE VELOCITY THEORY

Description of the physical problem

The physical problem to be examined is one of 3-dimensional heat flow in functional sapwood with differing thermal conductivities in the longitudinal (x), tangential (y) and radial (z) directions. A line heater lies along a radius (z axis at X = Y = 0) which is inserted through the bark, vascular cambium and into the sapwood. The heater may or may not penetrate the heartwood. One temperature sensor is installed in a similiar manner a positive distance Xd downstream (above the heater) from the heater and in the x-z plane. A second temperature sensor identical to the first, may or may not be installed at Xu, a negative distance upstream (below the heater). (Within this thesis, I will refer to the sensor(s) and heater collectively as "probes", individually as sensor or heater.) A probe configuration designated (-0.5,0,1.0 cm) means a temperature sensor at -0.5 cm upstream, a heater at the origin, and a second sensor 1.0 cm downstream. The probes occupy space originally occupied by sapwood within which sap moved through tracheids or vessels, and their thermal properties differ from those of bark, cambium, sapwood or heartwood.

Initially, the heater, temperature sensors, wood, cambium and bark are all at the same (ambient) temperature. The heater is activated for a short time period (1 to 4 s), raising its temperature from 5 to 40 °C. Heat is conducted in the longitudinal, tangential and radial directions in accordance with their directional thermal conductivities K^l, K^t and K^r respectively. In addition, heat is carried (convected) downstream by sap streams which are heated during their passage through the wood near the heater. The sap streams carry heat forward at a rate faster than it is conducted longitudinally and the convected heat wave loses heat to the colder wood as it passes through it. The sap streams are interrupted in the plane of the sensor-heater so that heat arrives at the sensor(s) by conduction through the sapwood in the plane of the sensors and by conduction plus convection through the wood immediately adjacent on both sides of the sensor-heater plane. Either continuously or at periodic intervals, the temperature registered by the sensor(s) is recorded. These temperature values are used to solve for heat pulse velocity using one or more of the solutions given below.

Idealized heat transport theory

Partial differential equation (PDE) in 3-dimensions

In the idealized case, a linear heater and point temperature sensors without physical size or mass are installed radially into the xylem. Heat conduction in the longitudinal, tangential and radial directions, plus convection in the longitudinal direction must be accounted for. With sap flow in the x-direction (longitudinal), one may write for temperature (Marshall 1958, Carslaw and Jaeger 1959).

$$PC(\partial T/\partial t) = K^l(\partial^2T/\partial x^2) + K^t(\partial^2T/\partial y^2) + K^r(\partial^2T/\partial z^2) + auPsCs(\partial T/\partial x) + Q(X,Y,Z,t) \quad (1)$$

where T (^oC) is temperature departure from ambient; t is time (s) from initiation of heat pulse; u is sap speed (cm s^{-1}); a is the fraction of xylem cross sectional area occupied by moving sap streams (cm^2 cm^{-2}); Ps (g cm^{-3}) and Cs (cal g^{-1} $^oC^{-1}$) are density and specific heat of the sap (considered equivalent to water); P (g cm^{-3}) and C (cal g^{-1} $^oC^{-1}$) are density and specific heat of the combined wood-sap mixture; K^l, K^t and K^r are the longitudinal, tangential and radial thermal conductivities (cal s^{-1} cm^{-1} $^oC^{-1}$) of the mixture; and Q is internally generated heat (cal cm^{-3} s^{-1}).

Definition of heat pulse velocity

Equation 1 is the same form as conduction in a moving medium with movement in the "x" direction (Jakob 1949). It is from this equation that the rather peculiar definition for HPV (Eq. 2) arises (Marshall 1958); i.e. "a weighted average of the velocities of the sap and stationary wood substance." One can extract sap velocity "u" from HPV if the fraction "a" and the specific heat and density of the combined wood-water mixture are known. However, according to Marshall, sap flux (Eq. 10, p. 23), the "au" portion of Equation 2, is more useful than sap speed for most comparison purposes.

$$HPV = au(PsCs)/PC \text{ cm h}^{-1} \quad (2)$$

Analytical solution to PDE, idealized case

Marshall's (1958) concern was with a two-dimensional simplification of the above three-dimensional heat flow equation in the longitudinal and tangential directions. He considered uniform sap movement and thermal properties along the z-axis (stem radius) and showed that when Q represents an instantaneous heat pulse at X=Y=t=0, the heater and sensors are infinitely small, the xylem infinitely large, thermally homogeneous and isotropic ($K^l = K^t$), and sap streams are uniformly distributed, Equation 1 may be solved for T:

$$T = (Q/4\pi Dt)\exp-\left\{\left[(X - HPVt)^2 + Y^2\right]/4Dt\right\} \ {}^oC \qquad (3)$$

where diffusivity $D = K/PC$.

Equations to extract HPV's from time-temperature data

Equation 3 may be manipulated in several ways to extract HPV from the temperature variation with time at one or more points (X,Y) in the xylem. Reference to Figure 2 will help to illustrate the following derivations.

Single sensor, fixed time, HPVM

Marshall (1958) considered a single temperature sensor downstream from a heater, read at three successive times t_1, t_2 and t_3 such that $t_3 = 3t_1$ and $t_2 = 2t_1$ (Fig. 2a), and derived:

$$HPVM = r\left[(t_1 \ln R_1 - t_3 \ln R_2)/t_1 t_2 t_3 \ln(R_1/R_2)\right]^{1/2} \ \text{cm s}^{-1} \qquad (4)$$

where $r = (X^2 + Y^2)^{1/2}$ is the distance from heater to sensor

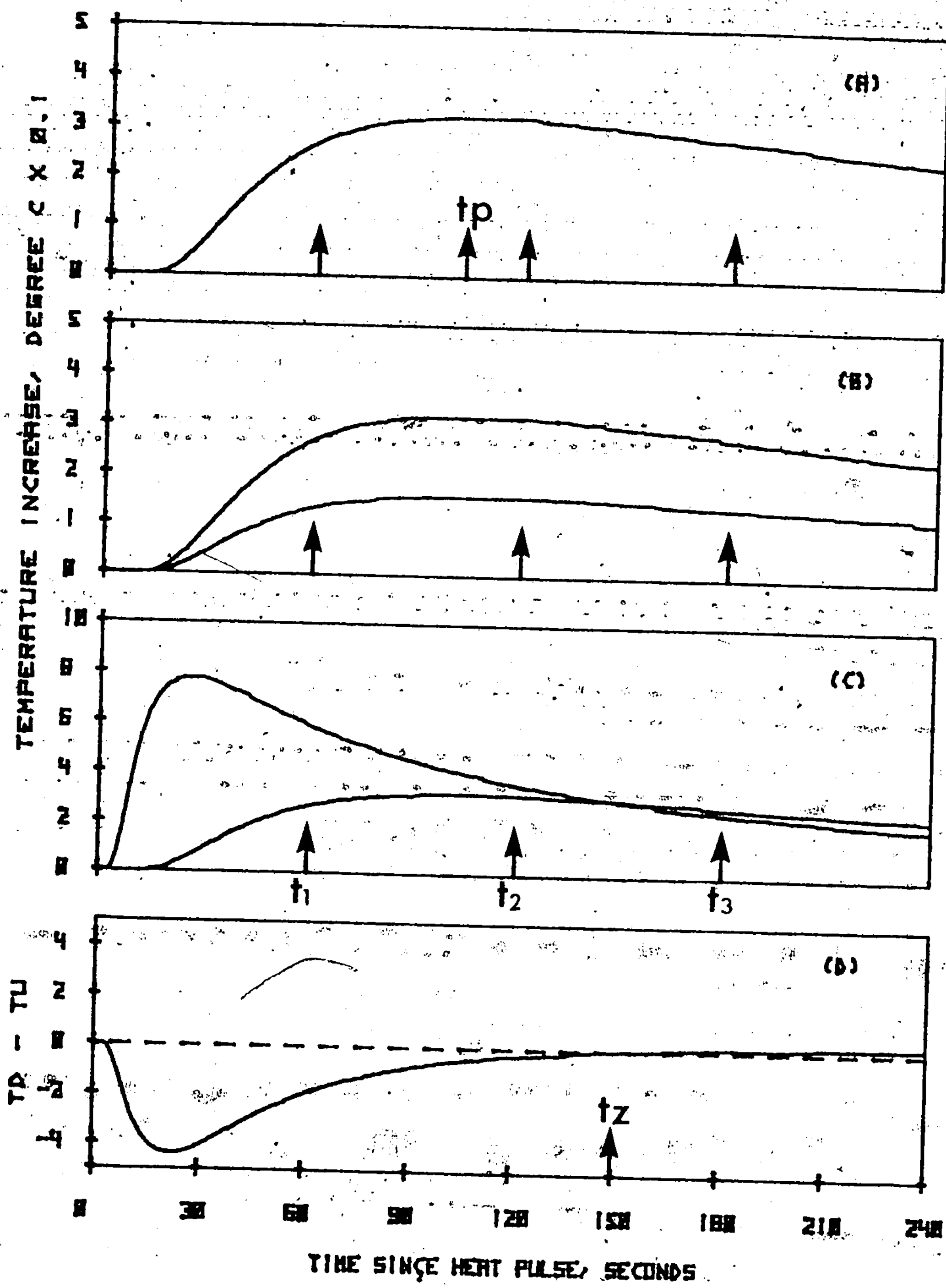

Figure 2. Plots of temperature rise versus time for the various solutions of Equation 3 with HPV = 5 cm/h. (A) Temperature rise at one sensor located 1 cm downstream from the heater (0,1.0 cm). (B) Temperature rise at the downstream sensor and at a second located 1 cm upstream (-1.0,0,1.0 cm). (C) Temperature rise at the downstream sensor and at a second located 0.5 cm upstream (-0.5,0,1.0 cm). (D) Temperature difference at 1 cm downstream, 0.5 cm upstream.

(note that since solutions are generally obtained at $Y = 0$, $r = X$), $R_1 = T_1t_1/T_2t_2$, $R_2 = T_2t_2/T_3t_3$ and T_1, T_2 and T_3 are temperature rise above ambient at times t_1, t_2 and t_3 respectively.

Single sensor, fixed time, thermal diffusivity, D

He also derived Equation 5 for thermal diffusivity (D) where the symbols have the same meaning as in Equation 4.

$$D = -0.5(t_2 - t_1)^2 r^2 / t_1 t_2 t_3 \ln(R_1/R_2) \ \ cm^2\ s^{-1} \qquad (5)$$

Two sensor symmetrical configuration, HPVS

Marshall (1958) suggested that Equation 6 might be more appropriate than 4 for very slow sap movement:

$$HPVS = (D/r)\ln(Td/Tu)\ cm\ s^{-1} \qquad (6)$$

where Td/Tu is the ratio of downstream to upstream temperatures at points Xu, Xd, equidistant upstream and downstream from the heater (Fig. 2b). This equation is independent of the time that the temperature ratio is measured but does require some measure of D.

Single sensor, time of peak temperature, HPVP

Marshall (1958) derived Equation 7, by setting the time derivative of Equation 3 equal to zero, to obtain a solution in terms of the time of maximum temperature rise, tp (Fig. 2a).

$$HPVP = (r^2 - 4Dtp)^{\frac{1}{2}}/tp \quad cm\ s^{-1} \qquad (7)$$

Two sensor, asymmetric, time of null temperature, HPVT

Swanson (1962) considered solutions to Equation 3 at two temperature sensors, one upstream a negative distance -Xu, and the other downstream, a distance Xd, from the heater (Xu + Xd ≠ 0, sap movement ≠ 0). After a temperature rise has been registered at the upstream sensor (Fig. 2c and 2d), then at time tz when Tu = Td:

$$HPVT = (Xu + Xd)/2tz \quad cm\ s^{-1} \qquad (8)$$

Equation 8 is particularily well adapted to manual determinations as it requires only a sensitive null detector and a stop watch to implement. The tz's are the only data that the observer must note.

Closs (1958) also derived Equation 8 but from theoretical analysis of a plane heat source in one dimension, demonstrating that this solution is independent of heater geometry. The identical working equation and the general similiarity of heat transport solutions (exponential form as in Eq. 3) apparently confused Morikawa (1972) who used the plane heat source theory to describe a line heat source application.

Two sensor, asymmetric, fixed times, HPVA

To obtain a solution more suited to digital recording than manual reading, the two sensors of Swanson's (1962) configuration can be read at any two times t_1 and t_2, (Fig. 2c):

$$HPVA = (Xu+Xd)(t_1 \ln S_1 - t_2 \ln S_2)/2t_1 t_2 \ln(S_1/S_2) \text{ cm s}^{-1} \quad (9)$$

where S_1 = Td/Tu at time t_1 and S_2 = Td/Tu at time t_2.

Note that none of these formulations require determination of actual temperature; only temperature ratio or difference. This has important implications for instrumentation.

Auxiliary equations

Sap flux

For most purposes, the quantity of interest is sap flux i.e., the unit-area rate of sap flow. This is the "au" term of Equation 2. Marshall (1958) showed that:

$$\text{Sap Flux} = au = Pb(Cdw + Mgw)HPV \quad \text{cm}^3 \text{ cm}^{-2} \text{ s}^{-1} \quad (10)$$

where Pb is basic wood density (oven dry weight)/(green volume), Mgw is the moisture fraction (wet weight - oven dry weight)/(oven dry weight), and Cdw is the specific heat of dry wood which Dunlap (1912) showed to vary slightly with temperature as:

$$Cdw = 0.266 + 0.00116T \text{ cal g}^{-1} \text{ }^{o}\text{C}^{-1} \quad (11)$$

where T is in ^oC.

Thermal conductivity of wood

The conductivity of wood is related to its moisture content and basic density (Siau 1971). Longitudinal conductivity (K^l), cal s^{-1} cm^{-1} $^oC^{-1}$, is given by Siau (1971) as:

$$K^l = 0.0001(21.0 - 20.0Va) \tag{12}$$

with fractional void volume per cm^3 of wood (Va) defined as:

$$Va = 1.0 - Pb(0.667 + Mgw) \tag{13}$$

Tangential and radial conductivity (K^t,K^r) are approximately equal and given by (Siau 1971):

$$K^t = K^r = 0.0001\left[12.2 - 11.3(Va)^{\frac{1}{2}}\right] \tag{14}$$

The literature contains few references to thermal conductivity of wood in living trees. According to Siau (1971), thermal conductivity in the longitudinal direction is about 2 to 2½ times greater than that in the tangential or radial directions. This is apparently true in cases where the wood moisture content is below fibre saturation point. However others have found that conductivity in all directions approaches that of water as wood moisture is increased above fibre saturation (Turrell and others 1967; Herrington 1969; Steinhagen 1977). Turrell and others (1967) calculated thermal conductivity of wood at a particular moisture content (Kgw) by summing the fractional conductivities of water and dry wood in the appropriate directions (Eq. 15).

$$Kgw = VgwKwa + (1.0 - Vgw)Kdw \qquad (15)$$

Where Vgw = PbMgw i.e. moisture content by volume, Kwa = thermal conductivity of water (0.00144 cal s^{-1} cm^{-1} $^oC^{-1}$), and Kdw = thermal conductivity of dry wood (cal $s^{-1} cm^{-1} {}^oC^{-1}$) in the desired direction. If one uses Equations 12 and 14 for dry wood thermal conductivity (Va is then a function of Pb only when Mgw = 0) in the appropriate directions, and Equation 15 to calculate the thermal conductivity of the wood-water mixture, then the longitudinal and radial or tangential values do approach that of water at high moisture contents.

Thermal conductivity K is related to thermal diffusivity D as:

$$D = K/PC \quad cm^2\ s^{-1} \qquad (16)$$

where P and C are density and specific heat, respectively.

Wood moisture content from thermal diffusivity and basic density

It is possible to calculate wood moisture content, Mgw, using Equation 17, from diffusivity, Equation 5 and basic density

(Pb), by combining Equations 12 and 13 or 12 and 14 and the definition for D, Equation 16 with Equation 15.

$$Mgw = (Kdw - 0.33PbDgw)/(Dgw - Kwa + Kdw) \quad (17)$$

The subscripts dw, gw, wa refer to drywood, greenwood and water respectively and Cdw is taken as 0.33. (Note that the diffusivity and conductivity of water are equal, i.e., Dwa = Kwa.) The Dgw is the thermal diffusivity of moist wood at Pb calculated from implanted sensors using Equation 5. Either D^{l}_{gw} or D^{t}_{gw} can be used in Equation 17 provided Kdw is similiarly defined. However, longitudinal diffusivity D^{l}_{gw}, is probably best suited to this application because of its wider range in magnitude over the moisture contents of physiological interest. D^{l}_{gw} in wood of Pb = 0.40 at theoretical saturation (Mgw = 1/0.40 - 0.65 = 1.85) (Skaar 1972) is 0.0014 $cm^2\ s^{-1}$, and at Mgw = 1.0, D^{l}_{gw} = 0.0018. In contrast, D^{t}_{gw} at saturation moisture content is 0.0013 and only increases to 0.001367 at Mgw = 1.0. I suspect that measures of D^{t}_{gw} to four significant figures would be quite difficult under field conditions. One can determine D^{l}_{gw} to two, or perhaps even three, significant figures. Although moisture content has been used to estimate thermal conductivity, I have not found reference to in situ determinations of sapwood moisture by this means (Eq. 17). If this proves to be a practical approach, it would represent a significant advance in the nondestructive monitoring of tree moisture content.

To estimate transpiration or total sap flow, one must integrate sap flux (Eq. 10, p. 23) over the sap conducting xylem area which must be measured or estimated. The integration requires determinations or estimates of HPV, Pb and Mgw over this area. The annual variation in wood basic density, Pb, in Engelmann spruce (Picea engelmannii Parry) and lodgepole pine (Pinus contorta Dougl.), was less than 5% (Swanson 1967a) and it can probably be taken as a constant for a particular tree. Both HPV and Mgw may be obtained *in situ* from the same data if it is taken to satisify Equations 4 and 5 (p. 19,20).

Conditions for application

Marshall (1958) stated, or implied through his discussion, that several physical conditions should be adhered to in the application of this idealized analytical theory to specific sap flow measurement situations. In my opinion the four most important ones are:

1) The tip of a temperature sensor must be implanted deeper than ½ to 1 cm in the sapwood in order to limit the effect of heat loss at the surface of the stem.

2) The sensor and heater diameters must be a small fraction of the distance(s) between them.

3) The sapwood must not contain layers of nonconvective material which require appreciable time to reach thermal equilibrium with their surroundings.

4) Sap flux, not heat pulse velocity, should be used to compare sap flow rates against each other or against external measurements such as evaporation at the leaves or water uptake by the roots.

The first criterion is reasonably objective. It limits application to the center of 1 to 2 cm diameter stems composed entirely of sapwood or to the center of sapwood layers 1 to 2 cm thick.

The second criterion was not specifically stated by Marshall (1958), but it is suggested by his discussion of experimental apparatus and absence of thermal homogeneity. He implies that the error in HPV measurement caused by finite-sized apparatus increases as the distance between sensor and heater decreases. I interpret these errors as arising from distortion of the temperature field caused by thermal interaction between the materials of the heater and sensor when in close proximity. The more they are separated, the larger each probe can be without increasing error arising from this source. Marshall's experimental apparatus consisted of a 0.076 cm diameter sensor 1.5 cm downstream from a 0.25 cm diameter heater. Their average diameter is 11% of the distance between centers: therefore, 10% of separation could be used as an approximate criterion for probe diameter.

The third criterion can be met if the thermal equilibrium time of any nonconvective layer can be made negligible. There will always be some nonconvecting tissue in the immediate vicinity of the HPV probes, because the act of drilling holes to implant them in functioning sapwood, must sever vessels or tracheids. Thermal equilibrium time, te, is dependent upon thickness of this nonconvective material and the thermal diffusivity of it. Marshall (1958) gives:

$$te = 3L^2/8D \text{ s} \tag{18}$$

where L = thickness of nonconvective material (cm). Marshall further implies that some fraction of measurement time may provide a criterion for specifying a minimum acceptable equilibrium time. The minimum duration of a measurement, that is the length of time from heat pulse initiation to the first temperature measurement used in the fixed-time Equations, 4 and 9 (p. 19 and p. 23), can be selected by the experimenter. For the purpose of this discussion, I am assuming that a te of 1% of the first time interval after the heat pulse, is acceptable. Marshall used 60 s intervals in his applications of Equation 4; therefore a te of 0.6 s may be appropriate. If Dgw = 0.0012 cm^2 s^{-1} in the tangential or radial direction (Herrington 1969), then any nonconvective thickness, L, less than 0.04 cm would not cause significant departure from thermal homogeneity. At first glance, it would appear that time measurement intervals could be made sufficiently long so that almost any size of probe, or sapwood with vessels in any arrangement, could be made to behave as thermally homogeneous. However practical time limits are set by the magnitude of temperature increase that can be conveniently created, without causing physiological damage to the tree, and by the exponential rate of decay of that temperature pulse with time. The temperature rise from a modest heat pulse input is detectable for a minimum of about 300 s (Swanson 1974a). If data to satisfy Equation 4 were taken at 100 s intervals: a te of 1 s with the above thermal constants would establish a maximum nonconvective thickness of 0.05 cm. Any nonconvective material wider than 0.05 cm within the 1.5 to 3 cm^2 cross section influencing the sensors, would make the tissue nonhomogeneous. This width could be used as a criterion to determine if Marshall's (1958) idealized analysis is usable or not.

The importance of the fourth criterion is illustrated on Figure 3. Waring and Running (1978) and Waring, Whitehead and Jarvis (1979) indicate that the relative water content (RWC) of stem sapwood may decrease by as much as 20 to 25% over a season. Considering Pb = 0.4, Mgw (dwb) at saturation would be 1.85. Curve A (Fig. 3) is at RWC = 0.8; curve B, is at a relative water content 25% less, i.e. 0.55. If the

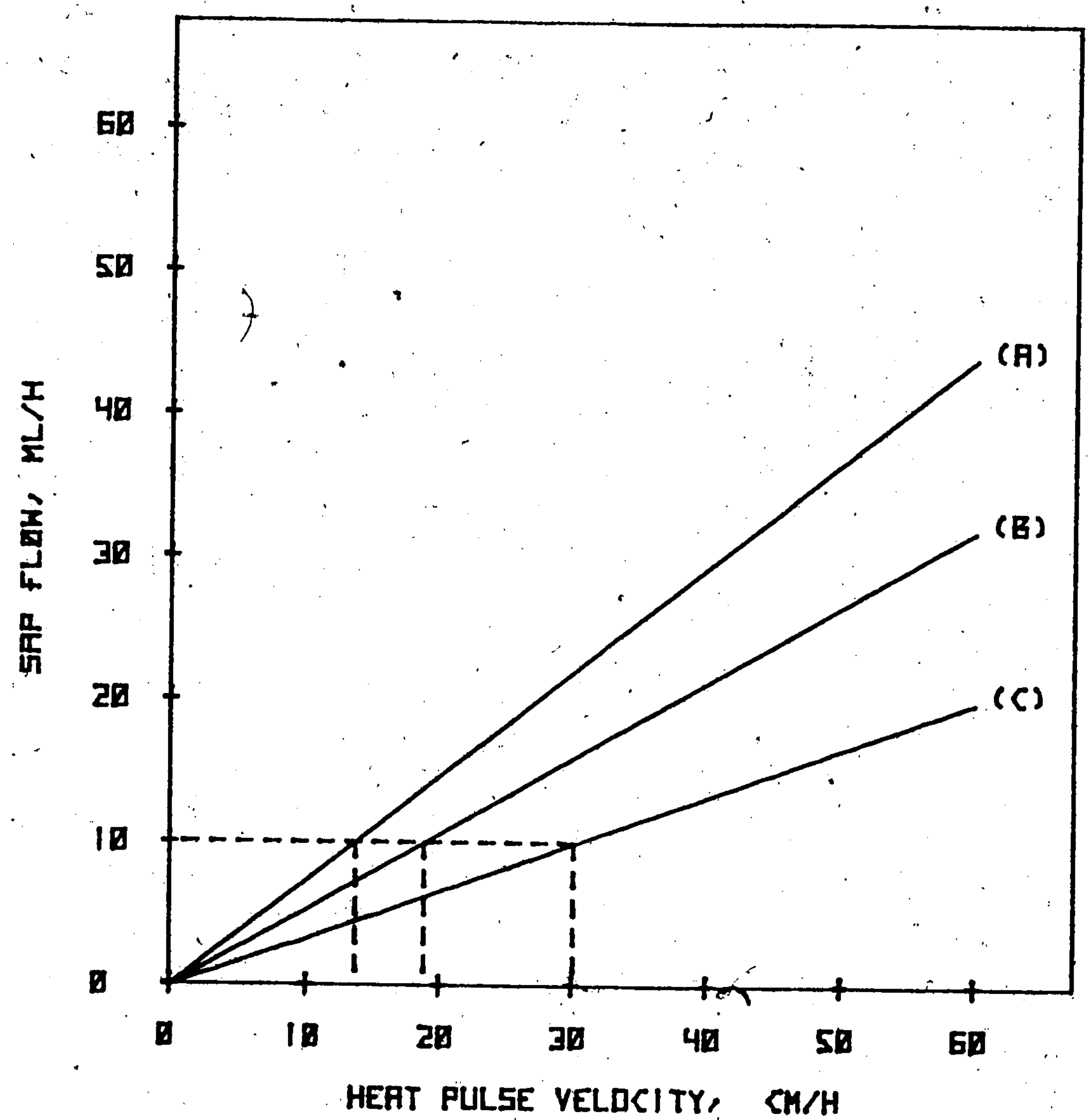

Figure 3. Theoretical plotting of sap flow through a constant sapwood area versus heat pulse velocities at Mgw's of (A) 1.5, (B) 1.0, (C) 0.5. The importance of a reasonably accurate estimate of current sapwood moisture content in calculating sap flow from heat pulse velocities is indicated by the example set out by the dashed lines. These show that at a constant sap flow of 10 mL/h, HPV's would be 13.7, 18.8 and 30.1 cm/h at the three moisture contents respectively. With a decrease in moisture content from 1.5 to 1.0, which is a physiologically realistic possibility, heat pulse velocities would overestimate actual sap flow by 40% if the sap flux calculation was not adjusted to the lower moisture content value.

same transpiration rate existed at both of these moisture contents, HPV would increase from 14 to 20 cm h^{-1} with no real change in sap flux. However it should be noted that the use of sap flux will produce the same results as would be obtained with HPV unless Mgw is determined concurrently with HPV.

CHAPTER III

IDEALIZED HEAT PULSE VELOCITY PRACTICE

Introduction

There is an evident need for a rapid, simple method for measuring tree transpiration. In forest hydrology or forest micro-meteorology one encounters numerous studies of the relationship between actual transpiration, potential transpiration and plant water stress in differing vegetative canopies (e.g. Idso, Reginato and Farah 1982; Bringfelt 1982). In forest physiology, transpiration is frequently one of the primary independent variables correlated with other physiological processes such as photosynthesis and respiration (e.g. Troeng and Linder 1982).

In view of such wide use for transpiration measurements, the relative simplicity and speed of obtaining heat pulse data, and the fact that the Marshall (1958) method is based on accepted heat transport theory, one would expect the heat pulse technique to be widely accepted and used. It is not. There are several accounts in the literature of new or improved instrumentation to implement Marshall's theory. There are a few reports on correlations of HPV's with environmental or physiological parameters affecting transpiration, a very few reports of attempts to correlate HPV measurements with actual transpiration, and even fewer of attempts to calculate transpiration directly from HPV's, sapwood moisture content, density and area.

My purpose in this chapter is to review the uses of Marshall's (1958) theoretical analysis by; 1) an examination of the ways in which the several analysis techniques have been implemented, 2) an examination of the type of problem that has been approached using HPV, and 3) my opinion as to whether or not each user's application violated any of the criteria given in Chapter II (p. 27). Lastly, I will summarize what I believe to be the sources of the difficulties that users have encountered in practical application of the heat pulse velocity method.

Both Marshall's (1958) analysis with line-heater point-sensor internal to a stem and Closs' (1958) analysis with plane-heater point-sensors external to a stem, have been used interchangeably or inappropriately in several of the reports reviewed. Closs' method is applicable only with small stems (probably less than 1 cm diameter); Marshall's with those much larger. All of Marshall's criteria (p. 27), except the one relating to probe implantation depth, are applicable to Closs' method as well. Where both have been cited in a report, or the application is not clearly one or the other, I will comment on the applicability of both. However, my focus in this study remains on the application of Marshall's method to large trees.

<u>Representative applications of Marshall's method</u>

<u>HPVM</u>

Wendt, Runkles and Hass (1967) report the only published use of the HPVM technique (Eq. 4, p. 19) that I could find. They obtained correlations between transpiration as indicated by weight loss of potted mesquite seedlings (Prosopis glandulosa var glandulosa Torr.) and HPVM. They do not state whether the sensor was implanted or external to the stem. They cite both Marshall (1958) and Closs (1958) but it is not clear whether either technique was actually used. They obtained regression equations with correlation coefficients ranging from 0.81 in 1.6 to 1.7 cm diameter stems, to 0.97 in 0.2 to 0.6 cm diameter stems. They do not mention encountering any difficulties in applying the technique, except that the analyses of the time-temperature curves were very time consuming.

Wendt and others (1967) appear confused about the theory as they indicate that the single sensor HPVM analysis (Eq. 4, p. 19) gives a "conduction velocity" that must be corrected (they do not state the nature of the correction) but that the two sensor HPVT analysis (Closs 1958) gives true sap velocity. Neither of these interpretations is correct as both give HPV as defined by Equation 2 (p. 18). Wendt and others (1967) results are little more than an empirical calibration of measured transpiration against some unknown type of "heat pulse velocity" determinations.

I suspect that my success in using the HPVM technique is more typical of the results that others may have experienced. I used a single 18 guage (0.13 cm diameter) stainless steel hypodermic needle thermistor temperature sensor 1.25 cm downstream from a similiar size line source heater (0,1.25; approximately the experimental configuration described by Marshall

1958). A heat pulse was created by connecting a 6-volt battery to the heater for 1 to 5 seconds. Relative temperature rise was read at 60, 120 and 180 s from a meter indicating the out-of-balance voltage across a bridge circuit in which the thermistor was the active arm. The results in using this apparatus, with sensors inserted 1 to 2 cm into the sapwood of 30 to 60 cm diameter ponderosa pine trees (Pinus ponderosa Laws), were an inordinate number of imaginary HPV's: in over 30% of the determinations, the term under the radical in Equation 4 (p. 19) was negative. My instrumentation was not an obvious violation of any of the criteria (p. 27). I therefore attributed the imaginary readings to instrumentation difficulties arising from the crude transistor amplifier circuitry then available (1959-60). I also found that the analysis of time-temperature data by Equation 4 (p. 19) was very time consuming. Marshall (1962) apparently anticipated this data reduction problem and published a set of nomograms to facilitate it.

HPVP

Cohen, Fuchs and Green (1981) used Equation 7 (p. 22) and a single 0.3 cm diameter sensor, implanted 1.5 cm (0,1.5 cm) downstream from the heater, that had six thermistors or thermocouples mounted at 1.0 cm intervals along it, in order to simultaneously sample the heat wave at several depths in a stem. They indicated that the main advantage of their technique was the capability of integration of sap flux by simultaneous measurement of HPVP at several depths in sapwood (this could be done with any of the analysis methods). They provided analyses of errors associated with determinations of D^1, tp and spacing of the sensor from the heater and concluded that a distance of 1.5 cm from heater to sensor was optimal. The diameter of their sensor is 20% of spacing, violating criterion 2 (p. 27). The nonconvecting material associated with a 0.3 cm diameter sensor would also violate criterion 3 (p. 28).

Stone and Shirazi (1975) used Equation 7 (p. 22) in an altered form to define "apparent heat pulse velocity" (Av) as Av = r/tp (where r and tp have the same meaning as in Eq. 7). They showed mathematically that Av is always in phase with HPVP if Pb and Mgw remain constant, i.e., they assumed constant sap flux coefficients. Since both their sensor and heater were placed on the surface of the stems of 1.25 cm diameter cotton plants, and the heater extended only halfway around the stem, their application was of neither the Marshall (1958) nor Closs (1958) method. Their assumption of constant Mgw is open to question. Variation in moisture content would violate criterion 4 (p. 28), even though they do not explicitly utilize the sap flux equation (Eq. 10, p. 23) in their calculations.

<u>HPV?</u>

Miller, Vavrina and Christensen (1980) reported an attempt to utilise Marshall's (1958) theory in ring porous oak trees. Although they used the same term "HPV" as in Equation 2 (p. 18), they defined it as X/t, where X is the distance between heater and temperature sensor, and t is the time from heat pulse start to first onset of heat at the sensor, i.e., a definition more akin to Huber (1932) than Marshall (1958). Because of this difference in definition and determination of HPV, the value they calculated was much more indicative of peak sap speed than it was of the heat pulse velocity defined by Equation 2. Values of HPV defined by Equation 2 have generally underestimated sap speeds by a factor of about 20 (Heine 1973). The "HPV's", as defined by Miller and others (1980), overestimated average sap speed in oak. (I informed these authors of this misuse of the definition of "HPV" prior to publication. For some reason, they still persisted in using it.)

Miller and others (1980) use of the instrumentation of Swanson (1974a), which was designed to measure HPV as defined by Equation 2, did not legitimize their misapplication of both technique and theory in ring porous oak. They could have determined tp with the same apparatus and calculated HPVP (Eq. 7, p. 22). This would have made their use of Marshall's (1958) theory correct even though the theoretical assumption of homogeneity, criterion 3 (p. 28), was probably not met.

HPVT

The asymmetrical two-sensor configuration of Figure 4 and Equation 8 (p. 22), (Closs 1958, Swanson 1962) is much simpler to use than Equation 4 (p. 19). I published details of instrumentation to measure HPVT's in 1962, with improved stability in 1963 and with updated electronics and commercially available temperature sensor probes in 1974 (Swanson 1962, 1974a; Skau and Swanson 1963). Accounts of other types or sizes of sensors, different spacings, differing electronic

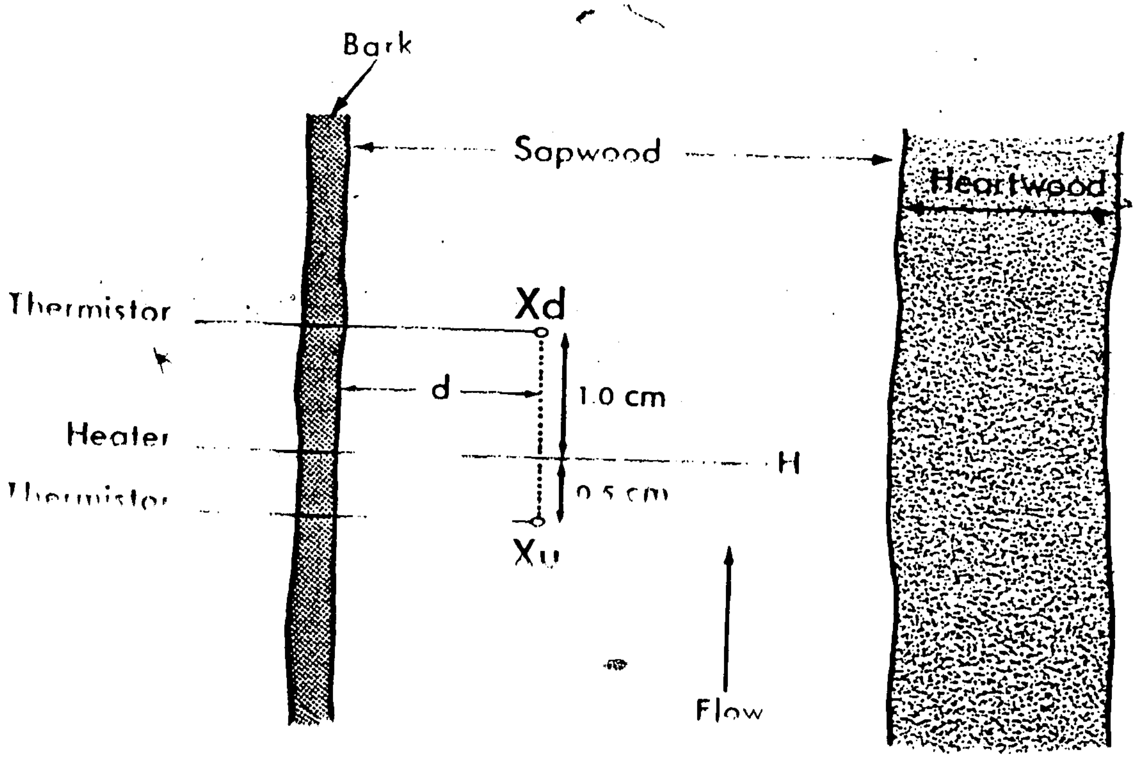

Figure 4. Diagrammatic sketch of the assymetrical, two sensor, HPVT sampling scheme. The configuration shown here is (-0.5,0, 1.0 cm). I install the heater 5 to 7 cm into the stem regardless of the depth, d, at the active tip of the sensors. The heater is heated uniformly all along its entire length.

indicating or recording instruments, but all still using the same general configuration of Figure 4 and Equation 8 were published by Gifford and Frodsham (1971); Hinckley (1971a) and Morikawa (1972)

Most implementations of the HPVT analysis technique violate criteria 2 and 3 (p. 27,28), in as much as the reported diameter of practically-sized sensors, (0.13 cm, Swanson 1962; 0.15 cm, Hinckley 1971a; 0.16 cm, Swanson 1974a), is much greater than 10% of the 0.3 to 0.5 cm separation used between the heater and the lower sensor, and the 0.04 to 0.05 cm width of nonconvecting material for negligible thermal equilibrium time.

Applications of idealized theory to specific problems

All of the remaining citations employed some form of instrumentation to exploit HPVT (Eq. 8, p. 22). The first six are published applications; the last two of unpublished studies that I started just prior to this thesis study.

Detection of moisture stress

Merkle and Davis (1967) used an external heater with sensors held gently against the stem (0.05 to 0.3 cm diameter) of a bean plant (Phaseolus vulgaris L. var. Black valentine) to measure HPV as an indirect indicator of moisture stress. This is similiar to the Closs (1958) technique but their references are only to Marshall (1958) and Swanson (1962). They concluded that, with their combination of sensors and analysis, HPV measurements were a sensitive indicator of the relative degree of moisture stress between plants, provided those compared had reasonably comparable leaf areas. Both heat loss, (criterion 1) and stem moisture content change (criterion 4, p. 28) may have influenced their results. They probably should have compared sap flux, rather than HPV, from stems with equal cross-sectional area (although plants with equal leaf area might well have similiar cross sections).

Effects of defoliation

Lopushinsky and Klock (1980) used heat pulse velocities to monitor the effects of defoliation on transpiration in Grand fir (Abies grandis (Dougl.) Lindl.) trees (31 to 48 cm dbh). They permanently implanted HPVT sensors (0.13 cm diameter, 1.0 cm deep, spaced -0.5,0,0.75 cm) during mid-June 1976 and read them through the rest of 1976 and 1977. They observed a rapid decline in HPVT's in severely defoliated trees and a much smaller decline in partially defoliated ones. My experience with sensors implanted over a long period of time such as this, is that the magnitude of the HPVT measurements may decline regardless of changes in transpiration rate, because a tree reacts physically and chemically to isolate the injured tissue (Merrill and Shigo 1979). The rate at which this isolation occurs is unpredictable. Their application violates criteria 2, 3 and 4 (p. 27,28). Therefore one must interpret the differences between partial and complete defoliation that Lopushinsky and Klock (1980) report with care.

Correlation between environmental parameters and transpiration

Heat pulse velocities, determined from idealized analytical theory, have generally correlated well with of those environmental parameters directly affecting transpiration such as vapour pressure deficit, solar radiation and air temperature. The method has been used in this application on conifers (Gale and Poljakoff-Mayber 1964; Swanson 1967b; Hinckley and Scott 1971; Shaw and Gifford 1975; Lassoie, Scott and Fritchen 1977; Lassoie and Salo 1981) and on diffuse porous hardwoods (Doley 1967; Gifford 1968; Lassoie and Scott 1972; Swanson, Benecke and Havranek 1979). Good correlations were found with respect to specific instrumentation and physiological conditions. But the coefficients relating HPVT to any specific environmental parameter were not generally transferable from one tree to another, nor useful in the same tree through extended time. This lack of general and prolonged applicability indicates violations of criteria 2 and 3 (and possibly criterion 4, p. 28).

Balek and Pavlik (1972) reported a unique application of the HPVT configuration and equation (Eq. 8, p. 22) to continuously monitor heat pulse velocities (wrongly called "sap stream velocities"). They permanently implanted sensors (size and exact spacing not given), in the configuration of Figure 4. A pulse of electric current was used to measure HPVT in the normal way for a range of environmental conditions. Then a steady electric current, approximately 0.01 of that for the pulse, provided a temperature difference (at the same sensors used for HPVT's) which, after correlation with the measured HPVT's, was recorded as a continuous estimate of HPVT. Their records extended over 52 d with the same sensors, with probable violations of criteria 3 and 4 (p. 28).

Simple correlations with sap flow or transpiration

Simultaneous measures of HPVT and transpiration as indicated by humidity increase in a plastic tent or cuvette enclosing all or a portion of a plant are reported by Decker and Skau (1964), Gale and Poljakoff-Mayber (1964), and Swanson, Benecke, and Havranek (1979). Gale and Poljakoff-Mayber (1964) found good correlations between hourly HPVT (0.13 cm diameter heater, diameter of sensors not given, spaced -0.5,0,1.0 cm) and transpiration in 0.6 to 1.2 cm diameter seedlings of aleppo pine and sour orange at soil water potentials higher that -0.4 MPa, but essentially no correlation between hourly values at -1.5 MPa. They also found that the coefficients of calibration equations did not remain constant as soil water potential decreased, nor did they return to the same values upon rewatering. This work probably violates all four criteria (p. 27).

Decker and Skau (1964) (0.13 cm diameter probes, spaced -0.5,0,1.0 cm) and Swanson and others (1979) (0.16 cm diameter probes, spaced -0.5,0,1.0 cm) found close relationship between hourly values of HPVT and transpiration in Pinus halapensis Mill., several Juniperus spp. and Nothofagus solandri var clif-fortioides Hook. F. Poole. Their application violated criteria 2 and 3 (p. 27,28) but probably ~~not~~ criterion 4 as these experiments did not include the effect of changing soil water availibility.

Simultaneous measures of HPVT and weight loss were reported by Hinckley (1971b) and Swanson (1972). Hinckley found close correlation between hourly HPVT's (0.15 cm diameter probes, spaced -0.5,0,1.0 cm) and hourly transpiration in Douglas fir (Pseudotsuga menzeisii (Mirb.) Franco) over a three day period while water was withheld. I found good correspondence between hourly HPVT (0.24 cm diameter probes, spaced -0.5,0,1.0 cm) and hourly transpiration in P. halapensis only when well-watered (xylem potential -1.1 MPa). HPVT and hourly transpiration rate were virtually unrelated at low xylem potentials (-2.7 MPa). Part of the disagreement between the hourly values may have been due to change in sapwood water content and the use of HPVT rather than sap flux as the independent variable. However my data does indicate good correlation between HPVT and transpiration averaged over 24 h as xylem potential decreased from -1.1 to -2.7 MPa and upon return to -1.1 MPa after rewatering. Both applications violated criteria 2, 3 and 4 (p. 27,28).

Direct calculations of transpiration

Doley and Greive (1966) report one of the most comprehensive efforts to compare actual water uptake (transpiration) with sap flow values calculated from HPVT, Pb, Mgw and sapwood area. Their application was in field grown Jarrah (Eucalyptus marginata Sm.) a diffuse porous hardwood. The HPV probes were placed on the surface of the sapwood (sensors spaced -0.5,0,1.0 cm). Water uptake, as measured by severing a stem and placing it in water, was used to calibrate the heat pulse calculations. Calculated sap flows values were approximately half those measured but the relationship between the two was linear at all rates of flow.

Doley and Grieve's (1966) apparatus does not correspond to the measurement configurations analysed by either Closs (1958) or Marshall (1958) so that none of the criteria for application fully apply. None-the-less, their results are excellent. In my opinion, their interpretation of measured HPV (with their apparatus) as being one-half of true, needs theoretical confirmation, because the empirical calibration was based on detection of sap movement in the outer 0.5 cm of sapwood where the HPV's may not be the same as those encountered at deeper depths (Swanson 1967b). Until this heat flow configuration is theoretically described, their technique is merely an empirical extension of Huber and Schmidt's (1937) "compensations method" with deference to Marshall's (1958) definition of HPV.

Swanson (1974a) re-examined the data of Swanson (1972) to compare daily sap flows calculated from HPVT, Pb, Mgw and sapwood area, with those measured by lysimetry. In this instance, sapflow calculated from HPVT averaged 46% of that measured. The lack of 1:1 correspondence was attributed to wound in the plane of the sensors (violation of criterion 3, p. 28).

Lastly, Cohen, Fuchs and Green (1981) reported a comparison of volumetric flow through excised wood cylinders and sap flow calculated from HPVP, Pb, Mgw and cross sectional area. Calculated sap flows averaged 55% of actual. These authors also attributed the lack of 1:1 correspondence to nonconvective wood in the plane of the probes (violation of conditon 3, p. 28).

Loss of sensor sensitivity with extended implantation time

When heat pulse probes are permanently implanted in trees to be read over an extended period of time, the magnitude of HPVT's measured may become progressively lower regardless of transpiration rate. From the last week of April 1975, through the last week of September 1975 and in the last week of May 1976, I installed one set of probes, (0.16 cm diameter; spaced -0.5,0,1.0 cm) to 1.25 cm xylem depth at breast height (1.35 m) in each of five lodgepole pine (*Pinus contorta* Dougl.) trees of mean dbh 21 cm, mean height 20 m. The five probe sets installed each month were placed at the same height on the stem and separated about 3 to 4 cm laterally from the previous month's installation. HPVT's were obtained from the current (control) and all previous probe installations on the day of, or the day following, installation. The HPVT's for each installation date were averaged and each past HPVT expressed as a fraction of current HPVT.

By the end of May 1975, just thirty days after installation, April HPVT's averaged 0.75 of current, and by May 1976, 0.6 of current (Fig. 5). Similiar values exist for each month's probe sets, except those installed in August, 1975, which still registered 85% of current after being installed over 300 d. The behavior of the August installations illustrate that one cannot predict how a tree will react to HPV probe implants through extended time. Apparently a tree's wound response is related to the phenological period during which it is wounded.

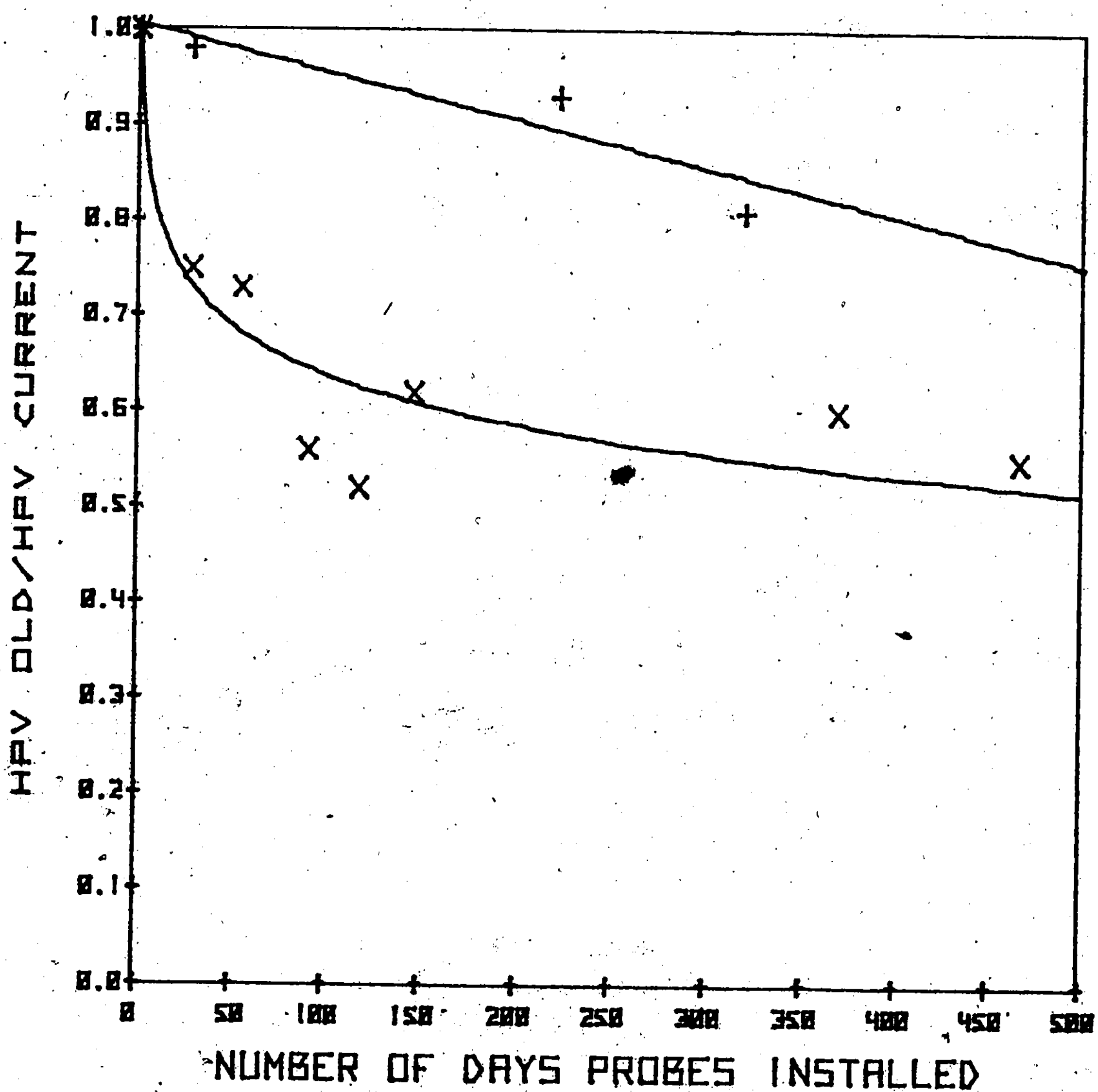

Figure 5. Decline in sensitivity with length of time that sensors have been installed: "x" denotes sensors installed in April 1975; "+" sensors installed in August 1975.

Shigo (personal communication) indicated that there are two periods, one at leaf emergence and the other broadly in "August" (in the northern hemisphere) when a tree may not react to a wound to isolate it.

According to Shigo and Hillis (1973), the normal first reaction of a tree to wounding, such as that necessary to implant HPV sensors, is to plug the vascular elements. This is followed by a change in color as the wood oxidizes and extractives accumulate in tissue above and below the wound site. The vertical extent of wound tissue formed in reaction to a single hole in the sapwood may be a column of discolored wood extending 15 cm or more above and below the point of wounding (Shigo 1976, Shortle 1979a, 1979b). These observations indicate that sap flow is interrupted for a considerable distance in the plane of heat pulse probes, both up and downstream. Since heat is not carried forward by sap movement within this plane, this slab of nonconvective tissue, which is greater than 0.16 cm in tangential width in my installations, is a violation of criterion 3 (p. 27).

The ~~late~~ Bir Mullick indicated that similiar oxidation and resin responses occur in xylem radially adjacent to wounds in the phloem (personal communication). If this is generally true, then those placing HPV sensors-heater on the surface rather than implanting them in the xylem (e.g. Doley and Greive 1966) may encounter a similiar loss in sensitivity, both upon initial installation and through extended time.

Incompatibility of data from differing sensor configurations

Several authors (Swanson 1962,1967; Gifford 1968; Morikawa 1972; Lassoie, Scott and Fritschen 1977) have shown that the use of sensors placed close to the heater increases instrument sensitivity, reduces sampling time and allows better resolution of slow HPVT's. The time spent in sampling is certainly less, but the magnitude of the HPVT's measured with one sensor configuration may not be the same as those measured using a different configuration. In each of the trees used for the sensitivity-through-time study above, I also installed a set of identical sensors physically near the control (-0.5,0,1.0 cm) installations but spaced (-0.5,0,0.75 cm). HPVT was determined for this set and that of the control on the day of installation or the day following. Assuming that both sets of a pair sample the same sap flow, then the HPVT data derived from each pair should be equal. This was not the case (Fig. 6). Data from the close spaced sets averaged 80% of the wider spaced controls. The average HPVT's for 25 readings were close spaced, 10.7 cm hr^{-1}, controls 13.6 cm hr^{-1}, and the difference, 2.9 cm hr^{-1} is statistically significant (Student's "t" = 7.93, $P < 0.01$). These data indicate the applicability of criterion 2 (p. 27).

Sources of problems in applications

The reports indicate that the difficulties users of the HPV method have encountered arise from four sources.

1) The definition of heat pulse velocity as the weighted average of the sap and nonmoving wood substance moving together, has often been disregarded.

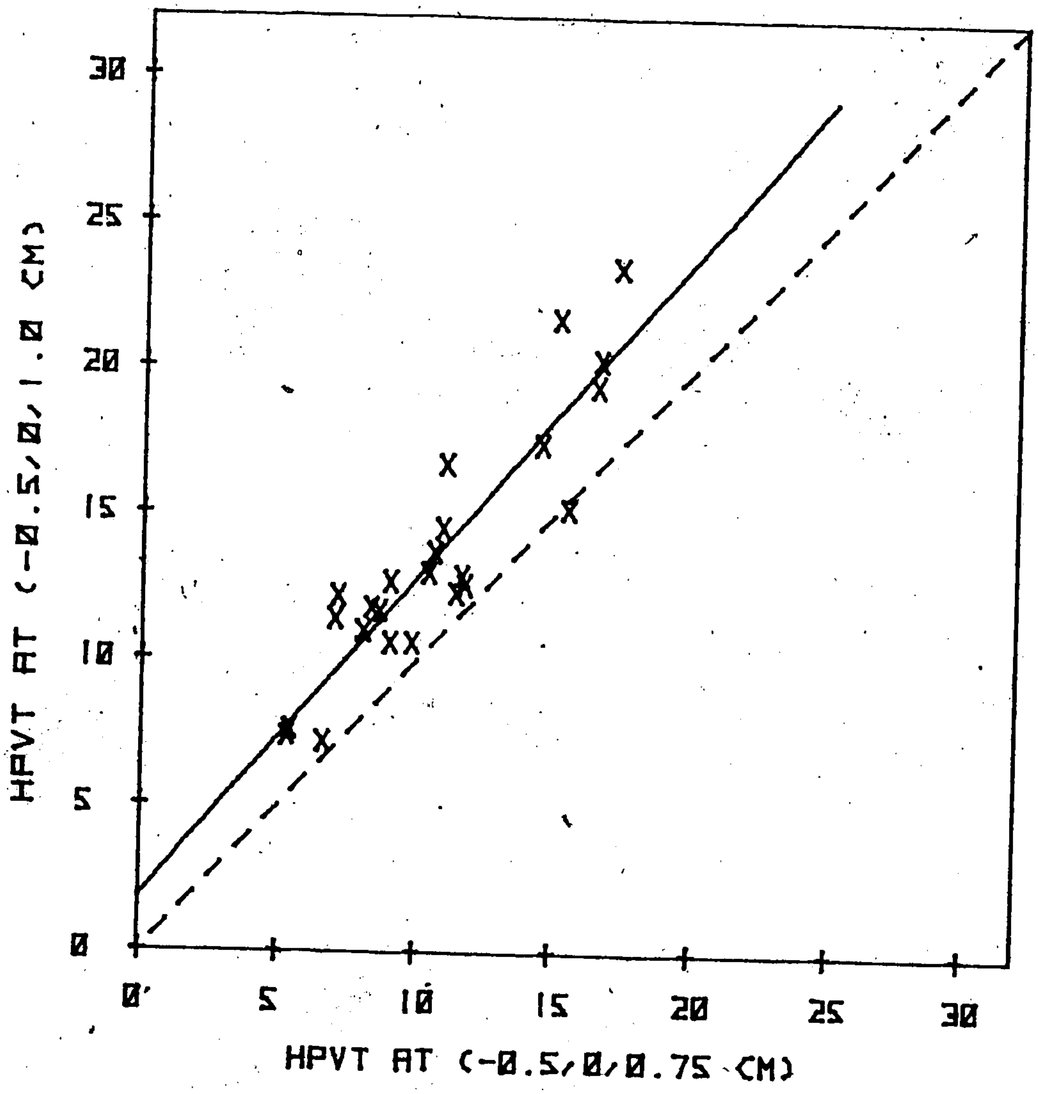

Figure 6. Least squares fitting of relationship between HPVT data obtained from sensors spaced -0.5,0,0.75 cm and those from sensors spaced -0.5,0,1.0 cm. The dashed line is 1:1.

2) The heat transport geometry for which solutions exist has not been applicable to the problem.

3) Vapour loss at the leaves may not be in phase with sap flow in the plane of the heat pulse probes at all levels of plant water stress.

4) All of the criteria stated for application of the idealized theory have not been met.

One, two and three above are "researcher" problems. They cannot be solved by providing better methods or more advanced theory. Their solution is simply to apply techniques as intended and to interpret measurements in light of what they actually represent. Only item 4 is a valid method problem.

All of the criteria that were assumed in deriving the analytical solution (Eq. 3, p. 19) to the heat transport equation (Eq. 1, p. 18) must be met in practice if the results are to provide accurate estimates of sap flux. This means that:

1) The sensing apparatus must be implanted sufficiently deep so that the heat losses to the outside are indeed negligible and will remain reasonably constant throughout the measurement interval. Using Marshall's (1958) criterion, there must be 1 to 2 cm of wood surrounding the sensor tip. The implanted HPV method is not applicable to most seedlings or herbaceous annual plant stems because their stems are generally too small to satisify this criterion.

2) The sensors must be infinitesimally small compared to the distance between them and the heater, so that

their material and physical presence does not distort the temperature field about them. It is probably impossible to meet this criterion with practically-sized heat pulse velocity probes.

3) The measurement section must not contain bands of nonconvecting sapwood greater than about 0.04 to 0.05 cm wide. This too is probably an impossible criterion to meet with practically-sized probes, because wounding will occur during initial implantation, resulting in a band of nonconvecting material at least as wide as the largest diameter probe. This band may or may not become wider as the tree responds to isolate the wound from the remaining sap conducting xylem. The effect of increasing wound width can be avoided by frequent renewal of sensor installations in new locations. The effect of initial wound cannot be avoided; it will be present in all heat pulse determinations in which implanted probes are used.

Nonconvecting bands of latewood may also be a source of error in some tree species. In conifers, only the earlywood conducts sap (Whitehead and Jarvis 1981). Longititudinal permeability measurements in the sapwood of New Zealand grown Douglas fir, indicates that nonpermeable latewood bands up to 0.6 cm wide, may be present (Booker and Swanson 1979). Cown and Parker (1979) show latewood widths 0.09 to 0.16 cm in Douglas fir of the Oregon to British Columbia region of North America. All of these widths are greater than the 0.04 to 0.05 cm criterion suggested as the maximum allowable for thermal homogeneity (p. 28). This may be a significant source of error in HPV measurements in Douglas fir, and other species with high proportions of latewood in their growth rings.

4) Sap flux, which is a function of heat pulse velocity, current sapwood moisture content and density, rather than HPV alone, must be used to correlate with, or to calculate transpiration. Sapwood moisture content is a dynamic variable that cannot be assumed constant, except perhaps over a period of 24 h at high plant or soil water potential.

I assumed that the practical problems, particularily 2 and 3 above, were the source of the persistent underestimation of HPV's and sap flow reported. I contacted D. C. Marshall, New Zealand Department of Scientific and Industrial Research, Auckland, to obtain some guidance as to how these problems might be overcome. He and Dr. D. W. A. Whitfield, Department of Botany, University of Alberta, Edmonton, suggested that I undertake a numerical analysis of Equation 1 (p. 18) to explore the effect of interrupted flow near the sensors as well as the effects of sensor material and configuration (Personal communication, D. C. Marshall, January 1977). These numerical analyses and their results are given in Chapter IV.

CHAPTER IV

NUMERICAL ANALYSIS OF HEAT PULSE VELOCITY THEORY

Introduction

The physical problem of 3-dimensional heat flow from a line heater in the thermally nonhomogeneous stem of a tree with implanted sensors is apparently difficult from an analytical standpoint. Pickard and Puccia (1972) and Pickard (1973) resolved a much simpler physical system consisting only of outer insulation, sapwood and heartwood, with constant thermal properties and uniform sap speed from bark to heartwood. Pickard and Puccia did not consider implanted sensors (although obviously one would need sensors of some sort to measure temperature) nor the effect that sensors might have on either heat or sap flow. They concluded that their analyses would only be applicable in ring porous stems with sapwoods less than 2 mm thick and in diffuse porous stems less than 5 cm diameter, composed entirely of sapwood, and that neither their heat step nor heat pulse methods were capable of yielding precise quantitative measures of sap flux. Their conclusion should not be surprising as few of the partial differential equations of physical interest have been solved analytically (von Rosenberg 1969, Saul'yev 1964).

The more realistic heat and sap flow system described in Chapter 2 (p. 16), can be approximated in a finite difference model by a succession of numerical values for the dependent variable (temperature) and the corresponding independent variables (wood, sensor and heater thermal properties, stem cross section, sap speed, sap flow geometry, etc.). These temperature values can provide a link between the numerical solution and its analytical solution (Harbaugh and Bonham-Carter (1970).

The finite difference method

In the finite difference method, the physical geometry of the system to be approximated is overlayed by a grid or network composed of a finite number of parallel lines (normally evenly spaced) in the x, y, and z planes. The intersections of these lines form nodes. An equation approximating the partial differential equation and thermal properties in the desired directions is written for each node. Equation 1 (p. 18), defines the temperature everywhere in a homogeneous solid: Equation 19, the finite difference approximation to each term of the parabolic partial differential equation (Eq. 1), defines the temperature at each node in terms of the temperature of its neighboring nodes, and the thermal properties of the materials between it and them (Saul'yev 1964; Carnahan, Luther and Wilkes 1969; von Rosenberg 1969).

$$\partial^2T/\partial x^2 = (K^l/PC)(T^{n+1}_{i-1,j,k} - 2T^{n+1}_{i,j,k} + T^{n+1}_{i+1,j,k})/(\Delta x)^2 \quad (19a)$$

$$\partial^2T/\partial y^2 = (K^t/PC)(T^{n+1}_{i,j-1,k} - 2T^{n+1}_{i,j,k} + T^{n+1}_{i,j+1,k})/(\Delta y)^2 \quad (19b)$$

$$\partial^2T/\partial z^2 = (K^r/PC)(T^{n+1}_{i,j,k-1} - 2T^{n+1}_{i,j,k} + T^{n+1}_{i,j,k+1})/(\Delta z)^2 \quad (19c)$$

$$\partial T/\partial x = (auPsCs/PC)(T^{n+1}_{i+1,j,k} - T^{n+1}_{i-1,j,k})/(2\Delta x) \quad (19d)$$

$$\partial T/\partial t = (T^{n+1}_{i,j,k} - T^{n}_{i,j,k})/(\Delta t) \quad (19e)$$

With each equation an error of aproximation, due to truncation of the infinite series approximation of the partial differential equation, that is a function of (Δt) and (Δx), must be considered. However, if the method used to solve the system is stable, then the error of approximation tends toward zero, Saul'yev (1964).

The formulation of Equation 19, where the values on the right hand side are all evaluated at the n+1 time step, is implicit in that the set of equations for the entire net must be solved simultaneously. The preferred method for parabolic partial differential equations (von Rosenberg 1969) is to solve the equations, using intermediate time steps (that have no physical meaning), by the alternating direction implicit (ADI) method. In the ADI method for two dimensions, the equations along one axis are written implicitly for a time step ½ of that desired, i.e., at n + ½, and the equations along the other axis are written explicitly using known temperatures at the previous time step, n. The intermediate solution to the implicit equations at n + ½ can be obtained by a back substitution technique (Carnahan, Luther and Wilkes 1969). The temperatures at n + ½ then become the known values. The implicit and explicit equations are interchanged between the two axes, and the temperatures at the desired time interval, n + 1, are calculated in the same manner. This process is repeated until the simulation arrives at times t = 60, 120, 180 s etc., as required to evaluate the appropriate analytical equation. A similiar technique is used for applying the ADI method in three dimensions.

Numerical models of 3-dimensional system.

My initial effort in numerical simulation was to approximate a tangential longitudinal slice in the sapwood of a 3-dimensional stem section, i.e., the same model that Marshall (1958) solved analytically. The results obtained with this model resolved many of the problems associated with sap flow interruption in the plane of the sensors (Swanson and Whitfield 1981). However my experience with applying the heat pulse technique in stems of various sapwood proportions indicated a need to consider heat exchange at the bark/sapwood and sapwood/heartwood borders as well. Ideally a 3-dimensional model should be used for this. But because the results using the 2-dimensional tangential longitudinal model were so successful and because of the extremely large computer memory requirement to accomodate even a modest 3-dimensional finite difference model (4 to 6 megabytes for the final and intermediate solution matrices alone), I chose to approximate this 3-dimensional heat flow system with two 2-dimensional finite difference numerical models: One a tangential longitudinal section perpendicular to the heater at approximately the centre of the sapwood (Fig. 7a); the other a radial longitudinal section in line with the heater and sensors encompassing bark, vascular cambium, sapwood and heartwood (Fig. 7b). The initial condition for both models is isothermal (T = 0). The border conditions are unique for each application of the models and comprise the specific cases to be examined below.

The main purposes of the tangential longitudinal model were to examine the effects of flow interruption by, and in

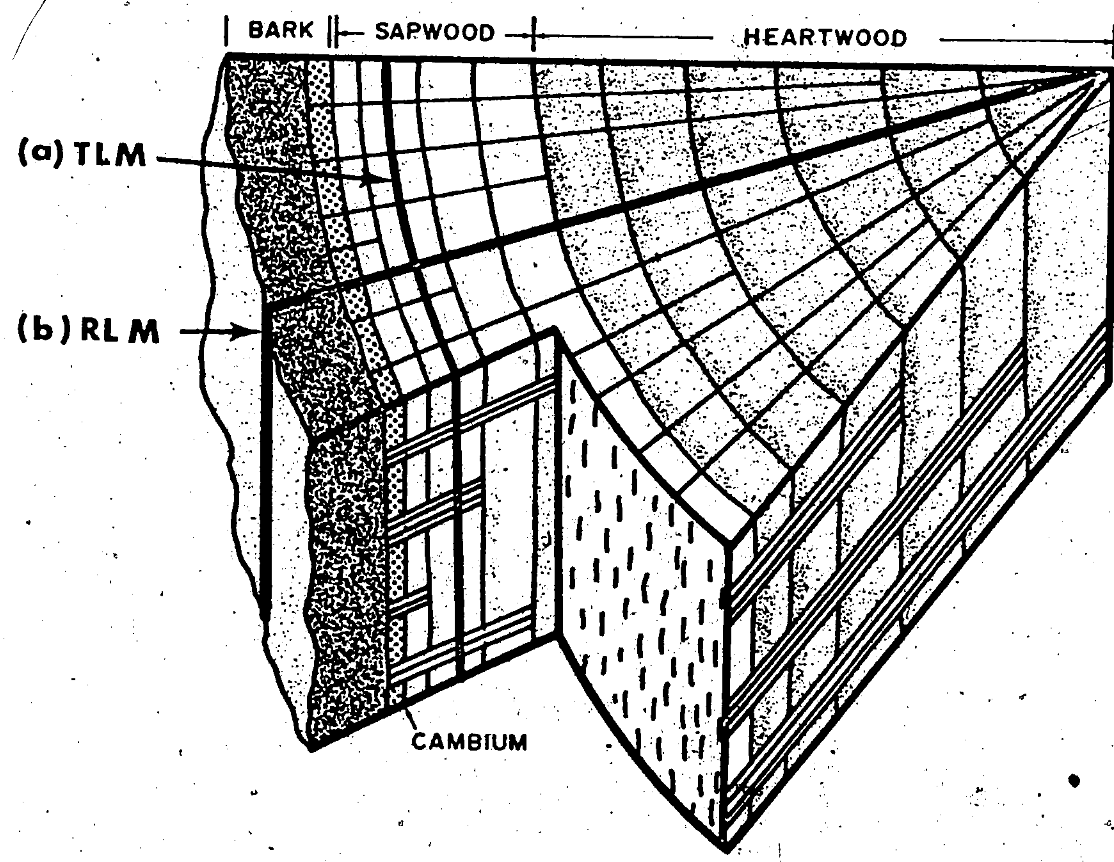

Figure 7. Stem cross sections simulated with numerical models. (a) Tangential-longitudinal. (b) Radial-longitudinal.

the near vicinity of, the sensors and of sensor configuration on the temperature field. The main purposes of the radial longitudinal model were to examine the effects of heat loss to the outside via the sensors, heat loss to the outside from the bark surface, the effect of abrupt cessation of xylem sap flow at the bark/sapwood, sapwood/heartwood or early/latewood interfaces and the differing thermal properties of bark, sapwood, heartwood, sensors and heater as these influence the temperature of sensors in the vicinity where these materials abut. A 0.04 cm node spacing (see discussion below for choice of this spacing) is a physical restriction common to both models that limits their usefulness to evaluating the effects of discontinuities of width 0.04 cm or larger. The normally uniserate rays of conifers and rays of diffuse porous woods at 0.001 to 0.002 cm wide (Esau 1977) are too small to be incorporated into the tangential longitudinal model. Both models apply to coniferous wood. They should also be applicable to porous woods where the nonconvecting material between vessels is sufficiently thin for a negligible "te" (criteria from Eq. 18 p. 29) or each vessel and each nonconvecting cross section, such as a multiserate ray, is wide and internally homogeneous enough to be approximated by one or more nodes.

Several features are common to both models. Initial and border conditions are set, the heat is "pulsed" at time t=0. Numerical approximations of the temperature at every node in the field are marched through time. At the times necessary, normally 60, 120 and 180 seconds, to solve the applicable analytical solution, the temperature values that exist at the sensor node(s) are recorded. The HPV or diffusivity value obtained from the analytical equation is compared with that imposed on the numerical solution to arrive at relationships between the numerical and analytical solutions that reflect the physical conditions imposed on the model. I have chosen to retain various forms of the analytical (Eq. 3, p. 19) solution of Marshall (1958) to Equation 1, as a base for expressing the numerical results, because they are as convenient as any and they allow myself and others to modify previously existing HPV's without recourse to the original raw temperature and/or time data used to obtain them.

The dimensions of the approximating grid network were chosen by trial. Every finite difference approximation is a compromise between physical reality and computing costs (Saul'yev 1964). To be relevant to this physical problem, the nodes were required to fall on sensor-wood material boundaries. The sensors and heater that I have used are 0.16 cm diameter, forcing node spacing to be a submultiple of 0.16 cm (the coarsest that could be used was 0.16 x 0.16 cm). As the distance between nodes is reduced ($\Delta x \rightarrow 0$) the numerical solution converges to the true solution. I settled on a mesh spacing of 0.04 cm by calculating the HPV's from the temperature field derived with mesh spacings of 0.16, 0.08, 0.04 and 0.02 cm. The values found at a spacing of 0.04 differed by less than 5% from those obtained at 0.02 cm. The 0.04 cm grid is a reasonable compromise between the greatly increased computing time at 0.02 cm and the difficulty of adequately describing the physical dimensions of sensors and heater in a 0.08 cm grid. The thermal properties at nodes where two or more materials met, were averaged in the appropriate spatial direction according to the method described by Saul'yev (1964).

Overall grid dimensions were set by increasing the size in each direction until the change ceased to affect the solutions obtained from sensors 1.6 cm above and below a heater, placed at the centre of the grid. The longitudinal dimension of both models was thus fixed at 8.0 cm. Tangential width was similiar-ily set at 1.6 cm each side of the sensor-heater plane. In the radial longitudinal model, radial depth is varied in accordance with the specific stem section boundaries for the case examined.

Time steps (Δt) were also chosen by trial. Theoretically the ADI solution technique is stable for any time and space step (Richtmyer and Morton 1967). A solution technique is considered stable if errors do not grow larger with each successive time step (Saul'yev 1964). Numerical solutions of some parabolic equations with a large first derivative coefficient (i.e., the "auPC" term in Eq. 19d) have been found to be unstable (von Rosenberg 1969). Also discontinuous coefficients, such as those at wood-sensor border nodes, and the sudden imposition of large temperature differences, such as at the heater node, may also introduce numerical instabilities (Carslaw and Jaeger 1959). Stability of the solution during imposition of the heat pulse was achieved by shaping the pulse with appropriate time steps as in Figure 8. Stability in cases when sensor material properties were vastly different from wood (an example would be the aluminum sensor material of Cohen, Fuchs and Green 1981) was achieved by setting ½ time steps of 0.1, 0.2, 0.5 and 1.0 s at solution times t = 0, 10, 30 and 60 s respectively. Stability was assumed to exist when temperatures varied smoothly between time and space intervals.

Wood and bark thermal properties were set as functions of basic density, Pb, and dry weight moisture fraction, Mgw. An average Pb of 0.4 g cm^{-3}, sapwood Mgw of 0.5, 1.0 and 1.5, heartwood Mgw of 0.4 and bark Mgw of 0.0 were used for most simulations. Thermal conductivities were calculated as functions of moisture content and basic density; tangential and radial from Equation 14 (p. 24); longitudinal from Equation 12 (p. 24). Bark was considered to be isotropic with conductivity 80% of dry wood tangential conductivity (Martin 1963). Sensors were composites of glass, brass or aluminum plus electrical insulating materals and lead wires. Their thermal properties were calculated as cross sectional area weighted averages of the materials involved. These thermal properties are tabulated in Appendix E.

Tangential longitudinal model (TLM)

This model is of a slice of sapwood in the tangential longitudinal plane perpendicular to a radius (Fig. 7a). Sap flow is in the positive "x" direction and is considered to be uniform at all points on a radius. An infinitely long heater lies on a radius through the centre of this slice. Infinitely long

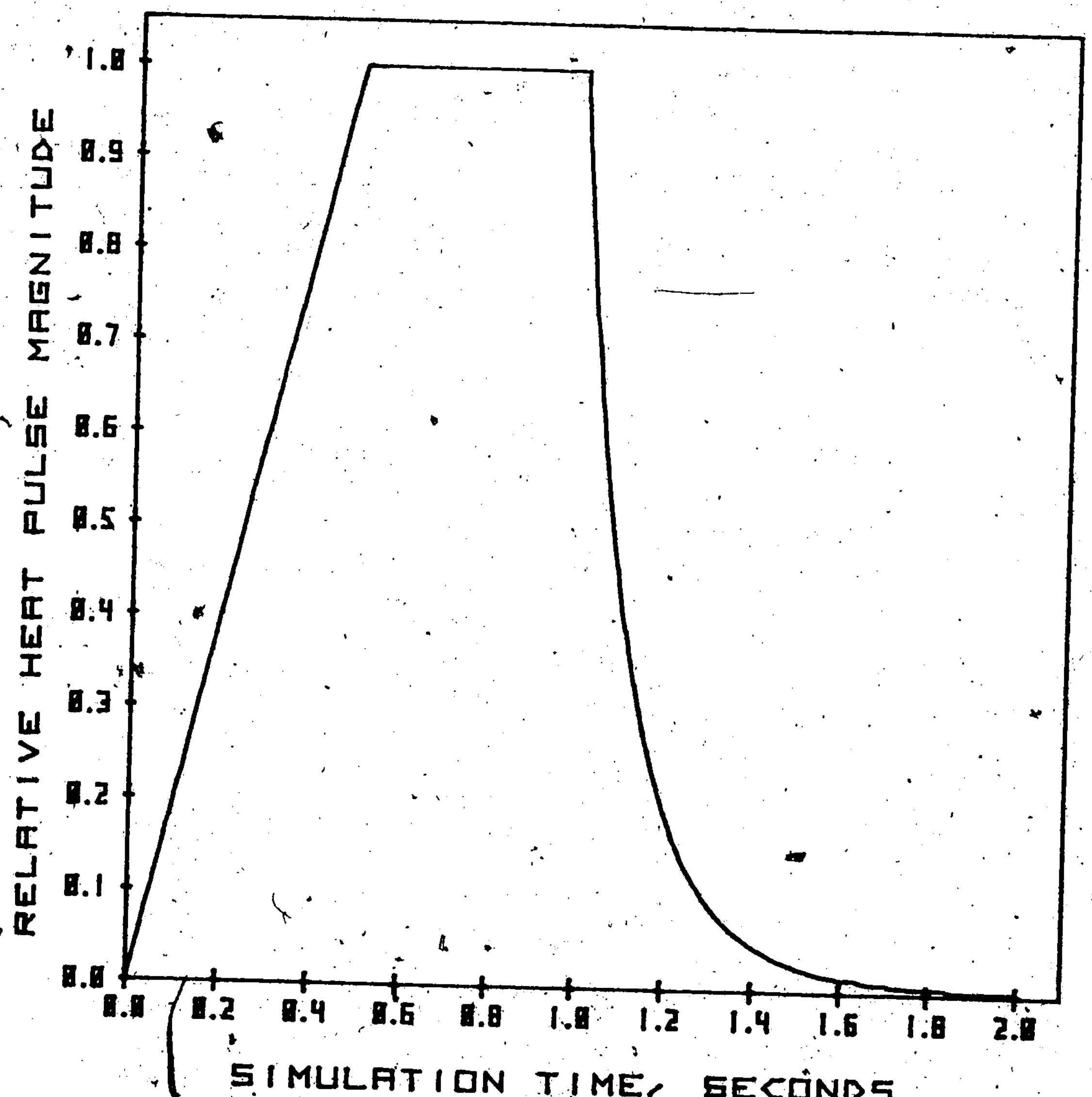

Figure 8. Heat pulse function, $Q(0,\delta,t)$, used in tangential-longitudinal simulations and $Q(0,y,t)$ used in radial-longitudinal numerical simulations. $Q = 2tQ_o$ from $t = 0$ to $t = 0.5$ s. $Q = Q_o$ from $t = 0.5$ s to $t = 1.0$ s. At all t greater than 1.0 s, $Q_c = Q_o/t^{10}$.

sensors, appropriately positioned to provide temperature rise data for solutions of Equation, 4 - 9, lie in the y = 0 plane. (Only downstream from the heater for one sensor simulations; both upstream and downstream from the heater for two sensor simulations.) Sap flow is stopped throughout the width (W) of a slab of wounded tissue enclosing the sensors and extending from the top to bottom of the slice. Except within W, sap flow is uniform at all nodes along the tangential axis, although any flow distribution that could be accomodated by the 0.04 cm node spacing could be imposed on the model. Temperature is held constant at T=0 at the borders of this model. It was programmed as a symmetrical half-plane with the axis of symmetry through the center of the heater-sensor plane.

Equation 1 is discretized in the x (longitudinal), y (tangential) directions twice as follows.

Implicit tangential, explicit longitudinal.

$$(1/2\Delta t)\Big[(PC)_{i+\frac{1}{2},j-\frac{1}{2}} + (PC)_{i+\frac{1}{2},j+\frac{1}{2}} + (PC)_{i-\frac{1}{2},j-\frac{1}{2}} + (PC)_{i-\frac{1}{2},j+\frac{1}{2}}\Big](T^{n+\frac{1}{2}}_{i,j} - T^{n}_{i,j})$$

$$= \Big[K^{l}_{i+\frac{1}{2},j}T^{n}_{i+1,j} - (K^{l}_{i+\frac{1}{2},j} + K^{l}_{i-\frac{1}{2},j})T^{n}_{i,j} + T^{n}_{i-1,j}\Big]/(\Delta x)^2$$

$$+ \Big[K^{t}_{i,j+\frac{1}{2}}T^{n+\frac{1}{2}}_{i,j+1} - (K^{t}_{i,j+\frac{1}{2}} + K^{t}_{i,j-\frac{1}{2}})T^{n+\frac{1}{2}}_{i,j} + K^{t}_{i,j-\frac{1}{2}}T^{n+\frac{1}{2}}_{i,j-1}\Big]/(\Delta y)^2$$

$$- au_{i,j}PsCs(T^{n}_{i+1,j} - T^{n}_{i-1,j})/(2\Delta x) + Q^{n}_{i,j} \qquad (20a)$$

Implicit longitudinal, explicit tangential.

$$(1/2\Delta t)\left[(PC)_{i+\frac{1}{2},j-\frac{1}{2}} + (PC)_{i+\frac{1}{2},j+\frac{1}{2}} + (PC)_{i-\frac{1}{2},j-\frac{1}{2}} + (PC)_{i-\frac{1}{2},j+\frac{1}{2}}\right](T^{n+1}_{i,j} - T^{n+\frac{1}{2}}_{i,j})$$

$$= \left[K^{l}_{i+\frac{1}{2},j}T^{n+1}_{i+1,j} - (K^{l}_{i+\frac{1}{2},j} + K^{l}_{i-\frac{1}{2},j})T^{n+1}_{i,j} + T^{n+1}_{i-1,j}\right]/(\Delta x)^2$$

$$+ \left[K^{t}_{i,j+\frac{1}{2}}T^{n+\frac{1}{2}}_{i,j+1} - (K^{t}_{i,j+\frac{1}{2}} + K^{t}_{i,j-\frac{1}{2}})T^{n+\frac{1}{2}}_{i,j} + K^{t}_{i,j-\frac{1}{2}}T^{n+\frac{1}{2}}_{i,j-1}\right]/(\Delta y)^2$$

$$- au_{i,j}PsCs(T^{n+1}_{i+1,j} - T^{n+1}_{i-1,j})/(2\Delta x) + Q^{n+\frac{1}{2}}_{i,j} \qquad (20b)$$

Radial longitudinal model (RLM)

This model represents a vertical slice of a stem along the radius of the sensors and heater (Fig. 7b). It is usually bounded on the outside by the bark/air interface and the inner boundary lies within the xylem. Sap flow is in the positive x direction, zero in bark, heartwood (and latewood if present), is not necessarily uniform at all radial positions in the sapwood and occurs through the sensors and heater materials if they are present. This is a purely hypothetical model because, in effect, the heater and sensors are represented as infinitely wide planes in the various tissues. The heat pulse velocity or diffusivity values derived from this model must be combined with those from one or more TLM simulations to portray a practical situation. Different analytical solutions apply to this plane heat source geometry than the line heat source Equations, 4 - 9 (Carslaw and Jaeger 1959). Plane heat source equations, comparable to each line heat source equation, are denoted 4a – 9a, and given in Appendix A. Temperature is held constant at both the upper and lower longitudinal borders.

The border conditions at nodes representing the interface of bark, sensor and heater nodes with the outside world were set in accordance with the following line of reasoning. In actual practice, the heater, sensors, bark, sapwood and heartwood are all assumed to be at the same initial temperature. Both sensors and heater extend through the bark a few millimeters into insulating material, such as fibreglass or styrofoam. The heater is heated along its entire length including that outside the bark. The condition, $\partial T/\partial z = 0$, was imposed at heater nodes on the outside border so that heat loss occurs only to the stem layers that the heater encounters. The sensors receive heat only through contact with the wood, bark and moving sap. The condition $T = 0$ was imposed on all sensor and bark nodes along the outside border. I generally avoided having to set inside boundary values by programming it as a symmetrical halfplane with the border of symmetry centered somewhere inside the stem.

An 8.0 by 4.0 cm grid with 0.04 cm node spacing was the maximum size that could be accomodated on the University of Alberta's Floating Point System Array processor. Most simulations using the radial longitudinal model were done with these maximum dimensions.

Equation 1 (p. 18) was discretized in the x,z directions in the same manner and with the same thermal and other physical properties as the tangential longitudinal model but with "z" and K^r replacing "y" and K^t in Equation 20. Heat was "pulsed" in the manner of Figure 8 uniformly along the entire radial depth.

Numerical solutions of general cases

The models were used to simulate a number of general cases, not related to specific instrumentation, in order to verify the numerical procedures and to separately quantify the effects of various violations of the idealized criteria (p. 27). Since neither the tangential longitudinal nor radial longitudinal simulations fully describe the true three dimensional situation, results obtained from both models must be interpreted in light of experimental results from actual heat pulse velocity measurements. These interpretations are given in Chapter V.

In the cases simulated, if sensor and heater materials are not specified, then the word "sensor" or "heater" refers only to a node in the finite grid where temperature is recorded or heat created. The thermal properties of these nodes were the same as the surrounding stem tissues.

If a sensor or heater materials are specified, then all of the nodes located within 0.08 cm of the position specified (which is at the center of the probe) for the heater or sensor location, were assigned the thermal properties of the given material. The usual material for a sensor was glass, for a heater, brass.

General cases simulated

1) Theoretical verification of the numerical analyses technique using both radial longitudinal and tangential longitudinal models of sapwood, to approximate the results if all of the idealized conditions (p. 27) were met.

2) Tangential longitudinal simulation of various wound widths in the plane of sensors installed in sapwood, to ascertain the effect of nonconvective wood on the solutions. These results relate to criterion 3 (p. 28).

3) Tangential longitudinal simulation of 0.20 cm wound and sensors positioned at several locations up and downstream from the heater, to ascertain the effect of sensor locations in nonconvective wood in the plane of the sensors. These results relate to criteria 2 and 3 (p. 27,28).

4) Tangential and radial longitudinal simulation of glass or brass sensors, brass heater, in sapwood, to ascertain the influence of sensor materials alone, i.e., without the effect on nonconvective wood in the plane of the sensors, or the effect of heat loss to the outside, bark or heartwood. These results relate to criterion 2 (p. 27).

5) Tangential longitudinal simulation of wound, glass sensor material and differing sensor spacings from a brass heater, to ascertain the effect of combined

sensor material placement and nonconvective wood in the plane of the sensors. These results relate to criteria 2 and 3 (p. 27,28).

6) Radial longitudinal simulation of the influence of tissue borders on the temperature field using various combinations of bark, sapwood and heartwood tissues to ascertain the effects of abrupt changes in thermal properties and sap movement that occur upon the transition from one tissue to another. These results relate to criterion 1 (p. 27).

7) Radial longitudinal simulation of the effects of alternating layers of earlywood with sapflow, latewood without. These results relate to criteria 1 and 3 (p. 27,28).

<u>General case results</u>

<u>Case 1, theoretical verification, no wound, no sensor material, TLM and RLM.</u>

The results of this case are summarized in Table 1 for the tangential longitudinal model, Table 2 for the radial longitudinal model.

When the data from the temperature field derived from the tangential longitudinal model were analysed using Equations, 4 -9, or the radial longitudinal model using Equations, 4a - 9a, the resulting HPVA or HPVS values were within 2% of those imposed (HPVI) from HPVI = 0 to 40 cm h^{-1}. HPVM's were within 1% and HPVP's within 5% for all HPVI's greater than 10 cm h^{-1}. HPVT's are not valid at HPVI = 0, and in any case, numerical

Table 1. Theoretical results—tangential longitudinal model, all sapwood. No sensor-heater materials or wound. Solutions for D, HPVM from numerically generated temperature data at 60, 120 and 180 seconds at the downstream points indicated. Solutions for HPVA, HPVT and HPVS are from temperature data at up and downstream points indicated at 60, 120 seconds, tz and 120 seconds respectively. Solutions for HPVP are from tp at the downstream point. Values for HPVM and HPVP marked 'im' are imaginary, i.e., the square root of a negative number. Values marked '--' mean that the tp or tz not reached during 180 second simulation time.

	Temperature measured at sensors spaced (-X=upstream, 0=heater, X=downstream, cm)															
	(-0.48,0,0.96)		(-0.96,0,1.44)			(-0.96,0,0.96)				(-1.20,0,1.20)				(-1.44,0,1.44)		
HPVI (1)	HPVA (2)	HPVT (3)	HPVA (4)	HPVT (5)	D^1 (6)	HPVM (7)	HPVS (8)	HPVP (9)	D^1 (10)	HPVM (11)	HPVS (12)	HPVP (13)	D^1 (14)	HPVM (15)	HPVS (16)	HPVP (17)
Imposed constants: Mgw = 0.5, Pb = 0.4, K^1 = 0.000795, K^t = 0.000490, D^1 = 0.0024, D^t = 0.0015																
0.0	0.1	--	0.0	--	.0024	2.3	0.0	im	.0024	2.6	0.0	1.0	.0024	2.7	0.0	--
5.0	5.0	5.0	5.0	5.0	.0024	5.5	4.9	im	.0024	5.6	4.9	4.9	.0024	5.7	4.9	--
10.0	9.9	9.8	9.9	9.8	.0024	10.2	9.9	8.9	.0024	10.3	9.9	9.6	.0024	10.3	9.9	--
20.0	19.7	19.6	19.8	19.6	.0024	20.0	19.7	18.4	.0024	20.0	19.7	19.0	.0024	20.1	19.7	19.4
40.0	39.2	38.6	39.4	39.3	.0023	39.7	39.3	38.1	.0023	39.8	39.3	38.8	.0024	39.8	39.4	38.3
Imposed constants: Mgw = 1.0, Pb = 0.4, K^1 = 0.000956, K^t = 0.000727, D^1 = 0.0018, D^t = 0.0014																
0.0	0.0	--	0.0	--	.0018	2.0	0.0	im	.0018	2.0	0.0	--	.0018	1.0	0.0	--
5.0	5.0	5.0	5.0	5.0	.0018	5.4	4.9	4.6	.0018	5.4	4.9	--	.0018	5.1	5.0	--
10.0	9.9	9.8	9.9	9.8	.0018	10.1	9.9	9.7	.0018	10.1	9.9	9.7	.0018	10.0	9.9	--
20.0	19.7	19.6	19.8	19.6	.0018	20.0	19.7	19.4	.0018	20.0	19.7	19.4	.0018	20.0	19.8	19.7
40.0	39.1	39.3	39.4	40.8	.0018	39.7	39.2	38.6	.0018	39.7	39.3	38.2	.0018	39.8	39.5	39.1
Imposed constants: Mgw = 1.5, Pb = 0.4, K^1 = 0.001117, K^t = 0.000965, D^1 = 0.0015, D^t = 0.0013																
0.0	0.0	--	0.0	--	.0015	1.7	0.0	im	.0015	1.2	0.0	--	.0015	im	0.0	--
5.0	5.0	5.0	5.0	5.0	.0015	5.3	4.9	4.0	.0015	5.1	5.0	--	.0015	4.6	5.0	--
10.0	9.9	9.8	10.0	9.8	.0015	10.1	9.9	9.6	.0015	10.0	9.9	--	.0015	9.8	10.0	--
20.0	19.7	19.6	19.9	19.6	.0015	19.9	19.7	18.8	.0015	19.9	19.8	19.4	.0015	19.9	19.9	--
40.0	39.1	39.3	39.6	41.5	.0015	39.6	39.2	38.1	.0015	39.7	39.4	39.1	.0015	39.8	39.6	39.9

Units are: Mgw (moisture fraction, d.w.b.), Pb ($g\ cm^{-3}$), K ($cal\ cm^{-1}\ s^{-1}\ {}^oC^{-1}$), D ($cm^2\ s^{-1}$), HPV ($cm\ h^{-1}$).

Table 2. Theoretical results radial longitudinal model, all sapwood. No sensor-heater materials or wound. Solutions for D, HPVM from numerically generated temperature data at 60, 120 and 180 seconds at the downstream points indicated. Solutions for HPVA, HPVT and HPVS are from temperature data at up and downstream points indicated at 60, 120 seconds, tz and 120 seconds respectively. Solutions for HPVP are from tp at the downstream point. Values for HPVM and HPVP marked 'im' are imaginary, i.e., the square root of a negative number. Values marked '--' mean that the tp or tz not reached during 180 second simulation time.

	Temperature measured at sensors spaced (-x=upstream, 0=heater, x=downstream, cm)															
	(-0.48,0,0.96)		(-0.96,0,1.44)			(-0.96,0,0.96)				(-1.20,0,1.20)				(-1.44,0,1.44)		
HPVI	HPVA	HPVT	HPVA	HPVT	D^l	HPVM	HPVS	HPVP	D^l	HPVM	HPVS	HPVP	D^l	HPVM	HPVS	HPVP
(1)	(2)	(3)	(4)	(5)	(6)	(7)	(8)	(9)	(10)	(11)	(12)	(13)	(14)	(15)	(16)	(17)
Imposed constants: Mgw = 0.5, Pb = 0.4, K^l = 0.000795, K^r = 0.000490, D^l = 0.0024, D^r = 0.0015																
0.0	0.1	--	0.0	--	.0024	2.5	0.0	--	.0024	2.9	0.0	--	.0024	3.1	0.0	--
5.0	5.0	5.0	5.0	5.0	.0024	5.6	4.9	--	.0024	5.7	4.9	--	.0024	5.8	4.9	--
10.0	9.9	9.8	9.9	9.8	.0024	10.2	9.8	10.0	.0024	10.3	9.8	--	.0024	10.4	9.8	--
20.0	19.7	19.6	19.8	19.6	.0023	20.0	19.6	19.6	.0023	20.0	19.6	19.8	.0024	20.1	19.7	--
40.0	39.3	38.6	39.5	39.3	.0023	39.7	39.2	38.2	.0023	39.7	39.2	38.3	.0023	39.8	39.3	39.2
Imposed constants: Mgw = 1.0, Pb = 0.4, K^l = 0.000956, K^r = 0.000727, D^l = 0.0018, D^r = 0.0014																
0.0	0.1	--	0.0	--	.0018	2.4	0.0	--	.0018	2.5	0.0	--	.0018	2.2	0.0	--
5.0	5.0	5.0	5.0	5.0	.0018	5.5	4.9	--	.0018	5.6	4.9	--	.0018	5.4	4.9	--
10.0	9.9	9.8	9.8	9.8	.0018	10.2	9.8	--	.0018	10.2	9.8	--	.0018	10.2	9.9	--
20.0	19.7	19.6	19.9	19.6	.0018	20.0	19.6	19.3	.0018	20.0	19.7	19.7	.0018	20.0	19.8	--
40.0	39.3	39.3	39.6	40.8	.0018	39.6	39.2	38.4	.0018	39.7	39.3	38.5	.0018	39.8	39.4	39.3
Imposed constants: Mgw = 1.5, Pb = 0.4, K^l = 0.001117, K^r = 0.000965, D^l = 0.0015, D^r = 0.0013																
0.0	0.1	--	0.0	--	.0015	2.2	0.0	--	.0015	2.1	0.0	--	.0015	0.0	0.0	--
5.0	5.0	5.0	5.0	5.0	.0015	5.4	4.9	--	.0015	5.4	4.9	--	.0015	5.0	5.0	--
10.0	9.9	9.8	10.0	9.8	.0015	10.2	9.8	--	.0015	10.1	9.9	--	.0015	10.0	9.9	--
20.0	19.7	19.6	19.9	19.6	.0015	19.9	19.6	19.4	.0015	20.0	19.7	19.5	.0015	19.9	19.8	--
40.0	39.3	39.3	39.8	41.5	.0015	39.6	39.2	38.3	.0015	39.7	39.3	38.5	.0015	39.8	39.6	39.3

Units are: Mgw (moisture fraction, d.w.b.), Pb ($g\ cm^{-3}$), K ($cal\ cm^{-1}\ s^{-1}\ {}^oC^{-1}$), D ($cm^2\ s^{-1}$), HPV ($cm\ h^{-1}$).

solutions at HPVI's less than 3 cm h^{-1} must be extended to 300 or more seconds for analysis with the HPVT technique. I did not undertake HPVT solutions at these slower HPVI's because the information gain would not justify the computational cost. HPVT's, where obtainable, were generally the same as HPVA's or HPVS's.

The imaginary values noted for HPVP near zero are not departures from theory but a result of the coarsness of the 2 s time steps used in the simulation at solution times greater than 60 s. In Tables 1 and 2, the HPVP's labled "imaginary", result from peak time determinations only 2 s from the correct value of tp, for the imposed HPV's.

Analysis of numerically derived temperature fields at HPVI's less than 3 cm h^{-1} with Equation 4 (Marshall's analysis method, p. 19) also resulted in minor departure of calculated from imposed HPV's near HPVI = 0. The source of these departures was discovered by imposing small temperature errors, $\pm$ 0.01 ^{o}C, on the simulated values. Such errors caused the HPVM's calculated by Equation 4 at HPVI = 0, to vary from imaginary to 3.6 cm h^{-1}. This oversensitivity of Equation 4 to small temperature errors at low HPV's (which here are probably due to finite difference truncation error) occurs in practice as well and this was acknowledged by Marshall (1958). He suggested that two sensors, equally spaced, (HPVS, Eq. 6, p. 21), be used to obtain HPV's less than 10 to 15 cm h^{-1}. Apparently the two sensor configuration with unequal spacing (HPVA, Eq. 9, p. 23) is also less sensitive to such temperature errors.

Longitudinal diffusivity, D^l, as calculated using Equation 5 (p. 21) or 5a (p. 237) and data from the numerically generated temperature field, is exactly the same as that imposed for all HPVI less than or equal to 30 cm h^{-1}. At HPVI = 40 cm h^{-1} and at wood moisture content 0.5, the calculated D^l is 4% less than that imposed which probably indicates some approximation error due to the first derivative term. However, the diffusivity equation appears to be far less sensitive to small temperature errors at HPVI = 0 than is the HPVM equation (Eq. 4, p. 19), which uses the same temperature ratios.

The departure of HPVP calculated from HPVI's near zero and the long simulation durations needed to resolve HPVT's at HPVI's near zero, imposed economical restrictions on generating numerical temperature data for these solutions. All of the other solutions, HPVA, HPVM, HPVS and D^l, can be obtained at specified time intervals of 60, 120 and 180 s, and the duration of a simulation run does not have to be extended beyond 180 s to incorporate HPVI's near zero. Since all of the solutions are approximately equal, I will use the HPVA, HPVM, HPVS and D^l solutions obtained from temperatures at simulation times 60, 120 and 180 seconds, unless otherwise noted (e.g. HPVT in case 6), in presenting numerically derived results throughout the remainder of this thesis.

Case 2, wound alone, TLM

The effects of wound widths 0.04 to 0.24 cm are shown in Figure 9 and Figure 10. The magnitude of the effect on calculated HPV varies considerably between the one and two

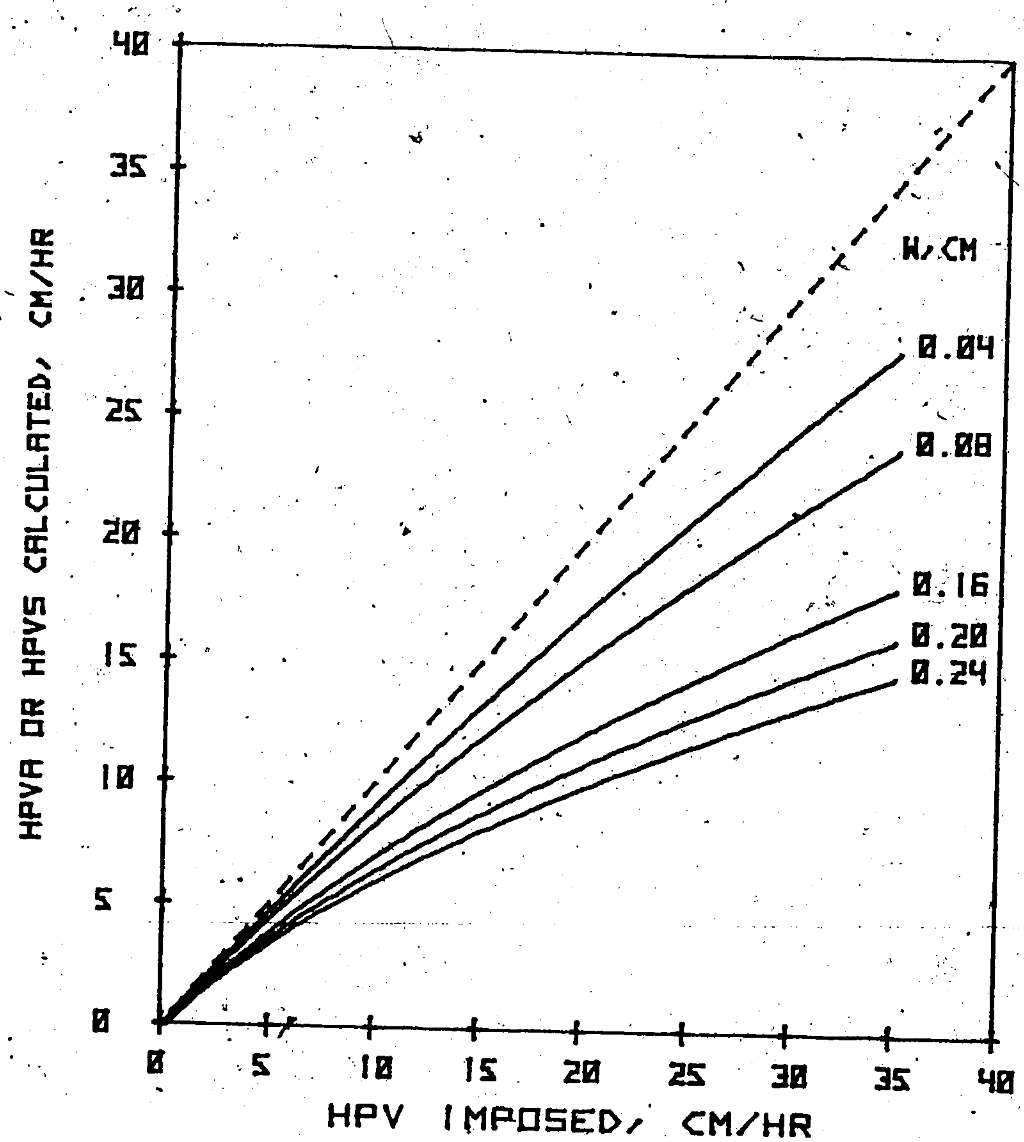

Figure 9. Influence of wound on two sensor configurations, no sensor materials, tangential longitudinal model. HPVA's or HPVS's measured at (-0.48,0,0.96 cm) or at (-0.96,0,0.96 cm). The dashed line is 1:1. These simulation results indicate that any width of nonconvective wood in the plane of the heat pulse probes is a significant violation of the idealized assumption regarding thermal homogeneity (criterion 3, p. 28).

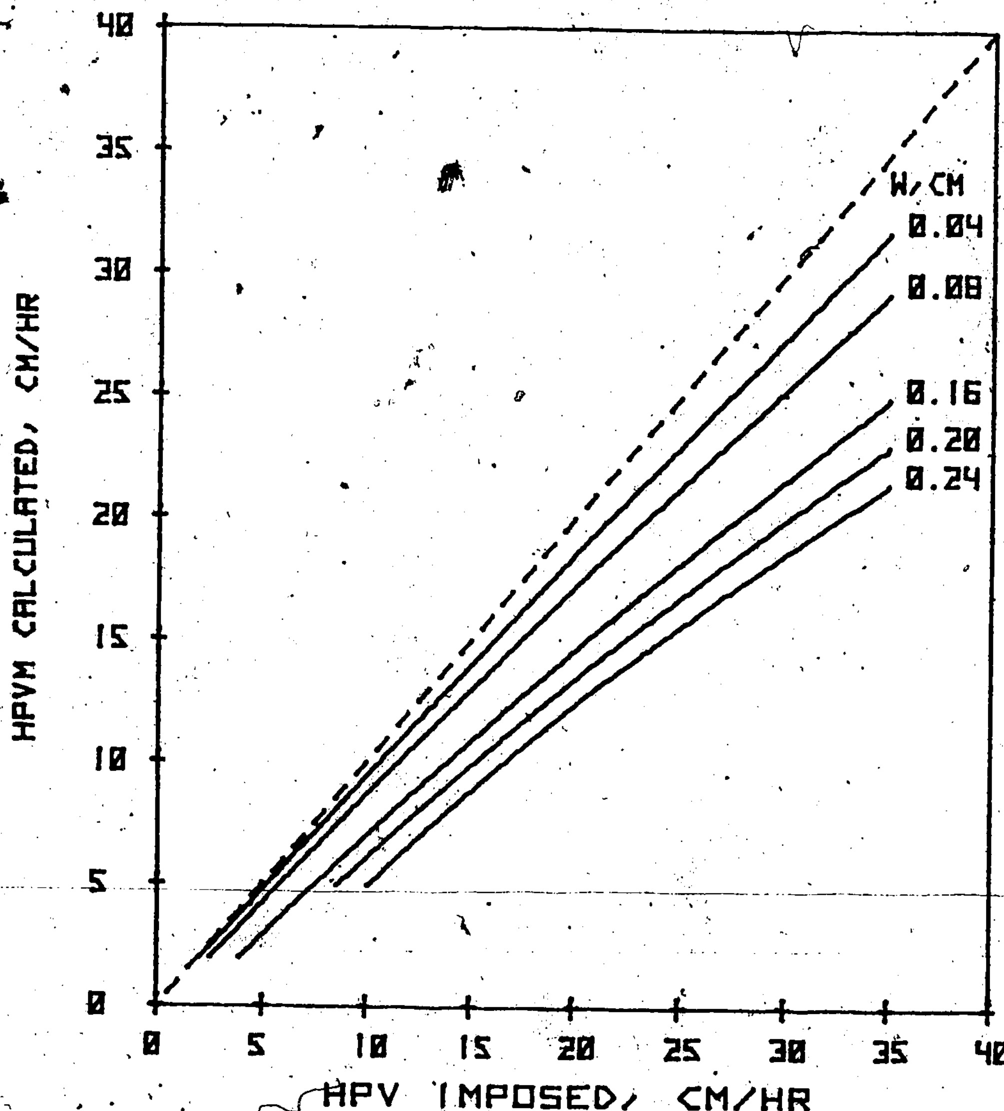

Figure 10. Influence of wound on one sensor configurations, no sensor materials, tangential longitudinal model. HPVM's measured at (0,0.96 cm) or at (0,1.44 cm). The dashed line is 1:1. The nonconvective slab associated with a practically sized sensor or heater would be greater than 0.08 cm, and would violate the idealized theoretical assumption regarding thermal homogeneity (criterion 3, p. 28).

sensor measurement configurations. HPV's determined with either of the two sensor configurations (-0.48,0,0.96 cm) or (-0.96, 0,0.96 cm), depart from the 1:1 line at W = 0.04 cm where calculated HPVA or HPVS are only 92% of HPVI at 5 cm h^{-1} and only 73% of HPVI at 40 cm h^{-1} (Fig. 9). HPVM's depart from the 1:1 line with increasing wound width too (Fig. 10), but, at W = 0.04 cm, the calculated values at either 0.96 or 1.44 cm are better than 90% of imposed even at 40 cm h^{-1}. At wound widths that would be imposed by any practical instrumentation, i.e., 0.08 cm or greater, the departures of calculated HPVM from HPVI are too great to ignore. These simulations clearly indicate that all implanted HPV instrumentation used to date has violated criterion 3 (p. 28).

The presence of nonconvecting wound tissue affects the temperature distribution through time in such a manner that analysis of the numerically generated temperature field at differing time combinations yields differing heat pulse velocities or longitudinal diffusivities (Table 3). HPVS's calculated from temperature ratios at 30 seconds are only 60 to 65% of those calculated from temperature ratios at 90 seconds. Similiar differences exist using ratios taken at 60 versus 180 seconds. The HPVA equation is not as sensitive to solution times as either HPVS, HPVM or D^1.

Longitudinal diffusivities, D^1, are affected by increasing wound width, decreasing from equal to imposed at HPVI = 0, to 80% of imposed at HPVI = 40 at all moisture contents when W = 0.16 cm or more (Table 4). Such variation raises a ques-

Table 3. Influence of changing the times at which temperatures or temperature ratios are measured on HPV solutions at wound = 0.20 cm with no sensor or heater materials, TLM. HPVA1-4 @ (-0.48,0,0.96 cm) using temperature ratios at 30/60, 60/90, 60/120 and 120/180 seconds respectively; HPVS1 @ (-0.96,0,0.96 cm) using k1; HPVS2 @ (-0.96,0,0.96 cm) using k2; HPVM1, k1 @ (0,0.96 cm) from temperatures at 30, 60 and 90 seconds; HPVM2, k2 @ (0,0.96 cm) from temperatures at 60, 120 and 180 seconds. Values for HPVM marked 'im' are imaginary, i.e., the square root of a negative number.

HPVI	HPVA1	HPVA2	HPVA3	HPVA4	HPVS1			HPVS2			HPVM1	HPVM2	k1	k2
					@30 s	@60 s	@90 s	@60 s	@120 s	@180 s				
(1)	(2)	(3)	(4)	(5)	(6)	(7)	(8)	(9)	(10)	(11)	(12)	(13)	(14)	(15)
Imposed constants: Mgw = 0.5, Pb = 0.4, K^l = 0.000795, K^t = 0.000490, D^l = 0.0024, D^t = 0.0015														
0.0	0.2	0.1	0.1	0.0	0.0	0.0	0.0	0.0	0.0	0.0	5.2	2.3	.0024	.0024
5.0	3.2	3.4	3.5	3.6	1.8	2.4	2.8	2.4	3.0	3.3	im	2.5	.0023	.0023
10.0	6.0	6.4	6.4	6.5	3.4	4.8	5.5	4.7	5.8	6.4	im	6.3	.0023	.0022
20.0	10.9	11.1	11.2	10.8	6.6	9.2	10.4	8.7	10.7	11.6	9.2	13.7	.0022	.0021
40.0	18.5	18.1	18.0	16.8	12.0	16.3	18.5	14.6	17.7	19.1	23.1	26.3	.0020	.0018
Imposed constants: Mgw = 1.0, Pb = 0.4, K^l = 0.000956, K^t = 0.000727, D^l = 0.0018, D^t = 0.0014														
0.0	0.0	0.1	0.0	0.0	0.0	0.0	0.0	0.0	0.0	0.0	3.0	2.0	.0018	.0018
5.0	3.1	3.4	3.4	3.6	1.7	2.4	2.8	2.4	3.0	3.2	im	2.1	.0017	.0017
10.0	5.8	6.2	6.3	6.4	3.3	4.7	5.4	4.6	5.7	6.2	im	6.0	.0017	.0017
20.0	10.6	10.9	11.0	10.6	6.4	8.9	10.2	8.4	10.4	11.4	8.0	13.4	.0016	.0015
40.0	18.1	17.7	17.6	16.6	11.5	15.8	17.8	14.1	17.1	18.5	22.6	25.9	.0015	.0014
Imposed constants: Mgw = 1.5, Pb = 0.4, K^l = 0.001117, K^t = 0.000965, D^l = 0.0015, D^t = 0.0013														
0.0	-0.1	0.0	0.0	0.0	0.0	0.0	0.0	0.0	0.0	0.0	im	1.7	.0015	.0015
5.0	3.0	3.3	3.4	3.5	1.7	2.4	2.8	2.3	2.9	3.2	im	1.7	.0015	.0015
10.0	5.7	6.2	6.3	6.3	3.3	4.7	5.4	4.5	5.6	6.2	im	5.9	.0015	.0014
20.0	10.5	10.8	10.9	10.6	6.2	8.8	10.2	8.2	10.3	11.3	6.9	13.3	.0014	.0013
40.0	17.9	17.5	17.5	16.6	11.4	15.5	17.5	13.9	16.8	18.1	22.4	25.7	.0013	.0012

Units are: Mgw (moisture fraction, d.w.b.), Pb ($g\ cm^{-3}$), K ($cal\ cm^{-1}\ s^{-1}\ {}^oC^{-1}$), D ($cm^2\ s^{-1}$), HPV ($cm\ h^{-1}$).

Table 4. Influence of wound from 0.00 to 0.24 cm and time at which temperatures are measured on calculated longitudinal thermal diffusivity. No sensor or heater materials, tangential longitudinal simulation at imposed heat pulse velocities ranging from 0 to 40 cm/h.

HPVI	D^l @ (0,0.96 cm) t= 30, 60 and 90 s						D^l @ (0,0.96 cm) t= 60, 120 and 180 s					
	0.00	0.04	0.08	0.16	0.20	0.24	0.00	0.04	0.08	0.16	0.20	0.24
(1)	(2)	(3)	(4)	(5)	(6)	(7)	(8)	(9)	(10)	(11)	(12)	(13)
Imposed constants: Mgw = 0.5, Pb = 0.4, K^l = 0.000795, K^t = 0.000490, D^l = 0.0024, D^t = 0.0015												
00.0	.0024	.0024	.0024	.0024	.0024	.0024	.0024	.0024	.0024	.0024	.0024	.0024
05.0	.0024	.0023	.0023	.0023	.0023	.0023	.0024	.0023	.0023	.0023	.0023	.0023
10.0	.0024	.0023	.0023	.0023	.0023	.0023	.0024	.0023	.0023	.0022	.0022	.0022
20.0	.0024	.0023	.0022	.0022	.0022	.0022	.0024	.0023	.0022	.0021	.0021	.0020
40.0	.0023	.0022	.0021	.0020	.0020	.0020	.0023	.0021	.0020	.0018	.0018	.0018
Imposed constants: Mgw = 1.0, Pb = 0.4, K^l = 0.000956, K^t = 0.000727, D^l = 0.0018, D^t = 0.0014												
00.0	.0018	.0018	.0018	.0018	.0018	.0018	.0018	.0018	.0018	.0018	.0018	.0018
05.0	.0018	.0018	.0018	.0017	.0017	.0017	.0018	.0018	.0017	.0017	.0017	.0017
10.0	.0018	.0017	.0017	.0017	.0017	.0017	.0018	.0017	.0017	.0017	.0017	.0017
20.0	.0018	.0017	.0017	.0017	.0016	.0016	.0018	.0017	.0016	.0016	.0015	.0015
40.0	.0018	.0017	.0016	.0016	.0015	.0015	.0018	.0016	.0015	.0014	.0014	.0013
Imposed constants: Mgw = 1.5, Pb = 0.4, K^l = 0.001117, K^t = 0.000965, D^l = 0.0015, D^t = 0.0013												
00.0	.0015	.0015	.0015	.0015	.0015	.0015	.0015	.0015	.0015	.0015	.0015	.0015
05.0	.0015	.0015	.0015	.0015	.0015	.0015	.0015	.0015	.0015	.0015	.0015	.0015
10.0	.0015	.0015	.0015	.0015	.0015	.0015	.0015	.0015	.0015	.0014	.0014	.0014
20.0	.0015	.0015	.0014	.0014	.0014	.0014	.0015	.0014	.0014	.0013	.0013	.0013
40.0	.0015	.0015	.0014	.0013	.0013	.0013	.0015	.0014	.0013	.0012	.0012	.0012

Units are: Mgw (moisture fraction, d.w.b.), Pb (g cm^{-3}), K (cal cm^{-1} s^{-1} $°C^{-1}$), D (cm^2 s^{-1}), HPV cm h^{-1}).

tion as to which diffusivity should be used in the diffusivity dependent equations, HPVS and HPVP. Leyton (1967) and Cohen and others (1982) used D^1 obtained when sap movement was assumed to be zero. The values for either HPVS or HPVP in the above tables have been calculated with D^1 obtained from temperatures measured at the downstream sensor and at the imposed HPV. Since the effect of wound must be accounted for in any practical application of the heat pulse velocity technique, the conditions of measurement, i.e. the times used in the solution of Equation 5 (p. 21) for D^1, and whether taken at zero or at current sap movement, must also be specified in defining any useful relationship between D^1 or HPVS and HPVI. Also, it should be noted that a temperature increase will always be registered by the downstream sensor so that it is always possible to calculate D^1 with downstream temperature data. The same can not be said for upstream temperature data. High rates of sap movement may carry the entire heat pulse downstream so that no temperature rise ever occurs at the upstream sensor (Miller and others 1980).

Since calculated HPV's and D^1's do vary with the times used in their solutions, there are numerous combinations that can be displayed. Marshall (1958) used temperature data taken at 1-minute intervals. This is as convenient a time interval as any. Unless otherwise noted, all subsequent HPVM or D^1 values in this chapter have been calculated from temperature data taken at 60 second intervals, i.e. 60, 120 and 180 s. HPVA's will be calculated from temperature ratios at 60 and

120 s; HPVS's from temperature ratios at 120 s; both HPVS and HPVP from D^1 at current HPVI with data from the downstream sensor.

Case 3, W = 0.20 cm, several sensor configurations, TLM

Difference in separation from the heater in the configurations with two unequally spaced sensors appears to be a very important consideration (Fig. 11). The simulated results are of various asymmetric sensor spacings that have been suggested by various authors, e. g: -0.3,0,0.8 cm (Gifford 1968); -0.5,0, 0[illegible] (Swanson 1962); -0.5,0,0.75 cm (Swanson 1967b); -0.5,0, 1.[illegible]m (Closs 1958, Swanson 1962, Decker and Skau 1964, Doley and Grieve 1966, Hinkley 1971a, Morikawa 1972); -0.7,0,1.0 cm (Morikawa 1972, Lassoie, Scott and Fritcshen 1977) and two spacings (-0.5,0,1.5 cm) and (-1.0,0,1.5 cm), that have not appeared in any publication. The simulated results from all configurations differ (Fig. 11), and in general, the smaller the difference in spacing from the heater of the two temperature sensors, the greater the departure of calclulated from imposed HPV. This indicates an interraction between wound and sensor spacing that is unrelated to the presence of sensor materials.

Spacing does not appear to be as critical in either the two sensor symmetrical or the one sensor configurations, as in those asymmetrical (Table 5). When sensor spacing was increased from 0.96 cm to 1.44 cm, HPVS's increased by about 12%, HPVM's by 5% and D^1's by 12%. HPVP's were included in this analysis because Cohen and others (1981) indicated that

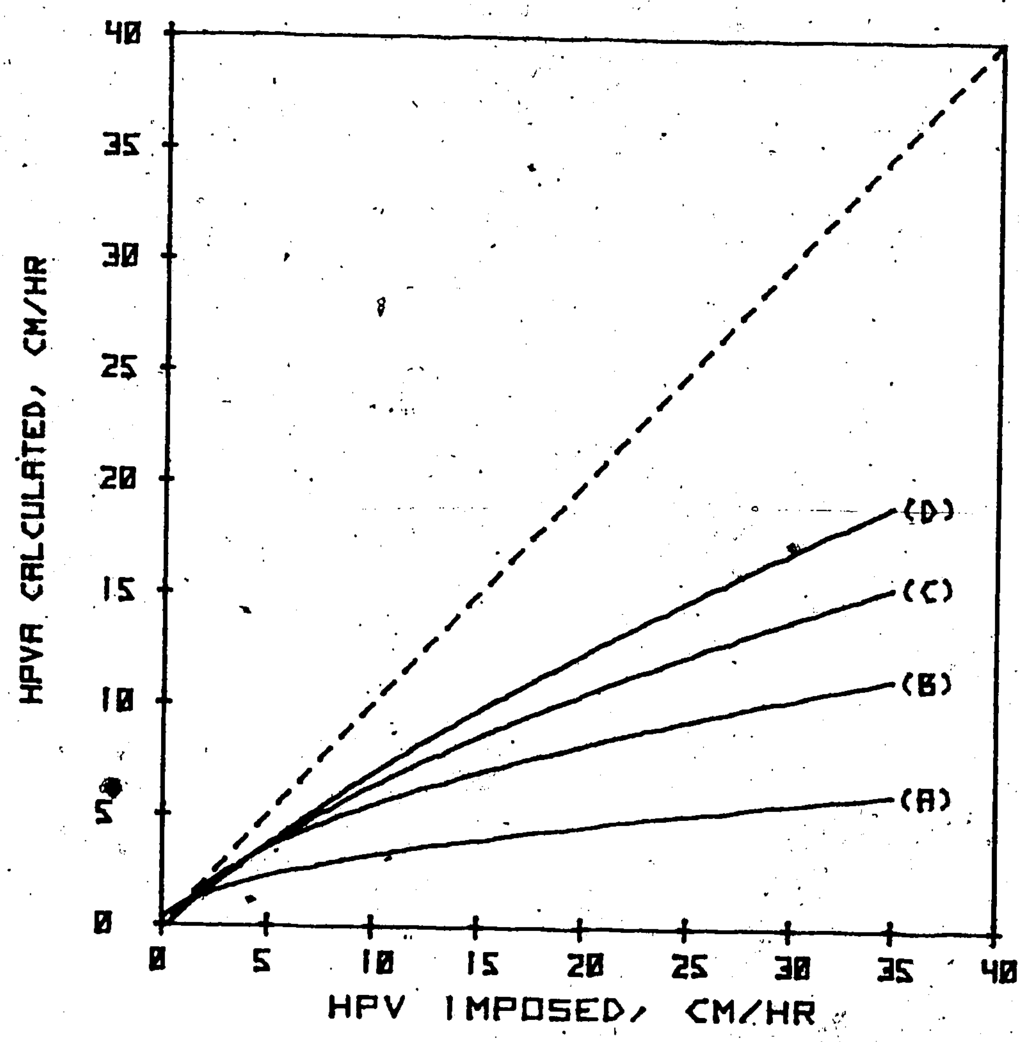

Figure 11. Influence of sensors placed at various spacings. Wound = 0.20 cm, no sensor material, tangential-longitudinal model. (A) (-0.5,0,0.6 cm), (B) (-0.5,0,0.75 cm) or (-0.7, 0,1.0 cm), (C) (-0.5,0,1.0 cm), (-0.3,0,0.8 cm) or (-1.0,0, 1.5 cm),(D) (-0.5,0, 1.5 cm). The dashed line is 1:1. These simulations indicate an interraction between wound and sensor spacing that is unrelated to sensor materials.

Table 5. Influence of sensor spacing on HPVS, HPVM, HPVP and D at wound = 0.20 cm, TLM. No sensor or heater materials. HPVS calculated using up and downstream temperatures @ t= 120 s and D at current imposed HPV; HPVM and D calculated using downstream temperatures @ 60, 120 and 180 s; HPVP calculated using current D and tp. Values for HPVM and HPVP marked 'im' are imaginary, i.e., the square root of a negative number. Values marked '--' mean that the tp or tz not reached during 180 second simulation time.

	(-0.96,0,0.96 cm)				(-1.20,0,1.20 cm)				(-1.44,0,1.44 cm)			
HPVI (1)	HPVS (2)	HPVM (3)	HPVP (4)	D^1 (5)	HPVS (6)	HPVM (7)	HPVP (8)	D^1 (9)	HPVS (10)	HPVM (11)	HPVP (12)	D^1 (13)
Imposed constants: Mgw = 0.5, Pb = 0.4, K^1 = 0.000795, K^t = 0.000490, D^1 = 0.0024, D^t = 0.0015												
0.0	0.0	2.3	im	.0024	0.0	2.6	1.0	.0024	0.0	2.7	--	.0024
5.0	3.0	2.5	im	.0023	3.0	2.0	im	.0023	3.1	0.8	--	.0023
10.0	5.8	6.3	1.6	.0022	5.9	5.9	4.6	.0022	6.0	5.3	--	.0023
20.0	10.7	13.7	12.5	.0021	11.0	13.5	12.9	.0021	11.3	13.2	--	.0022
40.0	17.7	26.3	25.3	.0018	18.9	27.0	26.0	.0019	19.8	27.4	26.2	.0020
Imposed constants: Mgw = 1.0, Pb = 0.4, K^1 = 0.000956, K^t = 0.000727, D^1 = 0.0018, D^t = 0.0014												
0.0	0.0	2.0	im	.0018	0.0	2.0	--	.0018	0.0	1.0	--	.0018
5.0	3.0	2.1	im	.0017	3.0	0.5	--	.0017	3.0	im	--	.0017
10.0	5.7	6.0	4.8	.0017	5.8	5.5	--	.0017	5.9	4.5	--	.0017
20.0	10.4	13.4	12.7	.0015	10.8	13.2	13.0	.0016	11.0	12.9	--	.0016
40.0	17.1	25.9	24.4	.0014	18.3	26.6	25.8	.0015	19.1	27.1	26.3	.0015
Imposed constants: Mgw = 1.5, Pb = 0.4, K^1 = 0.001117, K^t = 0.000965, D^1 = 0.0015, D^t = 0.0013												
0.0	0.0	1.7	im	.0015	0.0	1.2	--	.0015	0.0	im	--	.0015
5.0	2.9	1.7	im	.0015	3.0	im	--	.0015	3.0	im	--	.0015
10.0	5.6	5.9	5.4	.0014	5.7	5.2	--	.0014	5.8	3.9	--	.0015
20.0	10.3	13.3	12.5	.0013	10.6	13.1	--	.0014	10.9	12.7	--	.0014
40.0	16.8	25.7	24.9	.0012	18.0	26.5	25.7	.0013	18.8	26.9	26.3	.0013

Units are: Mgw (moisture fraction, d.w.b.), Pb ($g\ cm^{-3}$), K ($cal\ cm^{-1}\ s^{-1}\ {}^oC^{-1}$), D ($cm^2\ s^{-1}$), HPV ($cm\ h^{-1}$).

a spacing of 1.5 cm would be optimal. The data of Table 5 supports their contention. HPVP's, HPVM's and D^1's increased much more when the distance between the heater and sensor was increased from 0.96 to 1.20 cm then when increased from 1.20 to 1.44 cm. Whether or not one could realize this improvement in actual practice is debatable because the temperature signal that one has to work with is much reduced at 1.44 cm compared to that at 0.96 cm from the heater.

Case 4, effect of glass and brass sensor materials, TLM and RLM

In these simulations (Table 6, 7), sensors of the indicated materials were located both up and downstream from the heater. The presence of the upstream sensor is therefore reflected in the one sensor HPVM and D^1 results and most noticeable when it was brass.

These results clearly demonstrate that sensor materials are important violations of criterion 2 (p. 27) at least with the two sensor configurations. In the tangential longitudinal simulation results (Table 6), HPVA's were 20 to 25% less than imposed and even slightly negative at HPVI = 0. HPVS's were also 20 to 25% less than imposed but, because of symmetry, were not negative at HPVI = 0. HPVM's were erratic at imposed HPVI's less than 5 cm h^{-1}, but were better than 90% of imposed at all greater HPVI's.

In the radial longitudinal simulation results (Table 7), HPVA's and HPVS's were as in the TLM results (Table 6), except that HPVA is slightly more negative at HPVI = 0. HPVM's were

Table 6. Influence of glass or brass sensors and brass heater materials on solutions in sapwood, tangential longitudinal simulation. Values for HPVM and HPVP marked 'im' are imaginary, i.e., the square root of a negative number.

	Glass sensor material (-0.48,0,0.96 cm)			Glass sensor material (-0.96,0,0.96 cm)			Brass sensor material (-0.48,0,0.96 cm)			Brass sensor material (-0.96,0,0.96 cm)		
HPVI (1)	HPVA (2)	HPVM (3)	D^1 (4)	HPVS (5)	HPVM (6)	D^1 (7)	HPVA (8)	HPVM (9)	D^1 (10)	HPVS (11)	HPVM (12)	D^1 (13)
Imposed constants: Mgw = 0.5, Pb = 0.4, K^1 = 0.000795, K^t = 0.000490, D^1 = 0.0024, D^t = 0.0015												
0.0	-0.3	3.0	.0022	0.0	3.7	.0022	-0.3	3.4	.0022	0.0	4.1	.0021
5.0	4.1	5.2	.0022	4.2	5.7	.0022	4.0	5.4	.0022	4.1	5.9	.0021
10.0	8.3	9.4	.0022	8.4	9.7	.0022	8.1	9.4	.0021	8.2	9.7	.0021
20.0	16.2	18.3	.0022	16.5	18.4	.0022	16.0	18.1	.0021	16.1	18.2	.0021
40.0	30.8	35.7	.0020	31.3	35.6	.0020	30.3	35.2	.0020	30.5	35.1	.0020
Imposed constants: Mgw = 1.0, Pb = 0.4, K^1 = 0.000956, K^t = 0.000727, D^1 = 0.0018, D^t = 0.0014												
0.0	-0.3	im	.0018	0.0	im	.0018	-0.3	im	.0018	0.0	im	.0018
5.0	4.3	3.8	.0018	4.6	3.5	.0018	4.3	4.0	.0018	4.5	3.7	.0018
10.0	8.8	9.0	.0018	9.1	8.9	.0018	8.6	9.0	.0018	9.0	8.9	.0018
20.0	17.1	18.7	.0018	17.9	18.6	.0017	16.9	18.5	.0017	17.6	18.5	.0017
40.0	32.2	37.0	.0017	33.9	36.9	.0016	31.8	36.6	.0016	33.3	36.6	.0016
Imposed constants: Mgw = 1.5, Pb = 0.4, K^1 = 0.001117, K^t = 0.000965, D^1 = 0.0015, D^t = 0.0013												
0.0	-0.3	im	.0016	0.0	im	.0016	-0.3	im	.0016	0.0	im	.0016
5.0	4.4	2.7	.0016	4.8	1.9	.0016	3.4	3.9	.0016	4.5	2.1	.0016
10.0	9.0	8.7	.0016	9.5	8.6	.0016	8.9	8.8	.0016	9.4	8.6	.0016
20.0	17.5	18.8	.0016	18.6	18.8	.0015	17.4	18.8	.0015	18.4	18.7	.0015
40.0	32.9	37.6	.0015	35.2	37.6	.0015	32.6	37.3	.0015	34.8	37.3	.0014

Units are: Mgw (moisture fraction, d.w.b.), Pb ($g\ cm^{-3}$), K ($cal\ cm^{-1}\ s^{-1}\ {}^{o}C^{-1}$), D ($cm^2\ s^{-1}$), HPV ($cm\ h^{-1}$).

Table 7. Influence of glass or brass sensors and brass heater materials on solutions in sapwood, no wound or heat loss at radial borders, radial longitudinal simulation. Values for HPVM and HPVP marked 'im' are imaginary, i.e., the square root of a negative number.

	Glass sensor material						Brass sensor material					
	(-0.48,0,0.96)			(-0.96,0,0.96)			(-0.48,0,0.96)			(-0.96,0,0.96)		
HPVI (1)	HPVA (2)	HPVM (3)	D^l (4)	HPVS (5)	HPVM (6)	D^l (7)	HPVA (8)	HPVM (9)	D^l (10)	HPVS (11)	HPVM (12)	D^l (13)
Imposed constants: Mgw = 0.5, Pb = 0.4, K^l = 0.000795, $K^t = K^r$ = 0.000490, D^l = 0.0024, $D^t = D^r$ = 0.0015												
0.0	-1.8	im	.0022	0.0	im	.0021	-2.2	im	.0021	0.0	im	.0020
5.0	2.2	im	.0022	3.8	im	.0021	1.8	im	.0021	3.7	im	.0020
10.0	6.1	4.9	.0022	7.5	3.8	.0021	5.8	4.2	.0021	7.3	0.7	.0020
20.0	14.0	14.7	.0022	14.9	14.4	.0021	13.7	14.0	.0021	14.6	13.4	.0020
40.0	30.2	30.8	.0021	29.2	30.5	.0020	30.2	29.7	.0021	28.7	29.3	.0020
Imposed constants: Mgw = 1.0, Pb = 0.4, K^l = 0.000956, $K^t = K^r$ = 0.000727, D^l = 0.0018, $D^t = D^r$ = 0.0014												
0.0	-1.0	im	.0018	0.0	im	.0018	-1.2	im	.0018	0.0	im	.0018
5.0	3.2	2.2	.0018	4.2	im	.0018	2.9	1.7	.0018	4.2	im	.0018
10.0	7.2	8.0	.0018	8.5	7.2	.0018	7.0	7.7	.0018	8.3	6.4	.0018
20.0	15.3	17.2	.0018	16.8	16.9	.0018	15.1	16.7	.0018	16.5	16.3	.0018
40.0	32.2	34.5	.0018	33.0	34.4	.0018	32.0	33.6	.0018	32.5	33.4	.0017
Imposed constants: Mgw = 1.5, Pb = 0.4, K^l = 0.001117, $K^t = K^r$ = 0.000965, D^l = 0.0015, $D^t = D^r$ = 0.0013												
0.0	-0.6	im	.0017	0.0	im	.0017	-0.8	im	.0016	0.0	im	.0016
5.0	3.6	4.0	.0017	4.5	2.1	.0017	3.4	3.9	.0016	4.5	2.1	.0016
10.0	7.8	9.0	.0017	9.0	8.4	.0017	7.6	8.8	.0016	8.9	7.9	.0016
20.0	16.0	18.4	.0017	18.0	18.3	.0016	15.8	18.0	.0016	17.7	17.8	.0016
40.0	33.3	36.6	.0016	35.3	36.6	.0016	33.2	35.8	.0016	34.7	35.7	.0016

Units are: Mgw (moisture fraction, d.w.b.), Pb ($g\ cm^{-3}$), K ($cal\ cm^{-1}\ s^{-1}\ {}^oC^{-1}$), D ($cm^2\ s^{-1}$), HPV ($cm\ h^{-1}$).

again erratic (Table 7) at imposed HPV's less than 5 cm h^{-1} and were approximately 75% of imposed at Mgw = 0.5, 90% at Mgw = 1.5. This dependence on moisture content was much less pronounced in the TLM results (Table 6).

Calculated diffusivity values were lower at low moisture contents and higher at high moisture contents than in the "no sensor" simulations. It appears that if diffusivities are used to estimate wood moisture content, the estimates will be too high at low moisture contents and too low at high moisture contents. Therefore some correction for sensor material may be required. Both sensor materials and both models (Tables 6, 7) behaved approximately the same in this regard.

- <u>Case 5, TLM, combined effects of wound, glass sensor materials, brass heater at four sensor configurations</u>

These simulations describe practical heat pulse velocity probes implanted entirely in sapwood. The results (Tables 8, 9) should approximate those obtainable at the center of 2 cm of sapwood in coniferous or diffuse porous woods. The results integrate the combined effects of sensor materials (Criterion 2, p. 27) and nonconvective wood in the plane of the sensors (Criterion 3, p. 28).

The results with the asymmetrical configurations (Table 8) indicate that the effects of sensor materials that were noted in Case 4, are largely overshadowed by the effect of nonconvective wood. For example, with sensors configured (-0.48,0,0.96 cm), at W = 0.20 cm, no sensor, the HPVA's obtained at HPVI = 40 cm h^{-1} (see Table 3, column 4, p. 77) were

Table 8. Influence of glass sensor, brass heater material and 0.20 cm wound on HPVA, HPVM and longitudinal diffusivities with asymmetrical sensors configured (-0.48,0.0.96 cm) and (-0.96,0.0.96 cm). HPVA's calculated from temperature data at 60 and 120 s. HPVM's and longitudinal diffusivities calculated from temperature data at 60, 120 and 180 s. Values for HPVM marked "im" are imaginary, i.e., the square root of a negative number.

	(-0.48,0,0.96 cm)				(-0.96,0,1.44 cm)			
HPVI (1)	HPVA (2)	HPVM (3)	D^1 up (4)	D^1 dn (5)	HPVA (6)	HPVM (7)	D^1 up (8)	D^1 dn (9)
			Imposed Mgw = 0.5, D^1 = .0024					
0.0	-0.3	3.2	.0020	.0022	-0.1	im	.0022	.0022
5.0	2.9	3.1	.0020	.0022	3.2	im	.0022	.0022
10.0	5.6	6.1	.0021	.0021	6.1	3.4	.0023	.0022
20.0	10.1	12.9	.0021	.0020	10.9	12.1	.0024	.0021
30.0	13.7	19.2	.0020	.0019	14.7	19.5	.0024	.0020
40.0	16.7	24.9	.0018	.0018	17.8	26.2	.0024	.0020
50.0	19.4	30.0	.0017	.0017	20.7	32.3	.0024	.0019
60.0	22.0	34.6	.0016	.0016	23.2	37.9	.0024	.0019
			Imposed Mgw = 1.0, D^1 = .0018					
0.0	-0.3	im	.0017	.0018	-.02	im	.0018	.0018
5.0	3.0	im	.0018	.0018	3.3	im	.0018	.0018
10.0	5.9	5.2	.0018	.0017	6.2	im	.0019	.0018
20.0	10.6	13.0	.0018	.0016	11.0	11.8	.0020	.0017
30.0	14.3	19.7	.0017	.0015	14.9	19.7	.0020	.0016
40.0	17.4	25.6	.0016	.0014	18.1	26.7	.0021	.0016
50.0	20.3	30.9	.0015	.0014	21.0	33.0	.0021	.0016
60.0	23.1	35.6	.0015	.0014	23.9	38.6	.0021	.0016
			Imposed Mgw = 1.5, D^1 = .0015					
0.0	-0.3	im	.0015	.0016	-0.2	im	.0016	.0016
5.0	3.1	im	.0016	.0016	3.3	im	.0016	.0016
10.0	6.0	4.6	.0017	.0015	6.3	im	.0017	.0015
20.0	10.8	13.0	.0017	.0014	11.1	11.6	.0018	.0015
30.0	14.6	20.0	.0016	.0013	15.0	19.8	.0018	.0014
40.0	17.8	26.0	.0015	.0013	18.2	27.0	.0019	.0014
50.0	20.8	31.3	.0014	.0012	21.2	33.3	.0019	.0014
60.0	23.8	36.2	.0014	.0013	24.3	39.0	.0019	.0014

Units: HPV cm h^{-1}, D cm^2 s^{-1}

Table 9. Influence of glass sensor, brass heater material and 0.20 cm wound on HPVS, HPVM and longitudinal diffusivities with symmetrical sensors configured (-0.96,0.0.96 cm) and (-1.44,0,1.44 cm). HPVS's calculated from temperature ratios at 120 s. HPVM's and longitudinal diffusivities calculated from temperature data at 60, 120 and 180 s. Values for HPVM marked "im" are imaginary, i.e., the square root of a negative number.

	(-0.96,0,0.96 cm)				(-1.44,0,1.44 cm)			
HPVI (1)	HPVS (2)	HPVM (3)	D^1 up (4)	D^1 dn (5)	HPVS (6)	HPVM (7)	D^1 up (8)	D^1 dn (9)
Imposed Mgw = 0.5, D^1 = .0024								
0.0	0.0	3.8	.0022	.0022	0.0	im	.0023	.0023
5.0	2.7	3.8	.0022	.0021	2.9	im	.0023	.0022
10.0	5.2	6.5	.0023	.0021	5.7	3.2	.0024	.0022
20.0	9.7	13.1	.0024	.0019	10.8	12.1	.0024	.0022
30.0	13.4	19.4	.0024	.0018	15.3	19.5	.0025	.0021
40.0	16.3	25.0	.0024	.0017	19.1	26.2	.0026	.0020
50.0	18.6	30.1	.0024	.0016	22.4	32.3	.0026	.0020
60.0	20.6	34.7	.0024	.0016	25.3	37.9	.0026	.0019
Imposed Mgw = 1.0, D^1 = .0018								
0.0	0.0	im	.0018	.0018	0.0	im	.0018	.0018
5.0	2.9	im	.0018	.0017	3.1	im	.0019	.0018
10.0	5.6	5.0	.0019	.0017	6.0	im	.0019	.0018
20.0	10.4	12.9	.0020	.0016	11.3	11.7	.0020	.0017
30.0	14.1	19.7	.0020	.0015	15.8	19.7	.0020	.0016
40.0	17.1	25.6	.0021	.0014	19.6	26.7	.0021	.0016
50.0	19.6	30.9	.0021	.0014	22.9	33.0	.0021	.0016
60.0	21.8	35.6	.0021	.0014	25.8	38.6	.0022	.0016
Imposed Mgw = 1.5, D^1 = .0015								
0.0	0.0	im	.0016	.0016	0.0	im	.0016	.0016
5.0	3.0	im	.0016	.0016	3.2	im	.0016	.0016
10.0	5.8	4.2	.0017	.0015	6.1	im	.0017	.0015
20.0	10.7	12.9	.0018	.0014	11.5	11.6	.0017	.0015
30.0	14.5	19.9	.0018	.0013	16.0	19.8	.0018	.0014
40.0	17.5	26.0	.0019	.0013	19.8	27.0	.0018	.0014
50.0	20.0	31.3	.0019	.0012	23.1	33.3	.0019	.0014
60.0	22.4	36.2	.0019	.0012	26.1	39.0	.0019	.0014

Units: HPV cm h^{-1}, D cm^2 s^{-1}

18.0, 17.6 and 17.5 compared to 16.7, 17.4 and 17.8 cm h^{-1} (at Mgw = 0.5, 1.0 and 1.5 respectively) with both sensor materials and wound (column 2, Tables 8). (I did not perform similiar "no sensor" simulations to compare with those configured -0.96,0,1.44 cm). The effect of sensor material is such that the HPVA and HPVM at Mgw = 1.5 is slightly greater than that obtained at Mgw = 0.5 (Table 8, columns 2 and 3, 6 and 7); the opposite occured in the "no sensor" simulation (Table 3, column 4 and 13).

The results with the symmetrical configurations (Table 9) are much the same as with those asymmetrical. The comparative "no sensor" simulation results are given in Table 5.

The effect of sensor materials on longitudinal thermal diffusivity, D^1, is to reduce the magnitude of the value calculated in dry sapwood (Mgw = 0.5), and to increase its magnitude in wet sapwood (Mgw = 1.5). This sensitivity to sensor materials may be important if D^1 and Pb are used to estimate sapwood moisture content with Equation 17 (p. 26). Also, D^1's calculated with temperature data from the up and downstream sensors were different depending upon spacing and imposed HPV (Tables 8, 9; columns 4 and 5, 8 and 9); the value obtained from downstream sensor data became smaller, that from the upstream sensor larger, as HPVI was increased from 0 to 60 cm h^{-1}. However, the average of the D^1's obtained from the up and downstream sensor data was fairly close to that obtained at HPVI = 0 at all greater HPVI's with both symmetrical sensor arrangements (Table 9) and the asymmetrical one (Table 8) configured (-0.96,0,1.44 cm).

Case 6, effect of stem tissue borders, RLM only

This group was divided into five subcases. In each, I applied the RLM without sensor or heater materials to several "stem radii" composed of differing arrangements of bark, sapwood and heartwood. These were:

a) Bark, sapwood, no heartwood.

b) Sapwood, heartwood, no bark.

c) Bark, three centimeters of sapwood, heartwood.

d) Bark, two centimeters of sapwood, heartwood.

e) Bark, one centimeter of sapwood, heartwood.

In each instance, bark and heartwood moisture contents were held constant at 0.0 and 0.4 (moisture fraction, dry weight basis) respectively while sapwood moisture content was varied from 0.5 to 1.5. Uniform heat pulse velocities were imposed across the sapwood. My rationale for imposing uniform HPV's across the entire sapwood was to make these results a standard set against which to compare other, possibly more realistic, distributions (e.g. Xylem flow structure, p. 128). Sap movement in the bark and heartwood was considered to be nil.

The results for each subcase are presented on three graphs:

1) Longitudinal diffusivity, D^l, HPVM and HPVA at HPVI = 0.

2) HPVM at each of the three moisture contents and at HPVI's from 5 to 30 cm h^{-1}.

3) HPVS and HPVA at HPVI's from 5 to 30 cm h^{-1}.

HPVS has not been presented at HPVI = 0 because it was always zero there. HPVS's and HPVA's were only marginally different at the three moisture contents; therefore only those obtained at Mgw = 1.0 have been displayed. HPVM's varied the most widely among the subcases. Thus it has been displayed at all moisture contents and HPVI's. HPVP's, where obtained, behaved similiarily to HPVM's and the HPVM traces can be considered as applicable to both. Between HPVI = 5 and 30 cm h^{-1}, HPVS traces can be considered as applicable to HPVT's as well.

Case 6a, 0.32 cm bark, 3.68 cm sapwood, no heartwood

These results are shown in Figure 12, Figure 13 and Figure 14. The presence of bark and the heat loss through it are evident in all traces. At HPVI = 0 (Fig. 12), longitudinal diffusivity is affected to a depth of 2.0 cm at Mgw = 0.5 and to 1.0 cm at Mgw = 1.5. HPVM's are greatly in error at depths less than 2.0 cm, ranging from 9 to 15 cm h^{-1} at the bark/sapwood interface to imaginary between 1.6 and 2.0 cm deep. HPVM's are closer to those imposed at HPVI's greater than 5 cm h^{-1} (Fig. 13), but are still seriously in error at depths less than 2 cm at the lower HPVI's.

HPVA's at HPVI = 0 are little affected by the bark/sapwood border (Fig. 12). At HPVI's of 5 to 30 cm h^{-1}, both HPVA and HPVS are relatively stable and calculate the same as HPVI at depths greater than 1.0 cm (Fig. 14).

Case 6b, no bark, 3.32 cm sapwood, 0.68 cm heartwood

These results are shown in Figure 15, Figure 16 and Figure 17. At HPVI = 0 (Fig. 15), longitudinal diffusivity is affected by the sapwood/heart-wood interface at 1.3 cm from it. HPVM's

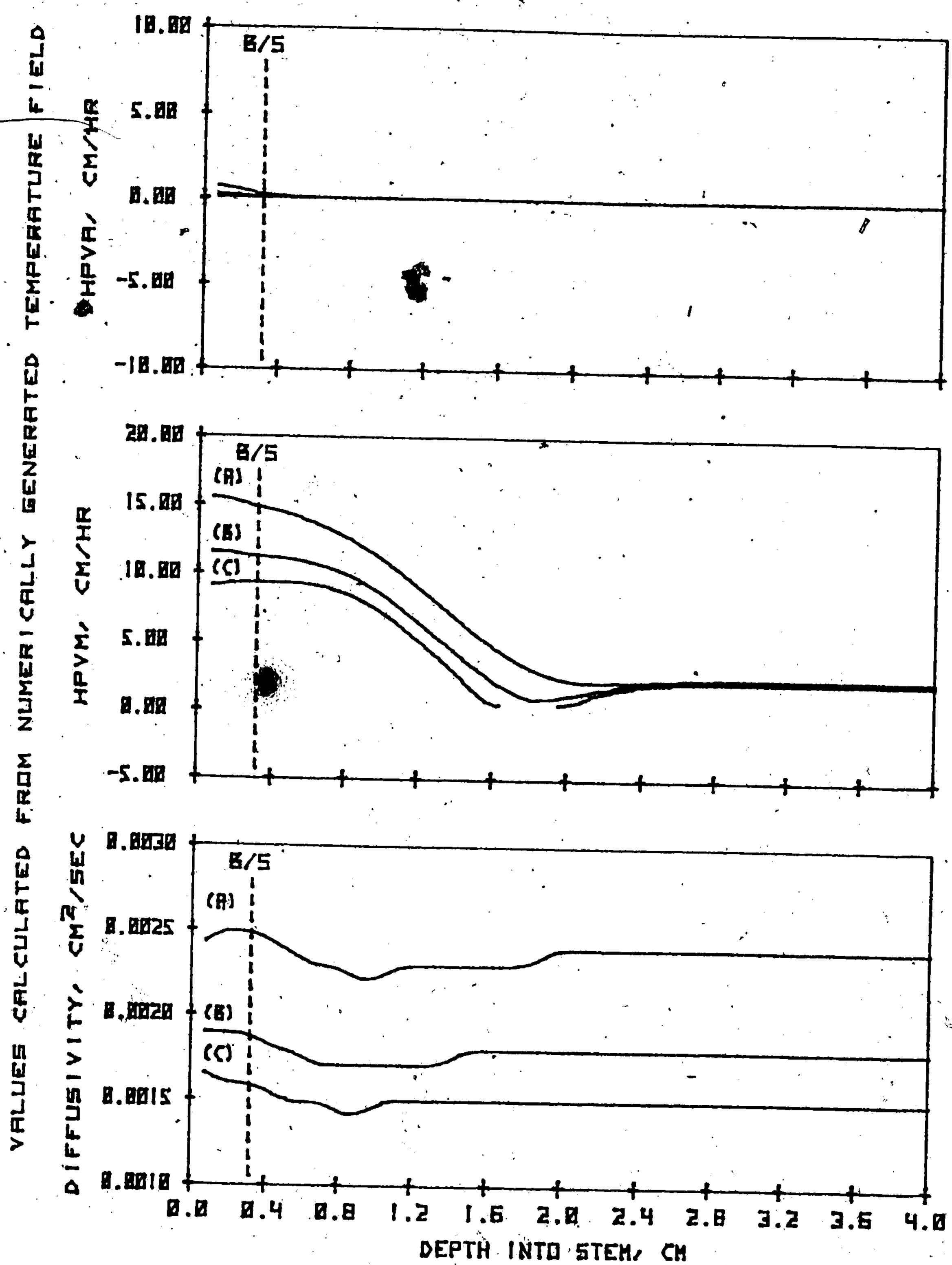

Figure 12. Influence of stem tissue borders on heat pulse calculations of longitudinal diffusivity, HPVM and HPVA at HPVI = 0. Radial-longitudinal model with 0.32 cm bark, 3.68 cm sapwood, no heartwood. Sapwood moisture fraction (dwb) (A) 0.5, (B) 1.0, (C) 1.5.

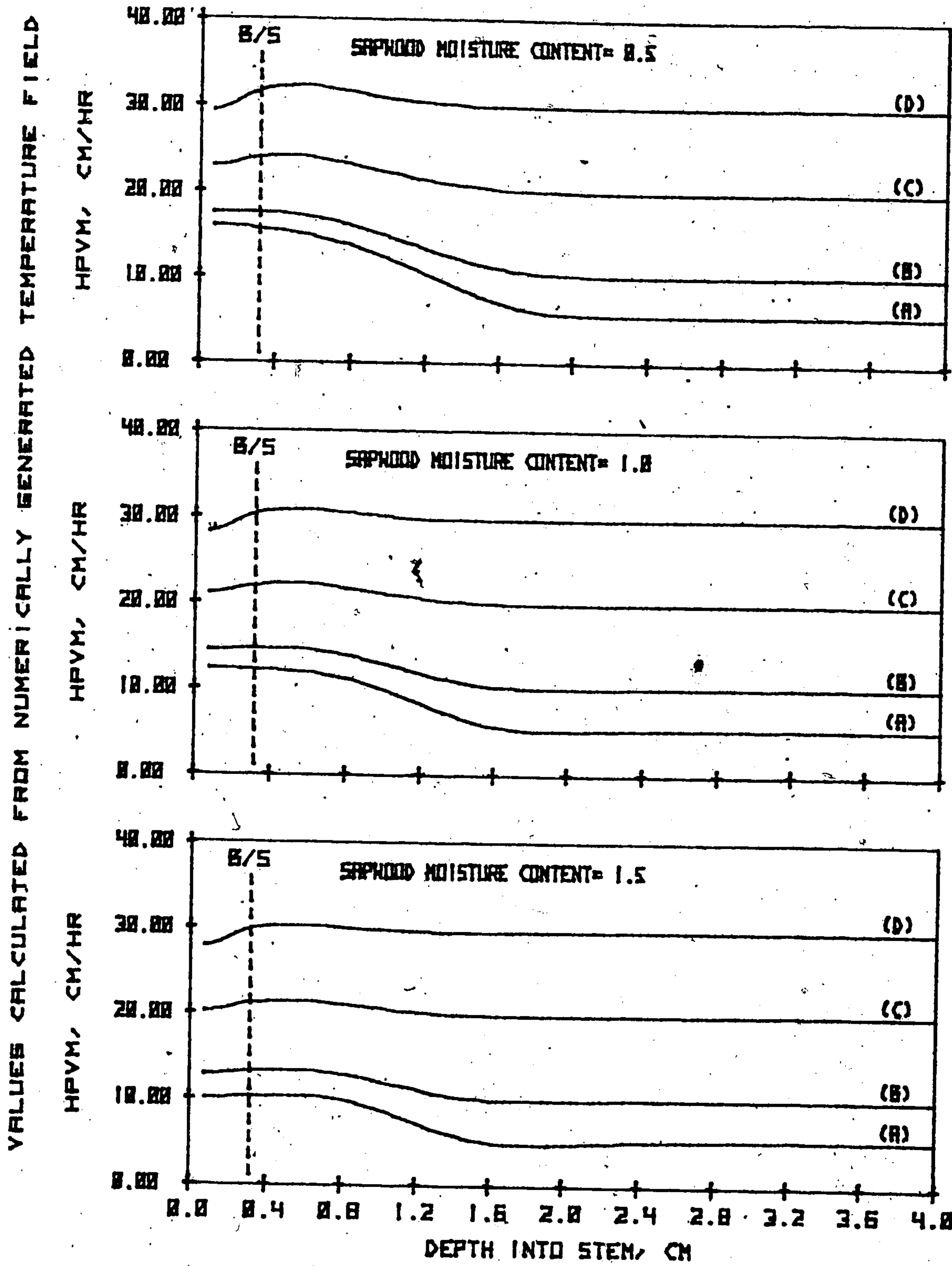

Figure 13. Influence of stem tissue borders on HPVM calculations. Radial-longitudinal model with 0.32 cm bark, 3.68 cm sapwood, no heartwood. HPVM's at HPVI's = (A) 5.0, (B) 10.0, (C) 20.0, (D) 30.0 cm/h.

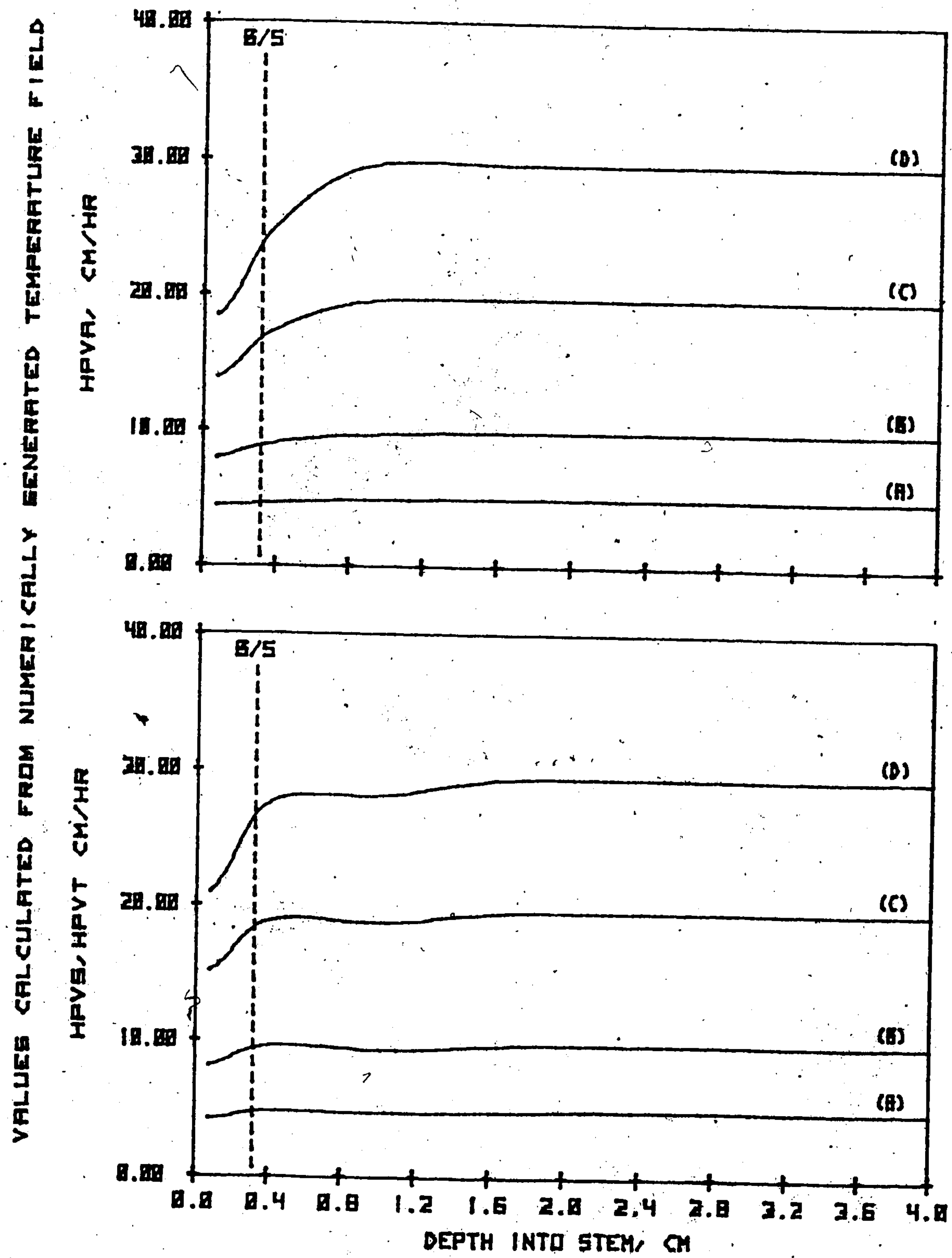

Figure 14. Influence of stem tissue borders on HPVA, HPVS and HPVT calculations. Radial-longitudinal model with 0.32 cm bark, 3.68 cm sapwood, no heartwood. HPVA and HPVS at sapwood moisture fraction 1.0. HPVI's = (A) 5.0, (B) 10.0, (C) 20.0, (D) 30.0 cm/h.

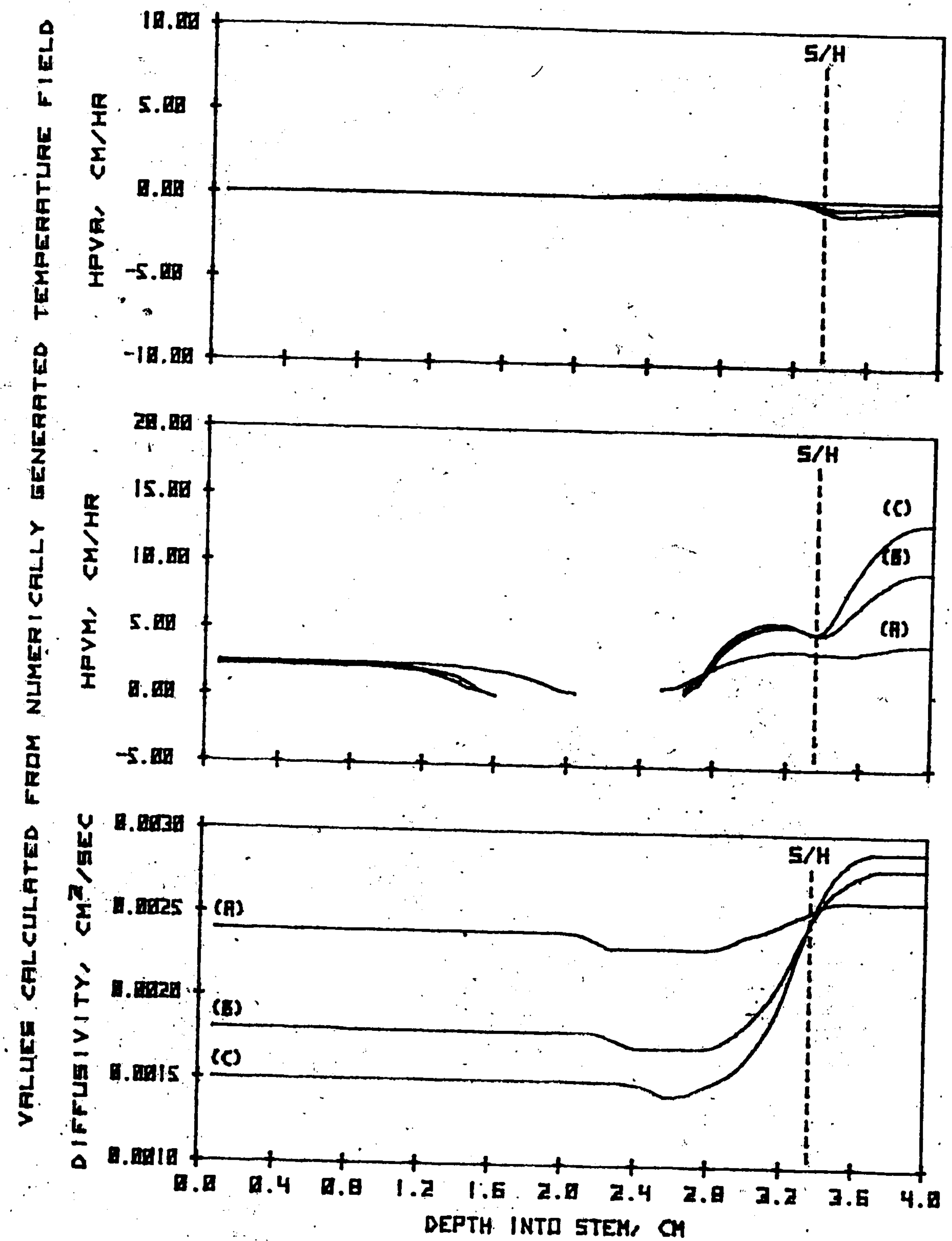

Figure 15. Influence of stem tissue borders on heat pulse calculations of longitudinal diffusivity, HPVM and HPVA at HPVI = 0. Radial-longitudinal model with no bark, 3.32 cm sapwood, 0.68 cm heartwood. Sapwood moisture fraction (dwb) (A) 0.5, (B) 1.0, (C) 1,5.

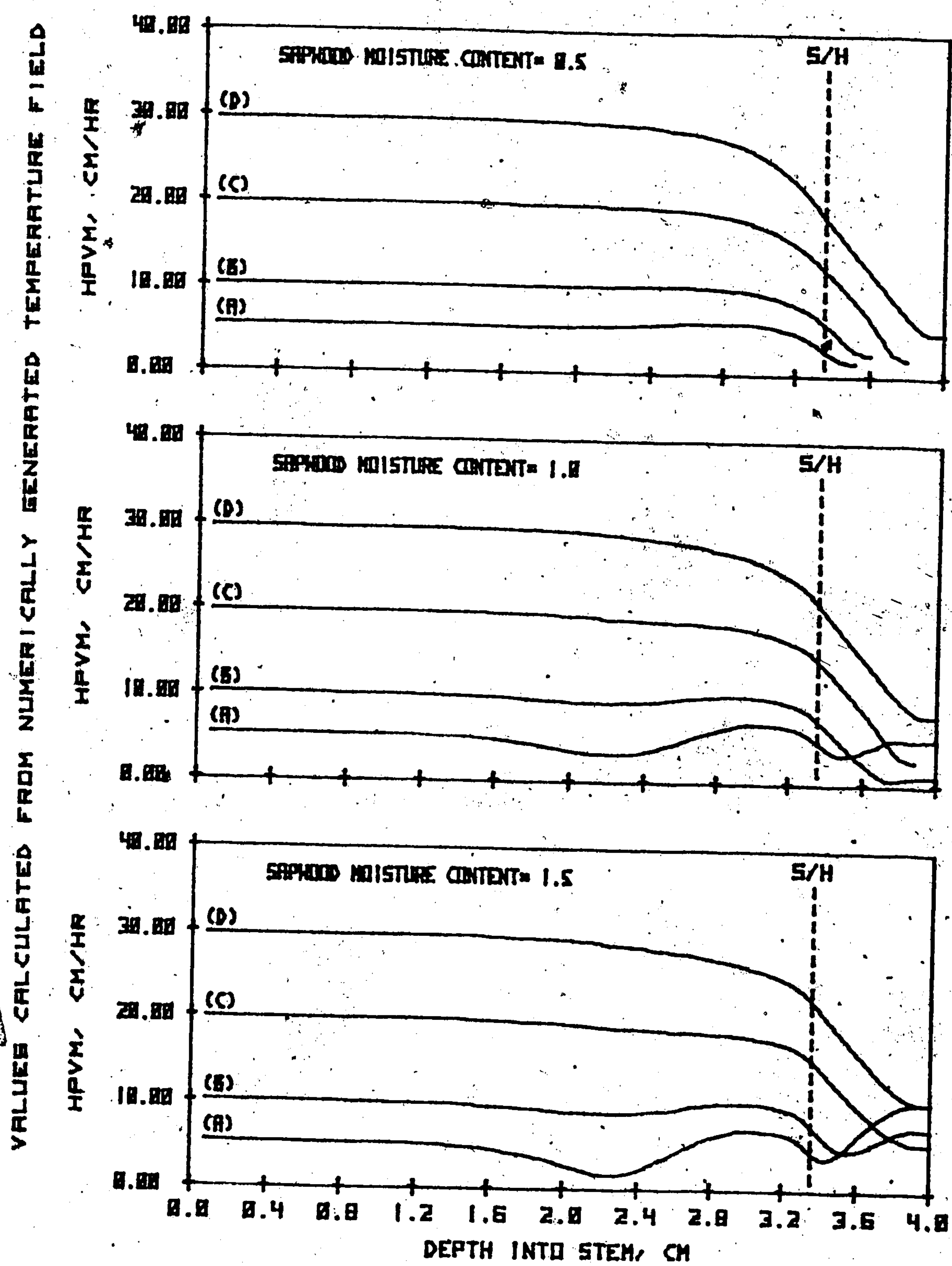

Figure 16. Influence of stem tissue borders on HPVM calculations. Radial-longitudinal model with no bark, 3.32 cm sapwood, 0.68 cm heartwood. HPVM's at HPVI's = (A) 5.0, (B) 10.0, (C) 20.0, (D) 30.0 cm/h.

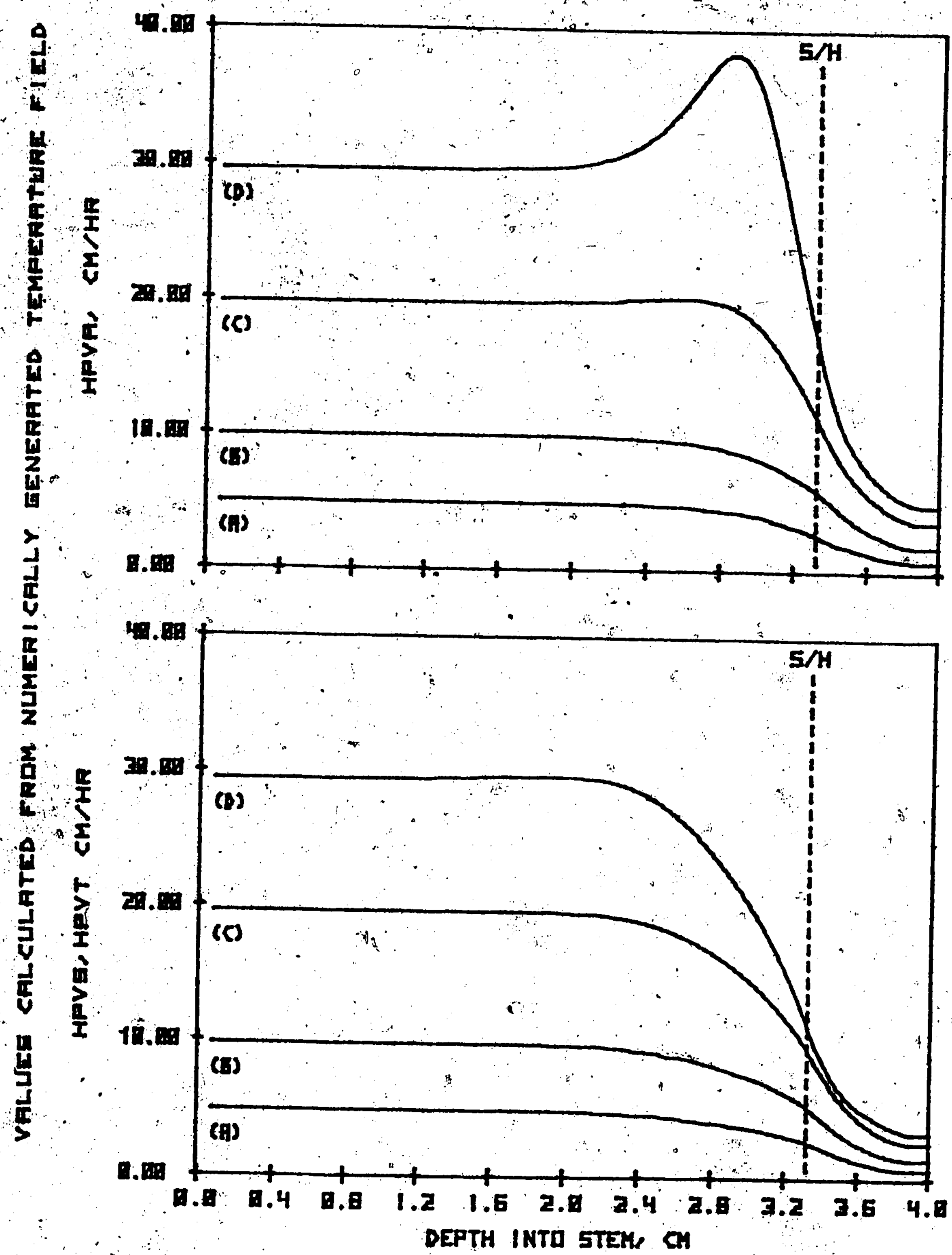

Figure 17. Influence of stem tissue borders on HPVA, HPVS and HPVT calculations. Radial-longitudinal model with no bark, 3.32 cm sapwood, 0.68 cm heartwood. HPVA and HPVS at sapwood moisture fraction 1.0. HPVI's = (A) 5.0, (B) 10.0, (C) 20.0, (D) 30.0 cm/h.

are influenced by the heartwood at 1.2 cm deep, i.e., 2.12 cm from the sapwood/heartwood interface. HPVA's in the sapwood are only mildly affected by the sapwood/heartwood border, but tend toward slightly negative values (ca. −0.4 cm h^{-1}) in the heartwood.

At HPVI's from 5 to 30 cm h^{-1} (Fig. 16), HPVM's in the sapwood are relatively free of the influence of the sapwood/heartwood border only when HPVI's are greater than 10 cm h^{-1} and at distances more than 1.2 cm from it. Both the HPVA and HPVS configurations give HPV values nearly equal to HPVI up to 1.4 cm from the sapwood/heart-wood border (Fig. 17). Near this border, HPVA's range from much greater to less than imposed. In the same portion of the sapwood, HPVS's decline more or less linearly into the heartwood.

The simulations were extended to 60 cm h^{-1} to further document the erratic behavior of HPVA near the S/H border. Similiar erratic behavior was found to occur with the HPVS, HPVM and D^1 solutions as well (Tables 10, 11). HPVT values were unaffected by this border (Table 12). The tz used in the HPVT equation (Eq. 9, p. 23) becomes smaller as HPVI increases (tz at HPVI = 10 was 86 s, at HPVI = 60, 14 s). This suggests that temperatures measured at shorter time intervals, e.g. 30,60 and 90 s, might produce more stable results than those displayed (at 60, 120 and 180 s). This is indeed the case. The results with 30 s time intervals (30, 60, 90 s, Table 10) indicates that HPVA still becomes erratic above HPVI = 50 cm h^{-1}. However, when HPVS and D^1 are calculated from temperatures taken at 30 s intervals, their values are stable at all points

Table 10. Influence of sensor position with respect to the sapwood heartwood border, and time interval used in the solutions to the equations HPVA, HPVM, HPVS and longitudinal diffusivity. Solutions obtained from temperatures at 60 s intervals, i.e., 60, 120 and 180 s from initiation of heat pulse. Solutions times used: HPVA 60, 120 s; HPVM and longitudinal diffusivity 60, 120 and 180 s; HPVS from temperature ratio at 120 s. Radial longitudinal model, no wound, no sensor materials. Sapwood Mgw = 1.0, Pb = 0.4; heartwood Mgw = 0.4, Pb = 0.4.

Depth HPVI	In sapwood				S/H	In heartwood			
	1.6	1.2	0.8	0.4	0.0	0.4	0.8	1.2	1.6 cm
(1)	(2)	(3)	(4)	(5)	(6)	(7)	(8)	(9)	(10)
					HPVA				
0.0	0.1	0.2	0.3	0.4	0.0	-0.2	0.0	0.1	0.2
5.0	5.0	5.0	4.8	4.4	3.1	1.0	0.3	0.2	0.2
10.0	9.8	9.8	9.6	8.7	6.0	2.1	0.6	0.2	0.2
20.0	19.5	19.6	19.9	19.0	11.4	3.9	1.2	0.3	0.2
30.0	29.2	29.7	32.7	37.8	17.0	5.2	1.6	0.4	0.2
40.0	39.0	40.8	58.2	484.3	26.8	6.0	2.0	0.5	0.2
50.0	48.9	55.9	--	-27.0	83.0	6.4	2.3	0.6	0.2
60.0	59.7	99.1	-28.0	-8.2	-36.1	6.5	2.5	0.6	0.2
					HPVS				
0.0	0.0	0.0	0.0	0.0	0.0	0.0	0.0	0.0	0.0
5.0	4.9	4.8	4.6	3.9	2.8	0.8	0.2	0.0	0.0
10.0	9.7	9.6	9.2	7.8	5.3	1.6	0.3	0.0	0.0
20.0	19.4	19.3	18.4	15.4	9.5	2.7	0.6	0.1	0.0
30.0	29.2	29.2	27.7	22.4	12.5	3.4	0.8	0.1	0.0
40.0	39.1	39.8	38.0	30.6	15.6	3.8	1.0	0.2	0.0
50.0	49.7	52.9	56.5	54.3	21.7	4.0	1.1	0.2	0.1
60.0	62.3	80.8	353.3	-212.6	46.0	4.2	1.2	0.2	0.0
					HPVM				
0.0	0.8	im	im	3.9	1.6	4.3	7.7	7.2	5.5
5.0	5.1	3.9	4.4	6.5	4.0	im	6.5	6.7	5.4
10.0	10.0	9.5	9.6	10.1	7.7	im	5.2	6.2	5.2
20.0	19.7	19.4	18.9	18.2	15.2	5.5	3.3	5.3	4.8
30.0	29.5	29.1	28.3	26.6	22.1	11.6	4.4	4.6	4.5
40.0	39.4	39.1	38.1	35.6	28.3	16.0	7.0	4.4	4.3
50.0	49.4	50.0	51.3	49.7	34.9	19.0	9.5	4.8	4.2
60.0	60.2	66.7	128.9	im	47.4	21.0	11.5	5.5	4.1
					Longitudinal Diffusivity				
0.0	.0017	.0017	.0017	.0017	.0021	.0027	.0026	.0025	.0025
5.0	.0017	.0017	.0017	.0017	.0021	.0026	.0026	.0025	.0025
10.0	.0017	.0017	.0017	.0017	.0021	.0026	.0026	.0025	.0025
20.0	.0017	.0017	.0017	.0018	.0020	.0024	.0026	.0025	.0025
30.0	.0017	.0018	.0018	.0019	.0020	.0022	.0025	.0025	.0025
40.0	.0018	.0018	.0020	.0023	.0023	.0021	.0024	.0025	.0025
50.0	.0018	.0020	.0027	.0040	.0031	.0020	.0024	.0025	.0025
60.0	.0019	.0027	.0166	-.0158	.0068	.0021	.0023	.0025	.0025

Units: HPV cm h^{-1}, D cm^2 s^{-1}

Table 11. Influence of sensor position with respect to the sapwood heartwood border, and time interval used in the solutions to the equations HPVA, HPVM, HPVS and longitudinal diffusivity. Solutions obtained from temperatures at 30 s intervals, i.e., 30, 60, and 90 s from initiation of heat pulse. Solutions times used: HPVA 30, 60 s; HPVM and longitudinal diffusivity 30, 60 and 90 s; HPVS from temperature ratio at 60 s. Radial longitudinal model, no wound, no sensor materials. Sapwood Mgw = 1.0, Pb = 0.4; heartwood Mgw = 0.4, Pb = 0.4.

Depth	In sapwood				S/H	In heartwood			
HPVI (1)	1.6 (2)	1.2 (3)	0.8 (4)	0.4 (5)	0.0 (6)	0.4 (7)	0.8 (8)	1.2 (9)	1.6 cm (10)
					HPVA				
0.0	0.4	0.4	0.5	0.9	-0.1	0.0	0.5	0.5	0.5
5.0	5.2	5.2	5.1	4.9	3.0	0.7	0.5	0.5	0.5
10.0	9.9	9.9	9.8	9.2	6.0	0.7	0.5	0.5	0.5
20.0	19.4	19.4	19.3	18.1	11.6	1.3	0.6	0.5	0.5
30.0	28.9	28.9	28.9	27.8	16.5	2.6	0.7	0.5	0.5
40.0	38.4	38.4	38.7	39.3	20.9	3.8	0.8	0.5	0.5
50.0	47.8	47.8	48.9	56.3	25.4	5.0	1.0	0.5	0.5
60.0	57.2	57.3	60.2	96.7	30.6	6.0	1.1	0.5	0.5
						6.8	1.3	0.6	0.5
					HPVS				
0.0	0.0	0.0	0.0	0.0	0.0	0.0	0.0	0.0	0.0
5.0	4.7	4.7	4.7	4.1	2.5	0.4	0.0	0.0	0.0
10.0	9.4	9.4	9.3	8.2	4.9	0.7	0.1	0.0	0.0
20.0	18.9	18.9	18.6	16.2	9.1	1.4	0.1	0.0	0.0
30.0	28.3	28.3	27.9	23.5	12.4	2.0	0.2	0.0	0.0
40.0	37.7	37.7	37.0	29.9	15.0	2.6	0.2	0.0	0.0
50.0	47.0	47.1	45.9	35.2	17.2	3.1	0.3	0.0	0.0
60.0	56.3	56.4	54.1	39.9	19.2	3.5	0.4	0.0	0.0
					HPVM				
0.0	7.7	6.6	im	8.1	1.9	11.5	13.1	10.4	9.1
5.0	9.1	8.4	6.4	10.3	3.8	9.0	12.5	10.5	9.1
10.0	12.4	12.0	11.0	13.5	7.6	5.7	11.8	10.1	9.1
20.0	20.9	20.7	20.3	21.0	15.7	im	10.3	9.9	9.1
30.0	30.1	30.0	29.6	29.3	23.8	im	8.6	9.6	9.1
40.0	39.6	39.4	39.0	37.8	31.5	im	6.7	9.4	9.1
50.0	49.0	48.9	48.3	46.3	38.6	11.0	4.8	9.1	9.0
60.0	58.6	58.4	57.7	54.8	45.0	17.3	3.3	8.9	9.0
					Longitudinal Diffusivity				
0.0	.0017	.0017	.0017	.0017	.0021	.0025	.0024	.0024	.0024
5.0	.0017	.0017	.0017	.0017	.0021	.0025	.0024	.0024	.0024
10.0	.0017	.0017	.0017	.0017	.0020	.0025	.0024	.0024	.0024
20.0	.0017	.0017	.0017	.0017	.0020	.0025	.0025	.0024	.0024
30.0	.0017	.0017	.0017	.0017	.0019	.0024	.0025	.0024	.0024
40.0	.0017	.0017	.0017	.0017	.0019	.0024	.0025	.0024	.0024
50.0	.0017	.0017	.0017	.0018	.0019	.0022	.0025	.0024	.0024
60.0	.0017	.0017	.0017	.0018	.0019	.0022	.0025	.0024	.0024

Units: HPV cm h^{-1}, D cm^2 s^{-1}

Table 12. Influence of sensor position with respect to the sapwood heartwood border. HPVT values, which are obtained at times dependent on the speed of HPVI, are given here for comparison with the fixed time solutions given in Tables 10 and 11. Radial longitudinal model, no wound, no sensor materials. HPVT's marked (--) means that tz not reached during 180 s simulation time. Sapwood Mgw = 1.0, Pb = 0.4; heartwood Mgw = 0.4, Pb = 0.4.

Depth	In sapwood				S/H	In heartwood			
HPVI	1.6	1.2	0.8	0.4	0.0	0.4	0.8	1.2	1.6 cm
(1)	(2)	(3)	(4)	(5)	(6)	(7)	(8)	(9)	(10)
0.0	--	--	--	--	--	--	--	--	--
5.0	4.9	4.8	--	--	--	--	--	--	--
10.0	9.8	9.8	9.6	8.6	5.9	--	--	--	--
20.0	19.2	19.2	19.2	18.0	11.4	--	--	--	--
30.0	28.8	28.8	28.8	27.0	16.3	5.2	--	--	--
40.0	37.9	37.9	37.9	36.6	21.1	5.8	--	--	--
50.0	47.0	47.0	47.0	47.0	25.4	6.1	--	--	--
60.0	56.8	56.8	56.8	56.8	30.0	6.1	--	--	--

Units: HPV cm h^{-1}

in the sapwood or heartwood from HPVI = 0 to 60 cm h^{-1} (Table 11). The values obtained for HPVM are unstable at some HPVI's at 0.4 cm into the heartwood (Table 10, 11; column 7), regardless of the time intervals used to obtain their solution.

Case 6c, 0.32 cm bark, 3.0 cm sapwood, 0.68 cm heartwood

These results are shown in Figure 18, Figure 19 and Figure 20. At HPVI = 0 (Fig. 18), calculated longitudinal diffusivity is equal to that imposed only between the 1.8 and 2.2 cm depths for all moisture contents. D^l behaves somewhat better at the higher moisture contents, equaling that imposed between the 1.5 to 2.2 cm depths when Mgw = 1.0 and between 1.0 to 2.3 cm depths when Mgw = 1.5. HPVM's are never the same as the imposed values anywhere in the cross section at HPVI = 0. Furthermore, the calculated values of HPVM are imaginary at the depths where the longitudinal diffusivities are relatively stable. HPVA's depart marginally (ca. 0.4 cm h^{-1}) from imposed at both the bark/sapwood and sapwood/heartwood borders.

At HPVI's from 5 to 30 cm h^{-1}, HPVM's behave somewhat better (Fig. 19), although at HPVI's of 5 and 10 cm h^{-1} the calculated values are different from imposed over most of the sapwood. HPVA's are again "humped" near the sapwood/heartwood border (Fig. 20). Both HPVA and HPVS calculate the same as HPVI between the 1.0 and 2.0 cm depths.

Case 6d, 0.32 cm bark, 2.0 cm sapwood, 0.90 cm heartwood

These results are shown in Figure 21, Figure 22 and Figure 23. At HPVI = 0 (Fig. 21), longitudinal diffusivity calculates

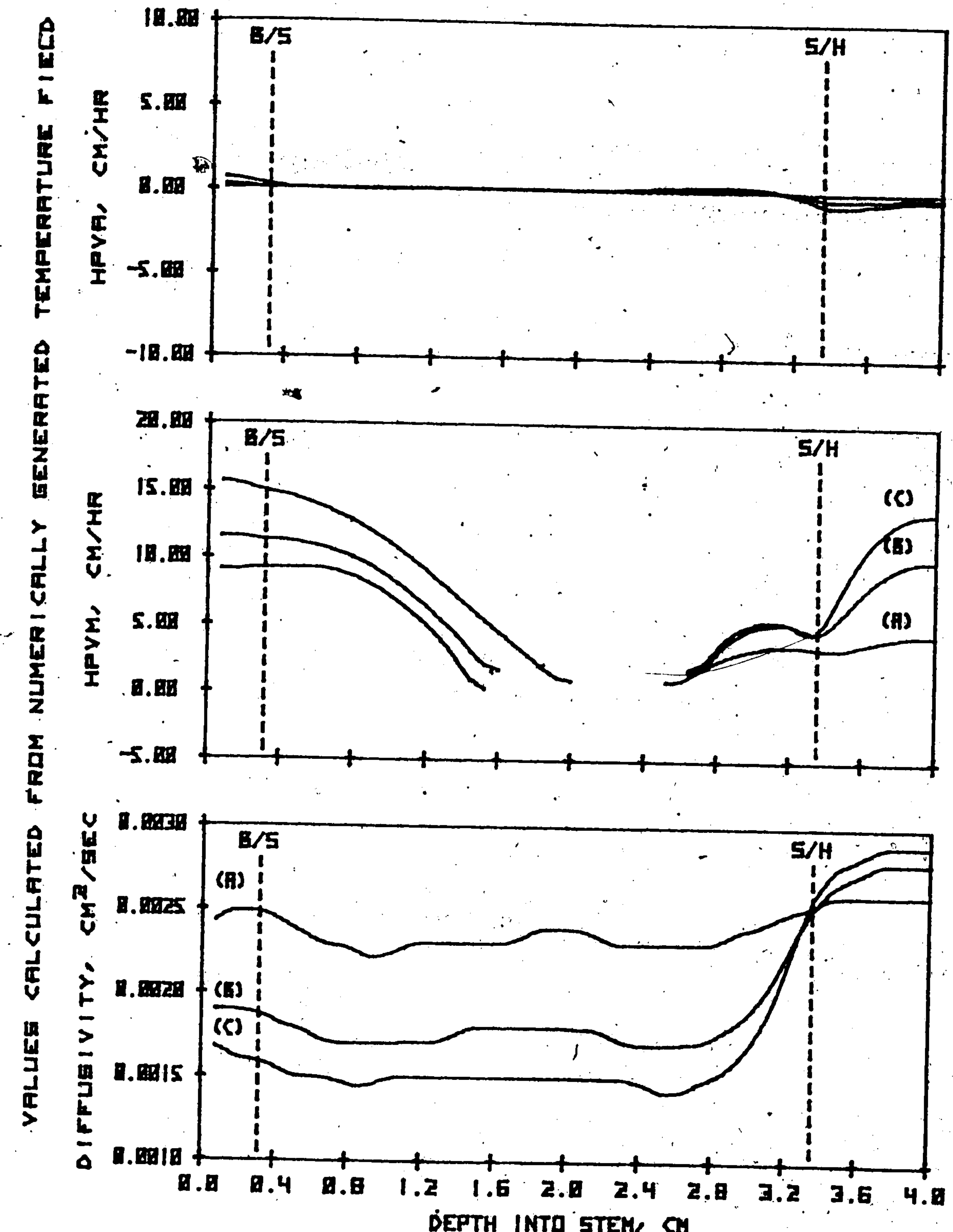

Figure 18. Influence of stem tissue borders on heat pulse calculations of longitudinal diffusivity, HPVM and HPVA at HPVI = 0. Radial-longitudinal model with 0.32 cm bark, 3.00 cm sapwood, 0.68 cm heartwood. Sapwood moisture fraction (dwb) (A) 0.5, (B) 1.0, (C) 1.5.

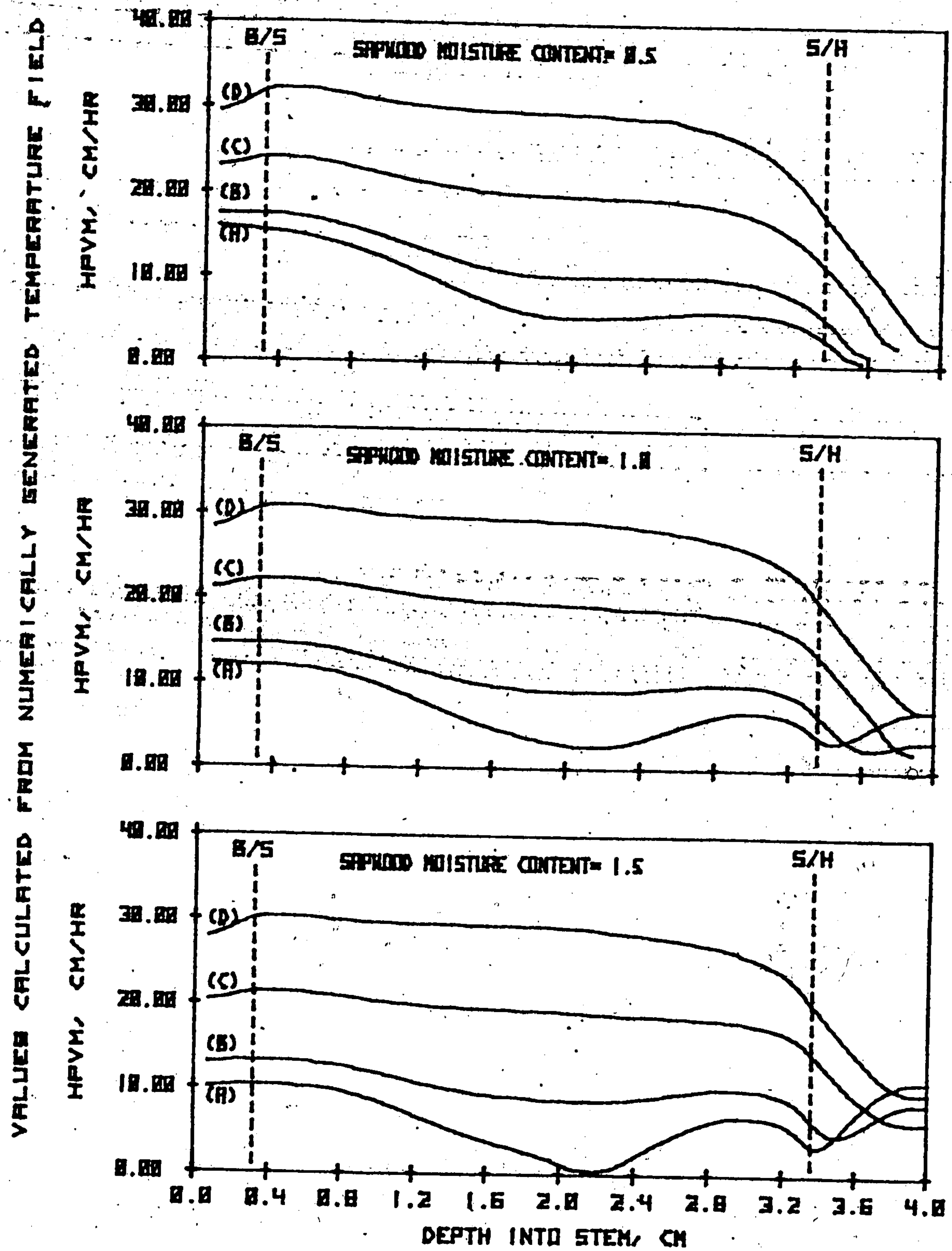

Figure 19. Influence of stem tissue borders on HPVM calculations. Radial-longitudinal model with 0.32 cm bark, 3.00 cm sapwood, 0.68 cm heartwood. HPVM's at HPVI's = (A) 5.0, (B) 10.0, (C) 20.0, (D) 30.0 cm/h.

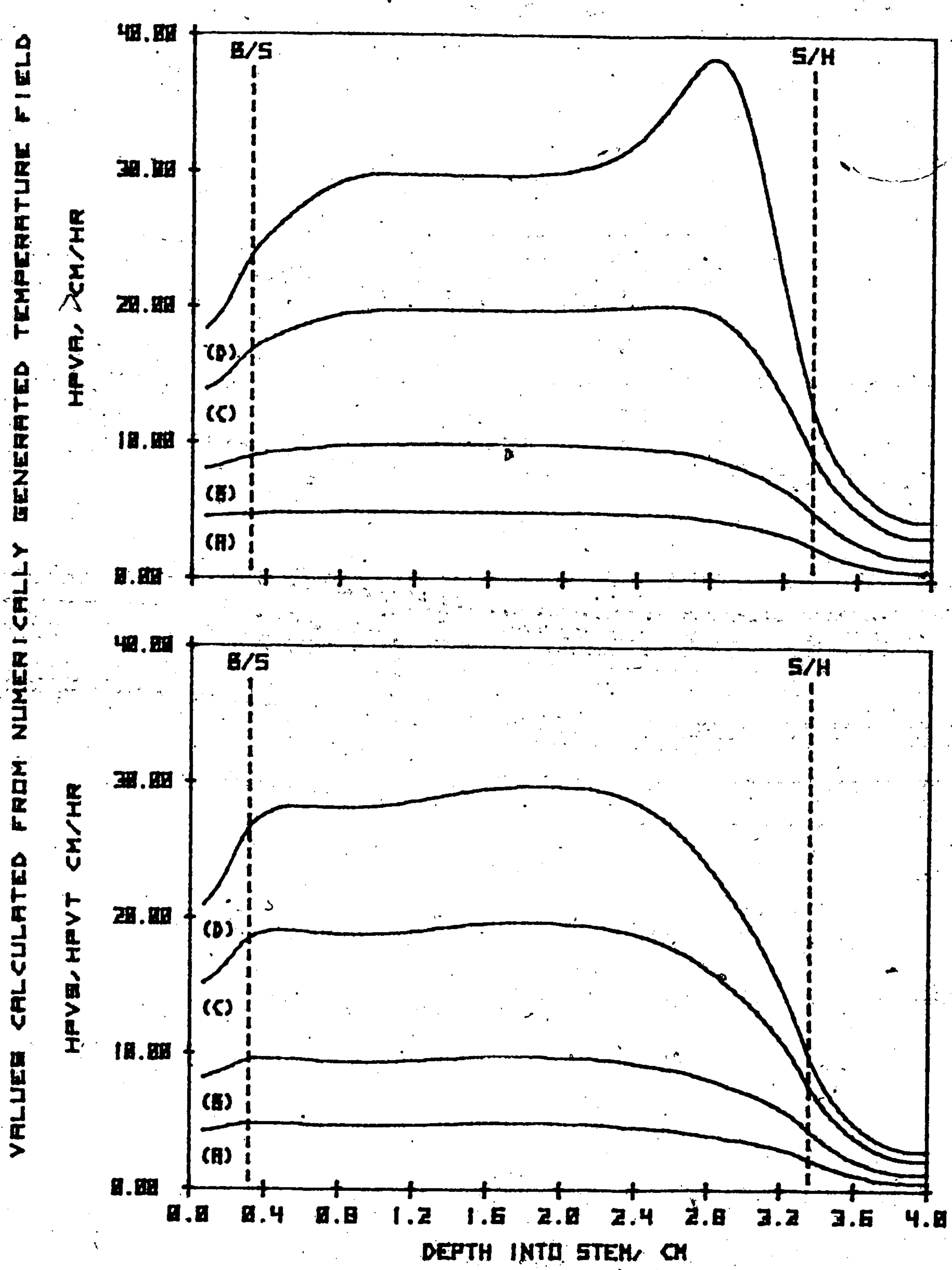

Figure 20. Influence of stem tissue borders on HPVA, HPVS and HPVT calculations. Radial-longitudinal model with 0.32 cm bark, 3.00 cm sapwood, 0.68 cm heartwood. HPVA and HPVS at sapwood moisture fraction 1.0. HPVI's = (A) 5.0, (B) 10.0, (C) 20.0, (D) 30.0 cm/h.

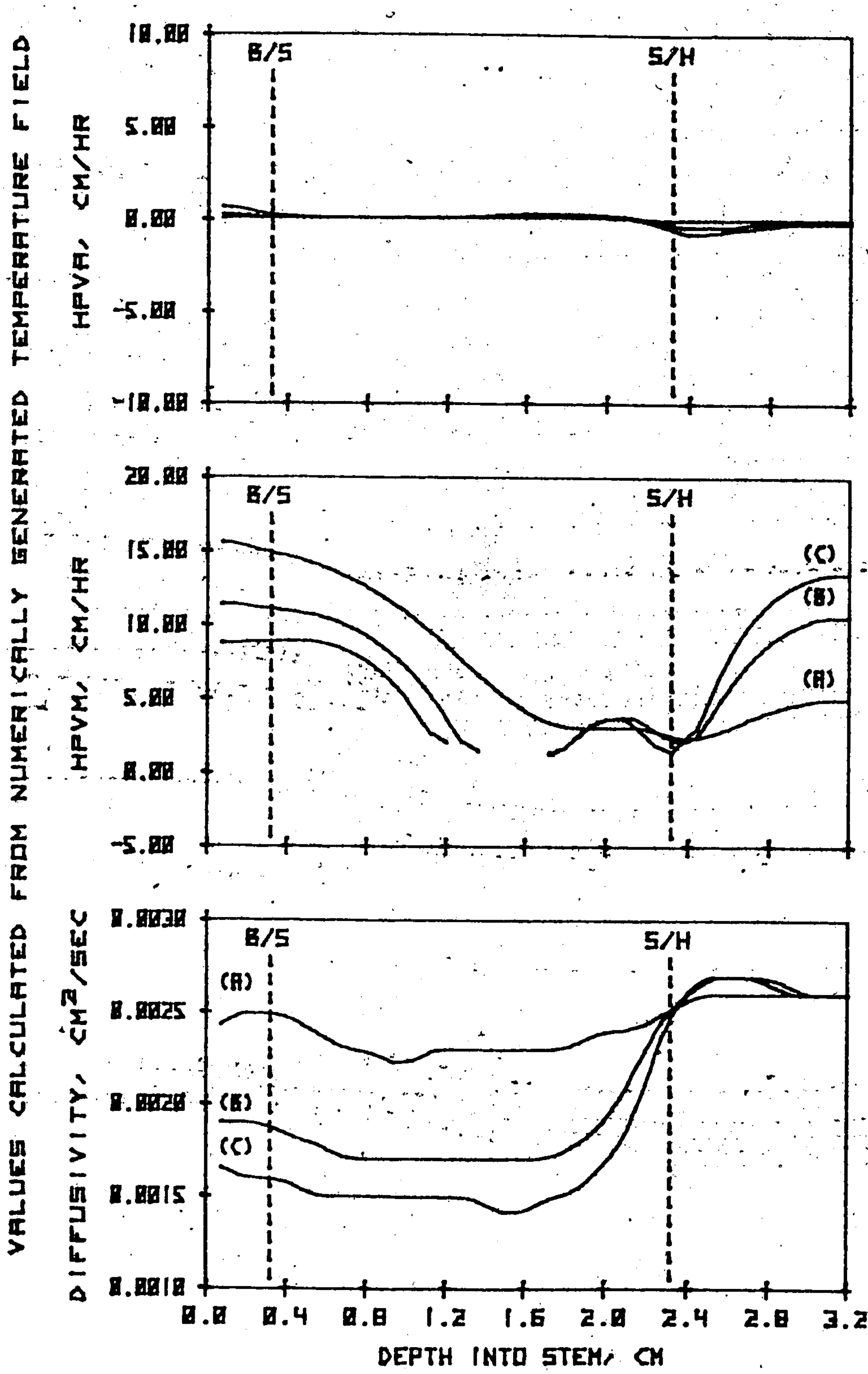

Figure 21. Influence of stem tissue borders on heat pulse calculations of longitudinal diffusivity, HPVM and HPVA at HPVI = 0. Radial-longitudinal model with 0.32 cm bark, 2.00 cm sapwood, 0.90 cm heartwood. Sapwood moisture fraction (dwb) (A) 0.5, (B) 1.0, (C) 1.5.

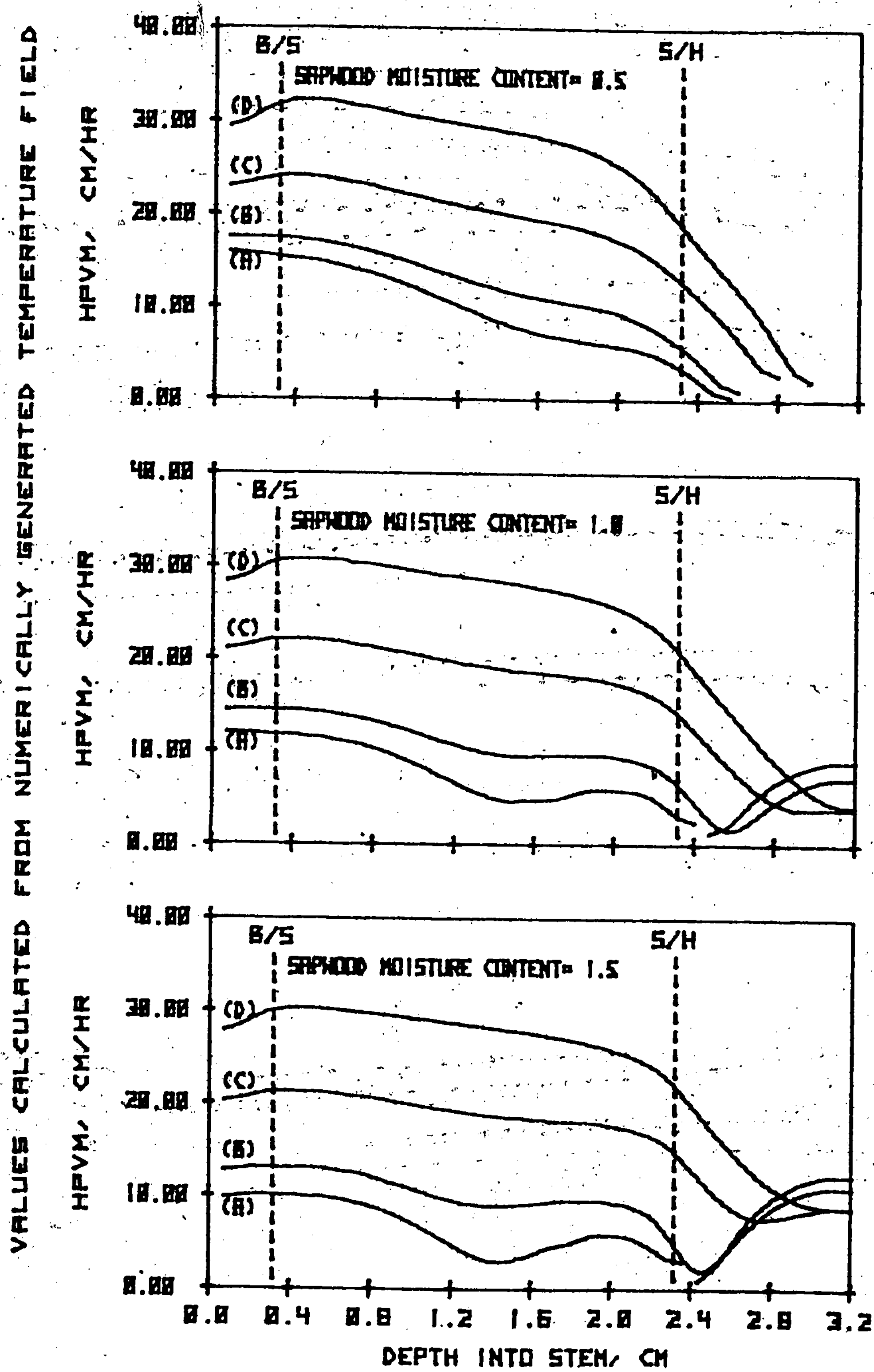

Figure 22. Influence of stem tissue borders on HPVM calculations. Radial-longitudinal model with 0.32 cm bark, 2.00 cm sapwood, 0.90 cm heartwood. HPVM's at HPVI's = (A) 5.0, (B) 10.0, (C) 20.0, (D) 30.0 cm/h.

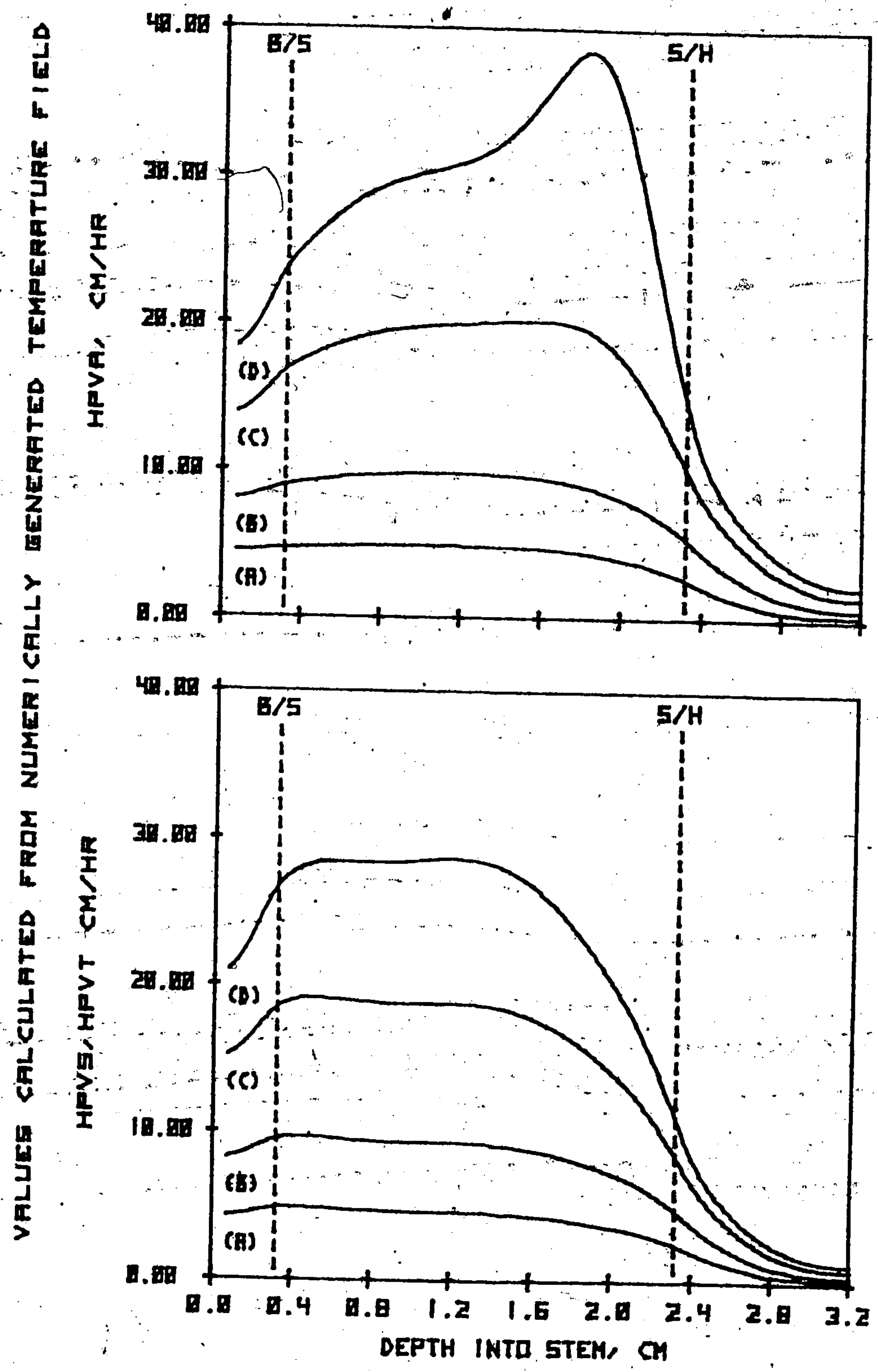

Figure 23. Influence of stem tissue borders on HPVA, HPVS and HPVT calculations. Radial-longitudinal model with 0.32 cm bark, 2.00 cm sapwood, 0.90 cm heartwood. HPVA and HPVS at sapwood moisture fraction 1.0. HPVI's = (A) 5.0, (B) 10.0, (C) 20.0, (D) 30.0 cm/h.

the same as imposed only for the 0.1 cm of sapwood between 1.2 and 1.3 cm depth at all moisture contents, and only between 0.7 and 1.3 cm at Mgw = 1.0 or 1.5. HPVM is defined over the entire sapwood at Mgw = 0.5, but is erratic and/or imaginary at depths greater than 1.2 cm at Mgw = 1.0 or 1.5. HPVA calculates close to zero over the entire sapwood.

At HPVI's from 5 to 30 cm h^{-1}, HPVM is inconsistent (Fig. 22). It ranges from that imposed at 30 cm h^{-1} near the bark/sapwood border to near zero at 5 cm h^{-1} just inside the heartwood. HPVA is again "humped" at HPVI = 30 cm h^{-1} near the sapwood/heartwood border (Fig. 23). HPVS behaves much as it did in the 3.0 cm sapwood simulations.

<u>Case 6e, 0.32 cm bark, 1.0 cm sapwood, 1.1 cm heartwood</u>

These results are shown in Figure 24, Figure 25 and Figure 26. At HPVI = 0 (Fig. 24), calculated longitudinal diffusivity never approaches steady values anywhere in the sapwood. HPVM's are defined but do not have the same value as those imposed. HPVA's are still relatively stable.

At HPVI's from 5 to 30 cm h^{-1}, HPVM's (Fig. 25), show much the same pattern as that found in the two greater sapwood thicknesses. HPVA and HPVS (Fig. 26), are also much as in the previous figures.

<u>Case 7, 0.32 cm bark, 3.0 cm alternate early-latewood, 0.68 cm heartwood</u>

Alternate 0.08, 0.12 and 0.20 cm wide layers of earlywood (EW) and latewood (LW) were imposed in the sapwood in the same general configuration as case 6c. This 50:50 ratio provided

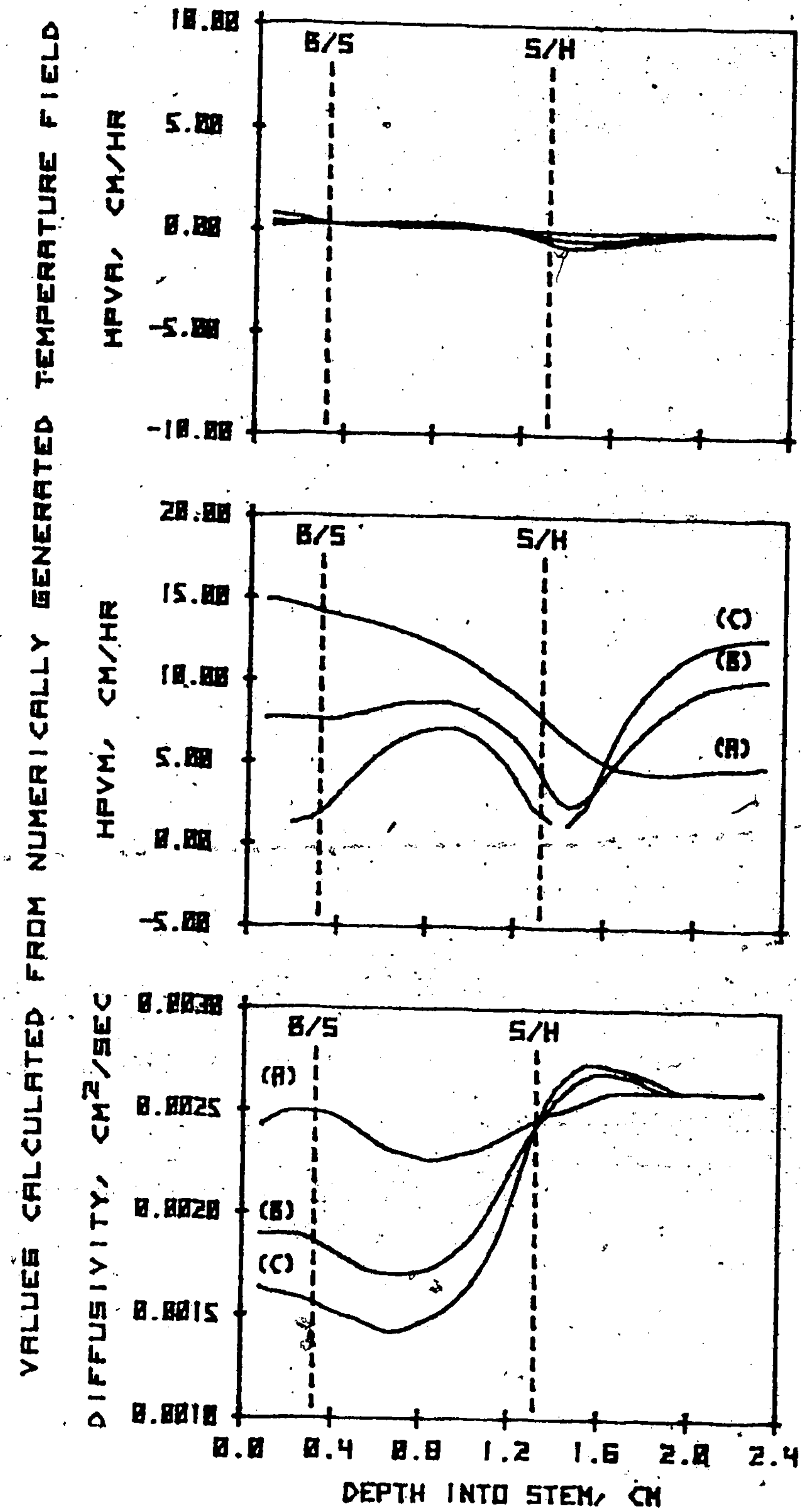

Figure 24. Influence of stem tissue borders on heat pulse calculations of longitudinal diffusivity, HPVM and HPVA at HPVI = 0. Radial-longitudinal model with 0.32 cm bark, 1.00 cm sapwood, 1.10 cm heartwood. Sapwood moisture fraction (dwb) (A) 0.5, (B) 1.0, (C) 1.5.

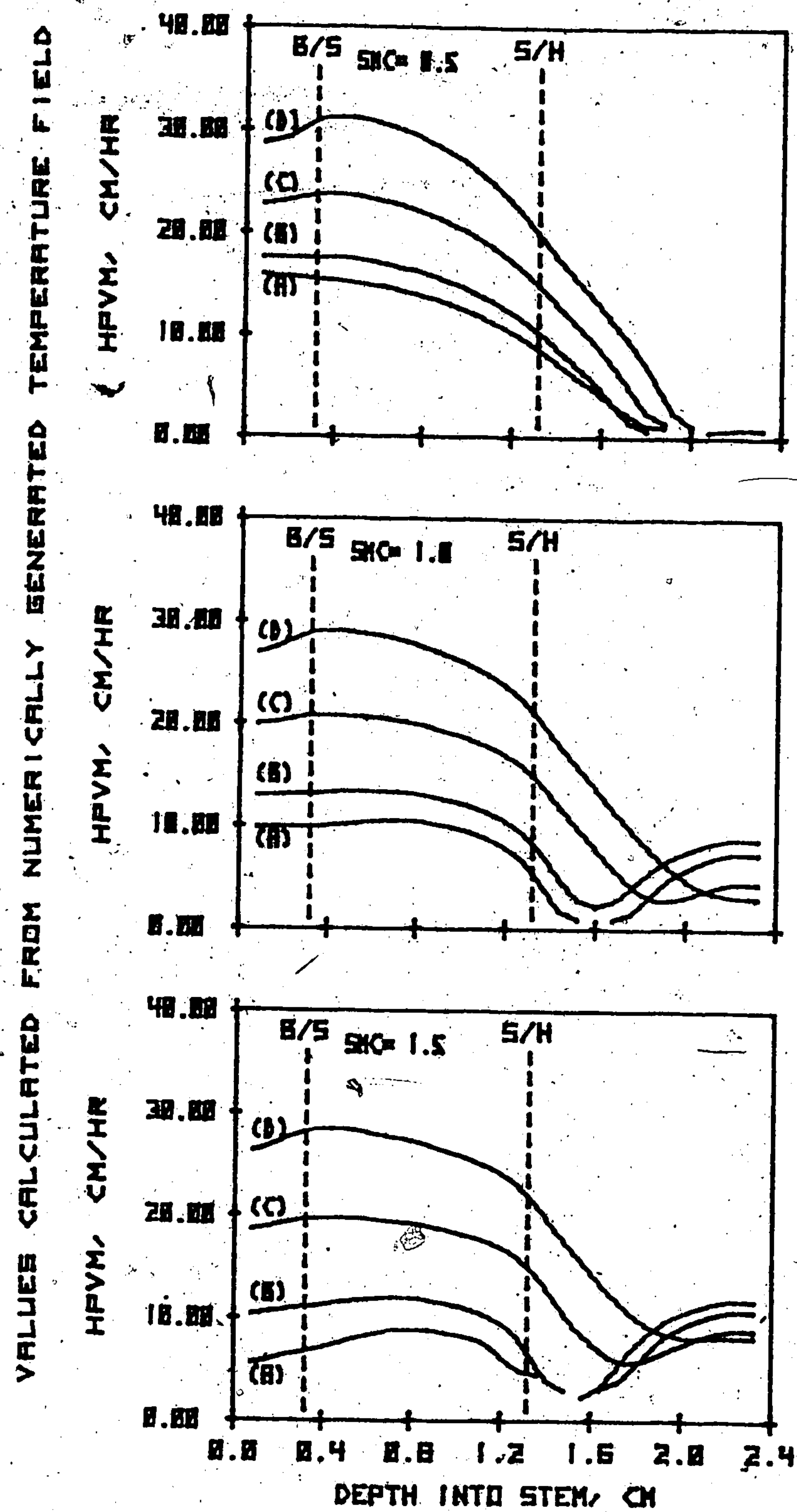

Figure 25. Influence of stem tissue borders on HPVM calculations. Radial-longitudinal model with 0.32 cm bark, 1.00 cm sapwood, 1.10 cm heartwood. HPVM's at HPVI's = (A) 5.0, (B) 10.0, (C) 20.0, (D) 30.0 cm/h.

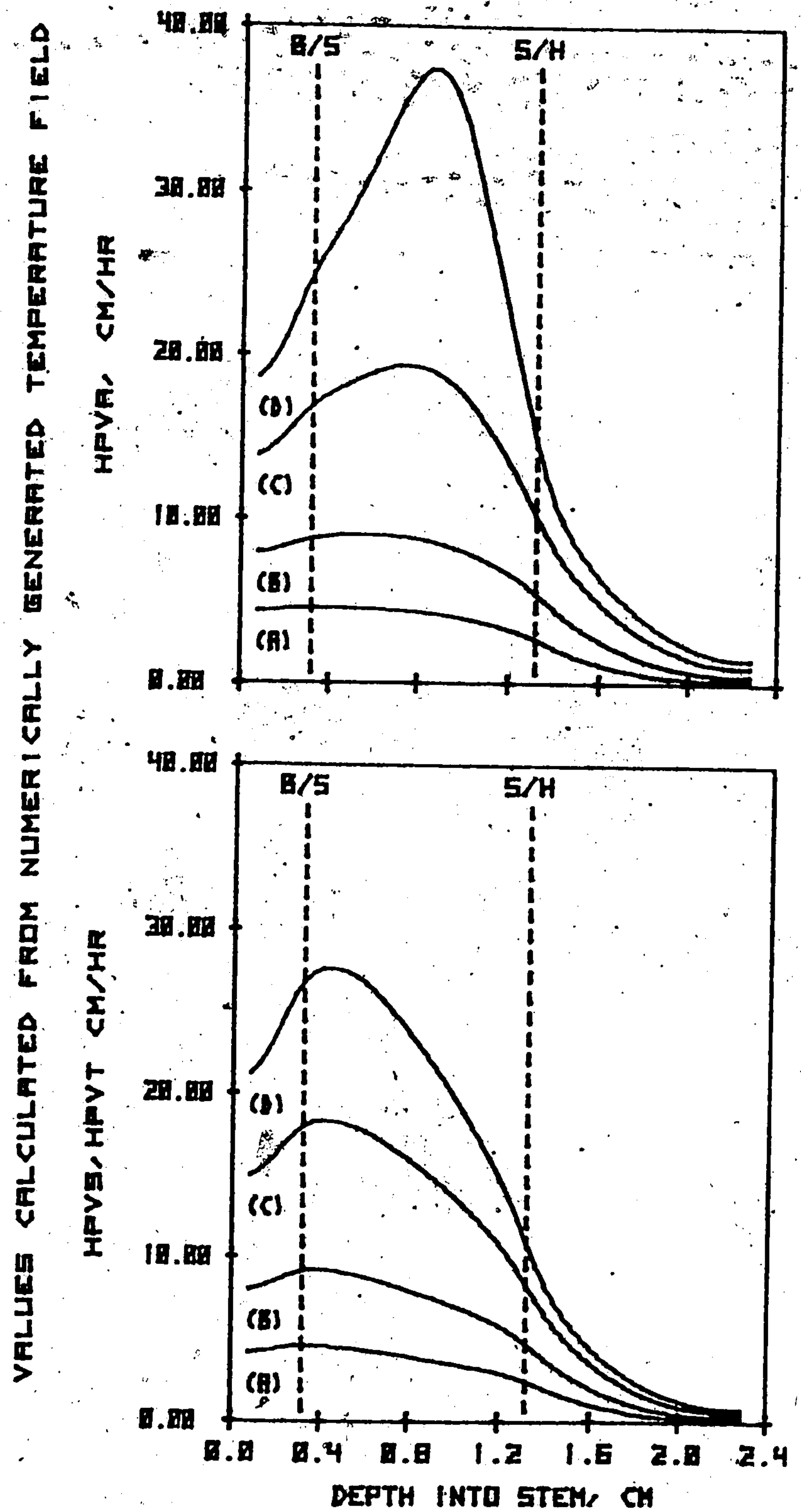

Figure 26. Influence of stem tissue borders on HPVA, HPVS and HPVT calculations. Radial-longitudinal model with 0.32 cm bark, 1.00 cm sapwood, 1.10 cm heartwood. HPVA and HPVS at sapwood moisture fraction 1.0. HPVI's = (A) 5.0, (B) 10.0, (C) 20.0, (D) 30.0 cm/h.

a slightly higher higher percentage of latewood than found in many North American conifers (Cown and Parker 1978). As such, these simulations represent the worst case conditions that should be encountered in woods where the latewood width is 0.20 cm or less. According to Booker and Kininmonth (1978), the liquid permeability of latewood is very near zero compared to earlywood. Thus the HPV imposed on the earlywood was HPVI; in the latewood, HPVI was set at zero. The average HPVI across the sapwood was therefore HPVI/2.

The results at all three EW:LW dimensions were identical. Calculated HPV's were one-half those imposed on the earlywood, i.e., exactly the true average. Except for this averaging effect, the plottings (which are not shown) were identical to those of Figure 18 to 20.

General conclusions from Case 6

Sensors must be emplaced at least 1 to 1½ cm deeper than the bark-sapwood interface and not closer that 1½ to 2 cm to the sapwood heartwood interface to approximate idealized conditions. This effectively rules out application of line heat source idealized heat pulse theory to ring porous stems of any size, and to the stems of seedlings or small saplings regardless of wood structure.

HPV's are a better indicator of imposed heat pulse velocities near the B/S border than they are at the S/H border. An explanation for this apparently ~~lies~~ in the amount of heat lost to the "outside" compared to that lost to the heartwood. Figures 14 and 15 tend to substantiate this line of reasoning.

In Figure 14, the heat loss from the inner border of the sapwood is zero and the calculated HPV's are the same as imposed. Likewise (Fig. 17), the heat loss from the sapwood to the "outside" is zero with comparable results. The sensitivity of the radial longitudinal model to outside border boundary conditions will probably make it difficult to exactly simulate real sensor installations, where the external heat losses can only be estimated within perhaps ± 100%.

Simulations with the radial longitudinal model indicate that relationships between the analytical solutions and imposed HPV or D^1, which are specific to the depth from bark and/or distance from the sapwood/heartwood interface, must be used if valid results are to be obtained from sensors emplaced within 1 to 2 cm of these tissue borders. Even with such specific solutions, HPVM (and HPVP) would not be usable much below HPVI = 20 cm h^{-1} in the near-border sapwood regions.

The "humped" behavior of HPVA at high HPVI's near the sapwood heartwood border casts some doubt as to its usefulness. The HPVT analysis method gives consistent results at all HPVI's (greater than about 5 cm h^{-1}) and at all radial positions. The HPVS configuration appears to be the most consistent at all depths sapwood thicknesses and HPVI's, but one may have to resort to 30 s time intervals to implement this technique. Although numerically generated temperature data are usable for HPVS at any HPVI, Marshall (1958) indicated that it was practically usable only up to a ratio of Td/Tu of 20, presumably because the quantity of heat reaching the upstream sensor becomes marginally detectable at these faster speeds. With sensors spaced (-1.0,0.1.0 cm), a ratio of 20 corresponds to an HPVS of 16 to 25 cm h^{-1} when D^1 varies from 0.0015 to 0.0024 as in the simulations above. These values for HPVS are marginally into the range where HPVM's may be usable for the higher HPVI's.

Summary and conclusions from the general simulations

A tangential longitudinal section through heat pulse probes, and a radial longitudinal section in the plane of the probes have been used to approximate a 3-dimensional heat and sap flow system representative of the implanted heat pulse method in a tree stem. The temperature fields that are created in stem sections in which heat pulse probes are emplaced were simulated using a numerical finite difference approach. These temperature fields were then analysed using an analytical solution for the idealized case of heat transport by coupled diffusion and convection in an infinite medium. The resultant calculated heat pulse velocities or thermal diffusivities are displayed in tabular or graphic form for comparison of the numerical simulation results against imposed heat pulse velocities and thermal diffusivities.

Both the tangential longitudinal and radial longitudinal models adequately represented the idealized case. Numerical simulations of the idealized cases reproduced the imposed values within acceptable limits set by the presence of truncation errors in the finite difference approximations.

The simulations of any departure from the idealized case, resulted in calculated heat pulse velocities different from those imposed. The most serious departures were those caused by nonconvecting material in the plane of the sensors, and at the junction of stem tissues, such as at the bark/sapwood and sapwood/heartwood interfaces.

An inescapable conclusion resulting from these analyses is that a heat pulse method, based solely on idealized heat transport theory for a line heat source, cannot be used to estimate sap flux to an acceptable accuracy in any practical situation. Solutions to the heat transport equation must be specific to the instrumentation and to the general anatomical characteristics and thermal properties of the stem into which the heat pulse probes are emplaced. The degree to which the simulated results can be expected to provide an accurate link between analytical theory and practical application, is reported in Chapter V.

CHAPTER V

APPLICATION OF NUMERICAL ANALYSES RESULTS

Introduction

The ultimate test of these new analyses is in their application to measurement of transpiration in diffuse porous and coniferous trees. Transpiration, considered here as equal to total sap flow expressed either as a rate or periodic summation, is the sum of the sap flow calculated for the torodial partial areas associated with each HPV sensor, or group of sensors, if several are installed at multiple depths into the sapwood (Fig. 27a). Wood basic density, Pb, and sapwood moisture fraction, Mgw, can be obtained destructively for each partial area or as an average common to all.

A quantitative test demands not only that one be able to determine true heat pulse velocities at any given point in a stem cross section to an acceptable accuracy, but that the sapwood moisture content, basic wood density and the sap conducting area be measureable to comparable accuracy. To determine true HPV's, one must have at his disposal, relationships that can be used to correct the measured HPV's for wound and position of the sensor tips. To evaluate such a quantitative comparison, one must also have an independent measure of the actual transpiration of known accuracy.

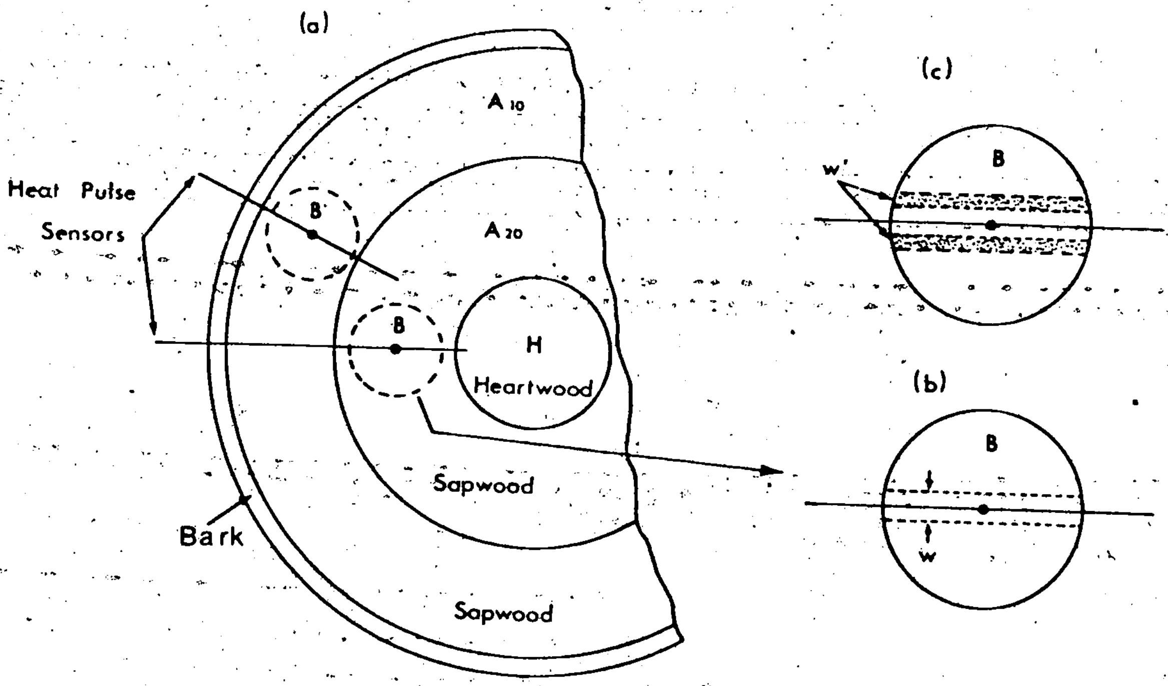

Figure 27. Schematic representation of the toroidal area and initial and subsequent wound widths associated with each heat pulse velocity probe installation. (a) Toroidal areas A_{10}, A_{20} associated with sensor tips at 1 and 2 cm depths, d, from the B/S interface. (b) Initial wound width upon probe implantation. (c) Increase in wound width as tree responds to isolate the damaged tissue.

HPV instrumentation

To a large degree, the type of experimental verification that can be done depends upon the type of instrumentation available for determining heat pulse velocities. Prior to 1981 (that is about two-thirds of the way through this study), the only instrumentation that I had access to, indicated or recorded temperature difference (Td - Tu) and tz used to calculate HPVT's (Swanson 1962, 1967b, 1974a). All but the most recent experiments reported below are of applications of HPVT data. During 1980 - 1981, a microprocessor controlled 16-channel digital "HPV logger" was constructed to record the relative temperature registered at an upstream and downstream sensor at times 60, 120 and 180 s after a heat pulse. Temperature rise data can be used to calculate HPVA, HPVM and D^1 or HPVS, HPVM and D^1 depending upon the configuration of the sensors. Neither HPVT nor HPVP can be obtained from these discrete time-temperature data.

As a result of this late instrument development, the number of HPVT data sets available far exceeds that of the latter type. In addition the "best" tree cross sections in terms of meeting the idealized criteria for sapwood thickness are with HPVT data sets. This is unfortunate as HPVT's less than about 2.0 cm h^{-1} and diffusivities (which might prove useful to provide a continuing estimate of moisture content for sap flux calculations) are not available for them.

Situations and results to be examined

The numerical solutions of the two models at various imposed conditions displayed in Chapter IV provide quantitative relationships between imposed and calculated heat pulse velocities. These relationships are testable to the extent that the models represent real situations encountered in heat pulse applications. Because of the sparseness of complete "transpiration" data sets, which would include HPV's, D^1's or sapwood moisture content and sapwood area, it is my intent to verify the model predictions that involve only heat pulse velocities and then to tackle the larger task of comparing calculated and measured transpiration. In this chapter I will thus examine the following:

1. Instrumentation and/or practice aimed at integrating HPV across the sapwood, ascertaining sap flux or area for which there are sufficient experimental data to compare with the numerical simulations from Chapter IV or those of simulations specific to the instrumentation in question.
2. Empirical studies of measured transpiration and comparisons of heat pulse velocities where the idealized conditions were most closely met, i.e., those where the sensors were emplaced at least 1 cm into sapwood of radial cross section 2 cm or greater.
3. Results of quantitative comparisons where the idealized conditions were marginally met, i.e., sapwoods less then 2 cm wide in radial cross section.

EXAMINATION OF INSTRUMENTATION AND PRACTICE

Heat pulse duration

According to Marshall's (1958) idealized theory, the heat pulse used should be instantaneous. Most workers have interpreted "instantaneous" rather loosely. Considering reports of application of both Huber's (1932) and Marshall's (1958) techniques, heat pulses ranging from 1 to 40 s have been considered instantaneous with the majority less than 10 s, i.e: 1 s (Swanson 1962; Edwards 1980; Miller, Vavrina and Christensen 1980); 1 to 2 s (Decker and Skau 1964); 1 to 10 s (Huber and Schmidt 1937); 2 s (Gifford and Frodsham 1971; Morikawa 1972); 4 s (Hinckley 1971b); 8 s (Bloodworth, Page and Cowley 1955); 10 s (Heine and Farr 1973) and 40 s (Ladefoged 1960). All of those cited considered their results to be satisfactory.

I simulated the effect of heat pulse durations ranging from 1 to 10 s using the tangential-longitudinal model, sapwood moisture fraction Mgw = 1.0, glass sensors, brass heater and 0.20 cm wound. Heat pulse durations of 1 to 4 s have minor effect (less than 5%) on HPVA's or HPVS's at all imposed HPV's, and above HPVI = 10 cm h^{-1}, minor effect on HPVM's and HPVP's as well (Table 13). Longitudinal diffusivity at HPVI = 0 decreased by 6% at heat pulse length 4 s and calculated values for D^1 at all HPVI's are 5 to 15% lower for heat pulse durations of 6 to 10 s than those for 1 to 4 s. I did not attempt the 40 s heating duration of Ladefoged (1960) as his technique

Table 13. Effect of heat pulse duration on HPVA, HPVM, HPVP, HPVS, HPVT and D^1 at wound = 0.20 cm, TLM simulations. Glass sensors, wood moisture =1.0, basic density =0.4. Values for HPVM, HPVP indicated "im", are square root of a negative number. Values marked "--" mean that tz or tp not reached during 180 s simulation time.

	Heat Pulse Duration = 1.0 s						Heat Pulse Duration = 2.0 s					
HPVI	HPVA	HPVM	HPVP	HPVS	HPVT	D^1	HPVA	HPVM	HPVP	HPVS	HPVT	D^1
00	-0.3	im	im	0.0	--	.0018	-0.2	im	im	0.0	--	.0018
05	3.0	im	im	2.9	--	.0017	3.0	im	im	2.9	--	.0017
10	5.9	5.0	3.3	5.6	5.9	.0017	5.9	5.4	3.0	5.6	5.9	.0017
20	10.6	12.9	11.4	10.4	10.3	.0016	10.5	13.0	11.7	10.2	10.3	.0016
30	14.3	19.7	18.3	14.1	13.9	.0015	14.2	19.7	18.5	14.0	13.9	.0015
40	17.4	25.6	24.8	17.1	17.6	.0014	17.3	25.6	24.1	16.9	17.3	.0014
50	20.3	30.9	30.2	19.6	20.6	.0014	20.0	30.8	29.3	19.3	20.1	.0014
60	23.1	35.6	35.1	21.8	23.4	.0014	22.9	35.5	34.0	21.5	22.7	.0013

	Heat Pulse Duration = 4.0 s						Heat Pulse Duration = 6.0 s					
HPVI	HPVA	HPVM	HPVP	HPVS	HPVT	D^1	HPVA	HPVM	HPVP	HPVS	HPVT	D^1
00	-0.1	3.0	im	0.0	--	.0017	0.0	4.5	4.0	0.0	--	.0017
05	3.1	3.0	im	2.8	--	.0017	3.2	4.4	2.6	2.7	--	.0016
10	5.8	6.2	5.2	5.4	5.8	.0016	5.8	7.0	5.9	5.2	5.8	.0016
20	10.3	13.2	12.5	9.9	10.0	.0015	10.2	13.4	12.6	9.6	10.0	.0015
30	13.9	19.6	18.3	13.6	13.5	.0014	13.6	19.6	18.9	13.1	13.5	.0014
40	16.9	25.4	24.5	16.4	16.9	.0014	16.6	25.2	24.1	15.9	16.6	.0013
50	19.7	30.5	29.7	18.8	19.6	.0013	19.2	30.2	29.0	18.2	19.2	.0013
60	22.3	35.1	34.4	20.9	22.2	.0013	21.8	34.8	33.5	20.2	21.6	.0013

Units: HPV cm h^{-1}, D cm^2 s^{-1}

Table 13. Continued.

HPVI	Heat Pulse Duration = 8.0 s						Heat Pulse Duration = 10.0 s					
	HPVA	HPVM	HPVP	HPVS	HPVT	D[1]	HPVA	HPVM	HPVP	HPVS	HPVT	D[1]
00	0.2	5.6	5.0	0.0	--	.0016	0.4	6.6	5.8	0.0	--	.0016
05	3.2	5.6	4.9	2.6	--	.0016	3.2	6.5	5.7	2.5	--	.0015
10	5.8	7.6	7.2	5.1	5.8	.0015	5.8	8.3	7.7	4.9	5.8	.0015
20	10.0	13.6	12.7	9.3	9.8	.0014	9.8	13.8	13.4	9.0	9.8	.0014
30	13.4	19.6	18.7	12.7	13.1	.0014	13.1	19.6	18.6	12.3	13.1	.0013
40	16.2	25.0	23.8	15.4	16.0	.0013	15.9	24.9	24.1	15.0	15.7	.0012
50	18.8	30.0	28.4	17.6	18.8	.0012	18.4	29.7	28.8	17.1	18.0	.0012
60	21.3	34.4	32.7	19.6	21.1	.0012	20.8	34.0	33.1	20.1	20.6	.0012

Units: HPV cm h^{-1}, D cm^2 s^{-1}

was totally alien to the theoretical analyses in question here; his heat pulse duration is only mentioned to indicate the wide interpretation of "instantaneous."

Sensor configuration

The sensor configurations for the data reported in Figure 6 (p. 50) were simulated (TLM) with glass sensors, brass heater, 0.20 cm wound and configurations (-0.5,0,0.72 cm; -0.5, 0,1.0 cm). In these installations, sensors tips were 1.25 cm from the B/S border, approximately 1.7 to 1.8 cm from the bark surface, and greater than 1.5 cm from the S/H border. This placement is comparable to the 1.6 to 2.0 cm depth in the RLM simulations for 3.0 cm sapwood (Fig. 20, p. 105) where the effects of either stem tissue borders are minimal. The data taken were HPVT's.

The TLM simulations are shown in Figure 28, the corrected experimental data in accordance with these simulations in Figure 29. Each of the 25 pairs of sensors is assumed to sample the same sap flow. Therefore, the HPV values obtained from both should be the same. For the raw data of Figure 6 (p. 50), the mean difference was 2.9 cm h^{-1}, (Student's) $t = 7.93$, $P < 0.01$, indicating a significant difference between HPV data pairs obtained from the two configurations (Freese 1967). By contrast, for the corrected HPV's (Fig. 29), the mean difference is 0.7 cm h^{-1}, $t = 0.51$, $P < .01$, indicating no significant difference between the corrected HPV's.

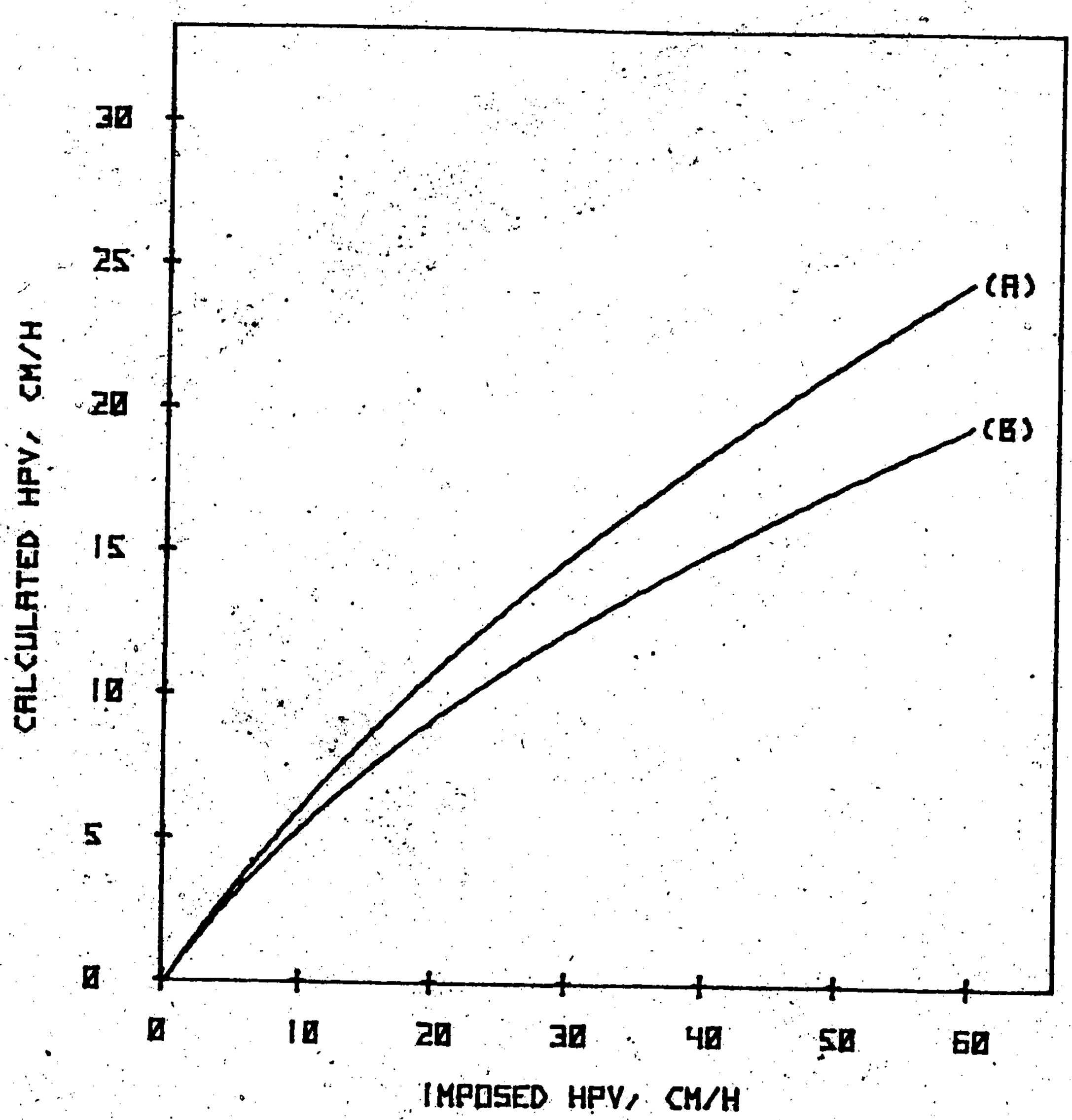

Figure 28. Tangential longitudinal simulation of HPV probes: effect of spacing 0.16 cm diameter glass rod thermistor sensors up and downstream from the heater, both plottings at W =0.20 cm. Sensor spacing (A) (-0.5,0,1.0 cm), (B) (-0.5,0,0.72 cm)

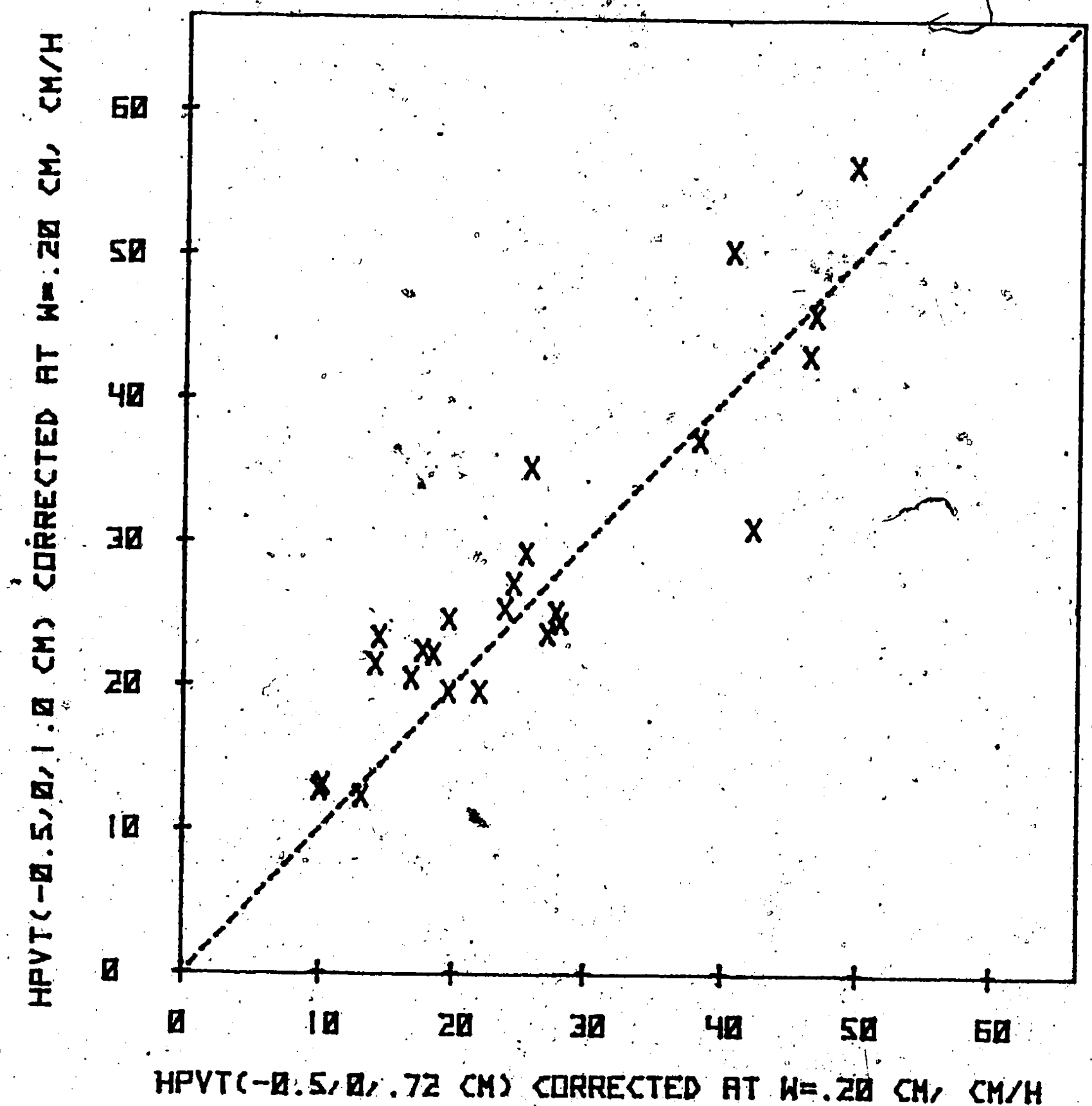

Figure 29. Corrections of Figure 28 applied to experimental data from sensors spaced (-0.5,0,1.0 cm) and (-0.5,0,0.72 cm). For these corrected data, the mean difference is 0.7 cm/h, (Students) t = 0.5, ($P < .01$) i.e., there is no significant difference between the corrected data pairs (cf. Fig 6, p. 50). Dashed line (---) is 1:1.

Effect of wounding

Wound width (width of nonconvecting tissue, W) upon initial installation cannot be less than the diameter of the largest diameter probe (sensor or heater) of an installation (Fig 27b). With painstaking care during installation, one can limit lateral excursion of the holes drilled to approximately ± 0.02 cm of a centerline drawn through the three probes. I always consider minimum wound, with 0.16 cm diameter probes, as 0.16 + 0.04 cm, i.e., 0.20 cm. The ones used in the experiment illustrated in Figure 5, (p. 47) were of 0.16 cm diameter glass materials, installed at 1.7 to 1.8 cm depth from the bark surface in the same trees as in the sensor configuration study above and the same imposed conditions apply except for spacing: all were configured (-0.5,0,1.0 cm).

TLM simulations, specific to the glass materials of these sensors at wounds of 0.20, 0.28, 0.36, 0.44 and 0.52 cm, provide coefficients (Table 20, p. 216; $HPVC = a + bHPVT + cHPVT^2$) for correcting HPVT data at a particular wound width. The wound width increases (Fig. 27c) and the sensors decline in sensitivity with time. At 30 d the ratio of old to current HPVT's is approximately 0.75 and at 100 d or more, 0.5 to 0.6 (Fig. 5, p. 47). Considering the "current" installations at W = 0.20 cm; "old" as those at wounds greater than 0.20 cm, at a mean measured current HPVT of 13.7 cm h^{-1}, a ratio "old" to "current" of 0.75 occurs at W = 0.32 cm, of 0.6 at W = 0.44 cm and of 0.5 at W = 0.52 cm. Wounds widths 0.32 to 0.60 cm were measured at comparable installations in trees in the same vicinity.

Xylem flow structure and sapwood thickness

Heat pulse velocities taken at various depths in the xylem have been used to infer the pattern that a curve drawn through the sap speed at several locations between the cambium and sapwood-heartwood border might exhibit as well as the location of the S/H border (Swanson 1967b, 1974b; Edwards 1980). I reported that sap speed, as indicated by heat pulse velocity, was faster at 1 to 2 cm into the sapwood than near the bark in lodgepole pine and Engelmann spruce (Figure 30A, Picea engelmannii Parry only; from Swanson 1967b). Waring and Roberts (1979) suggested a maximum rate of sap movement at 2-3 cm into the sapwood in Scots pine (Pinus sylvestris L.). Both of these results suggest a "parabolic" type radial distribution.

Practical application of the heat pulse technique to transpiration measurement would be simpler if a parabolic HPV radial depth pattern existed because: 1) fewer sensors would be required to integrate sap flux over the sapwood (Swanson 1970, 1974a); and 2) the position of the sapwood/heartwood border could be inferred from the pattern, so that the sap conducting area of a stem could be derived solely from HPV measurements. Unfortunately, sapwood permeability studies mitigate against such a radial distribution pattern as being consistently present, even in conifer sapwood (Booker and Kininmonth 1978, Booker and

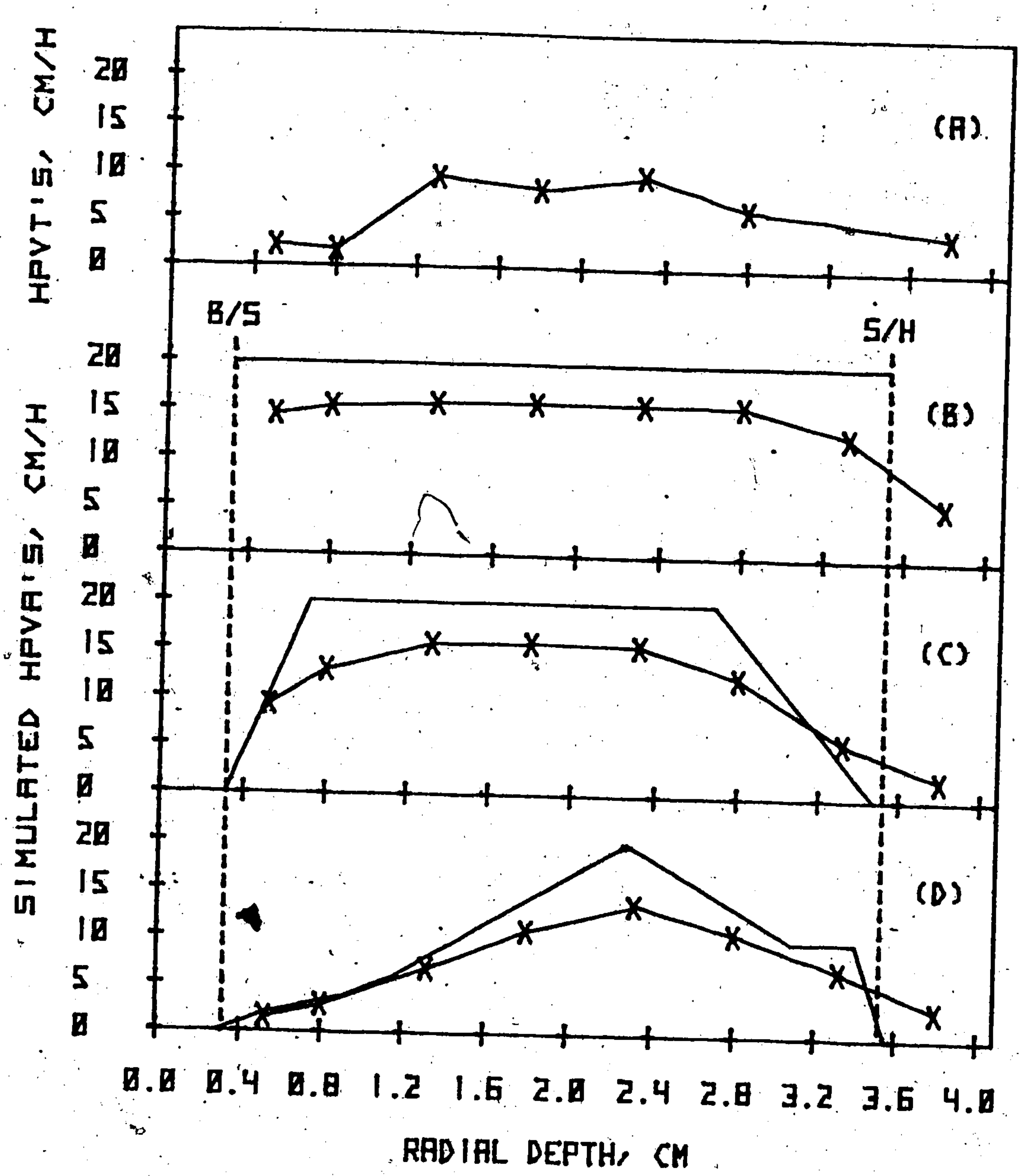

Figure 30. Radial depth profiles of experimental and RLM simulated HPV values obtained with 0.16 cm diameter brass point sensors located at various depths in a stem. (A) Experimental HPVT data, Picea engelmanii, (Swanson 1967b). The position of the S/H border is not indicated on the plotting because it was not determined when the data were taken. (B, C and D) Simulated HPVA data, (——) HPVI; (X——X) HPVA calculated from simulated temperature field.

Swanson 1979). However, a general parabolic pattern of radial sapwood permeability distribution similiar to Figure 30A was found in some sapwoods, and these HPV experimental data are useful to compare with the RLM results from similiar imposed HPV distributions (Fig. 30C and D).

RLM simulations with spherical brass "point" sensors (Swanson 1967) at 0.2, 0.5, 1.0, 1.5, 2.0, 2.5, 3.0 and 3.5 cm depths below the B/S interface, in 3.2 cm thick sapwood at three radial HPVT distributions are shown on Figures 30B, C and D. The experimental HPVT data (Fig. 30A) follow a radial pattern between the two non-uniform ones that were simulated (Fig. 30C and D). Barring major differences in sapwood moisture content at the differing radial positions, sap flux at each sensor is proportional to HPV. The implication of these experimental and simulated results (Fig. 30A, C and D) is that radial depth HPV patterns will resemble true radial depth sap movement patterns. And contrary to the expectations of some, (Kramer and Kozlowski 1979) sap speed in nonporous wood is not always fastest in the sapwood layers just inside the vascular cambium.

The position of the S/H border is unknown for the data of curve A (Fig. 30). And it is fairly clear from the simulated plottings (Fig. 30B to D) that the position of the S/H border would be difficult to discern from the minor change in HPV magnitude that occurs across it. A better indicator of the

S/H border is the radial pattern of liquid permeability across the sapwood. In P. contorta, the saturated liquid permeability of the sapwood was found to be as high one to two growth increments from the heartwood as at any shallower position (Booker and Swanson 1979). A more generally encountered pattern was indicated by the other species studied, (Cryptomeria japonica D. Don, Nothofagus solandri, Pinus montezumae Lamb., P. radiata, Pseudotsuga menzeisii) in which there was a gradual reduction in saturated longitudinal permeability with increasing radial depth to a value of 0.5 to 0.6 of peak permeability at the sapwood/heartwood border where it abruptly dropped to near zero (Booker and Kininmonth 1978, Booker and Swanson 1979). This abrupt change in liquid permeability is probably the best delimiter of the S/H border and the inner extent of sap conducting xylem.

Smoothing effect of sensor materials in radial profile

Upon preliminary work up of the potometer HPV and water uptake data (See Quantitative Comparisons, Hardwood Potometers, p. 168.), it became evident that the low thermal conductivity Teflon sensors installed in these stems (Appendix E) were behaving differently than the higher thermal conductivity glass rod sensors used (Fig. 31B) in most previous experiments (or a brass sensor, Fig. 31C, used in one instance; Pinus banksiana Lamb.). The data from a Teflon sensor, with tip placed in the heartwood, indicated an HPVA much closer to zero than that obtained with either the glass or brass sensors (Fig. 31).

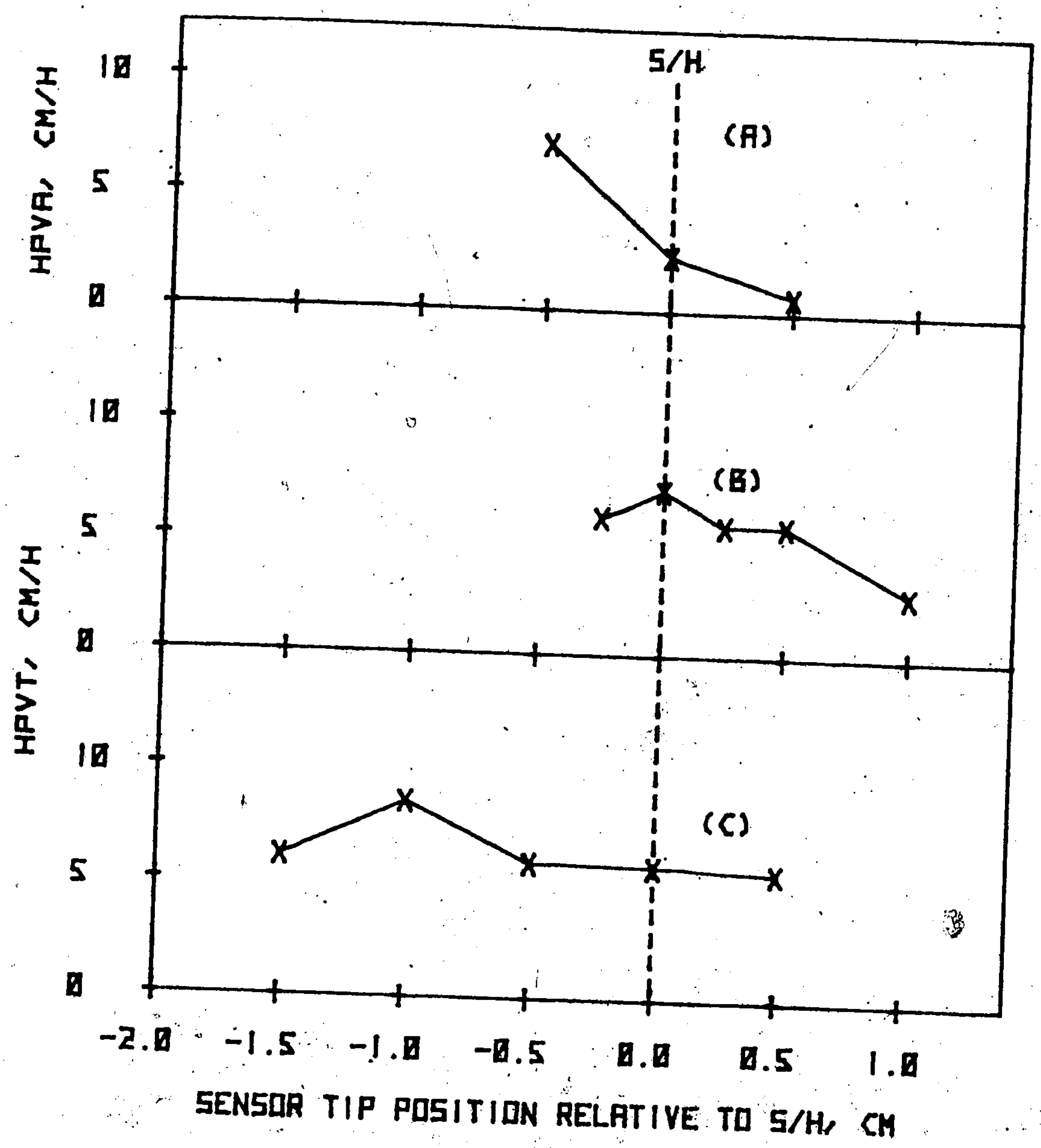

Figure 31. Experimental data obtained with (A) low thermal conductivity Teflon sensors in _Populus tremuloides_ Michx. (B) high thermal conductivity glass in _Picea glauca_ (Moench) Voss and (C) brass rod sensors in _Pinus banksiana_. Sensors emplaced at several positions relative to the S/H border. Note that HPV's from both glass and brass sensors are much the same magnitude within 0.5 cm on either side of the S/H border, and that none of them indicate HPV = 0 on the heartwood side of this border.

I undertook a few RLM simulations, with sensor materials along the entire radius from the outside border to the tip, to see if the observed data could be at least qualitatively described with this model.

The "no sensor" RLM simulations are for points, not planes, and are thus valid simulations of a physically realistic system. When probe materials lie along a radius, the RLM simulates each probe as a plane in the xylem cross section, not a line as it is in fact. Although the representation of the probes in this way is physically unrealistic and the absolute magnitude of the HPV's derived from the simulated temperature data is too low, the relative magnitude of HPV's obtained at differing positions along a radius from the RLM simulations with sensor materials, is apparently correct (Fig. 32). The relative change in HPVS, HPVT or HPVA magnitude across the S/H border in the "no sensor" and Teflon materials simulations (Fig. 32A,B) is on the same order of magnitude as the experimental data obtained with Teflon sensors (Fig. 31A). All of the higher thermal conductivity material simulations (Fig. 32C,D,E) are similiar to the experimental data for glass or brass sensors (Fig. 31B and C). These simulations and experimental data indicate that HPV's measured within 0.5 cm of either side of the S/H border will be more indicative of movement in the sapwood than the lack of movement in the heartwood. The high thermal conductivity materials tend to smooth out the abrupt transition

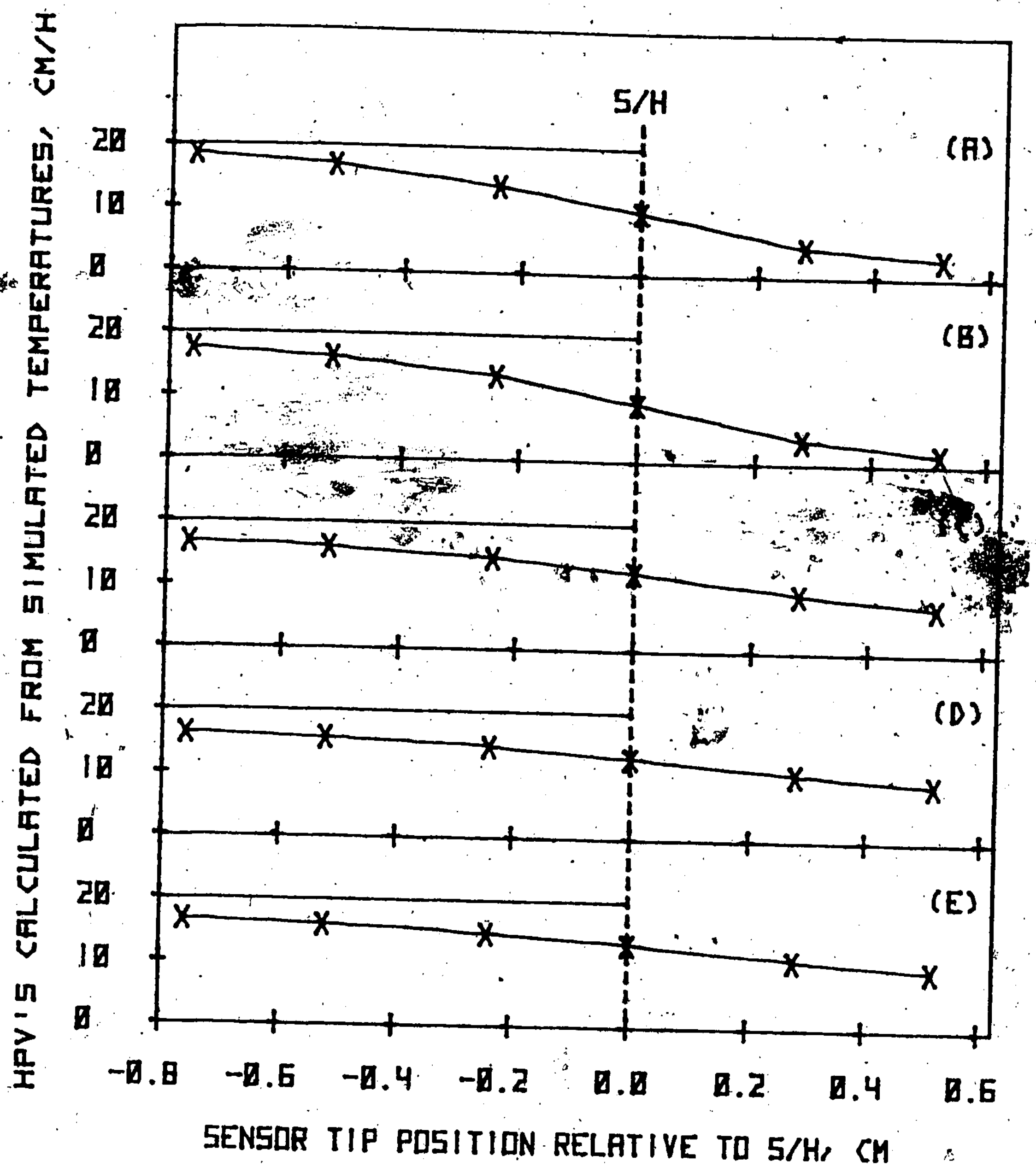

Figure 32. Radial longitudinal model simulations with several sensor materials. (A) no sensor material, (B) Teflon, (C) glass, (D) brass, (E) aluminum. HPVI (——); HPVA (X——X). These simulations tend to confirm the experimental results (Fig. 31) obtained using similiar sensor materials. The high HPVI's of the sapwood are indicated by HPVA's at the high thermal conductivity sensors 0.5 cm or more into the heartwood. The low thermal conductivity Teflon sensor behaves similiarly to the no sensor simulation (A). None of the simulations indicate that the S/H border would be clearly defined by a sharp decline in HPV's measured near it.

at the border. Thus corrections to HPV's, obtained from sensors positioned near the S/H border, may be less important for high thermal conductivity material sensors than for those constructed of low thermal conductivity materials.

HPVM's at low HPV's

The extreme sensitivity of the HPVM and HPVP solutions to outside border conditions, (Fig. 12, p. 92; Fig. 18, p. 103, etc.), was a surprise to me. Marshall (1958) indicated that the sensor needed to be embedded 0.5 to 1 cm below the surface to minimize the effect of unknown heat losses on the temperature rise data. I expected erratic performance for the HPVM configuration at these shallow depths as Marshall (1958) indicated that the square of the heat pulse velocity values were ± 10, giving a probable error of 3 to 4 cm h^{-1}. In Figures 12, 18, etc., HPVM's are much greater than 3 to 4 cm h^{-1} at all depths less than 1.6 to 2.0 cm. At Mgw = 0.5, HPVM's are between 10 and 15 cm h^{-1} and at Mgw = 1.5, they are generally between 5 and 10 cm h^{-1}.

The availability of the 16-channel HPV logger made it possible to experimentally test these simulated results. In the first test at HPV = 0, sixteen Teflon sensors were installed in a bolt cut from a standing dead tree (Mgw = 0.2 to 0.4; SWT 1 - 2 cm) and in a bolt of green wood (Mgw = 0.7 to 1.0; SWT 4 - 5 cm), both *Pinus contorta*. The sensors were initially installed to a depth of 3.0 cm from the bark surface, read 3 to 4 times at 1-hour intervals, then withdrawn by 0.5 cm to a depth of 2.5 cm, read for 3 to 4 hours and so forth to a final depth of 0.5 cm.

The experimental results are superimposed upon RLM simulated curves in Figure 33A, standing dead, and Figure 33B, green. In the "dead" log, all of the HPVM's measured were real (that is not imaginary in the mathematical sense) and lie above the simulated HPVM curve for sapwood moisture fraction 0.5, i.e., in the position one would expect for moisture fractions of 0.2 to 0.3. By contrast, 90% of the HPVM's obtained in the outer 1.5 cm of the green wood bolt were imaginary. The few values that were real fell below the simulated curve at sapwood moisture fraction for Mgw = 1.5, approaching the simulated values obtained with no heat loss to the outside (see Fig. 15, p. 95, HPVM, all plottings). This sensitivity to border heat loss at zero sap movement should be of use in determining boundary conditions to impose in future RLM simulations. Outside border heat loss conditions would be established by varying them until the simulated results approximated the single sensor experimental results.

Data for a second test at slightly higher HPV's, were available as simultaneous measures of HPVA, HPVS and HPVM for the hardwood potometer experiments (See Hardwood Potometers, p. 168). Teflon sensors were installed at 0.2, 0.5, 0.8 and 1.3 cm depths into sapwoods ranging from 1 to 1.4 cm thick.

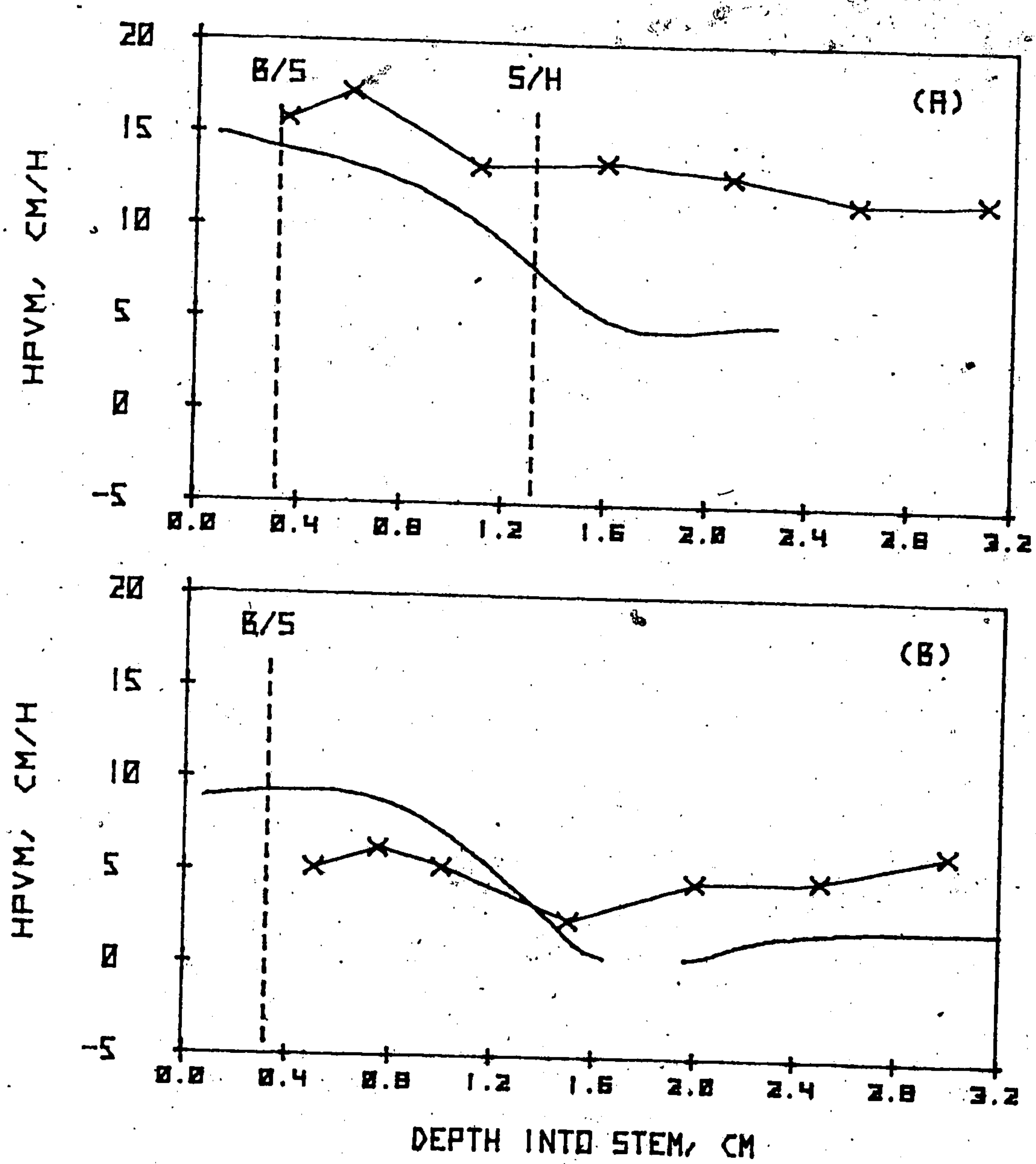

Figure 33. Simulated (RLM) and experimental results with the HPVM one-sensor configuration at zero sap movement in a standing dead dry (A) and green (B) wood bolt. In dry wood (A), where thermal conductivity is relatively low, the experimental results at wood moisture = 0.12 (X———X) lie at approximately the proper magnitude for them in comparison with the simulated result at Mgw = 0.5 (———). In the higher thermal conductivity green wood at Mgw = ca. 0.9 (X———X), the results lie in the wrong position compared to the simulated result at Mgw = 1.5 (———). (Simulations at all moisture contents in boundary situations comparable to these are given in Figure 24, p. 110, and Fig 12, p. 92.)

HPV data were selected from all four trees to cover all depths and a full range of magnitude of transpiration rates from 0 to 120 mL h^{-1}. Hourly sap flow rates calculated from the HPVA and HPVS values were within 5 to 15% of water uptake by the potometer trees.

Over the range of HPVA's and HPVS's encountered in these trees (-2.8 to 17.7 cm h^{-1}), they bear no relationship to HPVM's (Fig. 34). The coefficient of determination (Freese 1967), R^2, at each depth (0.2, 0.5, 0.8 and 1.3 cm) is 0.19, 0.12, 0.00 and 0.11 respectively, which indicates essentially no correlation between the two variables. These data indicate that the single sensor HPVM measurement technique is not usable for estimating transpiration in coniferous and diffuse porous trees where measured HPVA's or HPVS's are generally less than 20 cm h^{-1}.

<u>Accuracy of the HPVA and HPVS sensing configurations at zero flow</u>

The data sets obtained from the green and standing dead wood bolts above were also useful for determing the accuracy of the HPVA and HPVS sensing configurations at zero sap flow. Eight of the 16 sensors in each log were in the HPVA configuration (-0.5,0,1.0 cm) and eight arranged for HPVS (-0.1,0,1.0 cm).

Average HPVA's ranged from -0.81 to 0.66 cm h^{-1} and -0.64 to 1.06 cm h^{-1} at the indicated depths in the green and dry logs respectively (Table 14). Comparable HPVS's were -0.11 to 0.94 cm h^{-1} and 0.08 to 0.75 cm h^{-1}. This range is typical

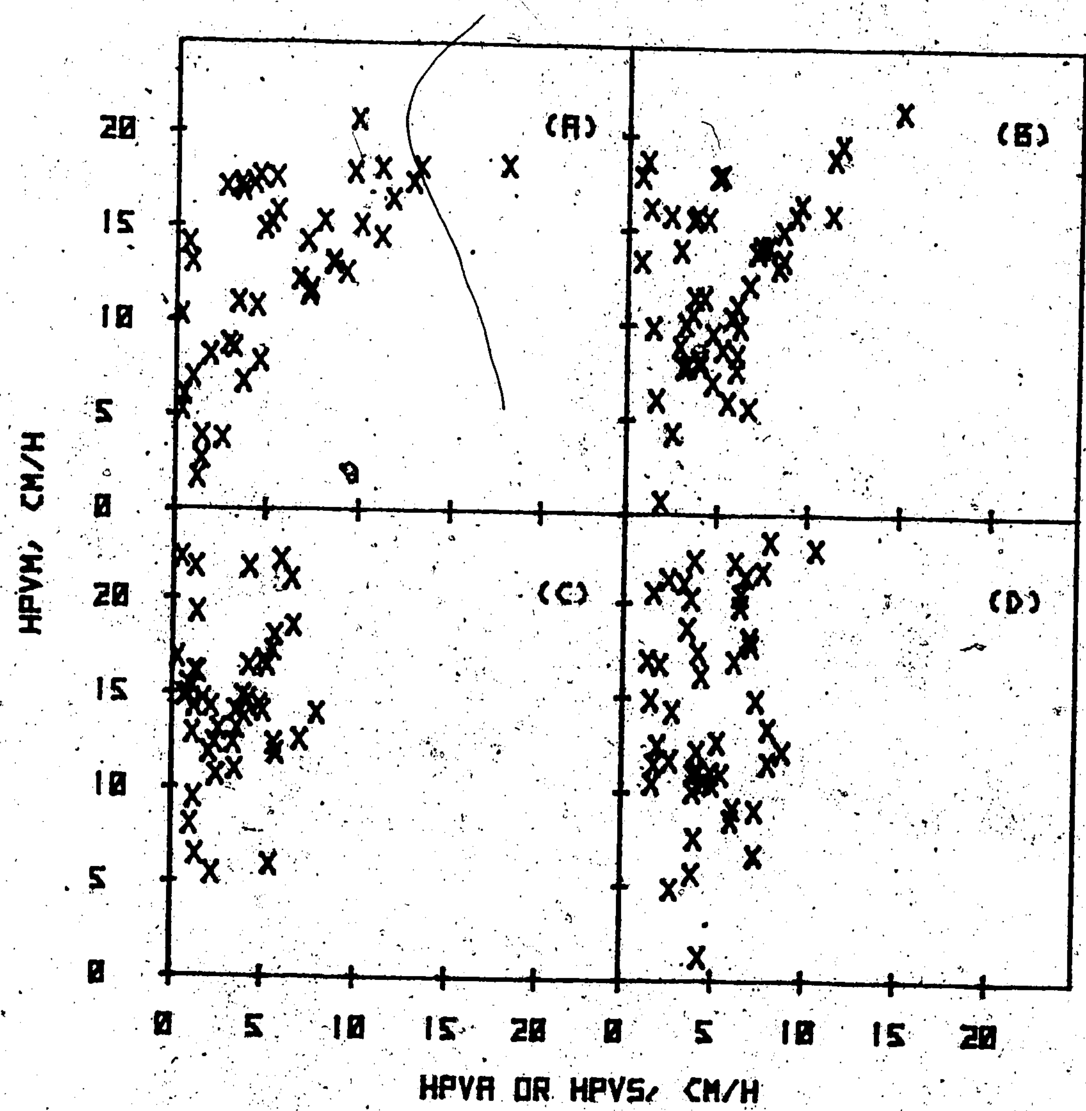

Figure 34. Experimental results using the single sensor HPVM configuration at several sapwood depths where the sap movement was greater than zero. The B/S border is the reference point for the sensor depths. Sapwood thickness was 1 to 1.4 cm. (A) 0.2 cm, (B) 0.8 cm, (C) 0.8 cm, (D) 1.3 cm. There is virtually no correlation between measured HPVA, HPVS values and HPVM's.

Table 14. Accuracy of HPVA and HPVS configurations at zero sap movement. Experimental data taken with 16-channel digital HPV logger. HPVA calculated from temperature data taken at 60 and 120 s; HPVS from temperature ratios at 120 s; longitudinal diffusivities from downstream temperature sensor at 60, 120 and 180 s. Teflon-enclosed thermistor bead sensors. (--) indicates sensor failure; usually replaced for the next depth. HPV's in cm/h.

	HPVA(60/120) at indicated depth, cm							HPVS(120) at indicated depth, cm						
	0.5	0.75	1.0	1.5	2.0	2.5	3.0	0.5	0.75	1.0	1.5	2.0	2.5	3.0
Green *Pinus contorta* bolt														
	-0.5	-0.9	0.3	0.1	0.1	--	--	-0.1	-0.4	-0.2	0.2	0.3	--	0.9
	-1.3	-0.5	-0.2	0.3	0.1	0.5	-0.2	-0.4	-0.1	0.0	0.6	0.2	1.0	0.6
	-2.0	-1.1	0.0	-0.4	0.1	0.1	0.0	-0.7	-0.5	0.0	-0.1	0.2	0.3	0.5
	-1.4	-0.4	-0.1	0.5	0.5	0.6	0.4	-0.5	0.0	-0.2	0.8	0.7	1.1	1.6
	-1.8	-1.4	-0.6	-1.0	-0.3	0.4	0.1	-0.8	-0.1	-0.6	0.1	0.0	-0.2	0.3
	-0.3	-0.6	-0.2	0.3	0.4	0.8	0.9	2.1	1.2	0.7	0.6	0.7	0.9	1.5
	1.1	0.8	0.7	0.8	1.5	1.1	1.8	-0.1	-0.2	0.2	-0.1	0.3	0.8	1.4
	-0.3	-1.3	-1.0	1.3	0.7	0.6	1.6	-0.4	-0.1	-0.3	0.3	0.2	0.1	0.7
Mean	-0.81	-0.68	-0.12	0.24	0.38	0.58	0.66	-0.11	-0.02	-0.06	0.30	0.34	0.57	0.94
$S_{\bar{x}}$	1.02	0.70	0.52	0.70	0.55	0.31	0.29	0.92	0.52	0.36	0.33	0.26	0.51	0.51
Standing dead *P. contorta* bolt														
	-0.8	-0.4	0.0	0.7	0.7	-0.1	-1.3	-1.4	-0.7	0.5	1.0	1.3	1.8	2.1
	-2.1	--	-0.5	0.7	1.0	1.8	--	-0.3	0.2	-0.4	-0.4	-0.5	--	0.0
	-0.4	-0.3	1.0	1.2	1.1	0.2	-0.6	-1.5	-1.5	-0.2	0.8	-1.0	--	--
	2.3	--	1.2	1.7	1.3	0.7	1.0	--	--	-0.1	-0.5	-2.0	--	--
	0.4	-0.6	0.2	0.9	0.7	--	1.6	0.4	0.1	0.5	0.8	0.7	0.8	1.1
	0.0	-1.0	-0.2	1.4	1.0	0.5	0.1	1.8	2.1	-0.1	-0.4	-0.8	-0.9	-1.2
	0.4	-0.8	0.0	0.5	-0.3	-0.7	0.3	1.5	0.9	1.7	1.8	2.1	2.4	2.0
	-0.1	-0.7	0.3	1.3	0.8	0.5	-0.8	0.2	-0.1	0.1	0.2	0.4	0.4	0.3
Mean	-0.01	-0.64	0.25	1.06	0.77	0.44	0.04	0.08	0.15	0.27	0.44	0.26	0.90	0.73
$S_{\bar{x}}$	1.25	0.27	0.59	0.41	0.47	0.77	1.03	1.29	1.13	0.66	0.83	1.29	1.30	1.28

of the few experimental data I have obtained using these analyses. The standard error varies from ± 0.25 to ± 1.02 cm h^{-1} in wood at physiologically relevant moisture contents, and from ± 0.25 to ± 1.30 cm h^{-1} in very dry wood. The standard error in HPVS measurements is slightly less than for HPVA's in moist sapwood, but the data from both configurations are of comparable accuracy.

Errors in HPV's at zero sap flow arise from three sources: 1) an inexact knowledge of the distance of each sensor from the heater; 2) nonuniform thermal diffusivities of the wood intervening between the heater and the up and downstream sensors; 3) longitudinal temperature gradients existing at the time of HPV measurement. The latter two are largely unavoidable. Therefore, these standard errors should probably be applied to all HPV's. ("Probably" because it is virtually impossible to establish uniform sap speeds greater than zero in order to obtain a similiar estimate of errors at higher heat pulse velocities.)

<u>Moisture content from longitudinal diffusivities</u>

As noted in Chapter II, Equation 17 (p. 26) can be used to calculate wood moisture content from measured longitudinal thermal diffusivity and wood basic density. The feasibility of doing so and the accuracy of wood moisture contents derived in this manner has not, to the best of my knowledge, been tested, although the dependence of wood thermal properties on moisture content is well known (MacLean 1956, Siau 1971). The data sets from the 16-channel HPV data logger provided an opportunity for a limited test of this technique here.

Longitudinal thermal diffusivities were available for two aspen and two birch trees (PT1, PT2, BP1, BP2), one spruce lysimeter tree (PG1) and two pine log sections. For each of the above, actual moisture fraction, (dwb), was determined at the end of an HPV data sequence. Moisture contents of the potometer stems and standing dead bolt were determined from four disks obtained at both ends and near the centre of the stem portion containing the HPV probes. The moisture contents of the potometer stems were obtained near, but not directly at, the probes because I needed to preserve these sections so that wound, sensor spacing and sapwood dimensions could be ascertained for calculating transpiration. Moisture content of the green bolt was determined from four sets of 4.5 mm diameter increment borings on the opposite side of the stem from the HPV probes, taken at the start and 72-hours later at the conclusion . In the lysimeter tree, PG1, wood samples at the probes could be excised for moisture content determinations because, shortly after this last set of sensors was installed, the tree failed to resume transpiration (after being held dormant for almost 3 years) and the physical measurements needed to estimate wound, were not needed for these probes.

Calculated, $Mgw(D^1,Pb)$, and actual, Mgw (dwb), moisture fractions (all data) were closely related over their full range (Fig. 35): $Mgw = -0.041 + 1.12Mgw(D^1,Pb)$; $R^2 = 0.8069$, $S_{\bar{x}} = 0.16$. In the range of physiological interest, Mgw = 0.6 to 1.2, the 1:1 line is as good a fit of the data as the least squares regression line. The standard error of 0.16 is not a great deal higher than the normal range one encounters in measuring Mgw from increment cores gravimetrically (unpublished measurements).

Average calculated and measured moisture contents in the spruce lysimeter tree, PG1 were essentially identical and the two values were highly correlated ($R^2 = 0.8547$). The calculated and measured moisture contents at each probe set were generally within 10% of each other.[1/]

QUANTITATIVE RESULTS IN SEMI-IDEALIZED SITUATIONS

Introduction

The radial longitudinal model simulations indicate that

1/ One thing I did note in this test: the average moisture content fraction at 24 probe sets installed 3-years earlier was 0.66 compared to the 0.88 obtained here. This difference could be the result of a gradual drying out of the nonconvecting wood in the plane of the sensors during wound development. The wound at freshly installed sensors in actively transpiring trees is first evident as a lighter colored tissue above and below the probes. Later this lighter tissue may become resin filled, darken and broaden as the tree reacts to the wound. No such lighter colored tissue was noted in the plane of these newly-installed probes presumably because no transpiration was occuring.

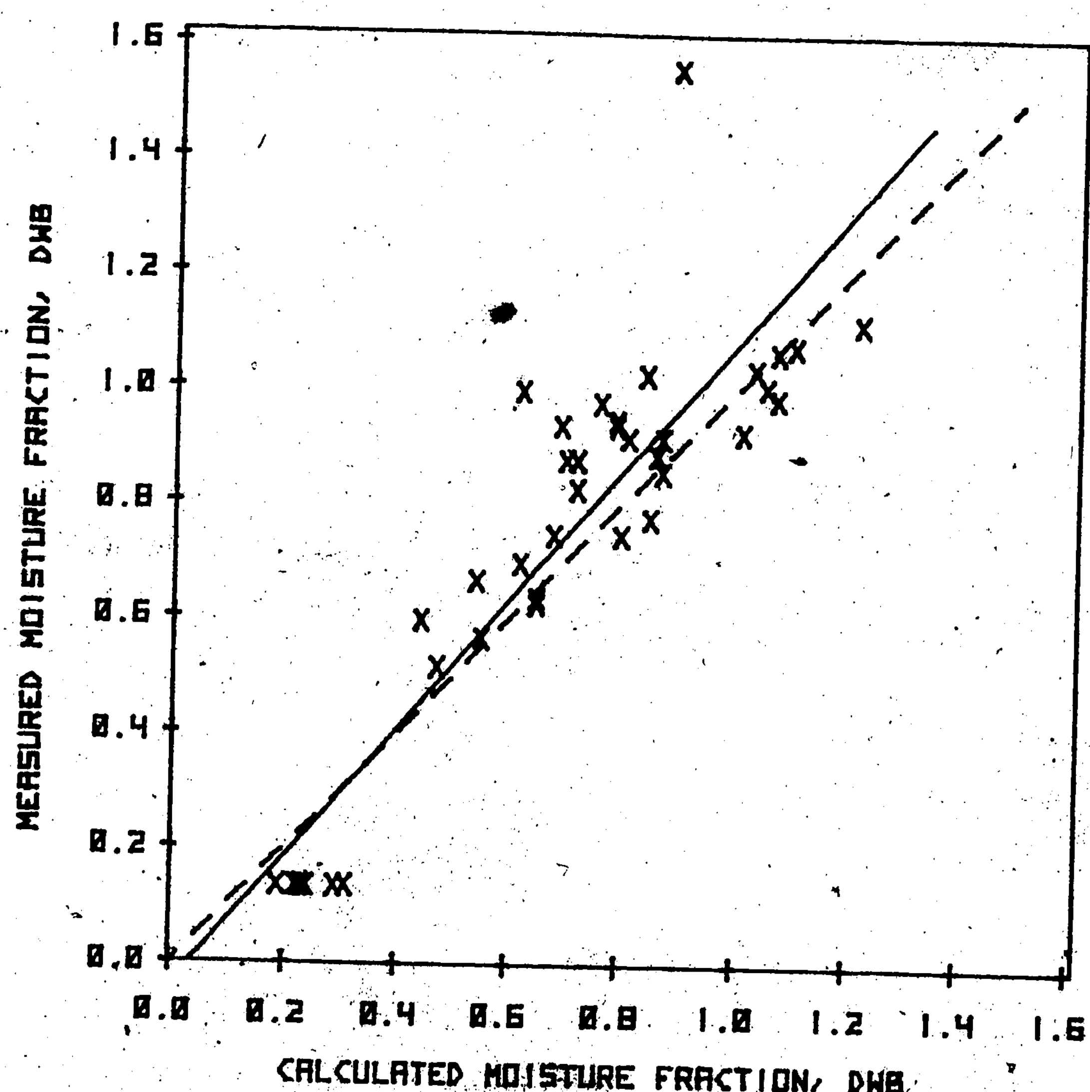

Figure 35. Actual wood moisture content (Mgw) versus that calculated from longitudinal diffusivities and basic wood density, $Mgw(D^1,Pb)$. $Mgw = -0.041 + 1.12\ Mgw(D^1,Pb)$, $R^2 = 0.8069$, $S_{\bar{x}} =$ 0.[illegible]6. Dashed line (---) is 1:1.

HPVS's or HPVT's measured in the sapwood at 1 cm or more from both the bark/sap wood and sapwood/heartwood borders are little influenced by these borders. If this finding also applies to real situations, then corrections for wound and sensor materials, as derived from the tangential longitudinal model, should account for most, if not all, of the departures from theory in these semi-idealized situations.

In cases where the idealized condition has been approached, empirical correlations between HPVT and measured transpiration have generally been excellent. Decker and Skau (1964) reported that hourly sap velocities (actually HPVT's) and hourly transpiration rates measured in a ventilated tent were closely correlated in several partial day determinations in aleppo pine (Pinus halepensis Mill), Utah juniper (Juniperus osteosperma (Torr.) Little) and alligator juniper (J. deppeana Steud). They do not state how closely correlated, but their graphs indicate R^2's of 0.9 or better.2/

Hinckley (1971b) reported similiarly good results (R^2 = 0.83) in 3.0 to 3.5 cm diameter Douglas fir seedlings (Pseudo-

2/ Neither do they state the diameter of the stems nor the placement of the sensors with respect to the S/H border in their article. I have their original HPV data. The stems were 10 to 15 cm diameter and the stainless steel sensor tips were placed at 1 cm depth increments from the B/S interface for 4 cm into a 3+ cm thick sapwood, so that at least 2 of the 4 or 5 sensors emplaced in each tree were relatively free of the border effects.

tsuga menzeisii (Mirb) Franco). HPVT's were compared with transpiration measured by weighing. All of the stainless steel sensors were inserted to the centre of the stem which was presumably all sapwood. Thus the sensor tips were 1.5 cm from the outside, approximating the idealized conditions for application.

Quantitative comparisons

Prior to this study, I conducted three experiments to empirically relate transpiration values calculated from HPV measurements with those obtained from weighing lysimeters with aleppo pine and Monterey pine (*P. radiata*), and one climatized cuvette on New Zealand mountain beech (*N. solandrii* var *cliffortioides*), a diffuse porous hardwood (Maylan and Butterfield 1972). In each of these experiments, the near idealized conditions above were met as at least some of the sensor tips were emplaced in sapwood 1 cm or more from both the B/S and S/H borders.

1. Aleppo pine on a lysimeter (PH1).

This test was carried out at the U. S. Department of Agriculture's Soil and Water Conservation Laboratory at Tempe, Arizona, during the summer of 1967 (Swanson 1972). An aleppo pine measuring 6 cm diameter outside bark, 5 m tall, was grown in a 1 m^3 container of soil. The container was covered with polyethelene to prevent evaporation from the soil, and placed on the Soil and Water Laboratory's lysimeter number 3, which was at ground level in a field adjacent to the main building complex. This lysimeter was capable of detecting weight changes as small as 10 g in a total weight of 3000 kg (van Bavel and Myers 1962). In my application, the permanently installed lysimeter was used as a sensitive weighing platform to detect weight loss as a measure of transpiration by the tree.

An HPV probe set (glass bead thermistors 0.24 cm diameter, 0.16 cm diameter brass heater, spaced -0.5,0,1.0 cm) was installed at mid-xylem depth between the soil and the first live branch. Sapwood thickness at this sensor, 2.3 cm, was taken as the depth at which the moisture fraction declined from approximately 1.2 to 0.4 (dwb), resulting in a sapwood area of 23.1 cm^2. Wood basic density, 0.45 g cm^{-3}, and moisture fraction, 1.21, oven dry weight basis, were determined from disks of the stem taken at this sensor at the conclusion of the study. Sap flux was calculated using Equation 21, i.e., a specific application of Equation 10 (p. 23) to this case, and transpiration (TR) from Equation 22. (In this case with only one sensor set the partial and entire sapwood area were the same.)

$$\text{Sap Flux} = 0.45(0.33 + 1.21)\text{HPV} = 0.69\text{HPV mL cm}^{-2}\text{ h}^{-1} \qquad (21)$$

and

$$\text{TR} = 0.69(\text{HPV})(\text{Sapwood area}) = 16.0(\text{HPV})\text{ mL h}^{-1} \qquad (22)$$

After installation on the lysimeter, the tree was watered for several days until predawn xylem pressure potential (base potential, BP), as measured with a pressure bomb, stabilized at about -1.1 MPa (Scholander, Hammell, Bradstreet and Hemmingsen 1965; Ritchie and Hinkley 1975).[3/]

Water was witheld, HPVT's and weight loss measured until transpiration reduced BP to -3.2 MPa, then the tree was rewatered to BP = -1.2 MPa, and a second cycle of post-drying HPVT's and weight losses were obtained. During the two week duration of the study, daily air temperature averaged 33°C; vapour pressure deficits 22 to 27 mm Hg. Data obtained from days during which rain fell were excluded.

HPVT's were calculated from hourly recorded time-temperature difference traces, using Equation 5 (p. 21), during 4 d of the initial drying period and for 3 d subsequent to rewatering. Transpiration and 24 h weight losses (00 to 23 h) expressed as hourly averages for these 7 d are plotted on Figure 36. Transpiration has been calculated using both uncorrected HPVT's (open squares), TR(00), and corrected HPVT's (filled squares), TR(28) at W = 0.28, (0.24 cm sensor diameter + 0.04 cm for vertical misalignment). Corrected HPV's (HPVC's) were

---

3/ I do not know why BP was so low at the well-watered condition in this tree but this is a possible explanation. Aleppo pine is a salt tolerant species and Tempe's water supply is somewhat brackish. A high salt content in the soil would cause low water potentials. The salinity of the soil was not measured at the time of the study.

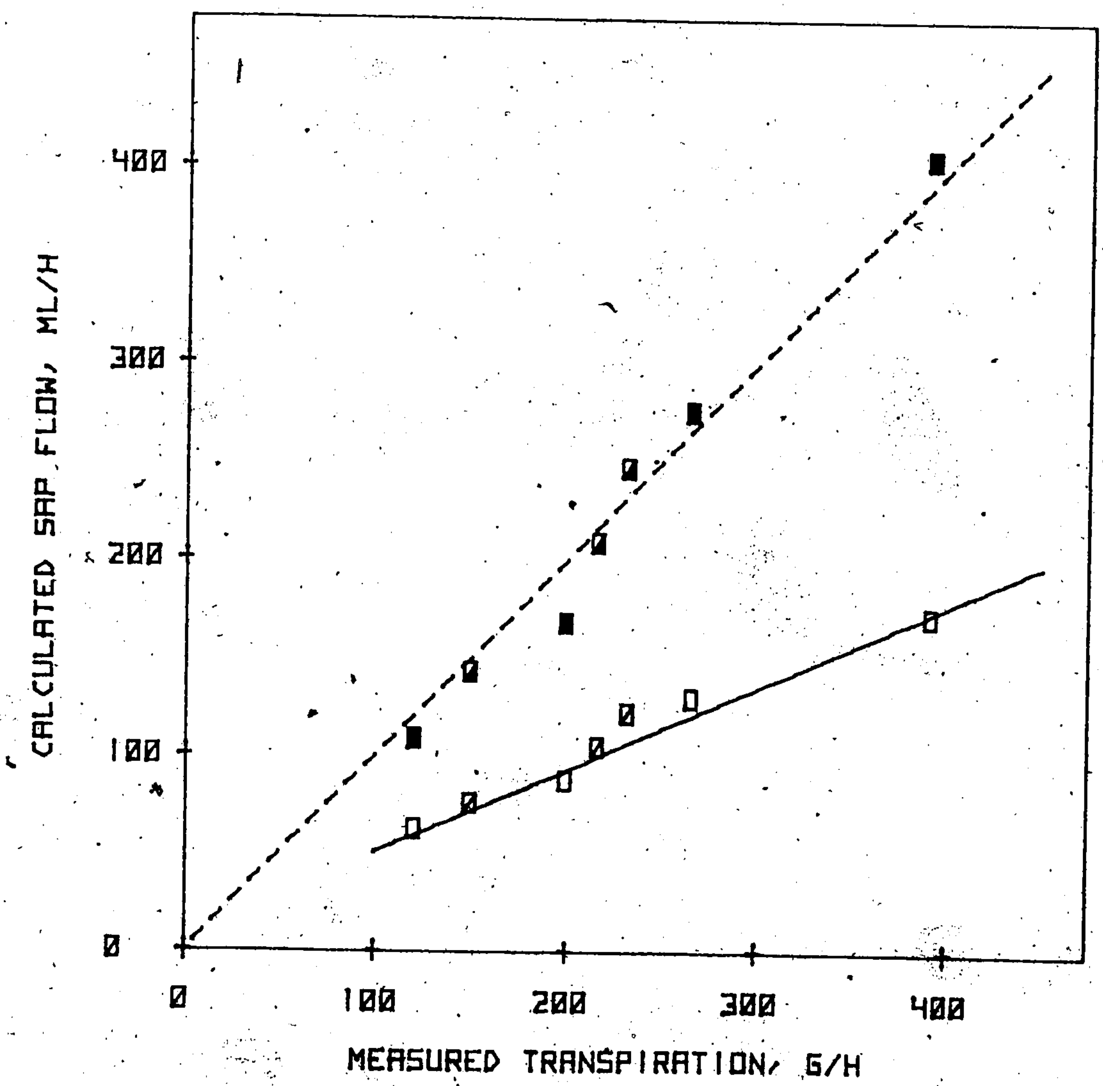

Figure 36. Transpiration of P. halepensis as determined by weighing lysimetry and calculated from heat pulse velocities. Open squares (□,▨) from raw HPV values before and after rewatering respectively. Filled squares (■,◩) from HPV values corrected in accordance with the TLM solutions at W = 0.28 cm. Dashed line (------) is 1:1.

obtained in accordance with Equation 23, derived from the TLM simulation results (Table 20, p. 216).

$$HPVC = 1.524 + 0.964(HPVT) + 0.124(HPVT)^2 \text{ cm h}^{-1} \quad (23)$$

The uncorrected values, TR(00), are in large disagreement with the lysimeter, while those corrected, TR(28), lie very close to the 1:1 line. The total of 7 d transpiration, TR(00) was 17.3 L, TR(28) 36.5 L and 37.2 Kg by lysimetery.

2. Monterey pine on load cell (PR1).

This test was carried out in the New Zealand Forest Research Institute's growth chambers at Rotorua, New Zealand, during 1974. The primary purpose of this study was to examine the reaction of *P. radiata* growth processes to drought stress (Rook, Swanson and Cranswick 1976). A tree measuring 5 cm diameter (dob), 3.2 m tall, was grown in a 1 m^3 container. The container was jointly supported by three load cells. The precision of this weighing system (250 g) was considerably poorer than that in the aleppo pine study because of mechanical noise generated by motion of the moveable floor in the growth chamber. This floor was designed to be vertically positioned to maintain various light intensities at foliage level.

Three HPVT probe sets (0.16 cm diameter glass rod thermistor sensors, brass heater, spaced -0.5,0,1.0 cm) were installed at 1 cm and 3 at 2 cm depths from the B/S boundary into the sapwood. The partial sapwood areas at the start of the study were:

1 cm sensors sapwood area (A_{10}) = 17.9 cm^2

2 cm sensors sapwood area (A_{20}) = 0.4 cm^2.

The sensor tips at 2 cm deep, were much less than the idealized 1 cm from the S/H border. However I have not applied position correction to these HPVT values because these sensors were glass rods, they represent barely 2% of the total area and whether corrected or not, their HPV values have litle bearing on total transpiration calculations. Their wound corrected values have been used in the transpiration calculations below.

The area applicable to the 1 cm depth sensor was adjusted for growth between the first and second drying measurement cycles. Sap flux was calculated using Equation 24; transpiration Equation 25.

$$\text{Sap Flux} = 0.30(0.33 + 2.15)\text{HPVC}$$

$$= 0.74(\text{HPVC})\ \text{mL cm}^{-2}\ \text{h}^{-1} \qquad (24)$$

$$\text{TR} = 0.74(A_{10}\text{HPV}_{10} + A_{20}\text{HPV}_{20})\ \text{mL h}^{-1} \qquad (25)$$

HPVT's were corrected at W = 0.20 (0.16 + 0.04 cm alignment error), using the TLM simulated coefficients (Table 20, p. 216) as:

$$HPVC = 0.807 + 1.203(HPVT) + 0.058(HPVT)^2 \text{ cm h}^{-1} \quad (26)$$

The day the HPV probes were installed was considered as day one in describing the sequence of events below.

Weight loss and HPVT were followed over two soil drying cycles. Air temperature was maintained at 21°C day (07 to 17 h), 17°C night. Day radiation was approximately 400 W m^{-2} (PhAR) supplemented with 3 h of low level incandescent radiation (approximately 10 W m^{-2}) on either side of the photosynthetic period. Day and night relative humidity was maintained at approximately 70%. The tree was well watered from day 1 to 11 to BP = -0.32 MPa, water withheld for 32 days to BP = 1.25 MPa, frequent watering for 62 days to BP = -0.64 MPa, water withheld to BP = -1.74 MPa and then rewatered for a second recovery period. The HPV probes installed on day one were used throughout the entire 152 days, including the second recovery period. Twenty-four hour average weight loss and TR(00), TR(20) calculated from hourly readings of HPVT's (03 to 21 h) on days 12 (BP = -0.32 MPa), 31 (BP = -1.00 MPa), 43 (BP = -1.25 MPa), 104 (after first rewatering; BP = -0.64 MPa), 123 (BP = -1.15 MPa) and 137 (BP = -1.74 MPa) are shown on Figure 37. The corrected values at W = 0.20 cm for the first drying cycle (filled squares) are virtually identical to those obtained from weight loss; those from the second drying cycle (half-filled squares) are not. Daily totals for the first drying

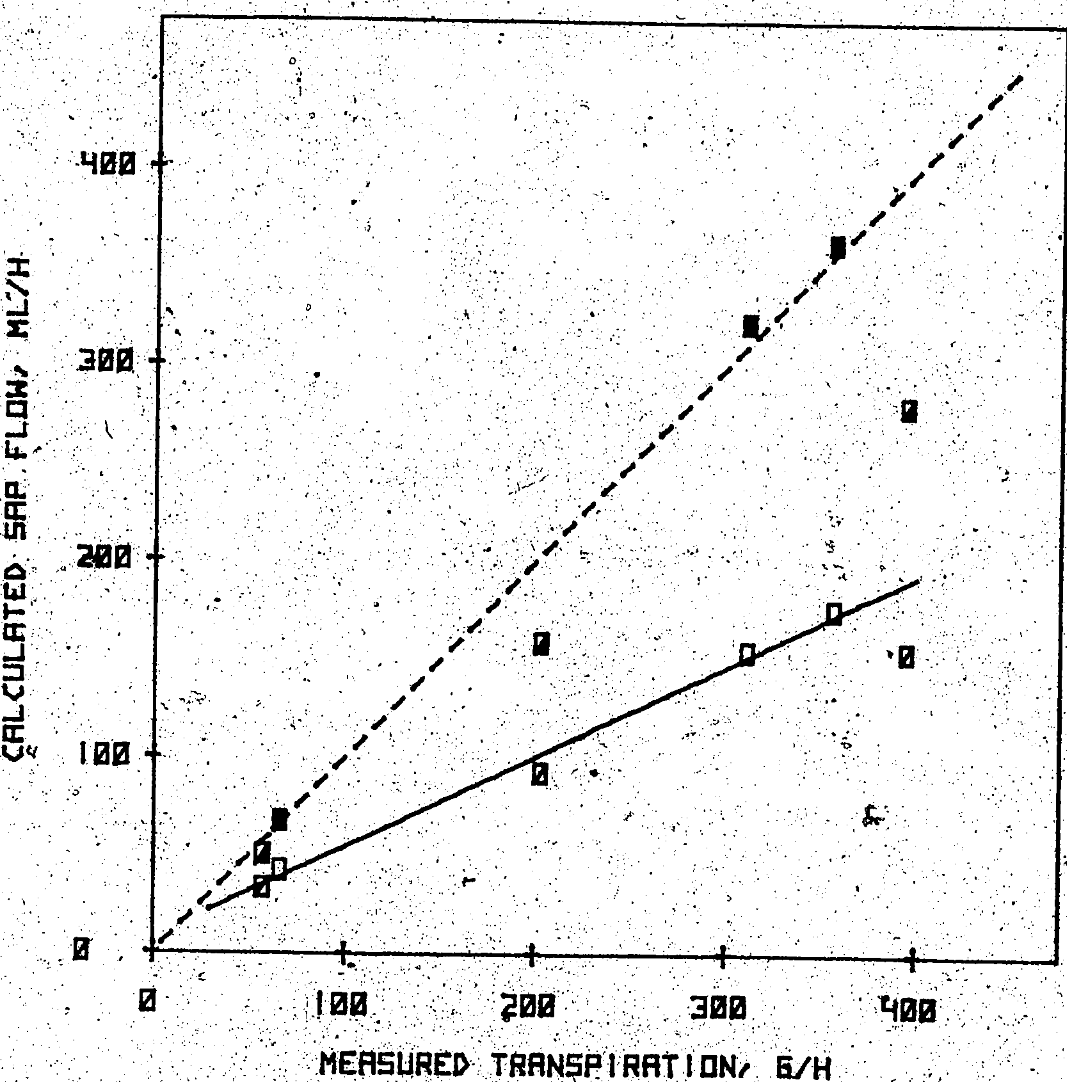

Figure 37. Transpiration of *P. radiata* as determined by weight loss and calculated from heat pulse velocities. Open squares (□) from raw HPVT values for days 12, 31 and 43 of the first drying cycle; or (▨) days 104, 123 and 137 after rewatering during a second drying cycle. Filled squares (■; ◩) are the same data corrected in accordance with the TLM simulations at W = 0.20 cm. The corrected values for the second drying cycle are well below the 1:1 (---) line.

cycle were TR(00) 3.6, 4.1, 0.9 L d^{-1}; TR(20) 7.6, 8.6, 1.5 L d^{-1}; versus weight losses of 7.4, 8.5, 1.5 Kg d^{-1} respectively. I tried corrections at W = 0.28 cm on the second drying cycle data and found that the calculated transpiration and weight loss values were essentially identical, i.e., 9.4, 4.6 and 1.3 L d^{-1} from TR(28) versus 9.4, 4.8 and 1.3 Kg d^{-1} weight loss. These data illustrate the necessity for measuring wound, or the use of freshly installed HPV probes, where initial wound width applies. In this case, the 0.28 cm wound was not measured nor were probes installed at fresh locations.

3. New Zealand mountain beech -- climatized cuvette (NS1).

This test was carried out in an open growing natural stand of mountain beech on a moist site with good drainage in Craigieburn Forest Park, New Zealand, during January 1975. Four trees in close proximity, measuring 10 to 12 cm diameter (dob), appproximately 6 m tall, and 20 years old, were each instrumented with two sets of HPV probes (0.16 cm diameter glass rod thermistor sensor, brass heater, spaced -0.5,0,1.0 cm); 1 set at 1.0 cm and a second at 2.0 cm into the sapwood from the B/S border. A thermoelectrically cooled cuvette coupled to a Koch-Siemens gas exchange unit was used to measure water vapour loss from one branchlet on one of the HPV-instrumented trees (6 m tall, 22 years, 11 cm dbh). The enclosed branchlet contained 253 leaves. At the end of several simultaneous HPV-vapour loss measurement runs, the branchlet and the entire tree were harvested to obtain an estimate of total crown leaf area, sapwood area, stem wood density, stem wood moisture content and wound width at the HPV probes. Half-hourly measurements of vapour loss in the cuvette were extrapolated, on the basis of crown leaf area, to the whole tree as an estimate of transpiration. Similiarly half-hourly values of HPVT's, obtained from all four trees, were averaged and applied to the appropriate partial sapwood area of the tree sampled by the cuvette, to estimate transpiration from it. These trees were well watered (BP = -0.20 MPa) by steady rain for 5 d prior to a 7 h period (1030 -1730) of simultaneous HPVT-vapour loss measurements on 30 January (Swanson, Benecke and Havranek 1979).

The accuracy of measurement of vapour loss in the cuvette was found to be ± 5% when properly calibrated (Swanson et al. 1979). Numerous critics of this type of technique have suggested an overall accuracy of ± 20%. This in not as accurate an independent transpiration measurement as weighing lysimetry.

Wound width at the sensors was indicated by darkly stained oxidized tissue in the sapwood 0.45 to 0.50 cm wide in line with and above and below the probes. The partial sapwood areas centered on each sensor tip were A_{10} = 49.5 cm^2, A_{20} = 51.0 cm^2. Sap flux derived from wood moisture and density at the end of the experiment was calculated using Equation 27; transpiration with Equation 28.

loss measurement runs, the branchlet and the entire tree were harvested to obtain an estimate of total crown leaf area, sapwood area, stem wood density, stem wood moisture content and wound width at the HPV probes. Half-hourly measurements of vapour loss in the cuvette were extrapolated, on the basis of crown leaf area, to the whole tree as an estimate of transpiration. Similiarly half-hourly values of HPVT's, obtained from all four trees, were averaged and applied to the appropriate partial sapwood area of the tree sampled by the cuvette, to estimate transpiration from it. These trees were well watered (BP = -0.20 MPa) by steady rain for 5 d prior to a 7 h period (1030 -1730) of simultaneous HPVT-vapour loss measurements on 30 January (Swanson, Benecke and Havranék 1979).

The accuracy of measurement of vapour loss in the cuvette was found to be ± 5% when properly calibrated (Swanson and others 1979). Numerous critics of this type of technique have suggested an overall accuracy of ± 20%. This in not as accurate an independent transpiration measurement as weighing lysimetry.

Wound width at the sensors was indicated by darkly stained oxidized tissue in the sapwood 0.45 to 0.50 cm wide in line with and above and below the probes. The partial sapwood areas centered on each sensor tip were A_{10} = 49.5 cm^2, A_{20} = 51.0 cm^2. Sap flux derived from wood moisture and density at the end of the experiment was calculated using Equation 27; transpiration with Equation 28.

$$\text{Sap flux} = 0.76(0.33 + 0.53)\text{HPV}$$

$$= 0.65\text{HPV mL cm}^{-2}\text{ h}^{-1} \quad (27)$$

$$\text{TR} = 0.65(49.5\text{HPVT}_{10} + 51.0\text{HPVT}_{20})\text{ mL h}^{-1} \quad (28)$$

HPVT's were corrected at W = 0.48 (Table 20, p. 216)

$$\text{HPVC} = 2.658 + 0.772(\text{HPVT}) + 0.424(\text{HPVT})^2\text{ cm h}^{-1}. \quad (29)$$

Transpiration for the 15 half-hourly periods was calculated using both measurement techniques (Fig. 38). The total transpiration for the 7 h period by the different methods was: cuvette 12.2 L; TR(00), 3.2 L; TR(48), 13.4 L.

QUANTITATIVE RESULTS IN MARGINAL SITUATIONS

Introduction

Marginal applications are those in which none of the HPV sensor tips can be positioned at least 1 cm from both the bark/sapwood and sapwood/heartwood borders. In this section I present the results of eight [illegible] quantitative tests of measured versus calculated transpiration in tree stems with sapwoods ranging from 0.9 to 1.4 cm thick. The first four of these were in white spruce (Picea glauca (Moench)Voss), the last four were in diffuse porous hardwoods, two aspen (Populus tremuloides Michx.), and two paper birch (Betula papyrifera Marsh.).

These tests were carried out in the environmental growth chambers of the Botany Department of the University of Alberta

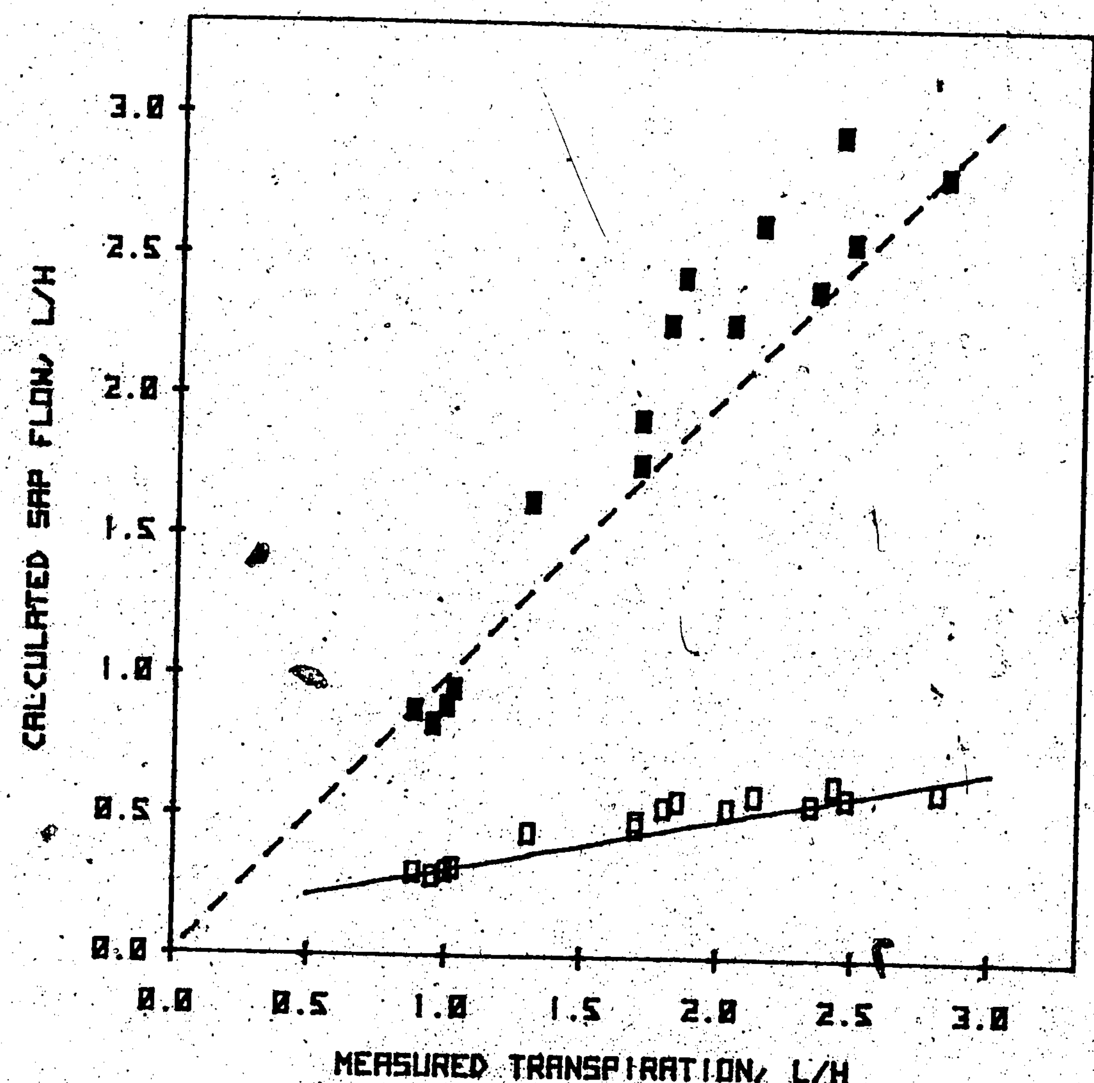

Figure 38. Transpiration of N. solandri var. cliffortiodes as estimated from a climatized cuvette and heat pulse velocity measurements. The open squares are from raw HPVT data, filled squares corrected in accordance with TLM simulations at W = 0.48 cm. The dashed line is 1:1.

during the period 1978 - 1981. Four weighing lysimeters were constructed from steel angle shelving material after a cable-pivot balance design of McIlroy (1975), (Appendix C), operated in null-balance mode. Weight loss over a given time period was determined by adding counter weights to the lysimeter to bring it back to the previous time's balance point. These lysimeters were capable of detecting weight changes of approximately 50 g in a total weight of 500 kg. Two were installed in chamber B009-2 and two in B009-3 to measure weight loss as an estimate of transpiration in P. glauca.

Severed stem, whole tree potometers (Appendix D), were used to measure water uptake as an estimate of transpiration in the P. tremuloides and B. papyrifera experiments. I could detect changes in water levels of 1 mm, representing an uptake of 3 mL, with this technique.

HPVT's were measured using a manually-read HPVT meter (Swanson 1962, 1974a) and recorded temperature-difference traces on a 4-channel strip chart recorder in the P. glauca experiments. Permanently emplaced HPV probes were 0.16 cm diameter glass rod thermistor sensors, brass heater, spaced -0.5,0,1.0 cm. Wood moisture contents, densities, sapwood thicknesses and sensor placements were determined by destructive sampling at the conclusion of each experiment. Various light intensities ranging from 64 W m^{-2} to 170 W m^{-2} (fluorescent, PhAR) were imposed to vary transpiration rate. Air temperature was maintained at 20 ± 2°C night and day (09 - 21 h). Relative humidity was not controllable, fluctuating between 20 and 60%.

In the potometer experiments, HPVA or HPVS, D^1 and HPVM were calculated from upstream and downstream temperature offset data obtained using a 16-channel HPV data logger especially designed and constructed for this study (Appendix E). Reusable 0.16 cm diameter thermistor sensors made of low thermal conductivity Teflon materials (Appendix E) were designed for, and used throughout, the four potometer experiments. Wood moisture content was estimated continuously, using Equation 17 (p. 26), from calculated longitudinal diffusivity at each probe set and an average wood basic density for each tree (ρb was determined for each stem at the end of each experiment). Both the HPVA and HPVS sensor configurations were used. The depth placement of sensors, which was different in each potometer experiment, is given in Appendix D.

Quantitative comparisons

1. White spruce lysimeters (PG1, PG2, PG3 and PG4).

Four white spruce trees, 4 - 6 cm diameter, 2½ to 3 m tall, 20 to 30 years old of unknown provenance were removed from an abandoned nursery on the Kananaskis Forest Experiment Station, Seebe, Alberta, during May 1977. A trench, 1 m deep, was dug around a 70 by 70 by 70 cm cube of soil and root material supporting each tree. A wooden container, with steel angle reinforcements on the sides and corners, was built about this soil volume taking care not to disturb the remaining roots within it. A hydraulic lift was used to transfer each container and tree to a truck for transport to the Northern Forest Research Centre nursery area at Edmonton, where all but one of the trees remained out doors until June 1978. One tree, PG1, was transfered into growth chamber B009-2 in January 1978; the remaining three into chambers B009-2 and B009-3 in June.

The containers were covered with plastic sheeting to reduce evaporation loss from the soil. A weighing apparatus (Appendix C) was assembled about each container. HPVT probes were permanently installed on various dates and to various sapwood depths (Appendix C) to acheive three goals:

(1) To calculate transpiration for comparison with weight loss under several xylem water potentials.

(2) To determine if simpl[illegible]rrelations of HPVT and weight loss became erratic [illegible]gative as BP decreased under drought stress.

(3) To see if the sapwood/heartwood boundary would be indicated by the radial depth pattern of HPVT values so that sapwood area could be calculated without a need for increment coring or other destructive sampling.

Measured and calculated transpiration values are given for the four trees for all complete data days in 1978 (Tables

15, 16 and 17). The sapwood moisture content and wood basic density for sap flux calculations were obtained when the trees were destructively sampled in 1981 (trees PG2, PG3 and PG4) or 1982 (tree PG1): (see Appendix C for sampling and sensor installation schedule for these trees). Calculated transpiration of each tree is the partial area (partial areas given in Appendix C) summation of that determined from all sensors in the sapwood that were installed on day one (for that tree) at no wound, TR(00), or W = 0.20 cm, TR(20). A constant sapwood moisture content and wood density, specific to trees PG1 and PG2, was applied to their data which commenced on 30/06/78 and continued through 20/08/78.

Weight loss, TR(WL), is the total weight loss less a correction for evaporation from the container (Appendix C) at the given light intensity and air temperature. The weight losses (09 - 21 h) of tree PG1 and PG2 (Tables 15 and 16) are the average of the losses from 09 - 13, 13 - 17 and 17 - 21 h with an error of estimate of ± 50 g for each of the three determinations. The cumulative error for the three weight determinations is ± 12 g h^{-1} for each 12 h data period 30/06 through 20/08/78. The weight losses of trees PG3 and PG4 (Table 17), 08 - 08 h are from a single determination at 08 h each day. The error estimate for these losses is 50 g averaged over 24 h or approximately 2 g h^{-1}.

Table 15. Quantitative comparison of transpiration as measured by weight loss and as calculated from heat pulse velocity data in white spruce, tree PG1. Air temperature constant day-night at 20°C, "daylight" 09-21 h. Transpiration calculations are: TR(00), no wound, raw HPV data; TR(20), 0.20 cm wound corrected HPVT's. Sapwood moisture content 0.88 dwb; wood basic density 0.44 g cm^{-3}.

1 1978 Da/Mo	2 Period h-h	3 BP MPa	4 RL s cm^{-1}	5 LI W m^2	6 TR(WL) g h^{-1}	7 TR(00) mL h^{-1}	8 (7/6) %	9 TR(20) mL h^{-1}	10 (9/6) %
30/06	09-21	-0.45	83	64	50	23	46	40	80
01/07	09-21	-0.45	17	106	83	51	61	87	105
02/07	09-21	-0.45	19	170	113	66	58	111	98
07/07	09-21	-0.35	45	64	31	13	42	27	87
08/07	09-21	-0.45	27	106	98	49	50	80	82
09/07	09-21	-0.40	25	170	145	74	51	127	88
14/07	09-21	-0.40	25	64	48	26	54	45	94
15/07	09-21	-0.45	20	106	112	60	54	99	88
16/07	09-21	-0.50	16	170	157	78	50	134	85
21/07	09-21	-0.60	25	170	129	80	62	140	109
22/07	09-21	-0.50	17	170	118	85	72	144	122
23/07	09-21	-0.45	25	170	126	81	64	140	111
28/07	09-21	-0.50	20	170	120	68	57	116	97
29/07	09-21	-0.50	25	170	131	75	57	130	99
30/07	09-21	-0.55	59	170	139	73	53	125	90
04/08	09-21	-0.70	40	170	104	50	48	83	80
05/08	09-21	-0.65	69	170	96	44	46	72	75
06/08	09-21	-0.70	69	170	92	37	40	60	65
11/08	09-21	-1.00	45	170	33	10	30	23	70
12/08	09-21	-1.00	65	170	39	17	44	31	79
13/08	09-21	-1.05	47	170	38	14	37	27	71
18/08	09-21	-1.25	134	170	27	10	37	22	81
19/08	09-21	-1.25	48	170	18	9	50	22	122
20/08	09-21	-1.40	62	170	19	14	74	28	147
				Mean	86.1	46.1	51	79.7	92

Table 16. Quantitative comparison of transpiration as measured by weight loss and as calculated from heat pulse velocity data in white spruce, tree PG2. Air temperature constant day-night at 20°C, "daylight" 09-21 h. Transpiration calculations are: TR(00), no wound, raw HPV data; TR(20), 0.20 cm wound corrected HPVT's. Sapwood moisture content 1.05 dwb; wood basic density 0.48 g cm^{-3}.

1 1978 Da/Mo	2 Period h-h	3 BP MPa	4 RL s cm^{-1}	5 LI W m^2	6 TR(WL) g h^{-1}	7 TR(00) mL h^{-1}	8 (7/6) %	9 TR(20) mL h^{-1}	10 (9/6) %
30/06	09-21	-0.40	32	64	60	31	52	52	87
01/07	09-21	-0.45	18	106	96	51	53	87	91
02/07	09-21	-0.50	12	170	122	66	54	116	95
07/07	09-21	-0.45	19	64	83	30	36	50	60
08/07	09-21	-0.40	21	106	87	50	57	86	99
09/07	09-21	-0.40	19	170	139	75	54	134	96
14/07	09-21	-0.40	13	64	71	38	54	62	87
15/07	09-21	-0.50	7	106	113	55	49	93	82
16/07	09-21	-0.50	10	170	134	67	50	119	89
21/07	09-21	-0.60	21	170	101	50	50	84	83
22/07	09-21	-0.55	12	170	92	47	51	79	86
23/07	09-21	-0.55	23	170	87	36	41	59	68
28/07	09-21	-0.60	34	170	84	40	48	65	77
29/07	09-21	-0.70	22	170	72	32	44	53	74
30/07	09-21	-0.70	19	170	61	27	44	46	75
04/08	09-21	-0.70	25	170	61	26	43	43	70
05/08	09-21	-0.60	48	170	69	25	36	42	61
06/08	09-21	-0.75	38	170	56	27	48	46	82
11/08	09-21	-0.90	9	170	45	23	51	39	87
12/08	09-21	-0.90	13	170	50	23	46	39	78
13/08	09-21	-0.90	26	170	44	22	50	37	84
18/08	09-21	-1.10	7	170	36	17	47	31	86
19/08	09-21	-1.10	19	170	37	15	41	29	78
20/08	09-21	-1.15	27	170	30	18	60	33	110
				Mean	76.2	37.1	48	63.5	83

Table 17. Quantitative comparison of transpiration as measured by weight loss and as calculated from heat pulse velocity data in white spruce, trees PG3 and PG4. Air temperature constant day-night at 20°C, "daylight" 09-21 h. Transpiration calculations are: TR(00), no wound, raw HPV data; TR(20), 0.20 cm wound corrected HPVT's.

1 Start Da/Mo	2 Stop Da/Mo	3 Period h–h	4 BP MPa	5 LI $W\ m^2$	6 TR(WL) $g\ h^{-1}$	7 TR(00) $mL\ h^{-1}$	8 (7/6) %	9 TR(20) $mL\ h^{-1}$	10 (9/6) %
(A) Tree PG3; Mgw = 1.00 dwb, Pb = 0.48 $g\ cm^{-3}$									
27/08	28/08	08-08	-0.95	170	54	33	61	56	104
02/09	03/09	08-08	-0.65	170	66	38	58	66	100
03/09	04/09	08-08	-0.75	170	65	39	60	69	106
				Mean	61.7	36.7	60	63.7	103
(B) Tree PG4; Mgw = 0.80 dwb, Pb = 0.47 $g\ cm^{-3}$									
27/08	28/08	08-08	-0.60	170	52	33	63	60	115
02/09	03/09	08-08	-0.55	170	92	48	52	87	95
03/09	04/09	08-08	-0.75	170	80	47	59	86	108
				Mean	74.7	42.7	58	77.7	106

Transpiration calculated from HPVT's measured on 30/06/78 to 02/07/78 (PG1 and PG2) and 27/08/78 to 03/09/78 (PG3 and PG4) is 100 ± 10% of measured weight loss for all four trees (Fig. 39). These transpiration calculations, made from data taken within the first week to 10 days after heat pulse probe installations, are the only ones I consider reliable because of the unpredictable speed of wound development and the lack of sapwood moisture content measurements specific to each data period.

The steadily declining percentage of weight loss that occurs with time in PG2 (Table 16, 30/06 to 06/08) is the type of wound response that I expected. The numerical simulations indicate that the effect of wound on calculated HPV's, becomes progressively less as imposed HPV's approach zero (Fig. 9; p. 74). Since calculated HPVT's can only approach, but never equal zero, the higher percentages of measured weight loss, that were calculated during the period 11/08 to 20/08 (Tables 15, 16) at very low HPVT's, were expected.

The results from PG1 (Table 15) are an interesting contrast to those of PG2. The higher percentages of weight loss calculated on 21/07 to 30/07 illustrates changing correlation of TR(HPV) to TR(WL) with time that cannot be explained by wound development. In this case, either sapwood area or sapwood water content must have decreased. The most likely explanation is that sapwood water content has decreased (Waring and Running 1978; Waring,

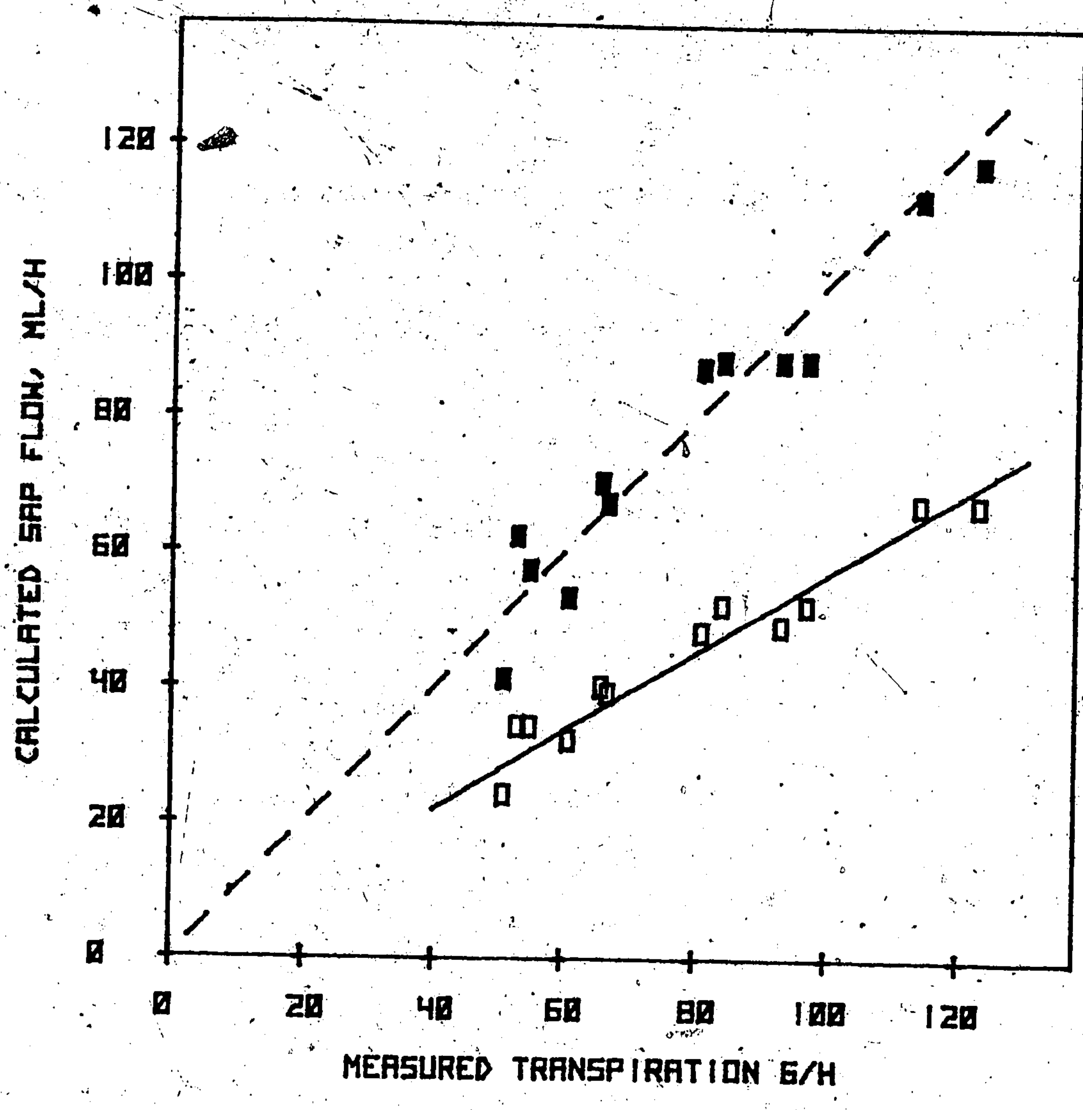

Figure 39. Transpiration of four P. glauca trees as determined by weight loss and calculated from heat pulse velocities measured within one week to ten days of sensor installation. Open squares from raw HPVT data. Filled squares from HPV values corrected with TLM simulations at W = 0.20 cm. The dashed line is 1:1.

Whitehead and Jarvis 1979). If sapwood water content decreases while sap flux remains the same, heat pulse velocity must increase (Fig. 3, p. 31). If sapwood water content has decreased and the equation to calculate TR(HPV) has not been adjusted to reflect this, then the result is a higher estimate, or in this case, (Table 15; 21-23/07) an overestimate of transpiration.

Gale and Poljakoff-Mayber (1964) reported constant or slightly decreasing total transpiration and increasing HPVT's at soil water potentials less than -15 atm. My results (Table 15, 30/06 - 23/07) are comparable to those of Gale and Poljakoff-Mayber (1964) in that, compared to data period 30/06 - 02/07, HPVT's increased by a greater amount than did weight loss by 21-23/07. A result almost identical to Gale and Poljakoff-Mayber's occured (Table 15, 18-20/08) where weight loss decreased from 27 to 19 g h^{-1} while TR(HPV) increased from 22 to 28 mL h^{-1}. The error band, $\pm$ 12 g h^{-1}, on the weight loss in this study is sufficiently broad so that no definite conclusion is possible. None-the-less, these data indicate that simple correlations between actual transpiration and HPV or TR(HPV) calculated with constant sapwood coefficients, are not reliable through extended time or changes in plant water status. In this, my results confirm the conclusions of Gale and Poljakoff-Mayber (1964).

The sapwood/heartwood border was not evident as a sharp reduction in HPVT's across it. A radial profile of the HPVT data from tree PG2 and PG3 was plotted earlier (Fig. 31B, p. 132). This profile, coupled with the results of the glass rod sensor RLM simulations (Fig. 32C, p. 134), indicate that it would be difficult to ascertain the S/H border within ± 0.5 cm. Even a 0.2 cm error in the determination of the 1.0 cm sapwood thickness of tree PG1 or PG4 would result in a 10 to 20% error in calculated transpiration. A radial profile of HPV values does not provide a sufficiently accurate estimate of sapwood thickness to use to calculate sapwood area.

2. <u>Hardwood potometers (BP1, BP2, PT1 and PT2).</u>

Four paper birch and four aspen trees were felled while in winter dormancy in March 1981 and stored in a cold room at 2 °C. Trees were selected with as large a diameter as possible (4 to 6 cm) consistent with a 3.5 m height limitation imposed by the environmental chamber dimensions (Appendix B). As needed, each stem was brought out of cold storage into an adjoining environmental chamber at 20°C, 12 hour days, 170 W m^{-2} (fluorescent, PhAR) for leaf out, where the stem was placed in a 25 L container of distilled water, and the basal end was freshly recut. (This leaf out procedure is a modification of a technique to induce out-of-season flowering in poplars described by Benson 1972.) Leaf out generally occured within 5 to 7 days with full development in 10 days. (Two trees of each species failed to leaf out after 8 weeks in cold storage.)

While the stem was still in the 25 L container, 8 sets of heat pulse velocity probes were installed between 40 and 60 cm, and 8 sets between 90 and 110 cm, from the basal end. Two layers of 6 mm inside diameter rubber tubing were wrapped around the 20 cm length of stem between the two groups of HPV probes. At an appropriate time in each experiment, chilled methanol (-30^{o}C) was circulated through this tubing to freeze the stem and create an ice block in the stem in order to temporarily stop water uptake (Zimmerman 1964, Hammel 1967) and possibly, to induce cavitation.

After the HPV probes and freezing coils were in place, and while the basal end still remained in the distilled water container, about 3 to 5 cm of the stem was cut off and the newly exposed surface was microtomed with a razor-sharp plane. A plastic bag full of water was placed over the cut surface to keep it continually under water while the stem was transfered to a 60 cm tall, 10 cm diameter cylinder. Distilled water was added to bring the level up to 30 cm above the cut surface. A 6 cm diameter graduated cylinder was used as an auxillary water supply so that quantities added to maintain the water level in the large cylinder, as depleted by transpiration, could be determined within about 3 mL independent of differing stem volumes. Sapwood thickness at the levels where the probes were installed was assumed, for installation purposes, to be the same as that at the basal end. At the conclusion of each potometer experiment, the exact location of each sensor tip with respect to the S/H border and wound widths were measured at each probe installation. The sapwood and heartwood moisture content and densities were determined from discs cut from the stem in the near vicinity of the upper and lower HPV probe groups.

Each potometer tree received differing configurations of HPV instrumentation (See Appendix D for instrumentation and data schedule.). The 0.16 cm diameter Teflon sensors were removed and reused in successive experiments. In tree BP1 (used here as an example) HPV probes were configured for HPVA determinations at -0.5,0,1.0 cm. The tips of the sensors of four sets in each 8 sensor group above and below the freezing coil were at 0.8 cm and four sets at 1.3 cm from the B/S border into a 1.4 cm thick sapwood. The 16-channel HPV logger was used to record all potometer HPV data.

The general schedule and environmental conditions for all of the potometer trees were 1 to 2 days of hourly HPV recordings, air temperature constant 25°C, daylight 09 - 21 h with water uptake measured at 2 to 4 h intervals from 08 to 22 h and at 08 h for dark uptake. The same schedule was repeated after a day of the stem freezing treatment. The ice block was created between 08 - 10 h and held until the leaves wilted (XPP = -1.4 to -1.8 MPa). Water uptake ceased after 30 minutes of circulating the coolant. HPV data could not be taken during this freezing treatment because rapidly changing temperatures at the sensors masked any temperature changes induced by sap movement. The ice block could be maintained for 10 to 12 hours at 25 °C air temperature before the coolant became too warm and thawing occured.

Transpiration was calculated for every time period during which both HPV's and water uptake values were available (Figs. 40 - 43).[4/] Sap flow was calculated for the partial area associated with each sensor depth, and summed to total transpiration as in the previous experiments, except that sap flux was calculated with constant Pb, and the current moisture content (as determined from Equation 17, p. 26, and D^1 at the downstream sensor). Sap flow at each sensor was calculated using three models:

a) HPV's without correction, TR(OO).

b) HPV's with correction for wound (which was very distinct in birch, very indistinct in aspen) as measured at the probes at the conclusion of the experiment, TR(NN).

c) HPV's with wound correction as above which was applied first, and then a correction for sensor tip position, TR(NNP).

4/ HPV data from tree BP1 were sparse due to frequent momentary power interruptions that often destroyed the contents of the volatile microprocessor memory. This problem was partially solved in subsequent runs by altering the configuration of the battery backup.

The equations and coefficients for these corrections are given in Appendix D.

These potometer experiments were intended to achieve three goals.

1) To calculate transpiration for comparison with water uptake in diffuse porous hardwoods.

2) To test the capability of the HPV technique to detect altered flow patterns under abnormal situations, in this case induced cavitation.

3) To test the HPVA, HPVS and HPVM sensing configurations. (HPVM results reported earlier in this chapter, Figure 34, p. 139.)

Potometer BP1.

All sensors were configured for HPVA. Sensors were installed at 0.8 and 1.3 cm depths below the B/S interface. The best data fit for BP1 (Fig. 40A) is with the wound only model TR(28). The averages for the entire experiment were: TR(00), 11.2 mL h^{-1}; TR(28), 23.9 mL h^{-1}; TR(28P), 26.9 mL h^{-1} compared to 20.7 mL h^{-1} measured.

Potometer BP2.

Tree BP2's sensors were as BP1 except half of them were configured for HPVS (-1.0,0,1.0 cm). The best data fit (Fig. 41A) is again the wound only model, TR(22). The averages for the entire experiment were: TR(00), 11.2 mL h^{-1}; TR(22),

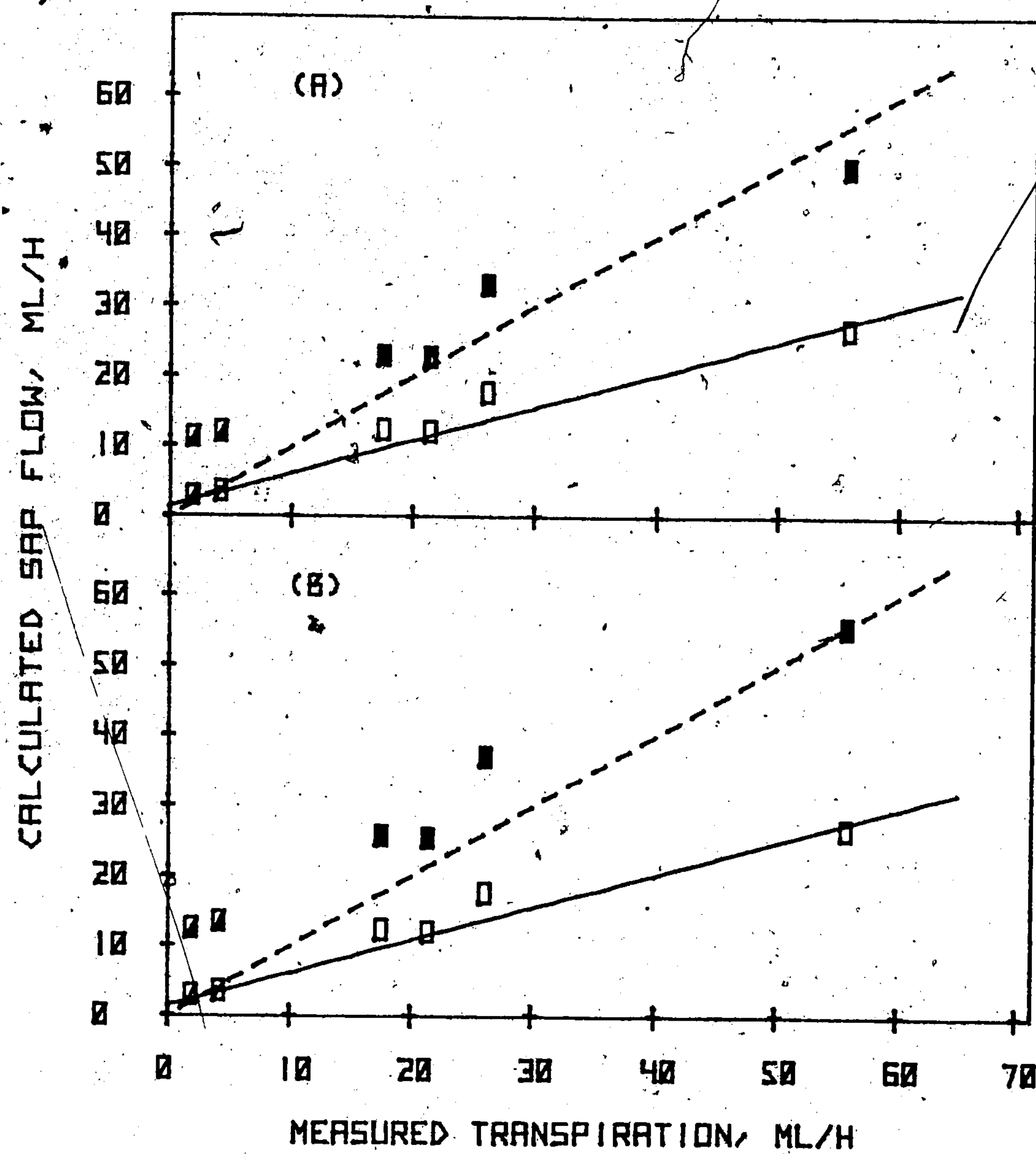

Figure 40. Transpiration of B. papyrifera, tree BP1, as determined by potometry and calculated from heat pulse velocities measured with 0.16 cm diameter Teflon-encased thermistor bead sensors. Open squares (□,▨) from raw HPVA values taken before and after a stem freezing treatment to induce cavitation. Filled squares (■,◪) are the same data corrected in accordance with: (A) TLM simulation at W = 0.28 cm; (B) TLM simulation at W = 0.28 plus a sensor position correction in accordance with the RLM simulations near the S/H border without sensor materials. Dashed line (---) is 1:1.

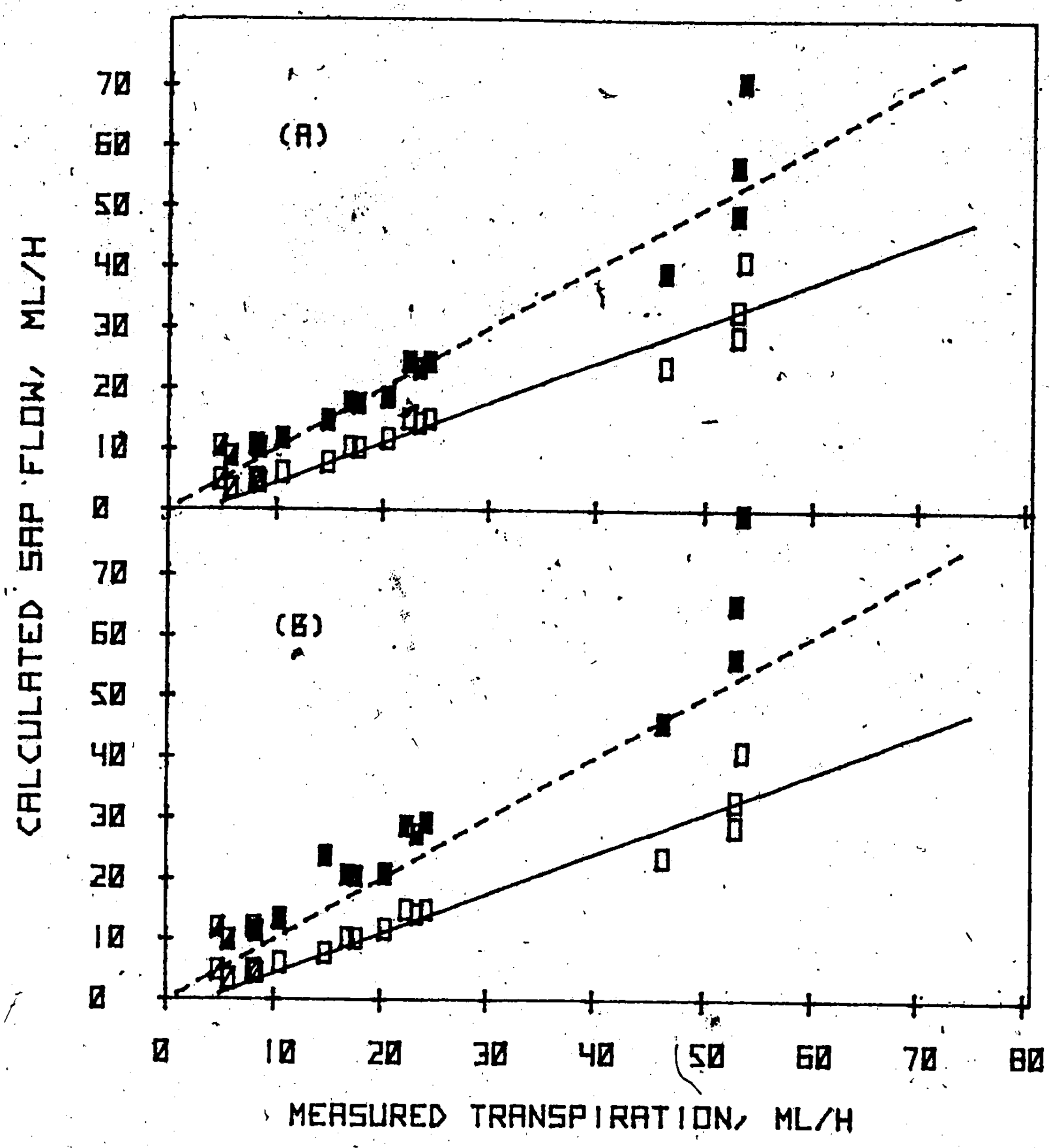

Figure 41. Transpiration of B. papyrifera, tree BP2, as determined by potometry and calculated from heat pulse velocities measured with 0.16 cm diameter Teflon-encased thermistor bead sensors. Open squares (□,◪) from raw HPVA and HPVS values taken before and after a stem freezing treatment to induce cavitation. Filled squares (■,◩) are the same data corrected in accordance with: (A) TLM simulation at W = 0.22 cm; (B) TLM simulation at W = 0.22 plus a sensor position correction in accordance with the RLM simulations near the S/H border without sensor materials. Dashed line (---) is 1:1.

24.0 mL h^{-1}; TR(22P), 28.3 mL h^{-1} compared to 23.4 mL h^{-1} measured.

Potometer PT1.

Four sensors were installed at 0.3 cm, 8 at 0.8 cm and 4 at 1.3 cm depths below the B/S interface with half HPVA and half HPVS, 8 above and 8 below the cooling coil. The best data fit (Fig. 42B) was the wound plus position correction model TR(24P). The averages for the entire experiment were: TR(00), 19.7 mL h^{-1}; TR(24), 39.7 mL h^{-1}; TR(24P),48.8 mL h^{-1} compared to 55.7 mL h^{-1} measured.

Potometer PT2.

Sensors were emplaced at 0.3, 0.55, 0.8 and 1.3 cm depths below the B/S interface, four at each depth, eight each in the HPVA and HPVS configurations, half above and half below the cooling coil. The no wound model TR(28) provided a good fit to the data (Fig. 43A) but the wound plus position model TR(28P) provided a marginally better one (Fig. 43B). The averages for the entire experiment were: TR(00), 25.0 ml h^{-1}; TR(28), 56.6 mL h^{-1}; TR(28P), 63.4 mL h^{-1} compared to 61.7 mL h^{-1} measured.

Cavitation.

The attempts to induce cavitation by stopping water supply to the leaves during high transpiration demand were intended to induce a "worst case" situation for the HPV technique. Hopefully sap flow patterns would be altered, i.e., new pathways,

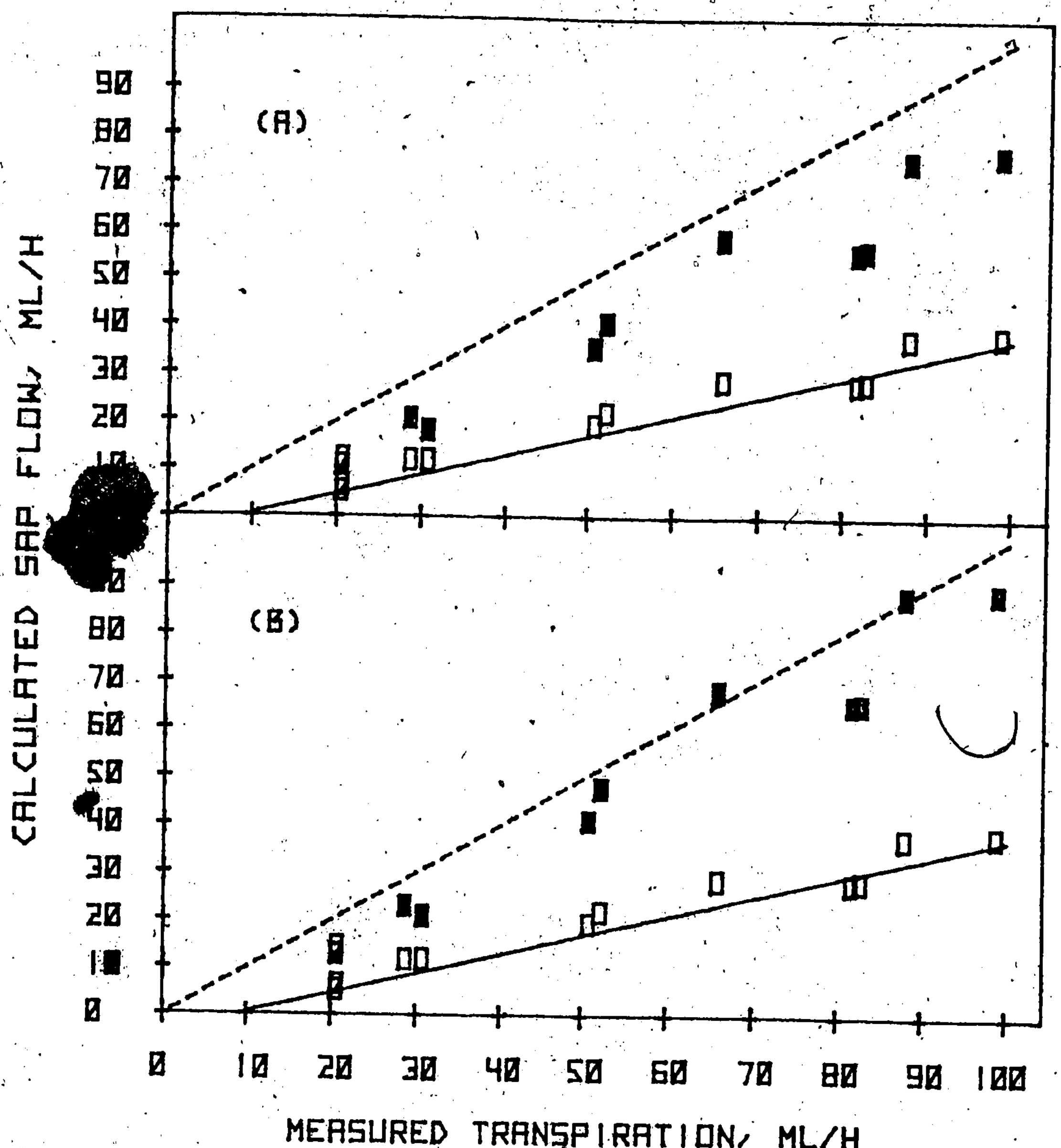

Figure 42. Transpiration of P. tremuloides, tree PT1, as determined by potometry and calculated from heat pulse velocities measured with 0.16 cm diameter Teflon-encased thermistor bead sensors. Open squares (□,▨) from raw HPVA and HPVS values taken before and after a stem freezing treatment to induce cavitation. Filled squares (■,◩) are the same data corrected in accordance with: (A) TLM simulation at W = 0.24 cm; (B) TLM simulation at W = 0.24 plus a sensor position correction in accordance with the RLM simulations near the S/H border without sensor materials. Dashed line (---) is 1:1

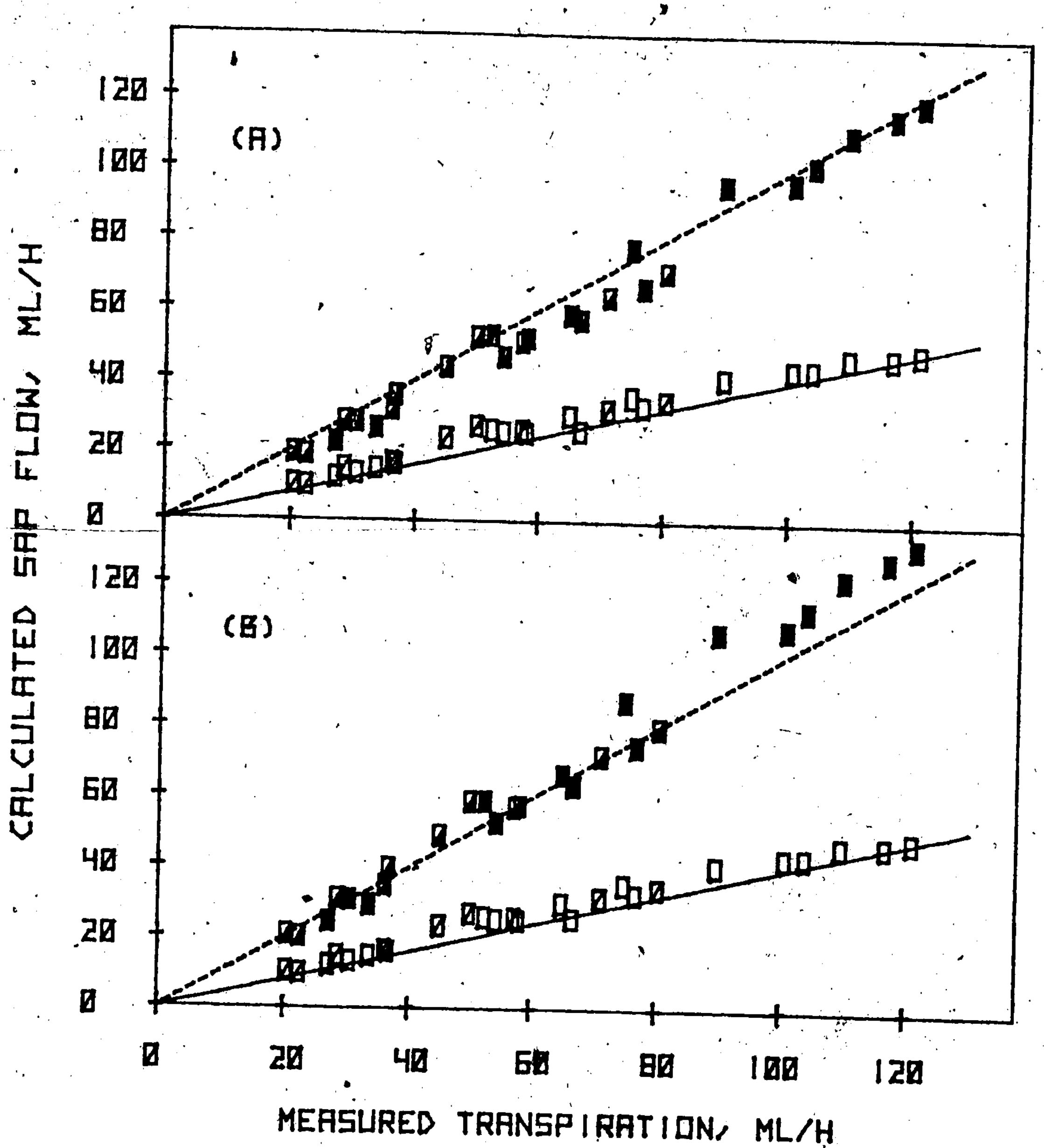

Figure 43. Transpiration of *P. tremuloides*, tree PT2, as determined by potometry and calculated from heat pulse velocities measured with 0.16 cm diameter Teflon-encased thermistor bead sensors. Open squares (□,▨) from raw HPVA and HPVS values taken before and after a stem freezing treatment to induce cavitation. Filled squares (■,◪) are the same data corrected in accordance with: (A) TLM simulation at W = 0.28 cm; (B) TLM simulation at W = 0.28 plus a sensor position correction in accordance with the RLM simulations near the S/H border without sensor materials. Dashed line (----) is 1:1.

reduced moisture content at various parts of the stem, etc (Hammel 1967). Partial cavitation was induced in both aspen potometers, but virtually total cavitation occured in both birch stems and very little water uptake occured after release of the ice block. In all four cases, the HPV sensors detected the change in water uptake (Figs. 40 - 43).

A change in both flow pattern and moisture content was detected in PT1 (Fig. 44A). Before application of the freeze block, 70% of the sap flow occured in the outer 5 mm of sapwood; after freezing, none occured there. The moisture fraction (calculated from D^1) decreased at each sapwood depth and the variability in moisture fraction increased: from 0.9 (0.82 to 1.04) before freezing to 0.8 (0.49 to 1.04) after freezing at 0.3 cm depth; from 1.0 (0.78 to 1.18) before freezing to 0.75 (0.42 to 1.04) after freezing at 0.8 cm depth (range of moisture contents at the individual sensors in parenthesis).

In PT2, the freezing treatment reduced flow in the outer 4 mm by 50% (Fig. 44B) but moisture fraction change at all sensors was less than 10%.

DISCUSSION OF APPLICATION RESULTS

Wound

Nonconvective material in the plane of the heat pulse probes is the source of the greatest departures from Marshall's (1958) idealized theory. This was shown numerically in Chapter IV and repeatedly demonstrated by the experimental results

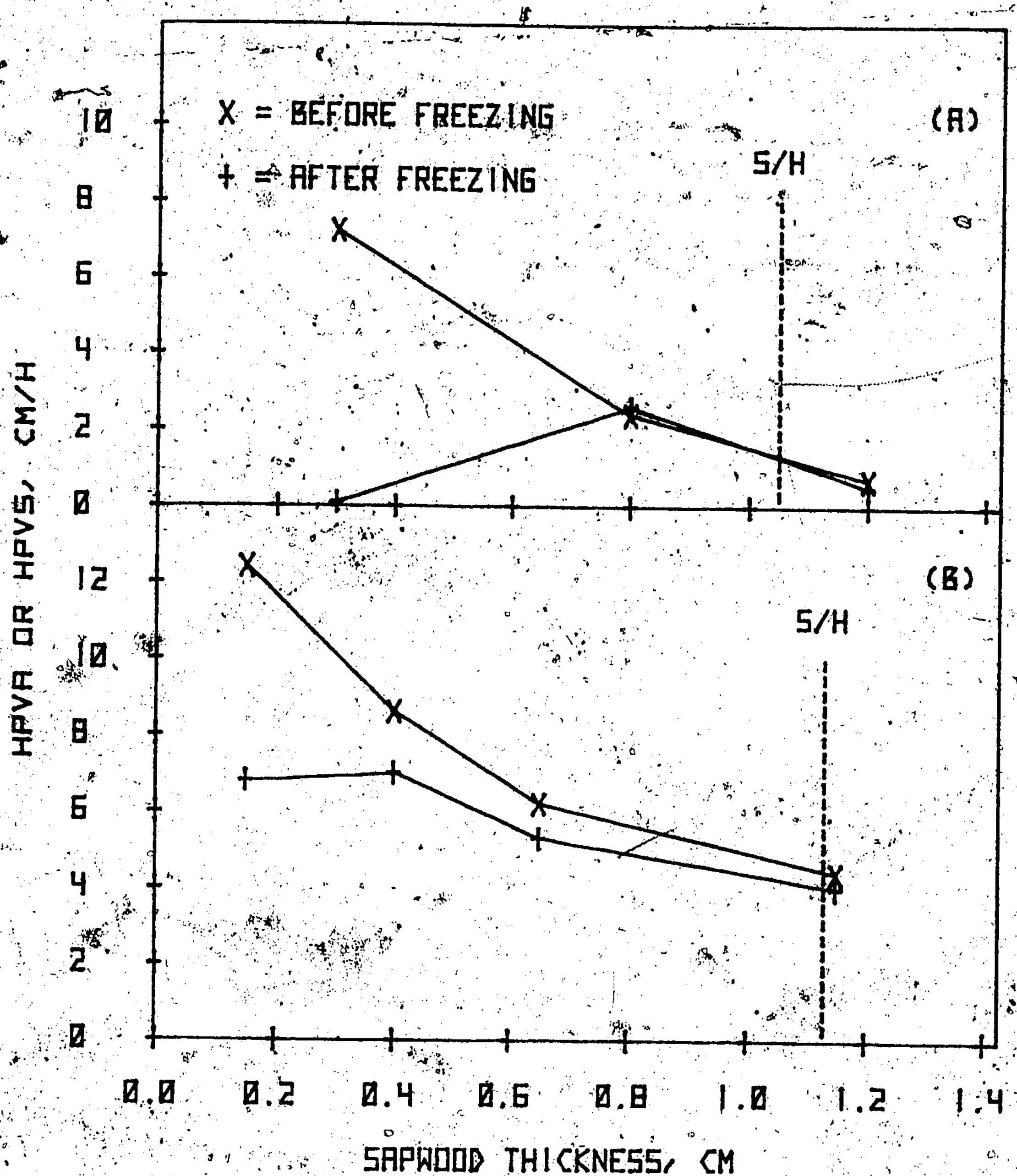

Figure 44. Heat pulse velocities in *P. tremuloides*, trees PT1 and PT2, at several positions in the sapwood before and after a stem freezing treatment. (A) Note the complete cessation of flow indicated by zero HPV's at 0.3 cm depth in PT1. (B) HPV's were considerably reduced in the outer 0.5 cm of PT2 but flow did not completely cease as in this position in PT1.

of this chapter. Transpiration calculated from uncorrected HPV's, no matter what technique or analysis method was used to obtain them, was generally less than 50 to 60% of that measured except at transpiration rates very near zero. If the HPVA's, HPVS's or HPVT's used to calculate TR(HPV) were corrected in accordance with the TLM simulation results at assumed or measured wound width, then calculated and measured transpiration rates, with few exceptions, fell within 10% of each other.

The appropriate wound width correction is not always easy to ascertain. In the potometer tree experiments, the stems were small and the drill jig used to align the holes for the sensors and heater wobbled from side to side during the drilling operation. Wound widths measured in these stems varied from 0.20 to 0.40 cm with the average being that used to calculate TR(HPV). Such lateral movement has not been a problem with larger stems where the misalignment error is ± 0.02 cm, as has been used in most of the above calculations.

Wound is generally easy to measure once the sensors have been excised. However, it was very indistinct in the *P. tremuloides* stems, particularily PT1, appearing only as a very faint band of slightly lighter wood in the plane of the sensors. In most conifers, wound is quite distinct, apearing as a band of resin filled tissue above and below the sensors. It was also quite distinct in the other diffuse porous experiments, appearing as a band of dark colored oxidized wood. Apparently I tend to overestimate wound width if it is distinct as in NS1, BP1 and BP2, and underestimate it if indistinct as in PT1 and PT2. (I consider the poorer results of PT1 to be mainly due to poor wound definition in the excised section.)

Wound and sensor configuration effects are closely associated. Probe configurations in which the sensors are located close to the heater are subject to greater wound effects than those with the sensors located further away. Sensors cannot be located sufficiently far from the heater so that wound effects become negligible because the temperature rise created by a practical-magnitude heat pulse becomes less detectable, at an exponential rate, as heater-sensor separation is increased. All sensor installations cause wound and each configuration is affected differently by wound. Simulations specific to each wound and sensor configuration must be used to obtain meaningful data. When sensors are differently configured, their data can be made compatible by applying simulation results specific to both wound width and sensor configuration.

Radial variation in stem anatomy

In simulation, nonconvective stem tissue borders were the next greatest source of departure from idealized theory. The radial longitudinal model simulations without sensor materials with varying thicknesses of sapwood (Chapter IV) indicated that sensors emplaced within 1 cm of the S/H border were subject to serious errors, especially in the HPVA configuration. The same simulations indicated that within 1 to 1.5 cm of the B/S border, data from the single sensor HPVM and HPVP configurations are virtually worthless.

The experimental results with respect to position are not so clear as they were for wound. Unknown heat losses to the "outside" and the averaging effect of sensors with thermal conductivities much greater than wood tend to mitigate tissue border effects.

High thermal conductivity sensor materials tend to produce HPV data in the vicinity of the S/H border that are biased toward the magnitude of HPV in the sapwood rather than the known zero velocity in the heartwood. The RLM simulations with glass, brass of aluminum sensor materials indicate that position corrections obtained from the no sensor simulations would, if applied, cause the data from these sensors to overestimate HPV data obtained within 0.5 cm of the S/H border. The experimental results support those simulated.

Both the RLM simulations and experimental results with Teflon sensors near the S/H border, indicate that these behave very much like the no sensor simulations. Teflon or other low thermal conductivity material sensors may be very useful in exploring xylem flow patterns. They are probably less desirable for transpiration studies where the averaging effect of the higher thermal conductivity materials would reduce sampling variation.

Sapwood area

The position of the S/H border cannot be established, with sufficient accuracy to estimate sapwood area, solely from HPV measurements in the vicinity of it. The "no sensor" RLM simulations indicate that sap movement in the sapwood affects HPV's measured up to 1 cm deep into the heartwood. Miller, Vavrina and Christensen (1980) referred to these HPV's at depths beyond known sap conducting tissue as a "heat shadow" affect. High thermal conductivity sensors make this "heat shadow" affect even more pronounced. That this shadow affect exists is unfortunate, as an abrupt change in HPV at or in the near vicinity of the S/H or sapconducting/nonconducting border, would have allowed sapwood area to be estimated solely from the relatively nondestructive heat pulse probe implants.

Miller and others (1980) considered sap-conducting area in oak as the current year's xylem. In my experiments confined to conifers or diffuse porous hardwoods, sapwood area has been determined from either a change in color or an abrupt change in moisture content at the S/H border and all of it has been assumed functional. This procedure appears to be justifiable in light of the abrupt decrease in liquid permeability that occurs there (Booker and Kininmonth 1978, Booker and Swanson 1979) and the closeness of the quantitative results reported herein.

Sapwood moisture content

The importance of a current knowledge of sapwood moisture content lies mainly in fine-tuning the TR(HPV) estimate to closer than within 10% of actual. Sapwood moisture content is used to determine sap flux (Eq. 10, p. 23). It is multiplied by basic wood density so that a change of 20 to 30% dwb, is necessary to change TR(HPV) by 10%. Waring and Roberts (1979) found that sapwood relative water content (RWC, defined as the fraction of saturated moisture content) normally varied by about 5% each day in Scots pine with 10% in one day being the largest variation encountered under normal circumstances. A 5% change in RWC may be as large as a 10% change in dry weight water content. Even so, TR(HPV) estimated using moisture contents measured at probe installation should be within 10% of actual for about 3 days. Since HPV probe installations should be renewed every 7 to 10 days to lessen the unpredictable effect of wound development, the time trend of moisture contents taken at each installation date should suffice to keep TR(HPV) estimates, well within a 10% error band, especially in large trees where repeated increment coring is possible.

In smaller trees, or in cases where destructive sampling is not possible, it would be advantageous to be able to continuously monitor sapwood water content. The technique tried in the potometer experiments (D^1 and Eq. 17, p. 26) appears to have promise. Longitudinal thermal diffusivity is sensitive to moisture content (Tables 8, 9; p. 87,88). Unfortunately, it is somewhat sensitive to HPV too. The variation in D^1 with HPV can be largely eliminated by using probe configurations where the upstream sensor is approximately 1 cm from the heater and by calculating Mgw from the average of the D^1 obtained at the up and downstream sensors. This average is almost identical to the D^1 obtained from either sensor when HPV = 0 (Tables 8, 9, p. 87,88).

In this study, the moisture contents calculated from D^1 and Pb were within reason and probably within the error band of the measured moisture contents used as controls which were always obtained at slightly different locations in the stem or at different times than the D^1 measurements. The moisture contents calculated from D^1's helped to provide the excellent fit observed in PT2 (Fig. 42) where moisture fraction, dwb, varied from 1.00 down to 0.65 during the course of this experiment (Fig. 45).

Some authors (Waring and Running 1978; Waring, Whitehead and Jarvis 1979) have suggested that sapwood moisture content is indicated by xylem pressure potential (XPP). Moisture content (as calculated from D^1) and XPP, for tree PT2, do appear to be related (Fig. 45). However Running's (1980a) results in *P. contorta* are not suggestive of a very close correspondence between XPP and RWC. Running (1980a) showed a decrease in RWC from 0.78 at XPP = -1.32 MPa to 0.33 at XPP = -2.10 MPa as taking place over an 8 to 30 day period. However, he also showed that XPP decreased from -0.5 to -2.1 MPa in less than 1 hour. It is virtually impossible that sapwood moisture content

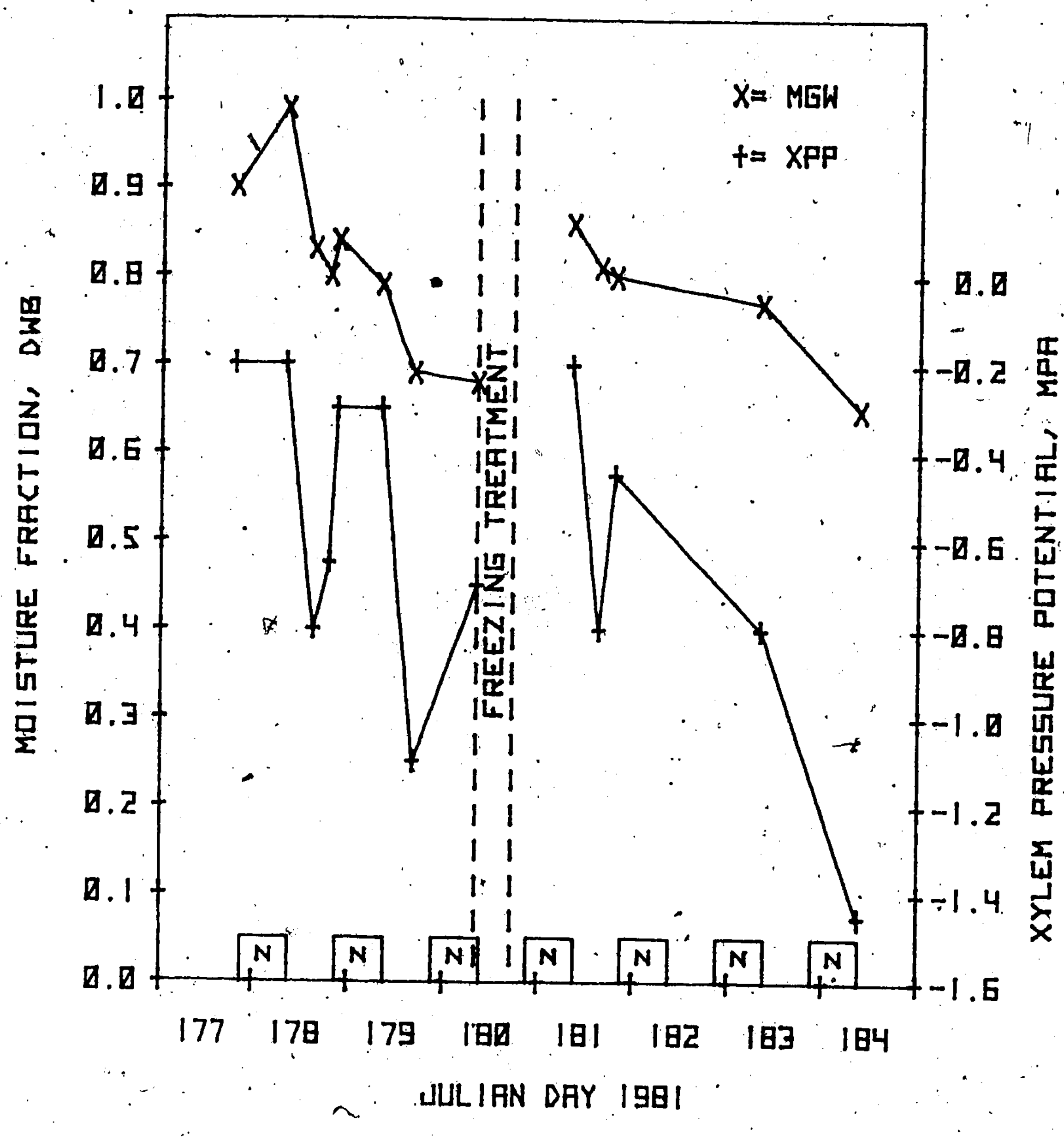

Figure 45. Time trend of Mgw(D[1],Pb) and XPP in P. tremuloides, tree PT2, before and after the stem freezing treatment. No thermal diffusivity data could be taken during the freezing treatment. Moisture contents appear to have an association with BP (XPP at 08 h, "N" indicates night 21 - 09 h), but does not follow the rapid flucuations in XPP noted during the daylight hours.

could drop from near total saturation to near fibre saturation in 60 minutes especially, since he (Running 1980a), reported an average total sapwood water content in these trees of 16.9 L, and a maximum transpiration rate of 1.9 L h^{-1}. Thus there is some question as to how closely one can estimate short term sapwood water content fluctuations from a relationship between RWC and XPP. Perhaps the near-continuous moisture content estimates that hourly D^1 measurements provide could be used to further explore the relationship between XPP and RWC.

Sampling

An adequate sample of HPV's throughout the sapwood is a necessity if transpiration calculations are to be valid. What constitutes an adequate number of sensors and their spatial placement in the sapwood is a good deal easier to determine after, rather than before, the fact. The results reported here were obtained with 1 to 16 sensors emplaced at various positions in the xylem. One sensor, apparently very strategically placed, gave good results in Aleppo pine. Sixteen sensors, apparently wrongly placed, produced what I consider to be poor results in B. papyrifera (trees BP1 and BP2), especially after induced cavitation.

The sampling system used in the P. radiata, N. solandri var. cliffortioides and P. tremuloides (tree PT2) experiments was to emplace sensors at predetermined depths to sample certain toroidal sections of sapwood (Fig. 27 p. 118). The results indicate that this was apparently a good scheme.

The imposition of artificial conditions, such as freezing the stem, or a naturally occuring phenomenon, such as drought stress, may cause a shift in flow paths from one area of the sapwood to another. If all areas are not sampled, then the HPV technique may not fully detect the change caused by the event (for example trees BP1 and BP2). Sampling to detect the effects of the desired phenomena is fundamental to good experimental design and not a peculiarity of the heat pulse technique. Therefore it is imperative, whatever sampling scheme is used, that a sufficient number of sensors be properly placed in the sapwood to detect the probable changes.

The "no sensor" RLM simulations indicate that zero flow boundaries begin to influence HPVA's, HPVS's or HPVT's at about 1 cm from them (Fig. 23, p. 108). The experimental results with Teflon sensors (Fig. 31A, p. 132) indicate that they behave similiarily (to the no sensor simulations) so that sap flow is sensed within an area of approximately 1 cm diameter centered on the sensor tip. The RLM simulations with high thermal conductivity sensor materials (Fig. 32C, D and E; p. 134) and the experimental results with glass and brass rod sensors (Fig. 31B and C, p. 132) suggest that a slightly larger area, approximately 1.5 cm diameter centered on the tip, is sensed by them. If it is critical to ensure the successful outcome of an experiment that all portions of the sapwood be sampled, then one Teflon sensor should be installed in each 0.8 cm^2, or one glass (or brass) rod sensor in each 1.8 cm^2 of sapwood area. This may require many more than the 16 sensors that I have used in the most dense arrangement reported here.

CHAPTER VI

GENERAL DISCUSSION

Idealized heat pulse velocity theory

Marshall (1958) provided a concise definition for the velocity of a heat pulse (Eq. 2, p. 18) as calculated from his analytical equations as "the weighted average of the velocities of the sap and stationary wood substance." Unfortunately the term heat pulse velocity has been applied to the data obtained from almost any thermometric sap flow measuring technique (e.g. Hinckley, Lassoie and Running 1978; Kramer and Kozlowski 1979; Miller, Vavrina and Christensen 1980). This has resulted in considerable confusion particularily in comparing data and results from studies using differing thermometric techniques such as Huber's (1932) "first onset", Huber and Schmidt's (1937) "compensation method", Marshall's (1958) "heat pulse velocity" or Daum's (1967) stem thermal budget. Failure to appreciate the basic theoretical differences between these differing methods and the type of data obtained from each has impeded progress toward realizing the potential of any of them in sap flow measurement. Further, the results of application of Marshall's (1958) theoretical analyses in cases where it did not apply (e.g. Gale and Poljakoff-Mayber 1964; Merkle and Davis 1967; Miller and others 1980) has discouraged development of an "applications" base upon which to build empirically. Even where Marshall's (1958) technique was applied with regard for his conditions, nonuniform analyses and/or instrumentation have produced data sets incompatible with each other, obscuring the serious practical and theoretical problems presented in application of the idealized analyses (e.g. Swanson 1967, 1972, 1975; Hinckley 1971b; Morikawa 1972; Lassoie, Scott and Fritschen 1977; Cohen, Fuchs and Green 1981). Lastly the plant medium-technique interraction has been a confounding influence as the affects of stem tissue borders, the severity of the influence of wounding caused by sensor implants and physical changes accompanying physiological stress have not been fully recognized and accounted for (e.g. Gale and Poljakoff-Mayber 1964, Lopushinsky and Klock 1980).

Marshall (1958) clearly set out the conditions under which his analyses were valid. He tested them, under the rather unique rapid growth circumstances that New Zealand grown _P. radiata_ offers, and found them to be valid. He did not forsee the problems that much slower sap speeds and smaller sapwood radii would create for future users. (Neither did he have any control over subsequent application and misapplication of his analysis.)

Practical theory based on numerical modeling

Numerical models of HPV probes and tree stems

In this study, I have used two numerical models of a stem, one in the tangential-longitudinal plane, the other in the radial-longitudinal plane, to demonstrate that significant departure from Marshall's (1958) analytical solutions for heat flux in sapwood arise from flow interruption due to finite probe size and, to a lesser degree, from both sensor thermal properties which differ from those of wood and the position of sensor tips with respect to the bark/sapwood or sapwood/heartwood borders. Both numerical simulations and experimental results further indicate that the results obtained depend upon sensor spacing, method of analysis and the time intervals chosen for application of Equations, 4 - 9 (Chapter II, p. 19 - 23), available for determining heat pulse velocities. Thus it is clear that the practical use of the heat pulse velocity method for determining sap flux requires solutions to the heat transport equation (Eq. 1, p. 18) for the particular conditions of measurement.

Several of the conditions imposed on Marshall's (1958) idealized theory were relaxed to obtain these more practical solutions. Sensors were of finite size and materials, the heat pulse of finite duration, and the xylem not infinite. Nonconvecting layers were present in the vicinity of the sensors. Heat pulse probes larger, smaller or of different shape than the 0.16 cm diameter circular ones I have used may be simulated in either model. The programs in Appendix F may be used with probes 0.04 to 0.32 cm diameter (TLM) and up to 4.0 cm long (RLM) without modification simply by inserting the appropriate thermal conductivity, specific heat and density values at each point in the node coefficient file (CPRB) indexed by the node index file (IPRB). Probe diameter is an extremely important practical as well as theoretical parameter as it sets the minimum width of nonconvecting wood (wound) in the plane of the sensors in the tangential-longitudinal model. Glass sensors, with thermal conductivity about 30 times that of wet sapwood, cause some offset in calculated HPV's with asymmetrically configured sensors, but only at zero sap flow. This offset remains relatively constant with even higher thermal conductivity sensor materials such as brass or aluminum. Therefore, a very detailed specification of sensor thermal properties is warranted only for materials with properties similiar to wood.

Macroscopic anatomical considerations

Only macroscopic anatomical features of a tree stem have been simulated in my application of the models. I have used the radial-longitudinal model to simulate several combinations of bark and/or sapwood and/or heartwood in a 4.0 (radial) by 8.0 cm (longitudinal) and the TLM to simulate wound values of 0.16 to 0.52 cm in a 3.2 cm (tangential) by 8.0 cm (longitudinal) grid. The only limitation on the fineness of the features that can be simulated by either model is node spacing, grid dimensions, computer memory capacity and computing cost.[5/] With the node spacing used in this study, the RLM can accommodate cork and phloem layers in the bark, early and latewood layers in the xylem, if each is a multiple of 0.04 cm in radial width. The TLM can handle xylem rays which are 0.04 cm or multiples thereof in tangential cross section.

5/ The 4.0 by 8.0 cm with 0.04 cm node spacing is the largest that can be accommodated with the ADI numerical solution technique in the University of Alberta's array processor. Much larger matrices can be accommodated in the University of Alberta's Amdahl 470V/8 mainframe, but the computation costs for even this 4.0 by 8.0 cm matrix in it, is roughly 10 times that in the array processor.

Microscopic anatomical assumptions

Convective and conductive thermal homogeneity must exist at each node in the grid of a numerical model as a point can have but one set of thermal properties. This means that the physical space represented by the node must exhibit similiar thermal homogeneity if the simulations are to be physically realistic, i.e., it must be isothermal (but may be anisotropic). In my models with 0.04 cm grid spacing, a node may be considered to represent a 0.0016 cm^2 area of stem tissue. To insure isothermal conditions within this area, the fine structure of the tissue simulated must be such that the node's temperature equilibrium time is negligible (Eq. 18, p. 29). Considering 0.3 s (1% of the shortest solution time, 30 s) as negligible, this means that any nonconvecting layer, in any 0.0016 cm^2 area partially occupied by functioning vessels or tracheids, must be 0.03 cm or smaller in the radial or tangential direction as appropriate to the radial-longitudinal or tangential-longitudinal model. The xylem of conifers may be assumed thermally homogeneous in this context (with the possible exception of areas containing longitudinal resin canals larger than 0.03 cm wide). Considering an average pore diameter of .04 mm, diffuse porous hardwoods, with more than 6 to 10 pores per square millimeter ($0.01^2/0.004^2 = 6.25$), may be assumed to be thermally homogeneous within this same context, i.e., te = 0.3 s (possible exception, an area of xylem including very large rays, 0.03 cm or more wide). Vessel arrangements in ring and semi-ring porous woods are so varied (Brown, Panshin and Forsaith 1949; McMillin and Manwiller

1980) that no general assumption on thermal homogeneity, or the lack of it, is warranted.

Future developments

Development and testing of heat pulse theory with numerical models is a continuing venture that will not terminate with this study. Since idealized heat transport theory does not apply in any practical sap flow measurement case, one loses the general applicability of it and must derive numerical solutions approximately applicable to each situation. The cases to which these 2-dimensional models have been applied have been, for the most part, those in which the results were verifiable by experiments conducted by me. Further work is required to verify the relationship between thermal diffusivity and sapwood moisture content. Verification is also needed of the averaging affect of high thermal conductivity sensor materials (glass, brass, aluminum etc.), in very nonhomogeneous sapwood such as Douglas fir (Cown and Parker 1979), especially that New Zealand grown, where the negligibly permeable latewood layers may be up to 0.6 cm wide (personal measurements, unpublished) in radial cross section. Also the simultaneous effects of sensor materials, sensor radial position, stem tissue borders and wound can only be explored with a 3-dimensional heat flow model.

Precautions

The new theoretical analyses presented and tested in this study, which are based on 2-dimensional simplifications of non idealized situations, explain much of the deviation from idealized theory that one encounters in practical applications. A number of cases, specific to the instrumentation and analyses techniques recommended below, have been simulated to provide a "standard" set of solutions for application to the measurement of xylem sap flow. These will provide no better results, and receive no better acceptance than Marshall's idealized analyses, if the recommended practice is not adhered to.

Practical sap flow measurement considerations

Wounding upon HPV probe implantation

Flow interruption (wound) occuring during and subsequent to heat pulse probe implantation has been shown to cause the most serious departure from idealized theory. The comparisons of transpiration calculated from HPV's with independent measurements of transpiration required selection of wound width values for the corrections. When HPV measurements were made within a few days of probe installation, good results were obtained by assuming that initial flow interruption was confined to a slab of nonconvecting wood as thick as the largest probes' diameter, plus 0.04 cm to account for probe misalignment, e.g. the *P. halepensis*, *P. radiata* (first drying cycle) and *Picea glauca* experiments.

Wound width increases with time after installation. This is to be expected as a consequence of oxidation and resin deposition in the sapwood surrounding the probes (Shain 1967, 1979, Shigo and Hillis 1973, Merrill and Shigo 1979, Shortle 1979). In *P. contorta*, wound width had increased to 0.32 cm (simulated result) at 30 d, and to 0.44 to 0.52 cm, 100 d after installation (confirmed by measurement). This means that either HPV measurements should be carried out with freshly installed probes, or wound width should be measured, a necessarily destructive procedure.

In the Picea glauca experiments, reasonably good results were obtained with the assumed W = 0.20 cm for 15 to 30 d after probe installation. In the Betula, Nothofagus and Populus experiments, where wounds were measured, corrections to HPV's based on these gave reasonably good results. During the second drying cycle of the P. radiata experiment, assuming W = 0.28 cm gave much better agreement than W = 0.20 cm. The apparently retarded wound development in the P. halapensis, P. radiata and Picea glauca experiments, where the original correction was valid for 14 to 40 d, may have been due to stress induced by the artifical environment and reduced water supply. This observation is supported by the work of Vite' (1961) and Puritch and Mullick (1975) who reported that resin exudation and physiological wound reactions may be delayed or postponed by high plant water stress (e.g. August data points, Fig. 5, p. 21). I feel that with 0.16 cm diameter probes, the use of a W = 0.20 cm correction will be valid for about 10 d under normal physiological conditions, but the actual speed and extent of wound development depends upon a complex series of successional events which, at present, are unpredictable (Merrill and Shigo 1979) so that actual wound, beyond that occuring upon implantation, must be ascertained in each situation.

Analysis method and probe configuration

Analytical technique, sensor spacing and sensor arrangement must be suited to the range of heat pulse velocities anticipated. Heine and Farr (1973) consider heat pulse velocities to be about 1/19 of actual sap speeds. The magnitude of HPV's (conforming with Marshall's definition, Eq. 2, p. 18) that have been encountered in conifers is 0 to 35 cm h^{-1} and 0 to 32 cm h^{-1} in diffuse porous hardwoods (Hinckley and others 1978) with most less than 25 cm h^{-1}.[6/] The fastest I have ever measured was an HPVT of 34 cm h^{-1} in P. radiata (unpublished data). The simulations indicate that no single analytical technique, sensor spacing or sensor configuration will produce satisfactory results over this 0 to 35 cm h^{-1} HPV range.

In the idealized case, the HPV data derived from all of the analytical equations is the same and may range in magnitude from zero to several meters per hour. In the nonidealized situations of interest, the HPV's derived from the several equations are not the same and the range of actual HPV's that can be detected with a particular sensor spacing is limited by wound, the proximity of the sensors to the sapwood boundaries and the choice

---

6/ Hinckley et al (1978) in their Table 5, give sap speeds as "HPV" if derived from thermometric data; "HTO", "32P" or "86Rb" if derived from tracers. To derive the above range of Marshall-type HPV's in conifers and diffuse porous woods, I considered that all of their "HPV's" attributed to Huber and cohorts, and those obtained from tracers were peak sap speeds. These I have converted to Marshall's HPV's by dividing them by 19 as was done by Heine and Farr (1973).

of times at which temperatures are determined. The analytical equation (Eq. 4 - 9, Chapter II, p. 19 - 23) used to convert temperature data to heat pulse velocities, the physical arrangement of the heat pulse probes in a tree stem, and the solution times at which temperatures are to be measured must be chosen with due regard for the xylem position of the sensors and the HPV's that they are likely to encounter there. Equations 4 and 7 are usable with temperature data from one temperature sensor located downstream from a heater. Equations 6, 8 and 9 require data from a second sensor located upstream from the heater.

The numerical simulations indicate that the one sensor HPVM (Eq. 4, p. 19) and HPVP (Eq. 7, p. 22) configurations are virtually useless at actual HPV's 0 to 20 cm h^{-1}. In RLM simulation, both of these techniques were seriously affected by the proximity of the S/H border and to a lessor extent by heat loss when near the B/S border. The HPVM equation may be of use at actual HPV's greater than 20 cm h^{-1} in combination with the two sensor HPVA or HPVS configurations because the data for it are those that would ordinarily be obtained at the downstream sensor of these two sensor arrangements. My experience in using the HPVA, HPVM and HPVS analysis techniques is that reported in Chapter V where the HPV's encountered were all less than 20 cm h^{-1}. Results obtained in quantitative tests from the few trees instrumented to obtain HPVA's or HPVS's were similiar to results obtained from the very many installations where HPVT's were obtained. I feel that I have some justification to recommend further use of the HPVA and HPVS techniques (but no basis to comment on further use of HPVM). The only reported work using the single sensor HPVP technique is that of Cohen, Fuchs and Green (1981) who were apparently satisfied with the consistency of their data. Aside from Marshall's (1958) initial experiments to verify the correctness of his theory, the use of the single sensor HPVM analysis to calculate sap flow in any practical situation has yet to be established.

One very important consideration in using the two sensor configurations, HPVA, HPVS or HPVT, is the magnitude of the temperature rise occuring at the upstream sensor. Miller, Vavrina and Christensen (1980) report that with a sensor 1.6 cm upstream from the heater, at peak sap speeds greater than 2 m h^{-1} (an HPV of approximately 10 cm h^{-1}) no heat reached the upstream sensor. Table 18 gives values for the theoretical temperature rise at 120 s (obtained using Eq. 3, p. 19) at sensors located 0.96 or 1.44 cm upstream from the heater. With my instrumentation, the minimum detectable temperature rise above ambient is approximately 0.005 ^{o}C. With a 4 s heat pulse, a true HPV of 60 cm h^{-1} (corresponding of an HPVA, HPVS or HPVT at W = 0.20 cm of 20 to 25 cm h^{-1}), the temperature rise would be marginally detectable at 0.96 cm, and undetectable at 1.44 cm upstream (Table 18). Therefore, the HPVA, HPVS or HPVT techniques, with an upstream sensor within approximately 1 cm of the heater, should be usable over the range of HPV's normally encountered in conifers and diffuse porous hardwoods.

Table 18. Theoretical temperature rise at a sensor 0.96 or 1.44 cm upstream from a heater, 120 s after a heat pulse of 1 to 4 s duration, in dry sapwood; HPV = 0, 30 or 60 cm h^{-1}, Mgw = 0.5 dwb, Pb = 0.4 cal g^{-1} $^oC^{-1}$, D^1 = 0.0024 cm^2 s^{-1}. The heater is composed of brass tubing, 0.16 cm diameter with No. 28 AWG nichrome wire insulated from the brass tubing by Teflon. At an electrical resistance of 0.16 ohms cm^{-1}, and a 4 ampere current, the temperature rise at the heater is approximately 40 ^oC s^{-1}. At higher sapwood moisture fractions, 1.0 to 1.5, the temperature rise would be about one-fourth to one-tenth that tabulated.

HPL sec	Temperature rise above ambient, ^oC at indicated HPV						
	at heater	Sensor at 0.96 cm			Sensor at 1.44 cm		
		0	30	60 cm/h	0	30	60 cm/h
1.0	40	4.6	0.23	0.01	1.94	0.09	0.001
2.0	81	9.2	0.46	0.02	3.87	0.18	0.002
3.0	121	13.8	0.70	0.03	5.81	0.27	0.002
4.0	161	18.5	0.93	0.04	7.75	0.37	0.003

Analysis method and sensor location

Marshall (1958) indicated that with sensors implanted less than 0.5 cm deep in a dowel, freshly milled from pine sapwood, heat loss at the surface noticeably affected HPVM measurements. (I interpert a "freshly milled dowel" to mean that no bark was present and flow occured just under the surface as well as at all deeper depths in the dowel.) The RLM simulations generally confirm the necessity for this depth beneath the flow surface with the single sensor analyses techniques, and with 0.32 cm of bark, the sensor must be installed to a total depth from the bark surface of 0.82 cm. With the two sensor techniques, this depth criterion can be relaxed considerably, as both simulated and experimental results indicated that sensors could be as shallow as 0.2 cm into sapwood if the bark was 0.3 cm thick.

The radial-longitudinal model simulations without sensor materials indicate that HPV's calculated from temperatures registered within 1 cm of the S/H border are affected in two ways.

1) By a gradual reduction in magnitude that begins about 1 cm on the sapwood side of the border and continues on for about 1 cm into the heartwood before indicating zero movement.

2) By distorting the temperature field at HPVI's greater than 20 to 30 cm h^{-1} so that the HPV's and D^1's calculated from temperatures taken at fixed time intervals (e.g. 60, 120 and 180 s) assume nonsensical values, i.e., either extremely high or negative (Table 10, column 4,5 6; p. 99).

In the potometer experiments, the relationship between calculated sap flow and actual transpiration was improved slightly in poplar and made worse in birch by inclusion of a correction for the gradual reduction in HPV's that the RLM simulations indicated. The PT2 poplar potometer was the best instrumented of the four. Here the position correction resulted in a minor improvement of calculated versus actual transpiration, but did not greatly improve the data fit about the 1:1 line over that provided by the correction for wound alone (Fig. 43A and B, p. 177).

The HPV's attained in the potometer experiments were all below the values (20 to 30 cm h^{-1}) where the instabilities began to become evident in the RLM simulations. Radial profiles of longitudinal permeability (Booker and Swanson 1979) indicate that, for the most part, liquid permeability near the S/H border is about 50 to 60% of that shallower in the sapwood. Presumably heat pulse velocities near the S/H border would be reduced on the same order of magnitude as the permeability values, and only rarely would the high HPV's, at which the nonsensical results were simulated, be attained in actual sapwood. I have never observed the simulated behavior, but since my experience in applying the HPVA, HPVS and D^1 analyses techniques is limited to that reported in Chapter V, where the fastest HPV measured was 17 cm h^{-1}, I cannot say that it will never be observed.

Because of the low HPV's encountered in conifers and diffuse porous hardwoods (0 to 35 cm h^{-1}), the use of one of the two sensor analytical techniques is mandatory. The HPVA, HPVS, HPVT and D^1 analyses are stable from HPVI = 0 to 60 cm h^{-1} if the sensor tips are not within 1 cm of the S/H border. Within 1 cm of the border, the behavior of the HPVA, HPVS and D^1 analyses that is indicated in the RLM simulations may indeed occur and one may have to avoid sampling in this portion of the sapwood, sample at time intervals shorter than 60 s (e.g. 30 s, Table 11, p. 100) or shift to the HPVT analysis technique which is relatively unaffected by the S/H border (Table 12, p. 101).

The results from potometer PT2 indicate that sampling with more than one sensor at each of several depths in the sapwood is far more important than correcting for errors in HPV measurement near the S/H border in order to extrapolate them over the whole sapwood. In most practical instances, one would only know in general the position of his sensor tips with respect to the S/H border. If the high thermal conductivity sensors are used, then the position correction is apparently not necessary. With good sensor distribution in the outer sapwood, application of the radial position correction is not generally warranted in application of implanted heat pulse theory to the measurement of sap flow in conifers and diffuse porous hardwoods.

Thermal diffusivity and moisture content

Longitudinal thermal diffusivity is sensitive to moisture content and appears to be of use in estimating it in conjunction with HPV measurements. Sensor spacing is more critical in obtaining D^1 than in obtaining HPV. At a sensor 0.48 cm upstream from a heater, the D^1 calculated at low sapwood moisture content simulation (Mgw = 0.5) was 0.0020 $cm^2\ s^{-1}$, compared to 0.0024 $cm^2\ s^{-1}$ imposed. At sensors 0.96 or 1.44 cm, the D^1's calculated were 0.0022 and 0.0023 $cm^2\ s^{-1}$ respectively. The difference between the values obtained at these spacings become smaller as Mgw becomes larger (see Tables 8 and 9, p. 87, 88, Mgw = 1.0 to 1.5).

In addition to the interraction between sensor spacing and D^1, the values obtained at either an up or downstream sensor are also influenced by the HPV imposed during simulation. At imposed HPV's greater than 5 to 20 cm h^{-1} (the range of applicable HPV's is dependent upon Mgw), the D^1 calculated at the upstream sensor is larger, that at the downstream sensor smaller, than that calculated at HPVI = 0 cm h^{-1}. With both sensors approximately 1 cm or more from the heater, the average of the D^1's obtained from both of them is quite close to that obtained at HPVI = 0 cm h^{-1} (Table 9, p. 88), and this average is the value that should be used to estimate sapwood moisture content.

Heat pulse probes

The diameter of the heat pulse probes should be as small as is practical to reduce wound width upon implantation. The 0.16 cm diameter heater used throughout this and most of my previous studies (Appendix E) is about the smallest that can be used and still produce a detectable temperature at 1 cm upstream. Since wound width is a function of the largest diameter probe in a heat pulse set, there is no reason for making the temperature sensors some smaller size -- although it is physically possible to do so.

The transpiration results (Figs. 36 - 39, Tables 15 - 17; p. 149 - 166) obtained with a few high thermal conductivity glass rod sensors were consistently better than those obtained with several of the lower thermal conductivity Teflon sensors (Figs. 40 - 43, p. 173 - 177). These results may have been due to the greater sapwood area that these glass sensors integrate or to the less artifical physiological conditions of trees in lysimeters versus severed stems as potometers. The Teflon sensors were used because they could be easily removed and used in subsequent studies. (I tried to use brass sensors but the electronics of the then operable HPV logger was incompatible with the multiple common electrical grounds that occur with more than one sensor set.) Glass sensors are not as mechanically robust as the Teflon ones, tending to crack upon insertion (and it is almost impossible to excise them without damage). The cracks allow sap to contact the thermistor lead wires which causes unpredictable electrical noise at the temperature detector. This can be a serious problem with the glass rod sensors if they are not very carefully installed.

In the RLM simulations, the brass rod sensors integrated HPV's over an area on the same order as the glass rod sensors. The brass rod sensors are mechanically robust (they are constructed almost identically to a heater except that a bead thermistor is installed instead of the nichrome wire) and in the one field test that I have conducted with them, they were not subject to electrical noise even after several insertions and removals to other locations. Their principal disadvantage is that the case is one side of the electrical circuit and it is common, via the tree, to one side of the heater as well. Electronic circuitry can be devised to accomodate these multiple common grounds, but the large electrical transient generated during the heat pulse may be propogated into the temperature measuring circuitry. Instrumentation to utilize the brass sensors in multiple probe installations is tricky at the millivolt temperature signal levels involved.

The Teflon sensors were moderately rugged. They were easily installed and about 95% could be removed for use in subsequent studies. They are electrically isolated from the tree and heater circuit. From both the mechanical and electrical standpoint they are an ideal sensor. The small amount of sapwood they integrate over may be an advantage in studying the relatively fine structure of sap movement near tissue borders, but a disadvantage in transpiration measurement.

To conclude this section on sensors: there is no ideal sensor suited to all applications of the heat pulse velocity technique. The choice, in each instance, must be made with due consideration for the objectives intended for the data and the electronic indicating or recording instrumentation available to the researcher.

Indicating or recording instruments

One does not have to take very many HPV measurements before he realizes the value of a recording instrument. Taking HPV's, particularily HPVT's, is a boring job! Sap flow may occur at all hours of a day. Both day and night HPV's are necessary to estimate diurnal transpiration. Several sites may need to be sampled simultaneously. All of these sampling schemes can be done with a number of direct indicating instruments and several observers, but recording of some sort is preferred, largely to eliminate errors caused by the boredom of taking the readings.

The easiest analysis technique to instrument is HPVT. One needs only a sensitive null detector to indicate when temperatures at the up and downstream sensors are equal, a means of activating the heater for some prescribed duration and a stop watch to indicate tz at null temperature after the heat pulse has been registered. Suitable indicating instrument designs are given by Swanson (1962, 1974a). This technique can be semi-automated to relieve operator error by replacing the indicating meter with a strip chart recorder and by providing some sort of elementary programmer to actuate the heat pulse. The tz is measured from the recorded temperature difference trace (Swanson 1967b).

The HPVT technique gives the least amount of useful information to go with HPV, and it is not useful at HPV = 0 or at negative HPV's. Also, normal heat dissipation from the test section, limits the tz one can determine, with either an indicating or recording instrument, to about 300 to 400 s (Swanson 1962) corresponding to an HPVT of 3.0 to 2.5 cm h^{-1} with the (-0.5,0,1.0 cm) sensing configuration. The time spent obtaining tz is inversely proportional to sap flow as tz is greatest at the slowest flows.

The use of the other time-dependent solution, HPVP, has been reported by Cohen and others (1980). The time of maximum is not sharply defined at low sap speeds (Fig. 2, p. 20), and is best obtained from a recorded temperature trace or with an electronic "maximum" detector. Measurement time is an inverse function of sap speed as with the HPVT technique.

The fixed time interval HPVA, HPVM, HPVS and D^1 solutions appear most useful with digital recording instrumentation. One can construct an instrument to sample several sensor sets at fixed intervals in multiplex or time sequence and record the temperature in digital code on magnetic tape for direct entry into a computer. The HPV logger that I had constructed read temperatures at -60, 0, 60, 120 and 180 s. The temperatures before (-60 s) and at the heat pulse (0 s) are ambient; temperatures at 60, 120 and 180 s after the heat pulse are referred to ambient for use in the appropriate equations. These data can be multiplexed over a relatively short time span (ca. 5 to 10 min for all of the probe sets, limited to 8 sensor sets in a group by heat pulse duration), i.e.: T_1 sensor 1, T_1 sensor 2, ... T_1 sensor m; T_2 sensor 1, T_2 sensor 2, ... T_2 sensor m; ... T_n sensor 1, T_n sensor 2, ... T_n sensor m. Or the temperatures may be taken sequentially at one sensor before advancing to the next set so that data are taken over a long time span (ca. 5 minutes for each probe set to a maximum of 12 sets if hourly data are needed), i.e.: T_1 sensor 1, T_2 sensor 1, ... T_n sensor 1; T_1 sensor 2, T_2 sensor 2, ... T_n sensor 2; .... T_1 sensor m, T_2 sensor m, ... T_n sensor m. (In both cases, n is the discrete time step, m is the sensor set number.) The sequential scheme can be easily adapted to a strip chart recorder or existing data logger; the multiplexing scheme is best suited to a dedicated heat pulse recorder. (See Appendix E for suggested multiplexed logger.)

Sap conducting xylem area

According to Kramer and Kozlowski (1979) the amount of the crosssectional area of a tree trunk involved in sap conduction varies widely. In diffuse porous hardwoods and nonporous coniferous woods, a number of growth increments are involved. In some ring porous hardwoods, only the most recently formed ring conducts sap.

In this study, which has been confined to diffuse porous and coniferous woods, I have assumed that all of the xylem lying outside of a central core defined by an abrupt change in moisture content or color was conducting. If xylem pressure potential is propagated uniformly across the conducting sapwood, then one should expect sap movement wherever the wood is sufficiently permeable to permit it. The saturated longitudinal permeability measurements of Booker and Kininmonth (1978) and Booker and Swanson (1979) indicated that the entire sapwood of the species studied was thus capable of conducting sap. In this study, the TR(HPV) values calculated using the total sapwood as conducting area did not consistently overestimate actual transpiration as would be the case if only the small outer portion of the sapwood was actually conducting.

The heat pulse technique with Teflon sensors may be useful in defining the approximate boundary of the sap conducting area even if it does not define it precisely enough for use in transpiration calculations. Likewise pulsed electrical resistance may provide an indication of the radial extent of discoloured wood or true heartwood (Skutt, Shigo and Lessard 1972). Certainly, the radial extent of sapwood indicated by saturated longitudinal permeabilty profiles could be verified or refuted with these techniques. Until such work is done, Kramer and Kozłowski's (1979) statement that the "anatomy of the conducting system needs more study" still stands.

Sapwood moisture content

In the artifical transpiration situation of the potometer experiments reported in Chapter V, calculated sapwood moisture content was shown to decrease through time as the tree was subjected to considerable stress (Fig 45, p. 186; XPP = -0.2 to -1.4 MPa). Edwards (1980) using a non destructive gamma attenuation technique on stems of *Pinus contorta* and *Picea sitchensis* (Bong.) Carr, found that sapwood moisture content was increasing at the top of a tree while decreasing near the bottom. Shain (1979) reported that in excised wood bolts, water was withdrawn from severed tracheids by tensions still existing in the intact xylem. Shain and Edwards measurements indicate that sapwood moisture content is not static, presumably undergoing continual spatial adjustments to equalize longitudinal gradients in xylem pressure potential. More importantly, Edwards found that sapwood moisture content returned to the previous day's value after undergoing a diurnal change when XPP fluctuated between -0.3 and 0.6 MPa. My results (Fig. 45, p. 186) show a range of diurnal fluctuation similiar to Edward's, but superimposed upon a decreasing moisture content trend as XPP decreases.

My results, combined with Edwards (1980), indicate that sapwood moisture content undergoes relatively minor diurnal fluctuation. If moisture content is measured at the beginning and end of a heat pulse measuring sequence under normal physiological conditions, the daily values in-between can be linearly interpolated. Under stress conditions, it should be possible to augment beginning and end moisture content with estimates from longitudinal thermal diffusivity measurements. Again, the sapwood moisture content of living trees is an area where further study is needed. Perhaps simultaneous estimates based on longitudinal thermal diffusivity measurements and gamma attenuation would improve our understanding of moisture content fluctuation in normal and stressed trees.

RECOMMENDED PRACTICE

Sap flow or transpiration measurements which are based on heat pulse velocities, require sound spatial and temporal HPV sampling procedures as well as accurate estimates of the sap conducting area, sapwood moisture content and sapwood basic density. The techniques and analyses to obtain HPV's at a point are based on the simulated and experimental results reported in this study and must be strictly adhered to in order to obtain comparable results. The techniques indicated for obtaining estimates of sap conducting area, sapwood moisture content and temporal-spatial HPV averages are those that I have used with some degree of success. This latter group is included in these recommendations primarily as a guideline that may or may not be adequate to obtain reasonably precise estimates of sap flow in a particular situation.

Applicability

The practice recommended here is applicable to all coniferous and diffuse porous woods meeting the following criteria.

1) Sapwood equal to, or greater than, 1 cm in radial width, i.e., stems at least 2 cm, dib.
2) Latewood portion of growth rings equal to or less than 0.2 cm in radial width and making up not more that 50% of the sapwood.
3) A minimum of six to ten vessels per square millimeter (diffuse porous woods only).
4) Sensors installed 10 or fewer days.

Heat pulse instrumentation

Sensor configuration

Sensors 0.16 cm diameter spaced 1.0 ± 0.1 cm at equal depths above and below a line heater extending from the bark surface to at least 1 cm deeper than the tips of the sensors.

Analysis technique

1) HPVS from temperature ratio at 120 s (Eq. 6, p. 21).
This technique is useful with the above sensor spacing from HPVS = 0 to 30 cm h^{-1}, which at W = 0.20 cm, corresponds to a true HPV range greater than 60 cm h^{-1} (Table 19).[7/] This range should be adequate for the applicable woods.

2) Longitudinal thermal diffusivity calculated at the downstream sensor with temperature data taken at 60, 120 and 180 s.

Sensor materials

Teflon, glass or brass depending upon the objectives of the study and the instrumentation available. Glass or brass materials are prefered for transpiration studies.

Recorder-controller

The block diagram of a controller to actuate a given length heat pulse and record the temperature rise at the up and downstream sensors of two HPV probe installations is given in Appendix

---

7/ The equations of Table 20 are presented as a convenience to those who have used Marshall's idealized theory with implanted, asymmetrically spaced temperature sensors. Although this Table was derived from simulations of 0.16 cm diameter glass sensors at (-0.5,0.1.0 cm), these equations give results (using HPVT) within 5% (at the appropriate wound width) with any sensor material if the sensors are spaced so that the difference in up and downstream distance is 0.5 cm, i.e. (-0.3,0,0.8 to -1.0,0,1.5 cm). I have also included equations for use with HPVA to resolve sap flows near zero. These last are valid for data from 0.16 cm diameter, glass or brass sensors spaced (-0.5,0,1.0 cm), analysed at t_1 = 60 s and t_2 = 120 s.

Table 19. Coefficients for calculating imposed HPV's with glass, brass or Teflon sensors spaced (−1.0,0,1.0 cm) calculated using Equation 6 (p. 21); HPVS, downstream to upstream temperature ratio at 120 s and longitudinal thermal diffusivity from the downstream temperature sensor at t = 60, 120 and 180 s. HPVC = a + bHPVS + c(HPVS)^2.

Wound	HPVS 4 to 30 cm/h			HPVS 0 to 5 cm/h		
cm	a	b	c	a	b	c
0.16	3.708	0.655	0.063	0.090	1.404	0.029
0.20	4.612	0.449	0.099	0.115	1.505	0.045
0.24	5.329	0.254	0.141	0.132	1.622	0.063
0.28	6.617	−0.162	0.214	0.146	1.767	0.088
0.32	7.577	−0.543	0.296	0.166	1.921	0.117
0.36	9.097	−1.241	0.434	0.179	2.113	0.158
0.40	10.432	−1.994	0.607	0.195	2.332	0.205
0.44	11.881	−2.912	0.832	0.205	2.607	0.261
0.48	12.910	−3.829	1.130	0.206	2.946	0.327
0.52	14.023	−4.897	1.473	0.207	3.333	0.401

Table 20. Coefficients for calculating imposed HPV's from those calculated using Equation 8 (p. 22), HPVT, or Equation 9 (p. 23), HPVA, at t = 60 and 120 s with glass or brass sensors spaced (-0.5, 0, 1.0 cm). (Use Table 19 with Teflon sensors in this configuration.) HPVC = a + b(HPVA or T) + c(HPVA or T)^2.

Wound	HPVA or HPVT 3 to 30 cm/h			HPVA 0 to 6 cm/h		
cm	a	b	c	a	b	c
0.16	0.392	1.356	0.036	0.444	1.332	0.029
0.20	0.807	1.203	0.058	0.465	1.396	0.037
0.24	1.184	1.072	0.087	0.495	1.487	0.046
0.28	1.524	0.964	0.124	0.533	1.604	0.056
0.32	1.826	0.879	0.169	0.580	1.747	0.068
0.36	2.090	0.818	0.221	0.634	1.916	0.082
0.40	2.317	0.779	0.281	0.697	2.110	0.098
0.44	2.506	0.764	0.349	0.769	2.331	0.115
0.48	2.658	0.772	0.424	0.848	2.577	0.134
0.52	2.772	0.802	0.507	0.936	2.850	0.154

E. Temperature values can be obtained from the recorded traces at any time intervals, but the equations given in Table 19 are valid only with temperature data taken at 60, 120 and 180 s.

Sap conducting area

The portion of the xylem defined by the depth at an abrupt decrease in moisture content or change in color is considered as conducting sapwood. This depth should be determined in a standing tree, as the average from at least 4 increment borings taken 30 to 40 cm above and below the sensors, or if the tree is felled and the wood near the sensors can be excised, the average of the actual depths at each sensor.

Moisture content

In trees not subjected to significant drought stress (BP between -0.3 to -0.6 MPa), moisture content can be determined gravimetrically from 6 to 8 increment cores taken near dawn (XPP at maximum for the day) at the beginning and end of each installation's 10 day sensor use limit. Moisture content may also be inferred from the longitudinal thermal diffusivity measurements if wood basic density is obtained or can be estimated. If this is done, the D^1 used should be the average of that obtained from the up and downstream sensors. The $Mgw(D^1,Pb)$ technique remains to be proven even though it was used in the potometer experiments reported in Chapter V with moderate to excellent results.

If heat pulse velocity measurements and sap flow calculations are to be carried out over extended time and a significant change in BP (from -0.4 to -1.0 MPa), then moisture contents should be determined periodically throughout the experiment. I do not trust the moisture content values obtained from increment borings from trees at low XPP's (-1.0 to -2.0 MPa) (Swanson 1970a), although Waring and Running (1978) and Waring and Roberts (1979) apparently do not share my concern in this regard. I feel that calculation of moisture contents from the D^1 and Pb measurements is a useful approach even though this technique is unproven. Gamma attenuation (Rothwell 1974, Edwards 1980) or capacitance (Swanson 1966) are nondestructive, but also unproven, alternatives to the increment core method for determining moisture content.

<u>HPV sampling guidelines</u>

1) All of the sensors should be placed in the sap conducting sapwood. There is no flow in heartwood or discolored wood; HPV's measured there are due to radial conduction of heat from the temperature pulse advancing longitudinally in the sapwood.

2) HPV measurements at a given point may be taken as frequently as once every 30 minutes without interference from the prior heat pulse. In general it is not necessary to sample this frequently. One measurement each hour from all sensors is the most frequent that I have used. This was more than adequate to describe the time rate of change of HPV under the rapidly changing "square wave" light regime of a controlled environment chamber.

3) HPV probe sets should not be installed within 4 cm (laterally) of each other in order to avoid temperature interference from the heat pulses. Neither should they be installed within 10 cm (direct line above or below) of each other in order to avoid interference from the wounded tissue that usually extends several centimeters above and below each probe set.

4) The spatial variation in HPV from point to point in the xylem of healthy and unstressed trees is assumed to be less than in those subjected to disease or stress. The number of HPV probes sets that should be installed in an unstressed individual tree is 8 to 12, i.e. 2 to 3 at the center of each of the toroidal areas defined by dividing the sapwood radius into 4 equal length segments. A similiar number and arrangement of probe sets should be used to sample a plot of unstressed trees: i.e. one probe set in each tree; 3 trees with probes centered in each of the 4 toroidal areas for a total of 12 trees per plot (Swanson 1970b).

The number of HPV probe sets that should be installed in a stressed tree is 1 Teflon sensor set for each 1 cm^2 of sapwood or 1 glass (or brass) sensor set for each 2 cm^2 of sapwood. For example, a 20 cm dib tree with 1.5 cm wide sapwood would require 30 glass (or brass) or 60 Teflon sensor sets to insure full areal coverage.

5) It is better to err towards too many probe sets than too few. One can always discard data not required but he cannot

generate that not taken. Sampling programs in studies conducted subsequent to an initial one can be modified downward if the results indicate that the initial one was too dense.

SUMMARY AND CONCLUSIONS

Theoretical

Idealized heat transfer theory describing the velocity of a heat pulse as propagated through sapwood by conduction through the wood and sap substance and convection by moving sap streams with implanted line heat source and point temperature sensors (Marshall 1958), is not directly applicable to the measurement of sap flux in coniferous or diffuse porous woods. The idealized theory does not account for the effect of nonconvecting wood in the plane of the implanted probes that necessarily results from the interruption of flow elements, the effects of probe materials with differing thermal properties than the 3-dimensionally anisotropic wood, nor the normal variation in wood thermal properties that exists at stem tissue borders such as bark/sapwood and sapwood/heartwood.

The 3-dimensional partial differential equation for heat transfer by coupled conduction and convection can be solved numerically for specific stem tissue and heat pulse probe implant situations. Two 2-dimensional finite difference numerical models, one in the tangential-longitudinal plane and the other in the radial-longitudinal plane were successfully used to explain most of the observed departures between practical application and idealized theory.

The tangential-longitudinal model was used to simulate the effect of nonconvecting (wound) material in the plane of the sensors. Simulations with wounds from 0.04 to 0.52 cm wide and imposed heat pulse velocities (HPV's) from 0 to 60 cm h^{-1}, indicated that significant departure from the idealized case occurs at 0.04 cm and at the width of practically-sized heat pulse probes (0.16 cm diameter), calculated values are approximately 50% of those imposed.

The radial-longitudinal model was used to simulate the effects of bark/sapwood and sapwood/heartwood in radial cross sections with sapwoods of 1, 2 and 3 cm wide, imposed HPV's 0 to 60 cm h^{-1}. Single sensor measurement and analysis techniques are shown to be virtually useless at imposed HPV's 0 to 20 cm h^{-1}, especially near either of the tissue borders. Both symmetrically and asymmetrically spaced two sensor measurement and analysis techniques were usable at imposed HPV's 0 to 60 cm h^{-1} at locations in the sapwood greater than 1 cm from the sapwood/heartwood border. Within 1 cm of this border, both of the two sensor techniques, HPVA and HPVS, were usable at imposed HPV's 0 to 30 cm h^{-1}, with the symmetrically spaced HPVS somewhat superior at HPV = 0.

Experimental

Experimental results indicated that wound width (W) in the plane of the implanted probes was the major source of departure of practice from idealized theory. In a *Pinus radiata*, calculated transpiration from idealized theory was 49% of actual (by lysimetery), but with a numerically derived correction equation at W = 0.20 cm, calclulated transpiration was 103% of actual. In a diffuse porous hardwood (*Nothofagus solandri* var *cliffortioides*), calculated transpiration from idealized theory was 26% of actual (by cuvette), but with numerically derived correction equation at measured wound = 0.48 cm, calculated transpiration was 110% of actual. Similiar results were obtained in *Pinus halepensis*, *Picea glauca*, *Populus tremuloides* and *Betula papyrifera*.

Stem tissue borders are important sources of departure from idealized theory with single sensor measurement and analysis techniques. HPV's measured with a single sensor showed little or no correlation with HPV's determined with two-sensor symmetrical or asymmetrical configurations in the 1 to 1.5 cm wide sapwoods of 4 diffuse porous hardwood potometer experiments.

High thermal conductivity HPV sensor materials cause some departure from "no material" numerical solutions with all physical arrangements and analyses techniques. Longitudinal thermal diffusivity measured at HPV = 0 with glass sensors at 0.48 cm upstream from the heater are in error by aproximately -20% to 0%; the errors with comparable sensors at 0.96 cm are -10 to 6% and at 1.44 cm, -4 to 6%.

Heat pulse velocities determined within 1 cm on either side of the sapwood/heartwood border are undeestimates on the sapwood side, overestimates on the heartwood side. Rod-shaped high thermal conductivity sensors tend to integrate HPV across the sapwood/heartwood border and over a greater area of xylem than bead-shaped sensors. This integration may prove advantageous in transpiration measurement but is a disadvantage in determining the physical characteristics of xylem sap flow.

Wood moisture content may be dynamically and nondestructively determined from longitudinal thermal diffusivity measurements and basic wood density. A limited test of the feasibility and accuracy of such determinations indicated that calculated and actual moisture contents over the range 12 to 150%, oven dry weight basis, were closely correlated, $R^2 = 0.81$, with a standard error of estimate of 16%.

The numerical and experimental results indicate that solutions to the heat transport equation, specific to heat pulse instrumentation and stem cross section, are necessary to achieve accurate results with the implanted line source heat pulse method. When such solutions are available, this method can yield very accurate estimates of sap flow and transpiration. I have given solutions for a suggested standard configuration of 0.16 cm diameter sensors symmetrically spaced 1 cm up and downstream from a similiar diameter heater, which is suitable for use in most coniferous and diffuse porous hardwoods with a sapwood radius greater than 1 to 1.5 cm. I have also included solutions for the same heat pulse probes in the two sensor, asymmetric 0.5 cm upstream, 1.0 cm downstream sensor, configuration that has been used in much of the previous heat pulse velocity work.

LITERATURE CITED

Balek, J. and O. Pavlik. 1977. Sap stream velocity as an indicator of the transpirational process. J Hydrol 34:193-200.

Bamber, R. K. 1976. Heartwood, its function and formation. Wood Sci and Technol 10:1-8.

Baumgartner, A. 1967. Energetic bases for differential vaporization from forest and agricultural lands. In Forest Hydrology (W. E. Sopper and H. W. Lull, eds), p 381-389. Pergamon Press, Oxford.

Benson, M. K. 1972. Breeding and establishment - and promising hybrids. pp 88-96 In: Aspen Symposium Proceedings. USDA Forest Serv, North Central Forest Experiment Station, St. Paul Minnesota, Gen Tech Rep NC-1.

Bloodworth, M. E., J. B. Page and W. R. Cowley. 1955. A thermoelectric method for determining the rate of water movement in plants. Soil Sci Soc Am Proc 19:411-414.

Booker, R. E. and J. A. Kininmonth. 1978. Variation in longitudinal permeability of green radiata pine wood. New Zeal J For Sci 8:295-308.

Booker, R. E. and R. H. Swanson. 1979. Radial variation of longitudinal permeability over a tree cross-section for a number of conifers. Forest Products Division, Forest Research Institute, New Zeal For Serv Timber Drying Rep No. 33. 7 p.

Bringfelt, B. 1982. Air humidity and radiation influences on forest transpiration. Agr Meteorol 26:297-307.

Brix, H. 1962. The effect of water stress on the rates of photosynthesis and respiration in tomato plants and loblolly pine seedlings. Physiol Plant 15:10-20.

Brown, H. P., A. J. Panshin and C. C. Forsaith. 1949. Text book of wood technology, Vol I, Structure, identification, defects, and uses of the commercial woods of the United States. McGraw-Hill, New York. 652 p.

Carnahan, B., H. A. Luther and J. O. Wilkes. 1969. Applied numerical methods. John Wiley and Sons, New York. 604 p.

Carslaw, H. S. and J. C. Jaeger. 1959. Conduction of heat in solids. 2nd Edition. Clarendon Press, Oxford. 510 p.

Cermak, J., M. Deml and M. Penka. 1973. A new method of sap flow rate determination in trees. Biol Plant(Praha) 15:171-178.

Church, M. and R. Kellerhals. 1970. Stream gauging techniques for remote areas using portable equipment. Canada Department of Energy, Mines and Resources, Inland Waters Branch, Ottawa. Tech Bul No. 25, 89 p.

Closs, R. L. 1958. The heat pulse method for measuring sap flow in a plant stem. New Zeal J Sci 1:281-288.

Cohen, Y., M. Fuchs and G. C. Green. 1981. Improvement of the heat pulse method for determining sap flow in trees. Plant, Cell and Environ 4:391-397.

Colman, E. A. 1953. Vegetation and watershed management. Ronald Press, New York. 412 p.

Cown, D. J. and M. L. Parker. 1978. Comparison of annual ring density profiles in hardwoods and softwoods by x-ray densitometry. Can J For Res 8:442-449.

Cown, D. J. and M. L. Parker. 1979. Densiometric analysis of wood from five Douglas-fir provenances. Silvae Genetica 28:2-3.

Crafts, A. S. 1968. Water deficits and physiological processes. In Water deficits and plant growth, Vol II. Plant water consumption and response (T.T. Kozlowski, ed), p 85-133. Academic Press, New York.

Daum, C. R. 1967. A method for determining water transport in trees. Ecology 48:425-431.

Decker, J. P. and C. M. Skau. 1964. Simultaneous studies of transpiration rate and sap velocity in trees. Plant Physiol 39:213-215.

Decker, J. P., W. G. Gaylor and F. D. Cole. 1962. Measuring transpiration of undisturbed tamarisk shrubs. Plant Physiol 37:393-397.

Dixon, H. H. 1937. The convection of heat and materials in the stem of a tree. Proc Royal Dublin Soc 21:269-278.

Doley, D. 1967. Water relations of *Eucalyptus marginata* Sm. under natural conditions. J Ecology 55:597-614.

Doley, D. and B. J. Grieve. 1966. Measurement of sap flow in a eucalypt by thermoelectric methods. Aust For Res 2:3-27.

Dunlap, F. 1912. The specific heat of wood. USDA Forest Serv, Forest Prod Lab Bul 110. 28 p.

Edwards, W. R. N. 1980. Flow of water in trees. Unpublished PhD Thesis, University of Edinburgh.

Esau, K. 1977. Anatomy of seed plants. 2nd Edition. John Wiley and Sons, Toronto. 555 p.

Freese, F. 1967. Elementary statistical methods for foresters. USDA For Serv, Agr Handbook 317. 87 p.

Fritschen, L. J., J. Hsia, and P. Doraiswamy. 1977. Evapotranspiration of a Douglas fir determined with a weighing lysimeter. Water Resour Res 13:145-148.

Gale, J. and A. Poljakoff-Mayber. 1964. Effect of soil moisture stress on the correlation between heat pulse velocity and transpiration. Plant and Cell Physiol 5:447-455.

Gifford, G. F. 1968. Apparent sap velocities in big sagebrush as related to nearby environment. J Range Mgt 21:266-268.

Gifford, G. F. and G. D. Frodsham. 1971. Improved heat pulse velocity meter. J Range Mgt 24:469-470.

Greenwood, E. A. N., and J. D. Beresford. 1979. Evaporation from vegetation in landscapes developing secondary salinity using the ventilated-chamber technique, I. Comparative transpiration from juvenile *Eucalyptus* above saline groundwater seeps. J Hydrol 42:369-382.

Greenwood, E. A. N., and J. D. Beresford. 1980. Evaporation from vegetation in landscapes developing secondary salinity using the ventilated-chamber technique, II. Evaporation from *Atriplex* plantations over a shallow saline water table. J Hydrol 45:313-319.

Hammel, H. T. 1967. Freezing of xylem sap without cavitation. Plant Physiol 42:55-66.

Harbaugh, J. W. and G. Bonham-Carter. 1970. Computer simulation in geology. Wiley-Interscience, New York. 575 p.

Heine, R. W. and D. J. Farr. 1973. Comparison of heat-pulse and radioisotope tracer methods for determining sap-flow velocity in stem segments of poplar. J Exp Bot 24:649-654.

Herrington, L. P. 1969. On temperature and heat flow in tree stems. Yale University, School of Forestry Bulletin No. 73. 79 p.

Hinckley, T. M. 1971a. Plant water stress and its effect on ecological patterns of behavior in several Pacific Northwest conifer species. Unpublished PhD. Diss, Univ Washington, Seattle. 178 p.

Hinckley, T. M. 1971b. Estimate of water flow in Douglas-fir seedlings. Ecology 52:525-528.

Hinckley, T. M., J. P. Lassoie and S. W. Running 1978. Temporal and spatial variation in the water status of forest trees. Forest Sci Monogr 20. 72 p.

Hinckley, T. M. and D. R. M. Scott. 1971. Estimates of water loss and its relation to environmental parameters in Douglas-fir saplings. Ecology 52:520-524.

Huber, B. 1932. Beobachtung und Messung pflanzlicher Saftstroeme (Observation and measurement of sap flow in trees). Ber dtsch bot Ges 50:89 -109. (Can Dep For Transl No. 208. Ottawa.)

Huber, B. and E. Schmidt. 1936. Weitere thermoelektrische Untersuchungen ueber den Transpirationsstrom der Baeume. (Further investigations of the transpiration stream of trees.) Tharandt Forstl Jahrb 87:369-412.

Huber, B., and E. Schmidt. 1937. Eine Kompensationsmethode zur thermoelektrischen Messung langsamer Saftstroeme. (A compensation method for the thermoelectric measurement of slow sap movements.) Ber dtsch bot Ges 55:514-529.

Idso, S. B., R. J. Reginato and S. M. Farah. 1982. Soil- and atmosphere-induced plant water stress in cotton as inferred from foliage temperatures. Water Resour Res 18:1143-1148.

Ittner, E. 1968. Der Tagesgang der Geschwindigkeit des Transpirationsstromes im Stamm einer 75-jaehrigen Fichte. Oecol Plant 3:177-183.

Jacob, M. 1949. Heat Transfer. Vol I. John Wiley and Sons, New York. 758 p.

Kline, J. R., K. L. Reed, R. H. Waring and M. L. Stewart. 1976. Field measurement of transpiration in Douglas-fir. J Appl Ecol 13:273-283.

Kozlowski, T. T. and C. H. Winget. 1963. Patterns of water movement in forest trees. Bot Gaz 124:301-311.

Kramer, P. J. 1962. The role of water in tree growth. In Tree growth (T. T. Kozlowski, ed), p 171-182. Ronald Press, New York.

Kramer, P. J. 1969. Plant and soil water relationships: A modern synthesis. McGraw-Hill, New York. 482 p.

Kramer, P. J. and T. T. Kozlowski. 1979. Physiology of woody plants. Academic Press, New York. 811 pp.

Ladefoged, K. 1960. A method for measuring the water consumption of larger intact trees. Physiol Plant 13:648-658.

Ladefoged, K. 1963. Transpiration of forest trees in closed stands. Physiol Plant 16:378-414.

Larcher, W. 1975. Physiological plant ecology. Springer-Verlag, New York. 252 p.

Lassoie, J. P. and D. J. Salo. 1981. Physiological response of large Douglas-fir to natural and induced soil water deficits. Can J For Res 11:139-144.

Lassoie, J. P. and D. R. M. Scott. 1972. Seasonal and diurnal patterns of water status in Acer circunatum. In Proceedings - research on coniferous forest ecosystems - a symposium (J. F. Franklin, L. J. Dempster and R. H. Waring, eds), p 265-271. Pac Northwest Forest and Range Exp Stn, Portland, Oregon.

Lassoie, J. P., D. R. M. Scott and L. J. Fritschen. 1977. Transpiration studies in Douglas-fir using the heat pulse technique. Forest Sci 23:377-390.

Lee, R. 1966. Effects of tent type enclosures on the microclimate and vaporization of plant cover. Oecol Plant 4:301-326.

Leyton, L. 1967. Continuous recording of sap flow rates in tree stems. Proc XIV IUFRO Congress Munich, Section II. pp 240-251.

Leyton, L. 1970. Problems and techniques in measuring transpiration from trees. In Physiology of tree crops, (L. C. Luckwill and C. V. Cutting, eds), p 101-102. Academic Press, New York.

Lopushinsky, W. and G. O. Klock. 1980. Effect of defoliation on transpiration in grand fir. Can J For Res 10:114-116.

Luvall, J. C. and C. E. Murphy, Jr. 1982. Evaluation of the triated water method for measurement of transpiration in young Pinus taeda L. Forest Sci 28:5-16.

McIlroy, I. C. 1975. A sensitive low-cost weighing system. pp 21-1 to 21-6 In Recent Advances in Measurement Technology, IICA'75. Institute of Instrumentation and Control of Australia, 29-31 July 1975, Melbourne.

MacLean, J. D. 1956. Thermal conductivity of wood. Heating, Piping, Air Conditioning 13:380-391.

McMillin, C. W. and F. G. Manwiller. 1980. The wood and bark of hardwoods growing on southern pine sites. USDA Forest Serv, Southern Forest Exp Stn, New Orleans. Gen Tech Rpt SO-29. 58 p.

Marshall, D. C. 1958. Measurement of sap flow in conifers by heat transport. Plant Physiol 33:385-396.

Marshall, D. C. 1962. Sap flow analysis charts. New Zeal J Sci 5:521-530.

Martin, R. E. 1963. Thermal properties of bark. Forest Prod J 13:419-426.

Maylan, B. A. and B. G. Butterfield. 1972. Three-dimensional structure of wood. Chapman and Hall, London. 80 p.

Merkle, M. G. and F. S. Davis. 1967. Effect of moisture stress on absorption and movement of picloram and 2,4,5-T in beans. Weeds 15:10-12.

Merrill, W. and A. L. Shigo. 1979. An expanded concept of tree decay. Phytopathology 69:1158-1160.

Miller, D. R., C. A. Vavrina and T. W. Christensen. 1980. Measurement of sap flow and transpiration in ring-porous oaks using a heat pulse velocity technique. Forest Sci 26:485-494.

Morikawa, Y. 1972. The heat pulse method and an apparatus for measuring sap flow in woody plants. J Jap For Soc 54:166-171.

Østrem, G. 1964. A method of measuring water discharge in turbulent streams. Geographical Bul 21:21-43.

Owston, P. W., J. L. Smith and H. G. Halverson. 1972. Seasonal water movement in tree stems. Forest Sci 18:266-272.

Panshin, A. J. and C. de Zeeuw. 1970. Textbook of wood technology, Vol 1, structure, identification, uses and properties of the commercial woods of the United States and Canada. McGraw-Hill, Toronto. 705 p.

Phillip, J. R. 1966. Plant water relations: some physical aspects. Annu Rev of Plant Physiol 17:245-268.

Pickard, W. F. 1973. A heat pulse method of measuring water flux in woody plant stems. Math Biosci 16:247-262.

Pickard, W. F. and C. J. Puccia. 1972. A theory of the steady-state heat step method of measuring water flux in woody plant stems. Math Biosci 14:1-15.

Puritch, G. S. 1971. Water permeability of the wood of grand fir (Abies grandis (Doug.)Lindl.) in relation to infestation by the balsam wooly aphid, Adelges piceae (Ratz.). J Exp Bot 22:936-945.

Puritch, G. S. and D. B. Mullick. 1975. Effect of water stress on the rate of non-suberized impervious tissue formation following wounding in Abies grandis. J Exp Bot 26:903-910.

Redshaw, A. J. and H. Meidner. 1970. A thermal method for estimating continuously the rate of flow of sap through an intact plant. Z Pflanzenphysiol 62:405-406.

Richtmeyer, R. D. and K. W. Morton. 1967. Difference methods for initial-value problems. Intersceince Publishers, John Wiley and Sons, New York. 405 p.

Ritchie, G. A. and T. M. Hinckley. 1975. The pressure chamber as an instrument for ecological research. Adv Ecol Res 9:165-254.

Roberts, J. 1977. The use of tree-cutting techniques in the study of water relations of mature Pinus sylvestris L. J Exp Bot 28:751-767.

Rook, D. A., R. H. Swanson and A. M. Cranswick. 1976. Reaction of radiata pine to drought. In Proceedings of Soil and Plant Water Symposium, Palmerston North, New Zealand, 25-27 May 1976. p 55-68.

Rothwell, R. L. 1974. Sapwood water content of lodgepole pine. Unpublished PhD Thesis, University of British Columbia. 105 p.

Running, S. W. 1980. Relating plant capacitance to the water relations of Pinus contorta. Forest Ecol Manage 2:237-252.

Rutter, A. J. 1968. Water consumption by forests. In Water deficits and plant growth, Vol II. Plant water consumption and response (T. T. Kozlowski, ed), p 23-84. Academic Press, New York.

Sakuratani, T. 1982. Two thermic methods for measuring water flux in the stem of intact plants and their applications. Bull Nat Inst of Agr Sci Ser A. No. 29. 112 p.

Salisbury. F. B. and C. W. Ross. 1978. Plant physiology. 2nd Edition. Wadsworth, Belmont, California. 436 p.

Saul'yev, V. K. 1964. Integration of equations of parabolic type by the method of nets. Pergamon Press, Oxford. 345 p.

Scholander, P. F., H. T. Hammel, E. D. Bradstreet and E. A. Hemmingsen. 1965. Sap pressure in vascular plants. Science 143:339-346.

Shain, L. 1967. Resistance of sapwood in stems of loblolly pine to infection by Fomes annosas. Phytopathology 57:1034-1045.

Shain, L. 1979. Dynamic responses of differentiated sapwood to injury and infection. Phytopathology 69:1143-1147.

Shaw, C. B. and G. F. Gifford. 1975. Sap velocity studies in natural stands of pinyon and juniper trees. J Range Mgt 28:377-379.

Shigo, A. L. 1976. Microorganisms isolated from wounds inflicted on red maple, paper birch, American beech, and red oak in winter, summer and autumn. Phytopathology 65:559-563.

Shigo, A. L. and W. E. Hillis. 1973. Heartwood, discolored wood and microorganisms in living trees. Annu Rev of Phytopathol 11:197-222.

Shortle, W. C. 1979a. Compartmentalization of decay in red maple and hybrid poplar trees. Phytopathology 69:410-413.

Shortle, W. C. 1979b. Mechanisms of compartmentalization of decay in living trees. Phytopathology 69:1147-1151.

Siau, J. F. 1971. Flow in wood. Syracuse University Press, Syracuse, N.Y. 131 p.

Skaar, C. 1972. Water in wood. Syracuse University Press, Syracuse, N.Y. 218 p.

Skau, C. M. and R. H. Swanson. 1963. An improved heat pulse velocity meter as an indicator of sap speed and transpiration. J Geophysical Res 68:4743-4749.

Skutt, H. R., A. L. Shigo and R. M. Lessard. 1972. Detection of discolored and decayed wood in living trees using a pulsed electric current. Can J For Res 2:54-56.

Slatyer, R. O. 1967. Plant-water relationships. Academic Press, New York. 366 p.

Steinhagen, H. P. 1977. Thermal conductive properties of wood, green or dry, from -40° to +100° C. USDA Forest Service Gen Tech Rpt FPL-9, Madison, Wisconson. 11 p.

Stewart, C. M. 1966. Excretion and heartwood formation in living trees. Science 153:1068-1074.

Stewart, C. M. 1967. Moisture content of living trees. Nature 214:138-140.

Stone, J. F. and G. A. Shirazi. 1975. On the heat-pulse method for the measurement of apparent sap velocity in stems. Planta 122:169-177.

Swanson, R. H. 1962. An instrument for detecting sap movement in woody plants. USDA Forest Serv, Rocky Mountain Forest and Range Experiment Station, Fort Collins, Colorado. Station Paper 68. 16 p.

Swanson, R. H. 1966. Wood moisture measurement above fibre saturation - a dielectric method. Unpublished MSc. Thesis Colo State Univ 46 p.

Swanson, R. H. 1967a. Improving tree transpiration estimates based on heat pulse velocity measurements. In Proc XIV IUFRO Congress, Munich, 4-9 Sep 1967. Vol 1, Sec 10-12-11, p 252-263.

Swanson, R. H. 1967b. Seasonal course of transpiration of lodgepole pine and Engelmann spruce. In Proc Int Symp on Forest Hydrol (W. E. Sopper and H. W. Lull, eds), p 417-432. Pergamon Press, Oxford.

Swanson, R. H. 1970a. The tree as a dynamic system in forest-water resource research, In Proceedings Third Forest Microclimate Symposium, (J. M. Powell and C. F. Nolasco, eds), p 34-39. Environment Canada, Northern Forest Research Centre, Edmonton.

Swanson, R. H. 1970b. Sampling for direct transpiration estimates. J Hydrol (N Z) 9:72-77.

Swanson, R. H. 1972. Water transpired by trees is indicated by heat pulse velocity. Agr Meteorol 10:277-281.

Swanson, R. H. 1974a. A thermal flowmeter for estimating the rate of xylem sap ascent in trees. In Flow - its measurement and control in science and industry, (R. B. Dowdell, ed), p 647-652. Instrument Soc Am, Pittsburgh.

Swanson, R. H. 1974b. Velocity distribution patterns in ascending xylem sap during transpiration. In Flow - its measurement and control in science and industry, (R. B. Dowdell, ed), p 1425-1430. Instrument Soc Am, Pittsburgh.

Swanson, R. H. 1975. Water use by mature lodgepole pine. In Proc Management of Lodgepole Pine Ecosystems, (D. M. Baumgartner, ed), p 264-277. Washington State Univ Coop Ext Serv, Pullman, Washington.

Swanson, R. H. and R. Lee. 1966. Measurement of water movement from and through shrubs and trees. J Forestry 64:187-190.

Swanson, R. H., U. Benecke and W. M. Havranek. 1979. Transpiration in mountain beech estimated simultaneously by heat-pulse velocity and climatized cuvette. New Zeal J For Sci 9:170-176.

Swanson, R. H. and D. W. A. Whitfield. 1981. A numerical analysis of heat pulse velocity theory and practice. J Exp Bot 32:221-239.

Troeng, E. and S. Linder. 1982. Gas exchange in a 20-year-old stand of scots pine. II. Variation in net photosynthesis and transpiration within and between trees. Physiol Plant 54:15-23.

Turrell, F. M., S. W. Austin, D. McNee and W. J. Park. 1967. Thermal conductivity of functional citrus tree wood. Plant Physiol 42:1025-1034.

van Bavel, C. H. M. and L. E. Myers. 1962. An automatic weighing lysimeter. Agric Eng 43:580-583, 586-588.

van den Honert, T. H. 1948. Water transport in plants as a catenary process. Disc Faraday Soc 3:146-153.

Venard, J. K. 1957. Elementary fluid mechanics, 3rd edition. John Wiley and Sons, New York. 401 p.

Vieweg, G. H. and H. Ziegler. 1960. Thermoelektrische Registrierung der Geschwindigkeit des Transpirationsstromes I. Ber dtsch bot Ges 73:221-226.

Vitè, J. P. 1959. Observations on the movement of injected dyes in Pinus ponderosa and Abies concolor. Contrib Boyce Thompson Inst 20:7-26.

Vitè, J. P. 1961. The influence of water supply on oleoresin exudation pressure and resistance to bark beetle attack in Pinus ponderosa. Contrib Boyce Thompson Inst 21:37-66.

Vitè, J. P. and J. A. Rudinsky. 1959. The water-conducting system in conifers and their importance to the distribution of trunk injected chemicals. Contrib Boyce Thompson Inst 20:27-38.

von Rosenberg, D. U. 1969. Methods for the numerical solution of partial differential equations. American Elsvier, New York. 128 p.

Waring, R. H. and J. M. Roberts. 1979. Estimating water flux through stems of Scots pine with tritiated water and phosphorus-32. J Exp Bot 116:459-471.

Waring, R. H. and S. W. Running. 1978. Sapwood water storage: its contribution to transpiration and effect upon water conductance through the stems of old-growth Douglas-fir. Plant, Cell and Environ 1:131-140.

Waring, R. H., D. Whitehead and P. G. Jarvis. 1979. The contribution of stored water to transpiration in Scots pine. Plant, Cell and Environ 2:309-317.

Wendt, C. W., J. R. Runkles and R. H. Hass. 1967. The measurement of water loss by mesquite (Prosopsis glandulosa var. glandulosa Torr.) using the thermoelectric method. Soil Sci Soc Am Proc 31:161-164.

Whitehead, D. and P. G. Jarvis. 1981. Coniferous forests and plantations. In Water deficits and plant growth. Vol VI, Woody plant communities (T. T. Kozlowski, ed), p 49-152. Academic Press, New York.

Zimmermann, M. H. 1964. Effect of low temperature on ascent of sap in trees. Plant Physiol 39:568-572.

Zimmerman, M. H. and C. L. Brown. 1971. Trees structure and function. Springer-Verlag, New York. 336 p.

APPENDIX A

PLANE HEAT SOURCE GEOMETRY EQUATIONS

The analytical solutions to Equation 1 (p. 18) for a plane heat source geometry, contains a square root term in the denominator of the nonexponential term that alters the forms of the working solutions from those for the line heat source geometry. The working equations listed below are for use in heat pulse studies in which the plane heat source geometry is used.

None of the simulations done in this report were intended to approximate plane heat source geometry. However, there is no tangential heat exchange in the radial-longitudinal model. Because of this lack of tangential heat exchange, the RLM represents a slice where both the sensors and the heater are infinitely wide and the plane heat source equations must be used to obtain solutions from the temperature field generated with this model.

1. Plane heat source geometry analytical equation comparable to Equation 3 (p. 19), (Carslaw and Jaeger 1959, Closs 1958).

$$T = Q/(4\pi Dt)^{1/2} \exp - \left[(X - HPVt)^2/4Dt\right] \ ^{o}C \qquad (3a)$$

Where all symbols are as defined in Chapter 2 (p. 19).

2. Plane heat source geometry working equation comparable to Equation 4 (p. 19).

$$HPVM = r\left[(t_1 \ln R_1 - t_3 \ln R_2)/t_1 t_2 t_3 \ln(R_1/R_2)\right]^{1/2} \ cm\ s^{-1} \qquad (4a)$$

Where $R_1 = T_1 t_1^{1/2}/T_2 t_2^{1/2}$; $R_2 = T_2 t_2^{1/2}/T_3 t_3^{1/2}$

Note that the only difference between Equations 4a and 4, 5a and 5, is the inclusion of the $t_n^{1/2}$ in the equations for R_n.

3. Plane heat source working equivalent to Equation 5 (p. 21).

$$D = -0.5(t_2 - t_1)^2 r^2 / t_1 t_2 t_3 \ln(R_1/R_2) \quad cm^2\ s^{-1} \tag{5a}$$

This diffusivity equation (Eq. 5a) must be used to obtain the "D" used in Equations 6a and 7a below.

4. Plane heat source working equivalent to Equation 6 (p. 21).

$$HPVS = (D/r)\ln(Td/Tu)\ cm\ s^{-1} \tag{6a}$$

Note that Equation 6a is identical to 6 except for the source of the "D" value.

5. Plane heat source working equivalent to Equation 7 (p. 22).

$$HPVP = (r^2 - 2Dtp)^{1/2}/tp\ \ cm\ s^{-1} \tag{7a}$$

Note 2D in 7a vice 4D in Equation 7.

Both Equations 8 and 9 are identical in either the plane or line heat source geometry. They are repeated here simply to complete the set of working equations.

$$HPVT = (Xu + Xd)/2tz\ \ cm\ s^{-1} \tag{8a}$$

$$HPVA = (Xu+Xd)(t_1 \ln S_1 - t_2 \ln S_2)/2t_1 t_2 \ln(S_1/S_2)\ cm\ s^{-1} \tag{9a}$$

APPENDIX B

ENVIRONMENTAL CHAMBERS, UNIVERSITY OF ALBERTA

Dimensions

Height 3.22 m
Depth 3.71 m
Width 2.34 m
Door:
Width 0.96 m
Height 2.84 m

Environmental capabilities

Air Temperature

-5 to 50 °C lights off
5 to 50 °C lights on

Humidity

at AT = 35 °C, 20 to 80% RH
= 16 50%
= 5 85%

Manufactured by

Environmental Growth Chambers
P.O. Box 407
Chagrin Falls, Ohio

Table 21. Light intensity (PhAR) at mid canopy level.

Lighting combination	$W\ m^{-2}$
1/3 Fluorescent	64
2/3 Fluorescent	106
Full Fluorescent	170
Full Fluorescent + Multivapour	187
Full Fluorescent + Lumalux	311
Full Fluorescent + Lumalux + Multivapour	326

APPENDIX C

WHITE SPRUCE LYSIMETER EXPERIMENTS

Strictly speaking, these were not trees in lysimeters; merely large potted plants. The weighing device was based on the weighing lysimeter design by McIlroy (1975) and I continued to use the term lysimeter. McIlroy (personal communication) refered to the construction as being similiar to a large "Mechano" set. Mine certainly had an "Erector" or "Mechano" set appearance as they were constructed from readily available industrial shelving support material. The general details of construction are shown in Figure 46. The circled areas (Fig. 46) contain the pivot points for the balance, and these should be as free of friction as possible. Initial balancing was done by casting an initial balancing weight (of lead) that was slightly greater than needed to balance the potted tree. Fine balance was acheived by adding water to a container attached to the tree container. The zero position of the off balance indicator arm was marked on the vertical support. As evapotranspiration occured, balance was restored by adding sufficient water to the counter weight container to restore the pointer to zero. The leads to the HPV probes were a source of friction so that counter weight added was not exactly equal to ET loss (Fig. 47). Also some evaporation occured directly from the soil and pot, even though plastic covered. A measure of pot evaporation at various light intensities was obtained at the end of the experiment. The average value of pot evaporation at each light intensity (Table 22) was subtracted from the periodic weight loss measurements to obtain transpiration.

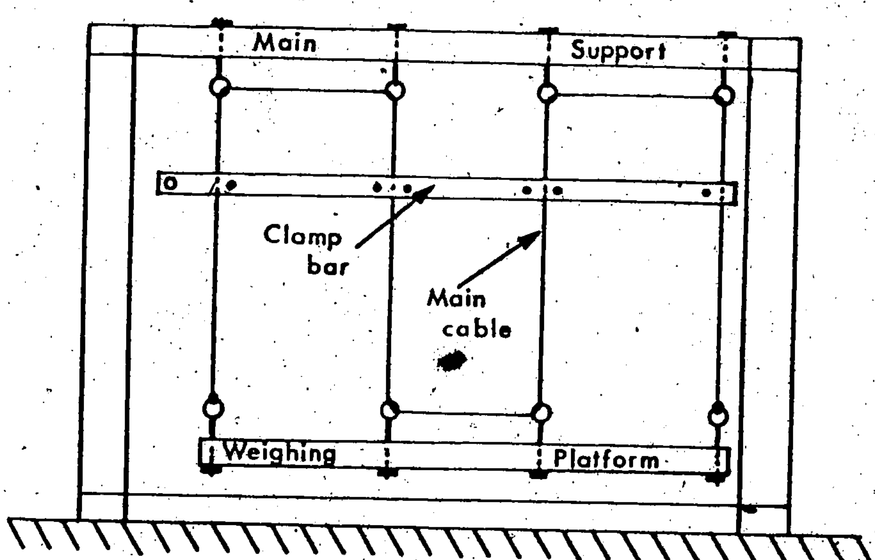

Side view

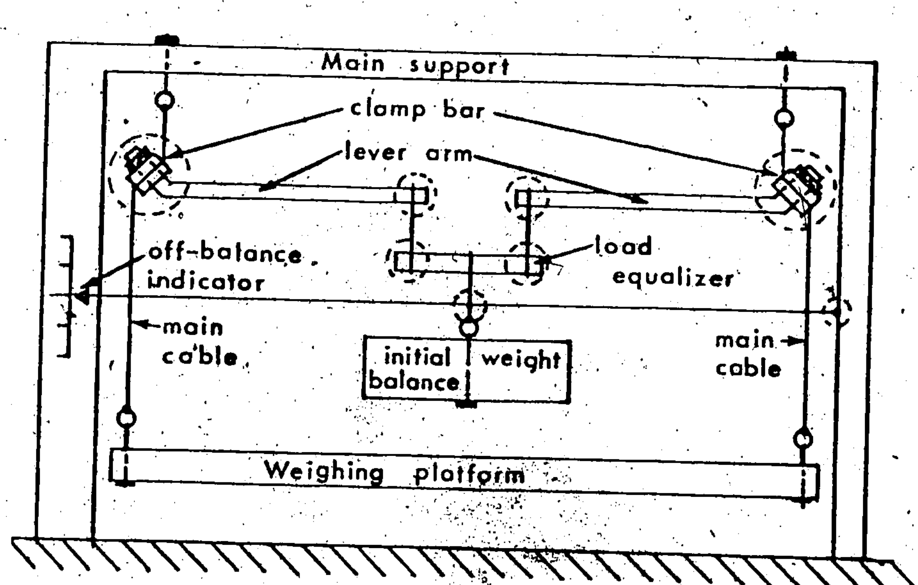

End view

Figure 46. "Lysimeter" construction details. The dimensions are not critical and were as needed to accomodate the hardware that was available locally. The clamp bars were 1.25 x 0.50 inch steel bar stock, the lever arms 0.75 inch iron pipe with 45° elbows and short nipples to connect to the clamp bars. The initial balance weight needed was determined with a spring scale before casting it from plumbers lead.

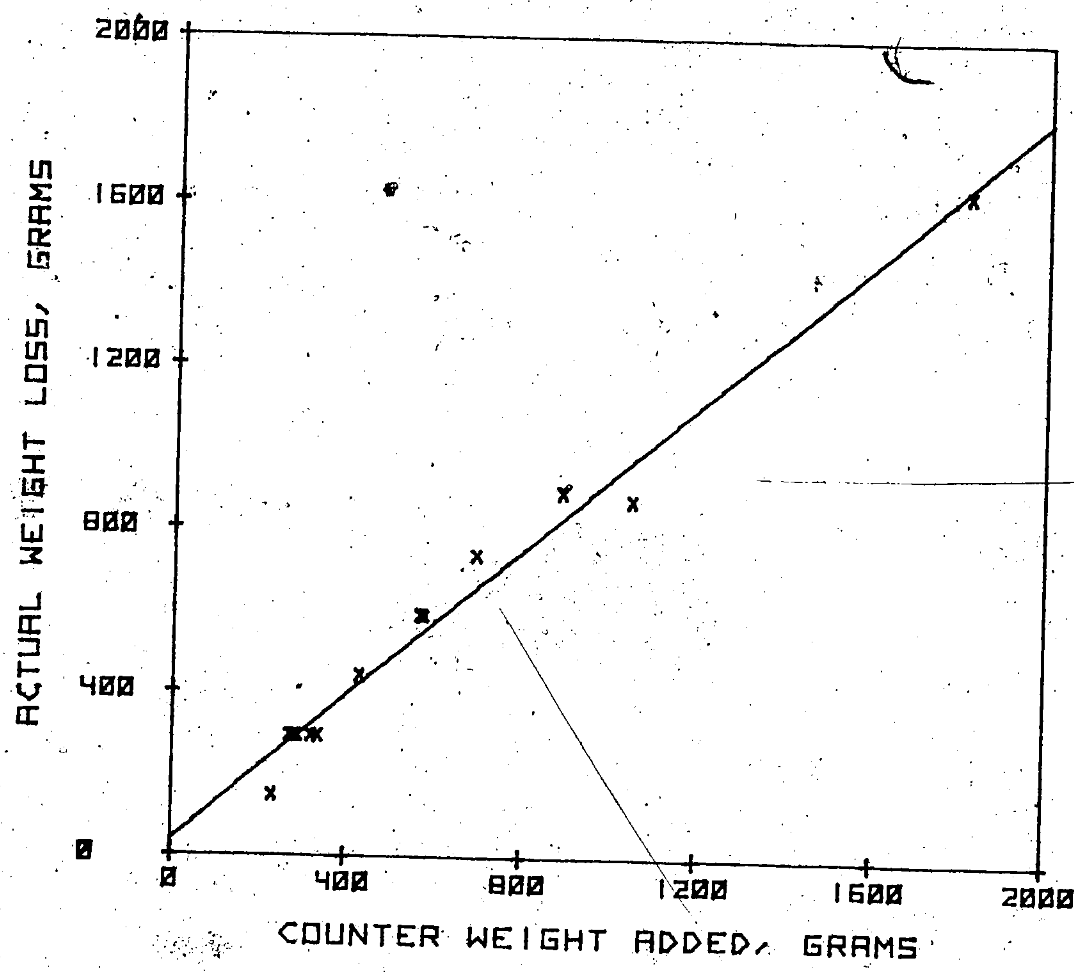

Figure 47. Lysimeter calibration curve. Least squares fitting, counter weight added (CWA) versus actual weight loss TR(WL), grams, with all HPV probe leads attached to tree. TR(WL) = 40.6 + 0.88(CWA), $R^2 = 0.9818$, $s_{\bar{x}} = 54$ g.

Table 22. Evaporation from lysimeter container alone, no tree, all HPV probe leads removed. AT = 20 to 25 °C.

Light Intensity (PhAR) $W\ m^{-2}$	Evaporation $g\ h^{-1}$
0	5.2
64	5.4
106	10.2
170	11.0

Table 23. Schedule of events white spruce lysimeter experiments. Lights on 0900 - 2100, chamber dark 2100 - 0900.

Date DA/MO/YR	Julian Date JD	LI(PhAR) $W\ m^{-2}$	Activity
28/06/78	179	170	12 hour shakedown run
29/06/78	180	170	No HPV data
30/06/78	181	64	12 hour reading schedule trees PG1, PG2
01/07/78	182	106	12 hour reading schedule trees PG1, PG2
02/07/78	183	170	12 hour reading schedule trees PG1, PG2
03/07/78	184	64	No HPV data until JD 188
07/07/78	188	64	12 hour reading schedule trees PG1, PG2
08/07/78	189	106	12 hour reading schedule trees PG1, PG2
09/07/78	190	170	12 hour reading schedule trees PG1, PG2
10/07/78	191	170	No HPV data until JD 195
14/07/78	195	64	12 hour reading schedule trees PG1, PG2
15/07/78	196	106	12 hour reading schedule trees PG1, PG2
16/07/78	197	170	12 hour reading schedule trees PG1, PG2
17/07/78	198	106	No HPV data until JD 202
21/07/78	202	170	12 hour reading schedule trees PG1, PG2
22/07/78	203	170	12 hour reading schedule trees PG1, PG2
23/07/78	204	170	12 hour reading schedule trees PG1, PG2
24/07/78	205	64	No HPV data until JD 209
28/07/78	209	170	12 hour reading schedule trees PG1, PG2
29/07/78	210	170	12 hour reading schedule trees PG1, PG2
30/07/78	211	170	12 hour reading schedule trees PG1, PG2
31/07/78	212	170	No HPV data until JD 216
04/08/78	216	170	12 hour reading schedule trees PG1, PG2
05/08/78	217	170	12 hour reading schedule trees PG1, PG2
06/08/78	218	170	12 hour reading schedule trees PG1, PG2
07/08/78	219	170	No HPV data until JD 223
11/08/78	223	170	12 hour reading schedule trees PG1, PG2
12/08/78	224	170	12 hour reading schedule trees PG1, PG2
13/08/78	225	170	12 hour reading schedule trees PG1, PG2
14/08/78	226	170	No HPV data until JD 230
18/08/78	230	170	12 hour reading schedule trees PG1, PG2
19/08/78	231	170	12 hour reading schedule trees PG1, PG2
20/08/78	232	170	12 hour reading schedule trees PG1, PG2
		No HPV data until JD 239. Start chamber B009-3; This chamber held at 5°C since April 1978, LI 64 $W\ m^{-2}$ (PhAR), 00 - 05 daily. Change to AT = 25 °C, LI = 170 $W\ m^{-2}$, 09 - 21 daily.	
27/08/78	239	170	12 hour reading schedule trees PG3, PG4
03/09/78	246	170	12 hour reading schedule trees PG3, PG4
04/09/78	247	170	12 hour reading schedule trees PG3, PG4

Table 24. Twelve hour reading schedule.

Period	Activity
0800-0900	Read HPVT's, XPP, RL. Rebalance lysimeter at 0900*
0900-0930	Work HPVT data off of strip charts
0930-1000	Read HPVT's
1000-1030	Break
1030-1100	Read HPVT's
1100-1200	Work HPVT data off of strip charts
1200-1300	Lunch
1300-1400	Read HPVT's, XPP, RL. Rebalance lysimeter at 1300
1400-1430	Work HPVT data off of strip charts
1430-1500	Break
1500-1530	Read HPVT's
1530-1700	Work HPVT data off of strip charts
1700-1730	Read HPVT's, rebalance lysimeter at 1700
1730-1830	Dinner
1830-1930	Read HPVT's, XPP, RL
1930-2030	Work HPVT data off of strip charts
2030-2100	Read HPVT, rebalance lysimeter at 2100
2100-2130	Break
2130-2230	Read HPVT's, XPP, RL.
2230	Secure for the day.

* Rebalance trees PG3 and PG4 only at 0830; other readings as indicated.

Table 25. HPV instrumentation installed in white spruce tree PG1. Sensors were 0.16 cm diameter glass rod; heater was 0.16 cm diameter brass.

Sensor No.	Date Inst DA/MO/YR	Xu cm	Xd cm	d cm	SWT cm	dib cm	A_{np} cm^2	Remarks
109	23/06/78	-0.48	1.00	1.00	1.2	8.50	27.5	
110	23/06/78	-0.50	0.98	1.25	1.1	8.50	25.6	In heartwood*
111	23/06/78	-0.50	0.99	1.50	1.1	8.50		In heartwood
112	23/06/78	-0.50	1.01	2.00	1.1	8.50		In heartwood
113	29/06/78	-0.49	1.00	0.75	1.0	5.96	15.6	
114	29/06/78	-0.50	0.96	1.00	1.0	5.96	15.6	
115	29/06/78	-0.50	1.00	1.25	1.1	5.96		In heartwood
116	29/06/78	-0.50	1.00	1.50	1.2	5.96		In heartwood
117	02/08/78	-0.50	1.00	0.75	1.0	5.88	15.3	
118	02/08/78	-0.50	1.00	1.00	1.2	5.88	17.6	
119	02/08/78	-0.51	0.97	1.25	0.8	5.88		In heartwood
120	02/08/78	-0.46	1.00	1.50	1.0	5.88		In heartwood
121	21/10/78	-0.50	0.98	0.75	0.8	5.90	12.8	
122	21/10/78	-0.47	0.99	1.00	0.9	5.90	14.1	In heartwood*
123	21/10/78	-0.50	1.00	1.25	1.2	5.90		In heartwood
124	21/10/78	-0.43	0.94	1.50	0.9	5.90		In heartwood

* Sensor used in TR calculations even though slightly in heartwood.

Table 26. HPV instrumentation installed in white spruce tree PG2. Sensors were 0.16 cm diameter glass rod; heater was 0.16 cm diameter brass.

Sensor No.	Date Inst DA/MO/YR	Xu cm	Xd cm	d cm	SWT cm	dib cm	A_{np} cm^2	Remarks
201	23/06/78	-0.46	1.00	0.75	1.4	6.24	21.3	
202	23/06/78	-0.50	1.00	1.00	1.1	6.24	17.8	
203	23/06/78	-0.50	0.97	1.50	1.1	6.24		In heartwood
204	23/06/78	-0.49	1.00	2.00	1.4	6.24		In heartwood
207	29/06/78	-0.49	1.00	0.75	0.9	5.10	11.9	
208	29/06/78	-0.49	1.00	1.00	0.8	5.10	10.8	In heartwood*
209	29/06/78	-0.50	1.00	1.50	0.9	5.10		In heartwood
210	29/06/78	-0.46	0.96	2.00	0.9	5.10		In heartwood
211	02/08/78	-0.50	0.99	0.75	1.2	5.17	15.0	
212	02/08/78	-0.50	0.99	1.00	1.1	5.17	14.1	
213	02/08/78	-0.41	1.00	1.25	1.0	5.17		In heartwood
214	02/08/78	-0.50	0.99	1.50	1.0	5.17		In heartwood
215	27/11/78	-0.49	0.98	0.75	1.0	4.84	12.1	
216	27/11/78	-0.47	0.95	1.00	1.0	4.84	12.1	
217	27/11/78	-0.50	1.00	1.25	1.1	4.84		Non functional
218	27/11/78	-0.51	0.98	1.50	1.1	4.84		In heartwood

* Sensor used in TR calculations even though slightly in heartwood.

Table 27. HPV instrumentation installed in white spruce tree PG3. Sensors were 0.16 cm diameter glass rod; heater was 0.16 cm diameter brass.

Sensor No.	Date Inst DA/MO/YR	Xu cm	Xd cm	d cm	SWT cm	dib cm	A_{np} cm^2	Remarks
305	24/08/78	-0.49	1.00	0.75	1.25	5.18	15.4	
306	24/08/78	-0.47	1.00	1.00	1.25	5.18	15.4	
307	24/08/78	-0.50	1.00	1.25	1.25	5.18	15.4	
308	24/08/78	-0.48	1.00	1.50	1.25	5.18		In heartwood
309	24/08/78	-0.50	1.00	0.75	1.04	4.83	12.4	
310	24/08/78	-0.42	0.99	1.00	1.04	4.83	12.4	
311	24/08/78	-0.50	0.98	1.25	1.04	4.83		In heartwood
312	24/08/78	-0.50	0.97	1.50	1.04	4.83		In heartwood
313	24/08/78	-0.49	0.99	0.75	1.10	4.57	12.0	
314	24/08/78	-0.50	1.00	1.00	1.10	4.57	12.0	
315	24/08/78	-0.49	0.98	1.25	1.10	4.57		In heartwood
316	24/08/78	-0.50	1.00	1.50	1.10	4.57		In heartwood

Table 28. HPV instrumentation installed in white spruce tree PG4. Sensors were 0.16 cm diameter glass rod; heater was 0.16 cm diameter brass.

Sensor No.	Date Inst DA/MO/YR	Xu cm	Xd cm	d cm	SWT cm	dib cm	A_{np} cm^2	Remarks
405	24/08/78	-0.50	1.09	0.75	1.42	5.81	19.6	
406	24/08/78	-0.50	1.00	1.00	1.42	5.81	19.6	
407	24/08/78	-0.50	0.99	1.25	1.42	5.81	19.6	Cracked sensor
408	24/08/78	-0.53	1.01	1.50	1.42	5.81		In heartwood
409	24/08/78	-0.50	1.00	0.75	1.19	4.80	13.5	
410	24/08/78	-0.50	0.99	1.00	1.19	4.80	13.5	
411	24/08/78	-0.50	0.97	1.25	1.19	4.80		In heartwood
412	24/08/78	-0.46	1.00	1.50	1.19	4.80		In heartwood
413	24/08/78	-0.50	1.00	0.75	1.08	4.87	12.9	
414	24/08/78	-0.50	0.99	1.00	1.08	4.87	12.9	
415	24/08/78	-0.50	1.00	1.25	1.08	4.87		In heartwood
416	24/08/78	-0.42	1.00	1.50	1.08	4.87		In heartwood

Table 29. Sample raw and corrected HPVT data, white spruce tree PG1.

DATE DA/MO/YR	PERIOD h-h	TR(WL) g/h	RAW HPVT cm/h				HPVC(0.20) cm/h			
			109	110	113	114	109	110	113	114
30/06/78	09-13	65	1.9	2.1	2.0	3.7	3.3	3.6	3.4	6.1
	13-17	40	1.8	1.8	1.5	3.1	3.2	3.2	2.7	5.1
	17-21	44	1.8	1.6	2.0	2.8	3.2	2.9	3.4	4.6
01/07/78	09-13	103	4.2	4.4	5.8	5.9	6.9	7.2	9.7	9.9
	13-17	62	4.0	4.5	6.1	5.6	6.5	7.4	10.3	9.4
	17-21	84	3.7	4.2	5.5	5.3	6.1	6.9	9.2	8.8
02/07/78	09-13	92	5.0	5.2	6.1	6.0	8.3	8.6	10.3	10.1
	13-17	133	5.3	6.1	7.6	6.3	8.8	10.3	13.3	10.7
	17-21	113	5.0	5.9	7.6	6.3	8.3	9.9	13.3	10.7

Sample transpiration calculations

09-13 h, 30/06/78, sap flux coefficient = 0.44(0.33 + 0.88) = 0.53

TR(00) = (1.9X27.5 + 2.1X25.6 + 2.0X15.6 + 3.7X15.6)(0.53)/4 = 25.8

TR(20) = (3.3X27.5 + 3.6X25.6 + 3.4X15.6 + 6.1X15.6)(0.53)/4 = 43.9

Table 30. Sample raw and corrected HPVT data, white spruce tree PG2.

DATE DA/MO/YR	PERIOD h-h	TR(WL) g/h	RAW HPVT cm/h 201	202	207	208	HPVC(0.20) cm/h 201	202	207	208
30/06/78	09-13	62	3.2	2.5	4.3	6.7	5.3	4.2	7.1	11.5
	13-17	57	2.4	1.8	3.4	4.6	4.0	3.2	5.6	7.6
	17-21	61	2.4	1.5	2.9	3.6	4.0	2.7	4.8	5.9
01/07/78	09-13	90	4.4	3.3	5.8	8.6	7.2	5.4	9.7	15.4
	13-17	95	4.6	3.0	5.7	9.4	7.6	4.9	9.5	17.2
	17-21	104	3.9	2.8	5.3	9.3	6.4	4.6	8.8	17.0
02/07/78	09-13	96	5.4	4.1	7.0	11.2	9.0	6.7	12.1	21.6
	13-17	146	5.6	4.6	6.9	11.2	9.4	7.6	11.9	21.6
	17-21	123	5.4	4.8	7.0	11.2	9.0	7.9	12.1	21.6

Sample transpiration calculations

09-13 h, 30/06/78, sap flux coefficient = 0.48(0.33 + 1.05) = 0.66.

TR(00) = (3.2X21.3 + 2.5X17.8 + 4.3X11.9 + 6.7X10.8)(0.66)/4 = 39.0

TR(20) = (5.3X21.3 + 4.2X17.8 + 7.1X11.9 + 11.5X10.8)(0.66)/4 = 65.4

Table 31. Sample raw and corrected HPVT data, white spruce tree PG3.

DATE DA/MO/YR	PERIOD START	PERIOD END	TR(WL) g/h	RAW HPVT cm/h 305	306	307	309	310	313	314
27/08/78	0830	2400		2.1*	4.3	8.2	6.0	4.8	8.3	4.5
28/08/78	0000	0830	54	-.1*	2.9	4.0	2.2	2.9	4.1	2.6
02/09/78	0830	2400		3.1	4.9	10.2	7.1	5.9	10.3	5.3
03/09/78	0000	0830	66	0.2	3.0	4.5	2.4	3.0	2.9	2.8
03/09/78	0830	2400		3.1	5.3	11.0	7.3	6.2	11.0	5.5
04/09/78	0000	0830	65	1.9	3.3	6.6	4.1	4.6	5.3	2.6

* Values less than 2.0 cm/h solved by iterative procedure in HPV, D[1], using ratios of $(Tu - Td)_{60}/(Tu - Td)_{120}$ and $(Tu - Td)_{120}/(Tu - Td)_{180}$ with Tu, Td defined at 60, 120 and 180 s by Equation 3, p. 19.

DATE DA/MO/YR	PERIOD START	PERIOD END	TR(WL) g/h	HPVC(0.20) cm/h 305	306	307	309	310	313	314
27/08/78	0830	2400		3.6	7.1	14.6	10.1	7.9	14.8	7.4
28/08/78	0000	0830	54	0.7	4.8	6.5	3.7	4.8	6.7	4.3
02/09/78	0830	2400		5.1	8.1	19.1	12.3	9.9	19.4	8.8
03/09/78	0000	0830	66	1.0	4.9	7.4	4.0	4.9	4.8	4.6
03/09/78	0830	2400		5.1	8.8	21.1	12.7	10.5	21.1	9.2
04/09/78	0000	0830	65	3.3	5.4	11.3	6.7	7.6	8.8	4.3

Sample transpiration calculation

0830 - 2400, 27/08/78, sap flux coefficient = 0.45(0.33 + 1.00)
= 0.60

TR(00) = (2.2 + 4.3 + 8.2)(15.4) + (6.0 + 4.8)(12.4) + (8.3 + 4.5)(12.0) (0.60)/7 = 43.9

TR(20) = (3.6 + 7.1 + 14.6)(15.4) + (10.1 + 7.9)(12.4) + (14.8 + 7.4)(12.0) (0.60)/7 = 75.4

Table 32. Sample raw and corrected HPVT data, white spruce tree PG4.

DATE DA/MO/YR	PERIOD START	PERIOD END	TR(WL) g/h	RAW HPVT cm/h 405	406	409	410	413	414
27/08/78	0830	2400		3.8	7.4	8.8	5.2	5.0	7.2
28/08/78	0000	0830	52	1.2*	2.0	0.5	0.9	2.0	2.9
02/09/78	0830	2400		5.1	9.2	10.2	6.7	5.5	8.3
03/09/78	0000	0830	92	3.2	4.5	5.2	3.3	3.2	6.3
03/09/78	0830	2400		5.3	9.6	10.4	7.1	5.4	8.7
04/09/78	0000	0830	80	3.2	4.2	4.6	3.0	2.0	4.1

* Values less than 2.0 cm/h solved by iterative procedure in HPV, D[1], using ratios of $(Tu - Td)_{60}/(Tu - Td)_{120}$ and $(Tu - Td)_{120}/(Tu - Td)_{180}$ with Tu, Td defined at 60, 120 and 180 s by Equation 3, p. 19.

DATE DA/MO/YR	PERIOD START	PERIOD END	TR(WL) g/h	HPVC(0.20) cm/h 405	406	409	410	413	414
27/08/78	0830	2400		6.2	12.9	15.9	8.6	8.3	12.5
28/08/78	0000	0830	52	2.3	3.4	1.4	1.9	3.4	4.8
02/09/78	0830	2400		8.5	16.8	19.1	11.5	9.2	14.8
03/09/78	0000	0830	92	5.3	7.4	8.6	5.4	5.3	10.7
03/09/78	0830	2400		8.8	17.7	19.6	12.3	9.0	15.7
04.09/78	0000	0830	80	5.3	6.9	7.6	4.9	3.4	6.7

Sample transpiration calculation

0830 – 2400, 27/08/78, sap flux coefficient = 0.47(0.33 + 0.80)
= 0.53

TR(00) = (3.8 + 7.4)(19.6) + (8.8 + 5.2)(13.5) + (5.0 + 7.2) (0.53)/6 = 50.0

TR(20) = (6.2 + 12.9)(19.6) + 15.9 + 8.6)(13.5) + (8.3 + 12.5)(12.9) (0.53)/6 = 86.0

APPENDIX D

BIRCH AND POPLAR POTOMETER EXPERIMENTS

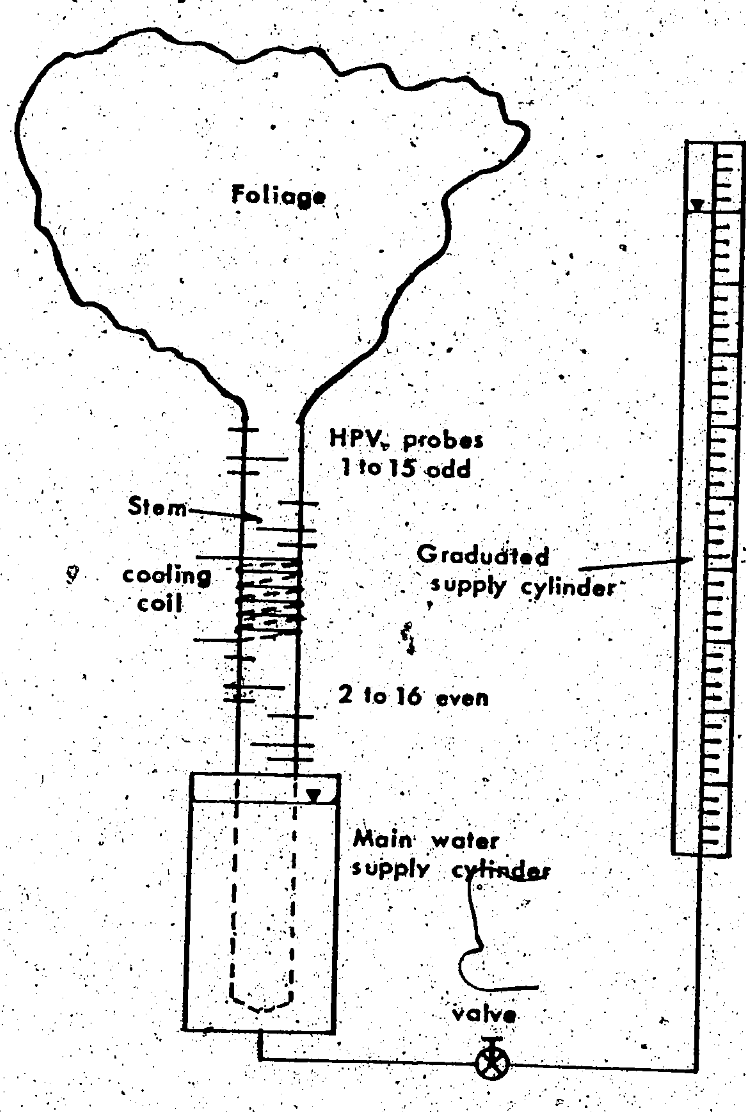

Figure 48. Sketch of potometer; physical placement of HPV probes and means of determining water uptake. Uptake could have been determined directly from graduations on the main supply cylinder if calibrated for each different stem volume. With the arrangement shown, the water needed to restore the original level in the main supply cylinder was read from the graduated cylinder, aproximately 28 mL/cm.

Table 33. Schedule of events, hardwood potometers.

Julian day 1981	Date DA/MO/YR	Activity
098	08/04/81 to 24/04/81	Cut dormant birch and poplars. Placed in cold room B009-2 at 2.5 °C, total darkness.
118	28/04/81	Started test of leaf out procedure on one birch and one poplar. Moved stems into chamber at 25 °C, lights 170 W m^{-2} (PhAR), 0900 - 0300.
124	04/05/81	Both test stems fully leafed out.
126	06/05/81 to 14/05/81	Trial stem freezing, etc., with leafed out stems.
134	14/05/81	Tree BP1 into warm chamber for leaf out.
142	22/05/81	BP1 fully leafed out, instrumented with Teflon HPV sensors 2101 - 2116 (Table 34).
143	23/05/81 to 29/05/81	Pre-freezing HPV, TR, tree BP1; chamber conditions AT = 25°C, RH aproximately 40%, LI 170 W m^{-2} (PhAR), 0900 - 2100, dark 2100 - 0900.
149	29/05/81	Stem freezing treatment tree BP1, 0850 - 2200.
150	30/05/81 to 02/06/81	Post freezing HPV, TR, tree BP1.
153	02/06/81	Tree BP2 brought into warm chamber for leaf out.
160	09/06/81	Tree BP2 fully leafed out.
161	10/06/81	1. Installed HPV sensors 2201 - 2216 in tree BP2, (Table 35). 2. Sectioned tree BP1 to get Mgw, Wound data. 3. Brought tree PT1 into warm chamber for leaf out.
162	11/06/81 to 13/06/81	Pre-freezing HPV, TR, tree BP2; chamber conditions as for tree BP1.
164	13/06/81	Stem freezing treatment tree BP2.

Table 33. Continued.

165	14/06/81 to 16/06/81	Post freezing HPV, TR data, tree BP2.
168	17/06/81	1. Instrument tree PT1 with sensors 1101 - 1116 (Table 36). 2. Section tree BP2 to ascertain Mgw, W. 3. Bring tree PT2 in to warm chamber for leaf out.
168	17/06/81 to 19/06/81	Pre-freezing HPV, TR, tree PT1; chamber conditions same as tree BP1.
170	19/06/81	Stem freezing treatment tree PT1, 1200 - 2200.
171	20/06/81 to 23/06/81	Post freezing HPV, TR, tree PT1.
177	26/06/81	1. Section tree PT1 to ascertain Mgw and W. 2. Instrument tree PT2 with sensors 1201 - 1216 (Table 37). 3. Bring tree BP3 into warm chamber for leaf out.
178	27/06/81 to 29/06/81	Pre-freezing HPV, TR, tree PT2; chamber conditions same as tree BP1.
180	29/06/81	Stem freezing treatment tree PT2, 0800 - 1700.
181	30/06/81 to 03/07/81	Post freezing HPV, TR, tree PT2.
184	03/07/81	Secured tree PT2 experiment, sectioned stem to obtain Mgw and wound.
192	11/07/81	No sign of leaves on tree BP3. Stems apparently dried out while in the cold room. No further potometer runs attempted.

END OF POTOMETER EXPERIMENTS

Table 34. HPV instrumentation installed in birch potometer tree BP1. Sensors were 0.16 cm diameter Teflon with glass bead thermistor; heater was 0.16 cm diameter brass. Installed 22 May 1981. Odd numbered sensors above freeze block, even numbered sensors below.

SENSOR	Xu	Xd	d	SWT	dib	A_d	W	POSITION EQUATION		
No	cm	cm	cm	cm	cm	cm^2	cm	a	b	c
2101	-0.50	0.98	1.3	1.40	3.89	1.58	0.32	-.306	1.890	-.024
2102	-0.50	0.99	0.8	1.48	4.40	11.05	0.30	-.261	1.173	-.007
2103	-0.50	0.97	0.8	1.40	3.89	9.37	0.40	-.292	1.202	-.008
2104	-0.46	1.01	1.3	1.48	4.40	2.53	0.26	-.211	1.651	-.021
2105	-0.50	0.91	1.3	1.40	3.89	1.58	0.36	-.306	1.890	-.024
2106	-0.49	1.00	0.8	1.48	4.40	11.05	0.30	-.261	1.173	-.007
2107	-0.49	1.00	0.8	1.40	3.89	9.37	0.30	-.292	1.202	-.008
2108	-0.47	0.99	1.3	1.48	4.40	2.53	0.28	-.211	1.651	-.021
2109	-0.49	0.99	0.8	1.40	3.89	9.37	0.36	-.292	1.202	-.008
2110	-0.44	1.01	0.8	1.48	4.40	11.05	0.20	-.261	1.173	-.007
2111	-0.49	0.95	1.3	1.40	3.89	1.58	0.40	-.306	1.890	-.024
2112	-0.50	0.96	1.3	1.48	4.40	2.53	0.25	-.211	1.651	-.021
2113	-0.49	1.00	0.8	1.40	3.89	9.37	0.24	-.292	1.202	-.008
2114	-0.47	1.02	0.8	1.48	4.40	11.05	0.23	-.261	1.173	-.007
2115	-0.50	0.96	1.3	1.40	3.89	1.58	0.30	-.306	1.89[illegible]	-.024
2116	-0.48	1.00	1.3	1.48	4.40	2.53	0.26	-.211	1.651	-.021

Average wound width = 0.30 cm

Table 35. HPV instrumentation installed in birch potometer tree BP2. Sensors were 0.16 cm diameter Teflon with glass bead thermistor; heater was 0.16 cm diameter brass. Installed 10 June 1981. Odd numbered sensors above freeze block, even numbered sensors below.

SENSOR	Xu	Xd	d	SWT	dib	A_d	W	POSITION EQUATION		
No	cm	cm	cm	cm	cm	cm^2	cm	a	b	c
2201	-0.47	0.96	0.8	1.42	3.96	9.60	0.24	-.273	1.190	-.007
2202	-0.47	0.96	0.8	1.40	4.32	10.79	0.23	-.273	1.190	-.007
2203	-0.93	0.98	0.8	1.42	3.96	9.60	0.20	-.074	1.192	-.004
2204	-0.96	0.91	0.8	1.40	4.32	10.79	0.22	-.074	1.192	-.004
2205	-0.50	0.94	1.3	1.42	3.96	1.75	0.20	-.251	1.765	-.023
2206	-0.50	0.95	1.3	1.40	4.32	2.06	0.20	-.251	1.765	-.023
2207	-0.93	0.93	1.3	1.42	3.96	1.75	0.25	0.014	1.551	0.001
2208	-0.92	0.96	1.3	1.40	4.32	2.06	0.24	0.014	1.551	0.001
2209	-0.49	0.99	0.8	1.42	3.96	9.60	0.22	-.273	1.190	-.007
2210	-0.49	0.96	0.8	1.40	4.32	10.79	0.23	-.273	1.190	-.007
2211	-0.96	0.97	0.8	1.42	3.96	9.60	0.21	-.074	1.192	-.004
2212	-0.93	0.95	0.8	1.40	4.32	10.79	0.20	-.074	1.192	-.004
2213	-0.49	0.93	1.3	1.42	3.96	1.75	0.20	-.251	1.765	-.023
2214	-0.50	0.91	1.3	1.40	4.32	2.06	0.30	-.251	1.765	-.023
2215	-0.98	0.96	1.3	1.42	3.96	1.75	0.28	0.014	1.551	0.001
2216	-0.91	0.97	1.3	1.40	4.32	2.06	0.20	0.014	1.551	0.001

Average wound width = 0.23 cm

Table 36. HPV instrumentation installed in poplar potometer tree PT1. Sensors were 0.16 cm diameter Teflon with glass bead thermistor; heater was 0.16 cm diameter brass. Installed 17 June 1981. Odd numbered sensors above freeze block, even numbered sensors below.

SENSOR No	Xu cm	Xd cm	d cm	SWT cm	dib cm	A_d cm^2	W cm	POSITION EQUATION a	b	c
1101	-0.50	0.92	0.8	0.95	3.42	2.04	0.22	-.777	1.704	-.020
1102	-0.50	0.92	0.8	1.18	3.88	3.22	0.22	-.654	1.422	-.016
1103	-0.95	0.95	0.8	0.95	3.42	2.04	0.23	0.044	1.468	0.018
1104	-0.95	0.97	0.8	1.18	3.88	3.22	0.22	0.022	1.320	0.004
1105	-0.45	0.99	0.3	0.95	3.42	4.96	0.24	-.549	1.271	-.010
1106	-0.51	0.91	0.3	1.18	3.88	5.74	0.26	-.460	1.191	-.003
1107	-0.97	0.95	0.3	0.95	3.42	4.96	0.22	0.012	1.221	-.001
1108	-0.98	0.91	0.3	1.18	3.88	5.74	0.23	-.020	1.148	-.001
1109	-0.46	0.99	0.8	0.95	3.42	2.04	0.23	-.777	1.704	-.020
1110	-0.46	0.98	0.8	1.18	3.88	3.22	0.22	-.654	1.422	-.016
1111	-0.94	0.98	0.8	0.95	3.42	2.04	0.24	0.044	1.468	0.018
1112	-0.95	0.98	0.8	1.18	3.88	3.22	0.23	0.022	1.320	0.004
1113	-0.46	0.93	1.3	0.95	3.42	--	0.22	In heartwood		
1114	-0.49	0.97	1.3	1.18	3.88	--	0.25	In heartwood		
1115	-0.99	0.95	1.3	0.95	3.42	--	0.26	In heartwood		
1116	-0.96	0.98	1.3	1.18	3.88	--	0.22	In heartwood		

Average wound width = 0.23 cm

Table 37. HPV instrumentation installed in poplar potometer tree PT2. Sensors were 0.16 cm diameter Teflon with glass bead thermistor; heater was 0.16 cm diameter brass. Installed 26 June 1981. Odd numbered sensors above freeze block, even numbered sensors below.

SENSOR	Xu	Xd	d	SWT	dib	A_d	W	POSITION EQUATION		
No	cm	cm	cm	cm	cm	cm^2	cm	a	b	c
1201	-0.50	0.95	0.3	1.20	4.55	3.69	--	-.417	1.159	0.002
1202	-0.49	0.96	0.3	1.06	4.95	4.04	0.26	-.417	1.159	0.002
1203	-0.99	0.94	0.3	1.20	4.55	3.69	--	-.014	1.108	0.001
1204	-0.96	0.98	0.3	1.06	4.95	4.04	0.30	-.014	1.108	0.001
1205	-0.50	0.95	0.6	1.20	4.55	2.94	0.36	-.461	1.214	-.006
1206	-0.50	0.96	0.6	1.06	4.95	3.26	0.20	-.461	1.214	-.006
1207	-0.96	0.98	0.6	1.20	4.55	2.94	0.28	-.014	1.175	-.001
1208	-0.95	0.98	0.6	1.06	4.95	3.26	0.20	-.014	1.175	-.001
1209	-0.45	0.91	0.8	1.20	4.55	3.68	0.26	-.565	1.301	-.012
1210	-0.50	0.97	0.8	1.06	4.95	5.66	0.20	-.565	1.301	-.012
1211	-0.95	0.94	0.8	1.20	4.55	3.68	0.30	0.006	1.251	-.001
1212	-0.93	0.99	0.8	1.06	4.95	5.66	0.30	0.006	1.251	-.001
1213	-0.50	0.99	1.3	1.20	4.55	--	0.20	In heartwood		
1214	-0.50	0.94	1.3	1.06	4.95	--	0.30	In heartwood		
1215	-0.98	0.97	1.3	1.20	4.55	--	0.20	In heartwood		
1216	-0.91	0.99	1.3	1.06	4.95	--	0.20	In heartwood		

Average wound width = 0.25 cm
Average wound width for sensors in sapwood = 0.27 cm
Wound marked --, accidently missed measurement.

Table 38. Sample data tree BP1, sensor 2103, at 0.8 cm depth, W = 0.40 cm. Longitudinal diffusivity and moisture content at up and downstream sensors, raw HPV (HPVA or HPVS, HPVM), that corrected for wound only (40), wound plus position (40P) and actual transpiration as measured by potometer uptake (TR).

DATE		Downstream		Upstream		HPV cm/h				TR
DA/MO/YR	h	D^1	Mgw	D^1	Mgw	HPVA	(40)	(40P)	HPVM	mL/h
26/05/81	1200	.00221	0.61	.00195	0.82	1.1	3.1	3.4	16.2	
	1400	.00218	0.63	.00213	0.67	1.5	4.1	4.5	13.7	21
	1600	.00246	0.47	.00256	0.42	1.5	4.1	4.5	4.5	
28/05/81	0800	.00243	0.48	.00244	0.48	0.0	0.7	0.5	10.7	26
	1000	.00224	0.59	.00316	0.23	3.3	8.7	9.6	12.7	
	1100	.00224	0.59	.00316	0.23	3.3	8.7	9.6	12.7	55
29/05/81	Freezing treatment, no HPV data									
30/05/81	0600	.00234	0.53	.00262	0.40	-2.0	-3.1	-4.1	15.7	
	0800	.00240	0.50	.00250	0.45	-2.8	-4.4	-5.8	15.0	
	1000	.00250	0.45	.00373	0.12	0.2	1.1	1.0	9.7	4
	1200	.00239	0.50	.00312	0.24	-2.1	-3.3	-4.4	15.1	
	1400	.00245	0.47	.00275	0.35	-1.3	-1.9	-2.6	12.8	
	1600	.00233	0.53	.00292	[illegible]	-1.1	-1.5	-2.1	14.3	
	1800	.00244	0.48	.00288	[illegible]	-1.7	-2.6	-3.5	13.0	
	2000	.00234	0.53	.00268	[illegible]	-1.9	-3.0	-3.9	16.1	
	2200	.00221	0.61	.00268	[illegible]	-0.9	-1.1	-1.7	17.2	
	2400	.00237	0.52	.00245	[illegible]	-1.9	-3.0	-3.9	14.7	

Table 39. Sample data tree BP2, sensor 2203, at 0.8 cm depth, W = 0.40 cm. Longitudinal diffusivity and moisture content at up and downstream sensors, raw HPV (HPVA or HPVS, HPVM), that corrected for wound only (20), wound plus position (20P) and actual transpiration as measured by potometer uptake (TR).

DATE		Downstream		Upstream		HPV cm/h				TR
DA/MO/YR	h	D[1]	Mgw	D[1]	Mgw	HPVA	(20)	(20P)	HPVM	mL/h
12/06/81	0000	.00276	0.35	.00278	0.34	1.9	3.1	3.6	12.8	
	0200	.00260	0.41	.00271	0.36	1.3	2.1	2.5	0.9	
	0400	.00239	0.50	.00223	0.60	0.8	1.3	1.5	11.9	
	0600	.00224	0.59	.00196	0.81	0.8	1.3	1.5	16.2	
	0800	.00227	0.57	.00216	0.64	0.4	0.7	0.8	12.1	16
	1000	.00234	0.53	.00260	0.40	1.4	2.3	2.7	15.9	10
	1200	.00231	0.54	.00239	0.50	0.8	1.3	1.5	16.6	
	1400	.00252	0.44	.00292	0.29	2.4	4.0	4.6	12.3	17
	1600	.00210	0.69	.00525	0.43	3.9	6.7	7.7	21.2	
	1900	.00202	0.75	.00192	0.85	6.6	12.0	13.7	26.2	46
	2000	.00219	0.62	.00302	0.26	5.1	9.0	10.3	18.6	52
	2200	.00205	0.73	.00271	0.36	5.3	9.4	10.8	20.6	52
	2400	.00213	0.67	.00284	0.32	7.0	12.9	14.7	20.1	
13/06/81	Stem freezing treatment, no HPV data.									
14/06/81	0000	.00209	0.70	.00212	0.68	1.2	2.0	2.3	18.6	
	0200	.00214	0.66	.00231	0.55	0.7	1.2	1.3	19.6	
	0400	.00227	0.57	.00225	0.58	0.7	1.2	1.3	14.9	
	1000	.00246	0.47	.00242	0.49	0.4	0.7	0.8	7.5	9
	1100	.00226	0.58	.00234	0.53	0.4	0.7	0.8	17.6	
	1400	.00244	0.48	.00240	0.50	0.9	1.5	1.7	14.9	8
	1600	.00240	0.50	.00245	0.47	0.3	0.6	0.6	14.9	4
	1800	.00225	0.58	.00236	0.52	0.0	0.1	0.1	16.4	8
	2000	.00215	0.65	.00211	0.68	-0.1	0.0	-0.1	20.4	
	2200	.00245	0.47	.00239	0.50	0.1	0.3	0.2	12.9	
	2400	.00260	0.41	.00262	0.39	-0.5	-0.6	-0.8	17.1	

Table 40. Sample data tree PT1, sensor 1107, at 0.3 cm depth, W = 0.22 cm. Longitudinal diffusivity and moisture content at up and downstream sensors, raw HPV (HPVA or HPVS, HPVM), that corrected for wound only (22), wound plus position (22P) and actual transpiration as measured by potometer uptake (TR).

DATE		Downstream		Upstream		HPV cm/h				TR
DA/MO/YR	h	D[1]	Mgw	D[1]	Mgw	HPVA	(22)	(22P)	HPVM	mL/h
18/06/81	0800	.00190	0.88	.00209	0.70	1.6	2.8	3.4	7.7	28
	1000	.00187	0.91	.00208	0.70	1.5	2.6	3.2	9.9	30
	1200	.00183	0.96	.00208	0.70	3.6	6.5	7.8	13.9	
	1500	.00181	0.99	.00207	0.71	4.1	7.4	9.0	14.7	65
	1600	.00178	1.02	.00190	0.88	4.6	8.5	10.3	16.6	
	1800	.00178	1.03	.00196	0.81	4.6	8.5	10.3	17.0	82
	2000	.00186	0.92	.00203	0.75	5.0	9.3	11.3	14.5	
	2200	.00180	1.00	.00196	0.81	4.8	8.9	10.8	16.2	81
19/06/81	0000	.00190	0.87	.00213	0.66	3.1	5.5	6.7	11.8	
	0200	.00192	0.86	.00226	0.58	2.6	4.6	5.6	10.4	
	0400	.00190	0.88	.00212	0.68	2.5	4.4	5.3	10.3	
	0600	.00187	0.91	.00206	0.72	2.4	4.2	5.1	11.4	
	0800	.00176	1.06	.00181	0.98	6.1	11.7	14.1	20.2	50
19/06/81	1200 to 2200, Stem freezing treatment, no HPV data									
20/06/81	0800	.00213	0.67	.00239	0.50	-0.1	0.0	0.0	17.3	22
	1000	.00219	0.62	.00235	0.53	0.8	1.4	1.7	14.8	
	1200	.00214	0.66	.00233	0.53	0.3	0.6	0.7	15.8	20
	1400	.00224	0.59	.00240	0.50	0.4	0.8	0.9	13.6	
	1600	.00223	0.60	.00234	0.53	0.2	0.4	0.5	14.5	20
22/06/81	0800	.00218	0.63	.00220	0.62	-0.4	-0.5	-0.6	15.1	8
	1000	.00222	0.60	.00235	0.52	-0.4	-0.5	-0.6	12.4	
	1200	.00223	0.59	.00231	0.55	-0.3	-0.3	-0.4	12.8	
	1400	.00225	0.58	.00233	0.54	-0.8	-1.1	-1.3	13.2	
	1600	.00223	0.59	.00231	0.55	-0.6	-0.8	-1.0	13.0	

Table 41. Sample data tree PT2, sensor 1207, at 0.6 cm depth, W = 0.28 cm. Longitudinal diffusivity and moisture content at up and downstream sensors, raw HPV (HPVA or HPVS, HPVM), that corrected for wound only (28), wound plus position (28P) and actual transpiration as measured by potometer uptake (TR).

DATE		Downstream		Upstream		HPV cm/h				TR
DA/MO/YR	h	D[1]	Mgw	D[1]	Mgw	HPVA	(28)	(28P)	HPVM	mL/h
27/06/81	1000	.00202	0.75	.00217	0.63	9.5	24.4	28.0	16.0	57
	1200	.00209	0.70	.00228	0.56	11.0	30.7	35.1	18.0	
	1400	.00219	0.62	.00246	0.47	12.7	39.1	44.2	19.1	100
	1600	.00214	0.66	.00258	0.41	12.9	40.1	45.4	21.5	109
	1800	.00215	0.65	.00234	0.53	12.4	37.5	42.5	20.6	120
	2000	.00219	0.62	.00243	0.48	12.1	36.0	40.8	19.4	116
	2200	.00219	0.62	.00236	0.52	5.6	12.4	14.4	11.3	52
28/06/81	0000	.00210	0.69	.00229	0.56	4.1	8.9	10.3	10.8	
	0200	.00226	0.58	.00222	0.61	3.6	7.6	8.9	7.2	
	0400	.00233	0.54	.00246	0.47	4.2	9.1	10.6	9.7	
	0600	.00225	0.58	.00226	0.58	3.8	8.1	9.5	2.8	
	0800	.00214	0.66	.00204	0.74	3.9	8.4	9.8	10.0	33
	1000	.00230	0.55	.00233	0.54	14.7	50.5	56.5	20.9	66
29/06/81	Stem freezing treatment, no HPV data									
30/06/81	1000	.00210	0.69	.00222	0.60	4.5	9.9	11.5	12.2	35
	1200	.00213	0.66	.00236	0.52	7.6	17.7	20.5	14.9	
	1400	.00217	0.64	.00225	0.58	7.7	18.1	20.8	15.1	
	1600	.00215	0.65	.00218	0.63	8.6	21.1	24.2	16.4	70
	1800	.00221	0.61	.00232	0.54	8.9	22.1	25.4	16.3	
	2000	.00220	0.61	.00225	0.58	8.2	19.7	22.7	15.6	79
	2200	.00226	0.58	.00234	0.53	3.9	8.4	9.8	10.4	56
01/07/81	0000	.00212	0.67	.00223	0.59	2.7	5.6	6.5	9.2	
	0200	.00220	0.61	.00218	0.63	2.3	4.7	5.5	6.3	
	0400	.00205	0.73	.00212	0.67	1.8	3.6	4.2	7.7	
	0600	.00208	0.71	.00218	0.63	2.0	4.0	4.7	9.3	
	0800	.00201	0.68	.00216	0.64	2.2	4.5	5.2	6.6	
	1000	.00221	0.61	.00229	0.56	9.4	24.0	27.6	17.5	28

APPENDIX E

HEAT PULSE VELOCITY INSTRUMENTATION

Sensor and heater construction and thermal properties

The general details of sensor and heater construction are shown in Figures 49 and 50. The thermistors were not matched for resistance as only ~~the~~ offset above ambient temperature is required, and that in arbitrary units.

The derived thermal properties that were used in the simulations are given in Table 42. The sensors and heater were considered to be isotropic within themselves, with the same conductivity in all directions.

Table 42. Thermal properties of materials used in simulating the sensor materials. The thermal properties of all materials (except Teflon) are from Carslaw and Jaeger (1959); Teflon from Modern Plastics Encyclopedia, 1968, Volume 45, No. 14A. p. 90.

SUBSTANCE	K	P	C	D
	$cal\ s^{-1}\ cm^{-1}\ {}^oC^{-1}$	$g\ cm^{-3}$	$cal\ g^{-1}\ {}^oC^{-1}$	$cm^2\ s^{-1}$
Air	.00006	.0013	.24	.19
Teflon	.0006	2.2	.25	.0011
Glass	.0028	2.4	0.2	.0058
Aluminum	.48	2.7	0.2	.86
Brass	.25	8.5	.09	.33
Copper	.93	8.9	.09	1.14
Glass composite*	.03	2.7	.2	.055
Teflon composite**	.024	1.4	.7	.024

* Glass composite 4.0% copper 96% glass
** Teflon composite 2.5% copper 52% Teflon 45.5% air

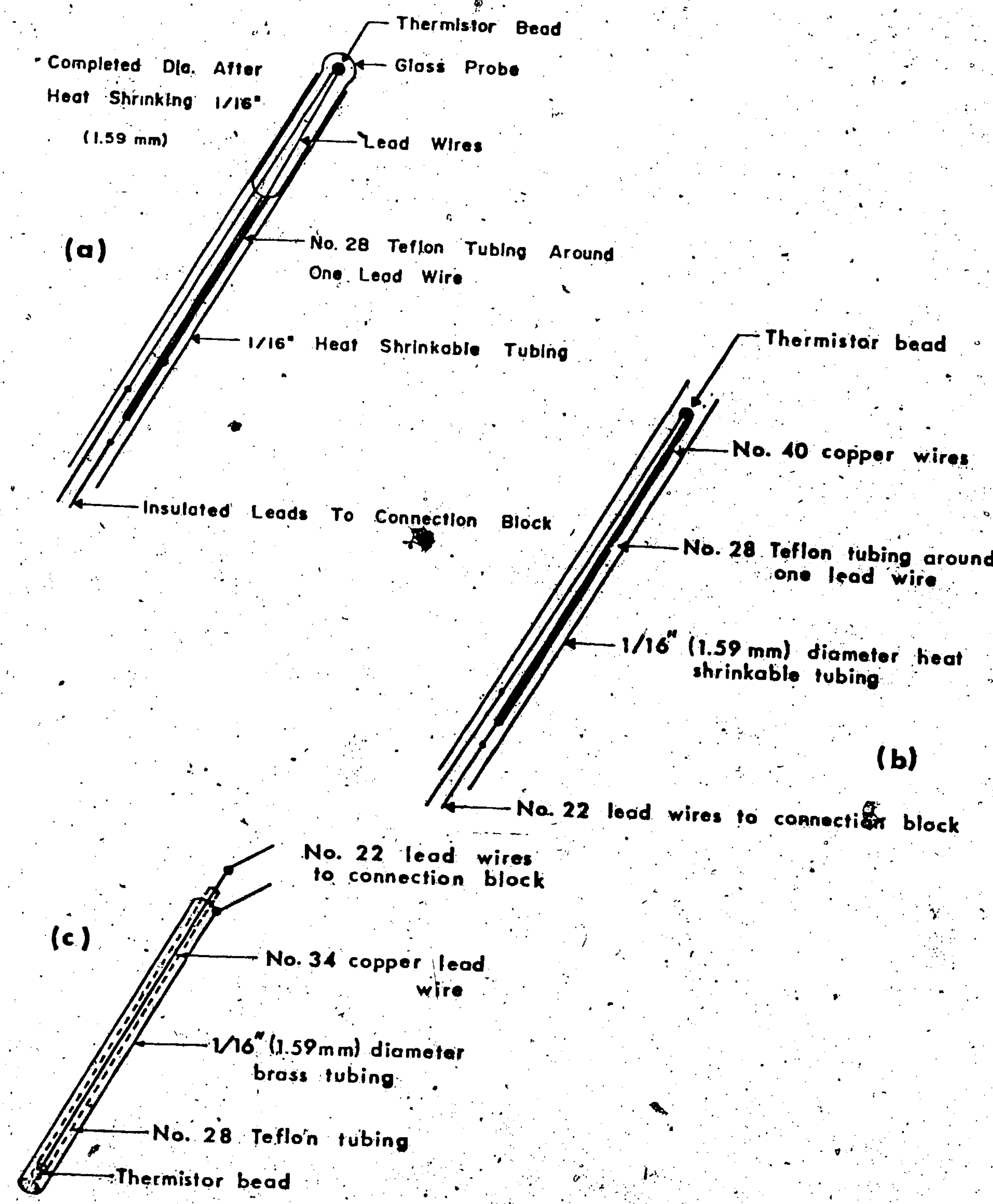

Figure 49. Construction details of thermistor sensors. (a) Glass rod, thermistor Fenwall type GB41M2. (b) Teflon, thermistor Fenwall type GB41J1. (c) Brass, thermistor Fenwall type GB41L1.

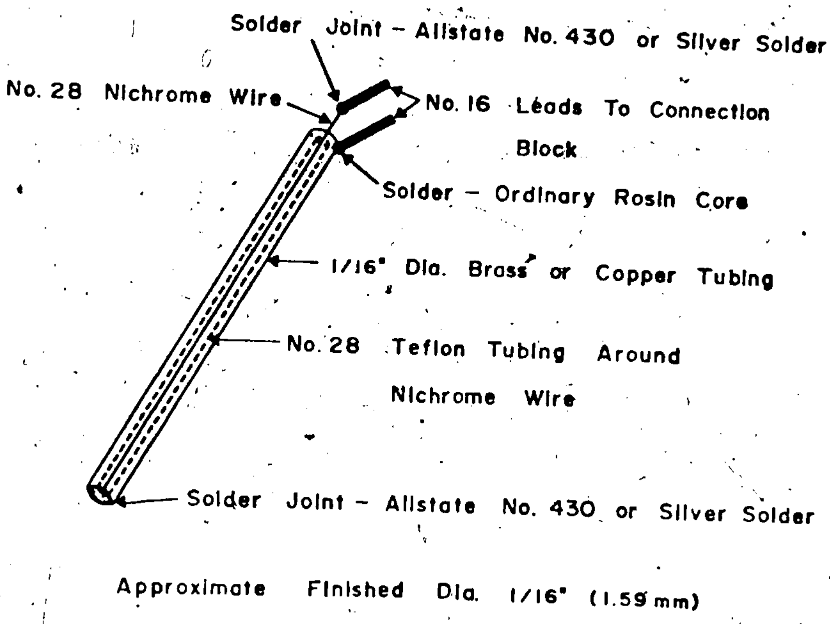

Figure 50. Heater construction details. The total electrical resistance of the heater wire varies with the length of heater constructed. The approximate resistance of the #28 AWG nichrome wire is 0.16 ohms/cm.

Heat plulse velocity indicating or recording instrumentation

Block diagrams for a single channel manual HPVT meter (Fig. 52), a 4-channel semi-manual HPVT recorder, (Fig. 53) and a 16-channel HPVA, HPVS, HPVM and/or D data logger (Fig. 54) are given below.

Sensor circuits

Each sensor (at Xu or Xd) was arranged in a bridge circuit as in Figure 51a for HPVT, or Figure 51b for HPVA, HPVS, HPVM or D.

HPV instruments

Separate power supplies (batteries) were used for the sensor and heater circuits to avoid propogation of the transient generated by the heat pulse back through to the low level temperature signal. A constant-current power supply maintained heat pulse current at 4 amperes to avoid burning out the heater wire. Heat pulse magnitude was varied between 8 to 32 Joules by extending the heat pulse duration from 1 to 4 s as needed to achieve a readable temperature-rise signal.

1) Manual instrument, HPVT (Fig. 52). Operator manually balances sensor output (Tu - Td) to zero, activates the heat pulse and watches the meter, M, for (Tu - Td) = 0 at some later time (tz). Elapsed time, seconds, is indicated by the counter.

2) Semi-manual HPVT recorder (Fig. 53). Operation as above except that the recorder relieves the operator of the task of watching the meter for tz; it is measured from the recorded temperature difference trace. The recorder operates at a chart speed of about 1 cm s^{-1}. The heat pulse is actuated at a convenient time line on the recorder chart. The recorder is then set to run for 5 to 15 minutes as necessary to allow all 4 channel tz's to be indicated by their respective traces.

3) Sixteen channel HPVA, HPVS, HPVM or D logger (Fig. 54). The microprocessor is programmed to select a group of 8 channels and then to access each channel in sequence. Xu and Xd are accessed ½ s apart. The initial offset from ambient for each sensor at t= -60 s is stored as offset error. This error is fed back into the input amplifier A_{in}, at each subsequent reading to maintain a constant reference signal for all future accesses to that sensor. At time t = 0, the up and downstream sensors (of channel 1) are read and the heat pulse actuated for 1 to 4 s. This sequence is repeated for sensors 2, 3, etc., at 7.5 s intervals until the heat pulse has occured on all 8 channels. Then each set of up and downstream sensors is read at 60 s intervals to t = 180 s. The second (and any additional groups of channels up to a maximum of 64) is selected and the individual sensors and heaters are accessed in exactly the same manner. At selected intervals, the data in memory is transferred to a cassette tape for processing into the desired HPV or D values in a Hewlett Packard 9825A desk top computer.

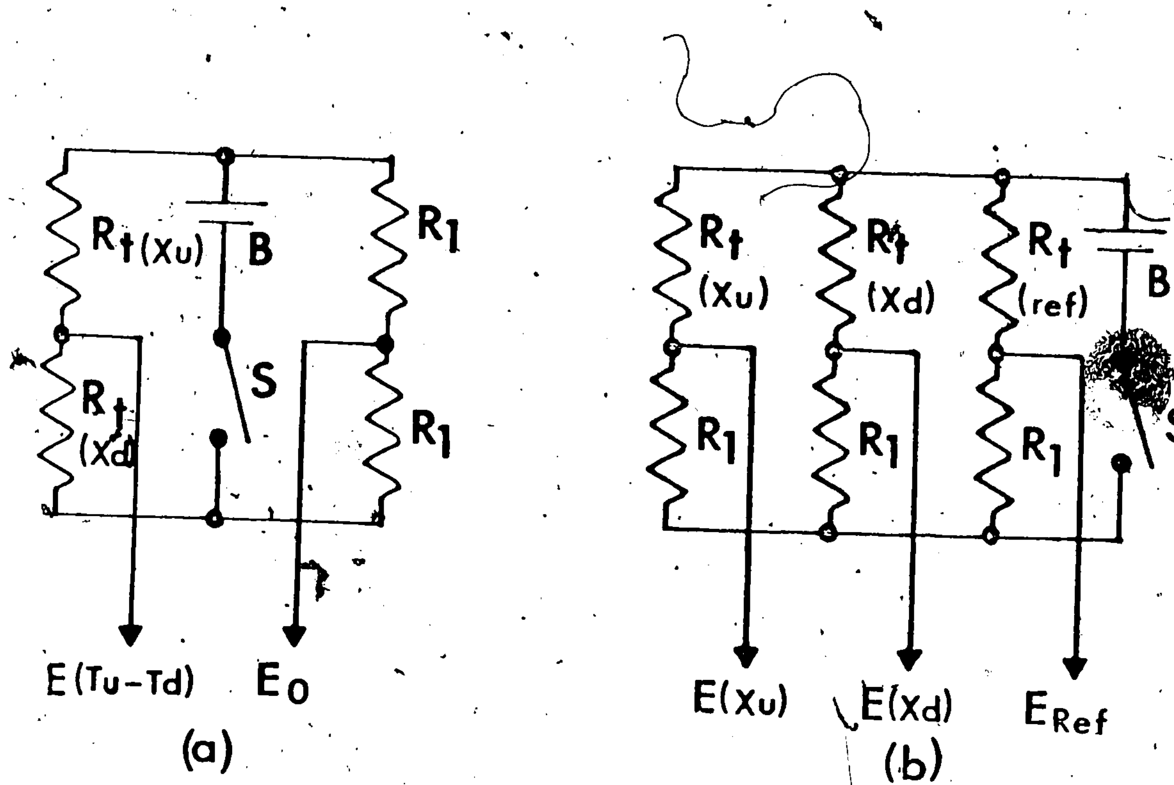

Figure 51. Thermistor bridge arrangements for HPVT (a) and HPVA, HPVS, HPVM or D (b) measurement. The sensors R_t located at Xd and Xu are active in that they are located directly above and below the heater to provide the temperature difference or temperature rise data for the several HPV or diffusivity calculations. In (b), the reference sensor R_{ref} provides a measure of ambient stem temperature, presumably unaffected by the heat pulse, to help maintain a constant bridge output under long term ambient temperature change. It should be located in the same stem as the active sensors but no closer than 4 to 5 cm laterally, 10 to 15 cm longitudinally, from any active pair. One reference sensor is sufficient for all of the active sensors in the same vicinity (±1 m) in the same stem. Resistors R_1 are located in the instrument, not in the stem.

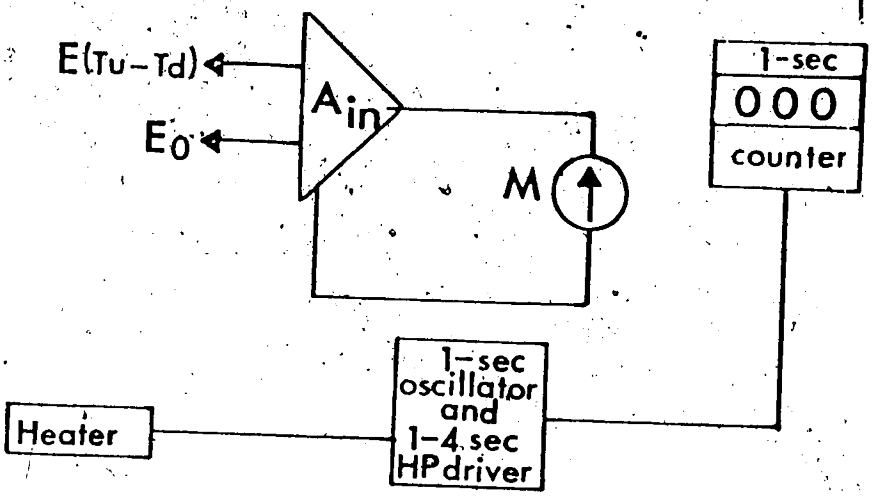

Figure 52. Manual instrument for measuring HPVT.

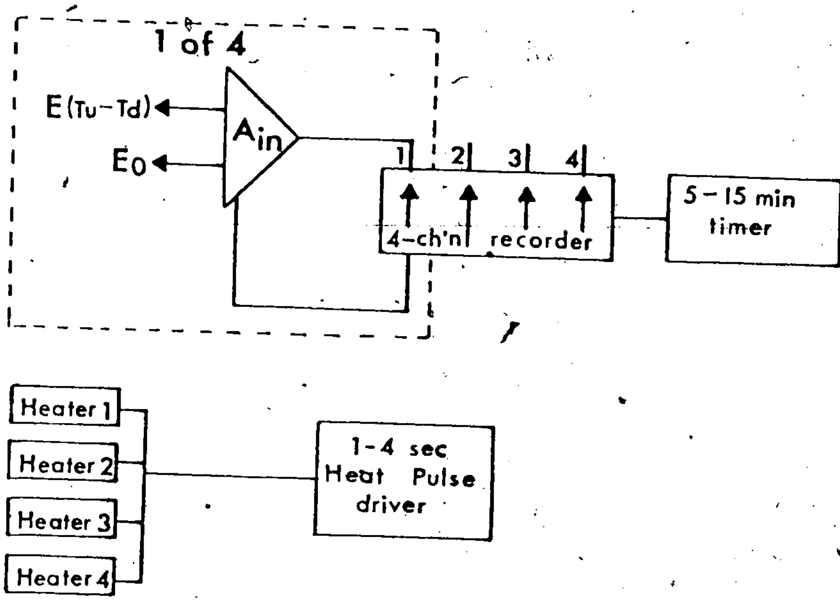

Figure 53. Semi-manual 4-channel HPVT recorder.

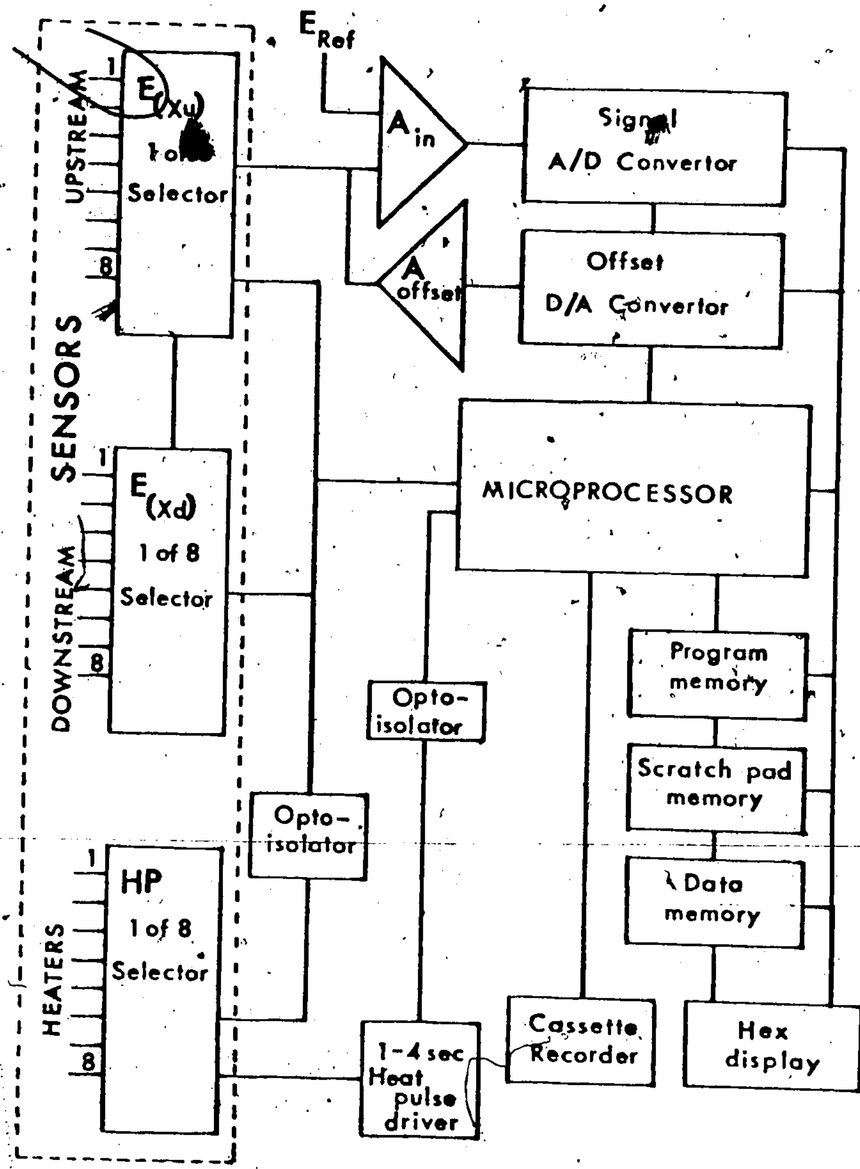

Figure 54. Sixteen channel HPVA, HPVS, HPVM or D logger.

APPENDIX F

COMPUTER PROGRAMS FOR TANGENTIAL AND RADIAL LONGITUDINAL MODELS

The program for both models is the same except for the plane heat source geometry equations for D^1, HPVM and HPVP. The TLM program is given in its entirety; however only the first 26 lines, containing the modified equations, are given for the RLM. Both programs access the same subroutine SOLVER which produces the finite difference solutions using the alternating direction implicit method (von Rosenberg 1969).

The thermal conductivity and density times specific heat for each node in the physical mesh are contained in file CPRB. The directional thermal conductivities are headed CAM, conductivity along the tree axis in the minus (upstream) direction from the point; CAP, as above except in the positive (downstream) direction; CTM, tangential in the minus direction (to the left) and CTP, as CTM except to the right. Density times specific heat (PC) is the weighted average for all materials meeting at the node.

The probe index number for the particular model is contained in file IPRB. The values assigned to each node in this file determines whether the simulation is TLM or RLM. Examples of a TLM IPRB index file with sensor materials (sensor-heater nodes indicated by boxed area) and an RLM IPRB without probe materials are given. One or two sensors up to 0.32 cm in diameter, may be located at any point in the physical grid, as positioned by variable ITC (top, downstream sensor location) or IBC (bottom, upstream sensor location). Similiarily the heater is positioned by variable IHC. In IPRB, the sensor, which must be of the same size and materials at both the up and downstream locations, is centered along IDX@6; the heater IDX@15.

A sample data printout for the TLM is given. Temperature field values are available at 15, 20, 30, 40, 45, 60, 80, 90, 120 and 180 s, but only the temperatures and solutions solutions at 60, 120 and 180 s are shown (temperature values are x100). With sensor materials in the temperature field, only the solutions at the sensor nodes are valid (circled on printout). All others are ignored. If sensor materials are not in the field, then solutions are valid at all points.

Variable KR controls the size of matrix used in the tangential or radial direction. KR x 0.04 cm is the dimension. KR also defines the centerline of symmetry of the solution matrix. The sensors and heater are normally centered at KR in the TLM, and KR is the center of the stem (up to 4 cm radius) in the RLM.

Wound is set by the HPV imposed at or in the vicinity of the sensor nodes: HPVI = 0 within the wound; HPVI = ½ HPV or zero on a sensor border depending upon the wound width imposed; HPVI = HPV at all other nodes. The values in IDX@1 in IPRB designate the HPVI assigned at each node. This index number is referenced to print out the HPVI at each tangential or radial position in the physical mesh.

```
C     THIS PROGRAM, TLM+SOLVER, PRODUCES A FINITE DIFFERENCE
C     NUMERICAL SOLUTION IN THE TANGENTIAL LONGITUDINAL PLANE
C     TO MARSHALL'S(1958) PARTIAL DIFFERENTIAL EQUATION
C     FOR HEAT TRANSPORT BY COUPLED CONDUCTION THROUGH
C     WOOD SUBSTANCE AND CONVECTION BY THE MOVING SAP.
C     PROBE THERMAL COEFFICIENTS AS WELL AS THOSE AT
C     VARIOUS EARLYWOOD/SAPWOOD OR LATEWOOD/HEARTWOOD
C     COMBINATIONS ARE CONTAINED IN MTS LINE FILE COEF.
C     AN INDEX TO WHICH COEFFICIENT IS TO BE USED AT EACH
C     NODE IS CONTAINED IN MTS LINE FILE PID(N).
C     CURRENT RUN PARAMETERS, I.E. WOOD MOISTURE, WOOD
C     DENSITY, SENSOR LOCATION, AND HPV'S TO RUN ARE
C     CONTAINED IN MTS LINE FILE RPAR(N).
C     FUNCTIONS ARE DEFINED BELOW TO SOLVE FOR HPVM,DIFFUSIVITY
C     HPVS, HPVA AND HPVP AT VARIOUS COMBINATIONS OF TIMES
C     FROM AMONG 15,20,30,40,45,60,80,90,120 AND 180 SECONDS,
C     AND AT VARIOUS SPACES RANGING FROM -1.20,-.96,-.48 TO
C     +.96, +1.20, AND TO +1.44 CM.
      VM(TM1,TM2,TM3,R1,R2)=(TM1*ALOG(R1) -TM3*ALOG(R2))
     1 /(TM1*TM2*TM3*(ALOG(R1/R2)))
      DIF(TM1,TM2,TM3,R1,R2,XU)=(XU*XU*(-.5*(TM2-TM1)**2))
     1 /(TM1*TM2*TM3*(ALOG(R1/R2)))
      VS(DF,R3,XU)=3600.*(DF*ALOG(R3))/XU
      VA(XT,XB,TM1,TM2,S1,S2)=(XT+XB)*(TM1*ALOG(S1)
     1 -TM2*ALOG(S2))/(2.*TM1*TM2*(ALOG(S1/S2)))
      VP(XU,DF,TVP)=(XU*XU-4.*DF*TVP)
      INTEGER LC(201)
      DIMENSION SNA(201,101),SNR(201,101),IPRB(19,101),
     1CPRB(200,6),HPVI(10),TH(10,101),TM48(10,101),TM96(10,101),
     2TM120(10,101),TM144(10,101),TP96(10,101),TP120(10,101),
     3TP144(10,101),TZ1(101),TZ2(101),TPK1(101),TPK2(101),
     4TPK3(101),DEPTH(101),VIMP(101),SOL(31,101)
      COMMON/NOSOL/DEPTH,SOL,VIMP
      COMMON /INT1/LC,IPRB
      COMMON /INT2/ IMAX,IMAX1,IMAX2,KR,KRM,KRP
      COMMON /INT3/ IT1,IT2,IT3,ITF,IT,ITC,IBC,IHC
      COMMON /INT4/ NH1,NH2,NH3,NH4,NH5,NH6,NH7,NH8
      COMMON /REA1/ SNA,SNR
      COMMON /REA2/ CPRB
      COMMON /REA3/TIME,DT,HT,HHPL,HPL,DT1,DT2,DT3,DT4
      COMMON/REA4/TM48,TM96,TM120,TM144,TH,TP96,
     1 TP120,TP144,TZ1,TZ2,TPK1,TPK2,TPK3
C     READ RUN CONTROL PARAMETERS
      READ(2'2000,503)MPT,MPC,NCOEF,NH1,NH2,NH3,NH4,NH5,NH6,NH7,NH8
      READ(2'3000,503)NRM,ITC,IHC,IBC,KR,IMAX
      READ(2'5000,504) (HPVI(I),I=1,NRM)
C     READ VALUES INTO COEFFICIENT FILE CPRB.
      READ(1'8000,500)((CPRB(I,J),J=1,6),I=1,NCOEF)
C     READ PROBE INDEX INTO FILE IPRB.
C     NOTE THAT THIS READ STATEMENT ROTATES THE FILE 90 DEGREES
```

```
      READ(3'1000,601)((IPRB(J,I),J=1,19),I=1,KR)
      READ(4'2000,504)DT1,DT2,DT3,DT4
      READ(4'4000,502)IT1,IT2,IT3,ITF
      READ(4'6000,500) HT,HPL
C     THIS READ STATEMENT ALLOWS ME TO INPUT THE NODE NUMBERS
C     AT WHICH I WANT DIFFERENT THAN THE STANDARD NODES
C     GIVEN HPV VALUES.  THE NODE NUMBERS ARE ASSIGNED
C     IN FILE CONPAR(N), WHICH IS ASSIGNED TO UNIT 4.
      READ(4'8000,502)NV1,NV2,NV3,NV4
      READ(4'10000,502)NP1,NP2,NP3
      CBARK=CPRB(67,1)/CPRB(67,5)
      CSWD=CPRB(1,1)/CPRB(1,5)
      CHWD=CPRB(2,1)/CPRB(2,5)
      DX=0.04
      HHPL=HPL/2.0
      KRM = KR-1
      KRP = KR+1
      IMAX1=IMAX-1
      IMAX2=IMAX-2
      ITT = ITC+4
      ITB = ITC-4
      IHT = IHC+4
      IHB = IHC-4
      IBT = IBC+4
      IBB = IBC-4
      ITM = ITB-2
      IHM = IHB-11
      IBM = IBB-2
      ITS = ITC-IHC
      IBS = IBC-IHC
      SPT = DX*ITS
      SPB = DX*IBS
      KWR = KR/17
      IF(KWR.EQ.0)KWR=1
      DO 200 I=2,IMAX1
      IF(I.GE.ITB.AND.I.LE.ITT) GO TO 192
      IF(I.GE.IHB.AND.I.LE.IHT) GO TO 193
      IF(I.GE.IBB.AND.I.LE.IBT) GO TO 194
191   LC(I)=1
      GO TO 200
192   LC(I)=I-ITM
      GO TO 200
193   LC(I)=I-IHM
      GO TO 200
194   LC(I)=I-IBM
200   CONTINUE
      DO 70 K=1,KR
70    DEPTH(K) = DX*(K-1)
      WRITE(6,610)
      WRITE(6,611)ITC,IHC,IBC,MPT,MPC
```

```
      WRITE(6,618)IT1,IT2,IT3,ITF,NH1,NH2,NH3,NH4,NH5,NH6,NH7,NH8
      WRITE(6,619)DT1,DT2,DT3,DT4,HT,HPL
      WRITE(6,622)NP1,NP2,NP3,NV1,NV2,NV3,NV4
      DDX=DX*DX
      D2DX=2.0*DX
C     ROUTINE TO PRINT OUT PROBE INDEX VALUES
      IF(MPC.EQ.0)GO TO 14
      WRITE(6,613)
      WRITE(6,614)
 14   DO 15 I=1,NCOEF
      IF(MPC.EQ.0) GO TO 15
      IF(I.EQ.51.OR.I.EQ.101.OR.I.EQ.151)WRITE(6,601)
      IF(I.EQ.51.OR.I.EQ.101.OR.I.EQ.151)WRITE(6,614)
      WRITE(6,612)I,(CPRB(I,J),J=1,6)
 15   CPRB(I,6) = 999.0
 16   IF(MPT.EQ.0)GO TO 13
      WRITE(6,608)NRM
      DO 71 I=1,[illegible]
      IF(I.EQ.[illegible].EQ.5.OR.I.EQ.7)WRITE(6,601)
      IF(I.EQ[illegible]I.EQ.11.OR.I.EQ.13)WRITE(6,601)
      K1 = 17[illegible]+1
      K2 = 17*[illegible]
      IF(K2.GT.KR)K2=KR
      WRITE(6,620)(K,K=K1,K2)
      WRITE(6,607)(DEPTH(K),K=K1,K2)
      DO 71 JJ=1,19
      J=20-JJ
 71   WRITE(6,609)J,(IPRB(J,K),K=K1,K2)
      WRITE(6,6[illegible])
      K1=K2+1
      IF(K1.GE.KR)GO TO 13
      WRITE(6,620)(K,K=K1,KR)
      WRITE(6,607)(DEPTH(K),K=K1,KR)
      DO 72 JJ=1,19
      J=20-JJ
 72   WRITE(6,609)J,(IPRB(J,K),K=K1,KR)
 13   DO 11 J=1,4
      DO 11 K=1,NCOEF
 11   CPRB(K,J) = CPRB(K,J)/DDX
      DO 50 NRUN = 1,NRM
      DO 12 K=1,KR
      DO 12 I=1,IMAX
      SNA(I,K)=0.0
 12   SNR(I,K)=0.0
      DO 17 K=1,KR
      TZ1(K)=999.99
      TZ2(K)=999.99
      TPK1(K)=999.99
      TPK2(K)=999.99
      TPK3(K)=999.99
```

```
      DO 17 I=1,31
17    SOL(I,K)=99.99
      HPV=HPVI(NRUN)
C     I AM ASSUMING THAT PHLOEM FLOW RATE = -0.01 XYLEM RATE
C     PHLOEM FLOW VALUES ARE SET AT NODES 39, 40 AND 41
C     THIS SETS PHLOEM VELOCITY AT -1% OF HPV XYLEM
      HPVPH=-0.01*(ABS(HPV))
      DO 10 K=1,KR
      KK=IPRB(1,K)
      IF(KK.EQ.1)VIMP(K)=HPV
      IF(KK.EQ.2.OR.KK.EQ.50.OR.KK.EQ.67)VIMP(K)=0.0
      IF(KK.EQ.37.OR.KK.EQ.38.OR.KK.EQ.51)VIMP(K)=0.5*HPV
      IF(KK.EQ.NP1)VIMP(K)=HPVPH/2.0
      IF(KK.EQ.NP3)VIMP(K)=(HPVPH + HPV)/2.0
      IF(KK.EQ.NP2)VIMP(K)=HPVPH
      IF(KK.EQ.NV1.OR.KK.EQ.NV2)VIMP(K)=HPV
      IF(KK.EQ.NV3.OR.KK.EQ.NV4)VIMP(K)=HPV/2.0
10    CONTINUE
      HPV=HPV/3600
      HPV=HPV/D2DX
      HPVPH=HPVPH/3600
      HPVPH = HPVPH/D2DX
      CPRB(1,6)=HPV
      CPRB(2,6)=0.0
      CPRB(37,6)=0.5*HPV
      CPRB(38,6)=CPRB(37,6)
      CPRB(NP1,6) = 0.5*HPVPH
      CPRB(NP2,6) = HPVPH
      CPRB(NP3,6) = (HPV + HPVPH)/2.0
      CPRB(50,6) = 0.0
      CPRB(51,6) = 0.5*HPV
      CPRB(67,6) = 0.0
      CPRB(NV1,6)=HPV
      CPRB(NV2,6)=HPV
      CPRB(NV3,6)=HPV/2.0
      CPRB(NV4,6)=HPV/2.0
      TIME = 0.0
      IT = 0
      DT = DT1
C     PRINT OUT PARAMETERS USED IN THIS RUN.
      WRITE(6,615)SPT,SPB,KR
      WRITE(6,605)
      DO 97 I=1,KWR
      K1 = 17*(I-1)+1
      K2 = 17*I
      IF(K2.GT.KR)K2=KR
      WRITE(6,620)(K,K=K1,K2)
      WRITE(6,607)(DEPTH(K),K=K1,K2)
97    WRITE(6,606)(VIMP(K),K=K1,K2)
      K1 = K2+1
```

```
      IF(K1.GE.KR)GO TO 40
      WRITE(6,620)(K,K=K1,KR)
      WRITE(6,607)(DEPTH(K),K=K1,KR)
      WRITE(6,606)(VIMP(K),K=K1,KR)
C     ROUTINE TO PRINT HPV VALUES AT SOLUTION NODE POINTS
40    WRITE(6,616)
      DO 98 I=1,NCOEF
      IF((CPRB(I,6)).GE.500.)GO TO 98
      VHPV = CPRB(I,6)*3600.0*D2DX
      WRITE(6,617)I,VHPV
98    CONTINUE
      CALL APTRAC(0,0,0,2)
      TIME=0.
      DT=DT1
      IT=0
41    CONTINUE
      CALL APINIT(1,0,ISTAT)
      CALL SOLVER
      CALL APRLSE
      WRITE(6,621)TIME
C     PORTION OF MAIN PROGRAM THAT CALLS ROUTINE
C     TO PRINT OUT TEMPERATURE MATRIX VALUES
93    DO 95 IPT=1,5
      GO TO(801,802,803,804,805),IPT
801   ITIME=30
      IP=3
      GO TO 811
802   ITIME=60
      IP=6
      GO TO 811
803   ITIME=90
      IP=8
      GO TO 811
804   ITIME=120
      IP=9
      GO TO 811
805   ITIME=180
      IP=10
      GO TO 811
811   WRITE(6,600)ITIME
      DO 94 I=1,KWR
      K1=17*(I-1)+1
      K2=17*I
      IF(K2.GT.KR)K2=KR
      CALL DPRT(K1,K2,IP)
94     CONTINUE
      K1=K2+1
      IF(K1.GE.KR)GO TO 95
      CALL DPRT(K1,KR,IP)
95    CONTINUE
```

```
C     ROUTINE TO CALCULATE DIFFUSIVITIES AND HEAT PULSE
C     VELOCITIES FROM NUMERICALLY GENERATED TEMPERATURE
C     DATA AT VARIOUS INDICATED TIMES.
      DO 81 KI=1,2
      DO 82 I=1,31
      DO 82 K=1,KR
82    SOL(I,K)=99.99
      GO TO(821,822),KI
821   K1=3
      K2=6
      K3=8
      TK1=30.
      TK2=60.
      TK3=90.
      GO TO 830
822   K1=6
      K2=9
      K3=10
      TK1=60.
      TK2=120.
      TK3=180.
830   CONTINUE
      DO 80 K=2,KR
      IF(TZ1(K).LT.(1.))TZ1(K)=1.0
      IF(TZ2(K).LT.(1.))TZ2(K)=1.0
      IF(TPK1(K).LT.(1.))TPK1(K)=1.0
      IF(TPK2(K).LT.(1.))TPK2(K)=1.0
      IF(TPK3(K).LT.(1.))TPK3(K)=1.0
C     SOLUTIONS FOR HPVA, HPVT @ -.48, +.96 CM.
      S1=999.99
      S2=999.99
      S3=999.99
      IF(TP96(K1,K).LE.(0.0).OR.TM48(K1,K).LE.(0.0))GO TO 701
      S1=TP96(K1,K)/TM48(K1,K)
701   IF(TP96(K2,K).LE.(0.0).OR.TM48(K2,K).LE.(0.0))GO TO 702
      S2=TP96(K2,K)/TM48(K2,K)
702   IF(TP96(K3,K).LE.(0.0).OR.TM48(K3,K).LE.(0.0))GO TO 703
      S3=TP96(K3,K)/TM48(K3,K)
703   IF(S1.EQ.(999.99).OR.S2.EQ.(999.99))GO TO 704
      IF(S1.EQ.S2)GO TO 704
      IF(S2.LT.(0.1))S2=0.1
      SOL(1,K)=3600.*VA(0.96,-.48,TK1,TK2,S1,S2)
704   IF(S1.EQ.(999.99).OR.S3.EQ.(999.99))GO TO 705
      IF(S1.EQ.S3)GO TO 705
      IF(S3.LT.(0.1))S3=0.1
      SOL(2,K)=3600.*VA(0.96,-.48,TK1,TK3,S1,S3)
705   IF(S2.EQ.(999.99).OR.S3.EQ.(999.99))GO TO 706
      IF(S2.EQ.S3)GO TO 706
      SOL(3,K)=3600.*VA(0.96,-.48,TK2,TK3,S2,S3)
706   IF(TZ1(K).EQ.(999.99))GO TO 707
```

```
      IF(TZ1(K).LE.(0.0))GO TO 707
      SOL(4,K)=864./TZ1(K)
      SOL(5,K)=TZ1(K)
  707 CONTINUE
C     SOLUTIONS FOR HPVA, HPVT @-.96, +1.44 CM
      S1=999.99
      S2=999.99
      S3=999.99
      IF(TP144(K1,K).LE.(0.0).OR.TM96(K1,K).LE.(0.0))GO TO 711
      S1=TP144(K1,K)/TM96(K1,K)
  711 IF(TP144(K2,K).LE.(0.0).OR.TM96(K2,K).LE.(0.0))GO TO 712
      S2=TP144(K2,K)/TM96(K2,K)
  712 IF(TP144(K3,K).LE.(0.0).OR.TM96(K3,K).LE.(0.0))GO TO 713
      S3=TP144(K3,K)/TM96(K3,K)
  713 IF(S1.EQ.(999.99).OR.S2.EQ.(999.99))GO TO 714
      IF(S1.EQ.S2)GO TO 714
      IF(S2.LT.(0.1))S2=0.1
      SOL(6,K)=3600.*VA(01.44,-.96,TK1,TK2,S1,S2)
  714 IF(S1.EQ.(999.99).OR.S3.EQ.(999.99))GO TO 715
      IF(S1.EQ.S3)GO TO 715
      IF(S3.LT.(0.1))S3=0.1
      SOL(7,K)=3600.*VA(01.44,-.96,TK1,TK3,S1,S3)
  715 IF(S2.EQ.(999.99).OR.S3.EQ.(999.99))GO TO 716
      IF(S2.EQ.S3)GO TO 716
      SOL(8,K)=3600.*VA(01.44,-.96,TK2,TK3,S2,S3)
  716 IF(TZ2(K).EQ.(999.99))GO TO 717
      IF(TZ2(K).LE.(0.0))GO TO 717
      SOL(9,K)=864./TZ2(K)
      SOL(10,K)=TZ2(K)
  717 CONTINUE
C     SOLUTIONS FOR HPVM,D,HPVP DOWNSTREAM AND HPVS @-.96,+.96 CM
      R1=999.99
      R2=999.99
      R3=999.99
      R4=999.99
      R5=999.99
      D1=999.99
      IF(TP96(K1,K).LE.(0.0).OR.TP96(K2,K).LE.(0.0))GO TO 721
      R1=(TK1*TP96(K1,K))/(TK2*TP96(K2,K))
  721 IF(TP96(K2,K).LE.(0.0).OR.TP96(K3,K).LE.(0.0))GO TO 722
      R2=(TK2*TP96(K2,K))/(TK3*TP96(K3,K))
  722 IF(R1.EQ.(999.99).OR.R2.EQ.(999.99))GO TO 727
      IF(R1.EQ.R2)GO TO 727
      IF(R2.LT.(0.1))R2=0.1
      SL=VM(TK1,TK2,TK3,R1,R2)
      IF(SL.LT.0.0)GO TO 723
      SOL(11,K)=3600*0.96*SQRT(SL)
  723 D1=DIF(TK1,TK2,TK3,R1,R2,0.96)
      IF(D1.EQ.(999.99))GO TO 727
      SOL(12,K)=D1
```

```
      IF(TM96(K1,K).LE.(0.0))GO TO 724
      R3=TP96(K1,K)/TM96(K1,K)
      IF(R3.LE.(0.0))GO TO 724
      IF(R3.LT.(0.1))R3=0.1
      SOL(13,K)=VS(D1,R3,0.96)
724   IF(TM96(K2,K).LE.(0.0))GO TO 725
      R4=TP96(K2,K)/TM96(K2,K)
      IF(R4.LE.(0.0))GO TO 725
      IF(R4.LT.(0.1))R4=0.1
      SOL(14,K)=VS(D1,R4,0.96)
725   IF(TM96(K3,K).LE.(0.0))GO TO 726
      R5=TP96(K3,K)/TM96(K3,K)
      IF(R5.LE.(0.0))GO TO 726
      IF(R5.LT.(0.1))R5=0.1
      SOL(15,K)=VS(D1,R5,0.96)
726   IF(TPK1(K).EQ.(999.99))GO TO 727
      IF(TPK1(K).LE.(0.0))GO TO 727
      HVP=VP(0.96,D1,TPK1(K))
      IF(HVP.LT.0.0)GO TO 728
      SOL(16,K)=3600.*SQRT(HVP)/TPK1(K)
728   SOL(17,K)=TPK1(K)
727   CONTINUE
C     SOLUTIONS FOR HPVM,D,HPVP DOWNSTREAM AND HPVS @-1.20,+1.20 CM
      R1=999.99
      R2=999.99
      R3=999.99
      R4=999.99
      R5=999.99
      D1=999.99
      IF(TP120(K1,K).LE.(0.0).OR.TP120(K2,K).LE.(0.0))GO TO 731
      R1=(TK1*TP120(K1,K))/(TK2*TP120(K2,K))
731   IF(TP120(K2,K).LE.(0.0).OR.TP120(K3,K).LE.(0.0))GO TO 732
      R2=(TK2*TP120(K2,K))/(TK3*TP120(K3,K))
732   IF(R1.EQ.(999.99).OR.R2.EQ.(999.99))GO TO 737
      IF(R1.EQ.R2)GO TO 737
      IF(R2.LT.(0.1))R2=0.1
      SL=VM(TK1,TK2,TK3,R1,R2)
      IF(SL.LT.0.0)GO TO 733
      SOL(18,K)=3600.*1.20*SQRT(SL)
733   D1=DIF(TK1,TK2,TK3,R1,R2,1.20)
      IF(D1.EQ.(999.99))GO TO 737
      SOL(19,K)=D1
      IF(TM120(K1,K).LE.(0.0))GO TO 734
      R3=TP120(K1,K)/TM120(K1,K)
      IF(R3.LE.(0.0))GO TO 734
      IF(R3.LT.(0.1))R3=0.1
      SOL(20,K)=VS(D1,R3,1.20)
734   IF(TM120(K2,K).LE.(0.0))GO TO 735
      R4=TP120(K2,K)/TM120(K2,K)
      IF(R4.LE.(0.0))GO TO 735
```

```
      IF(R4.LT.(0.1))R4=0.1
      SOL(21,K)=VS(D1,R4,1.20)
735   IF(TM120(K3,K).LE.(0.0))GO TO 736
      R5=TP120(K3,K)/TM120(K3,K)
      IF(R5.LE.(0.0))GO TO 736
      IF(R5.LT.(0.1))R5=0.1
      SOL(22,K)=VS(D1,R5,1.20)
736   IF(TPK2(K).EQ.(999.99))GO TO 737
      IF(TPK2(K).LE.(0.0))GO TO 737
      HVP=VP(1.20,D1,TPK2(K))
      IF(HVP.LT.0.0)GO TO 738
      SOL(23,K)=3600.*SQRT(HVP)/TPK2(K)
738   SOL(24,K)=TPK2(K)
737   CONTINUE
C     SOLUTIONS FOR HPVM,D,HPVP DOWNSTREAM AND HPVS @-1.44,+1.44 CM
      R1=999.99
      R2=999.99
      R3=999.99
      R4=999.99
      R5=999.99
      D1=999.99
      IF(TP144(K1,K).LE.(0.0).OR.TP144(K2,K).LE.(0.0))GO TO 741
      R1=(TK1*TP144(K1,K))/(TK2*TP144(K2,K))
741   IF(TP144(K2,K).LE.(0.0).OR.TP144(K3,K).LE.(0.0))GO TO 742
      R2=(TK2*TP144(K2,K))/(TK3*TP144(K3,K))
742   IF(R1.EQ.(999.99).OR.R2.EQ.(999.99))GO TO 747
      IF(R1.EQ.R2)GO TO 747
      IF(R2.LT.(0.1))R2=0.1
      SL=VM(TK1,TK2,TK3,R1,R2)
      IF(SL.LT.0.0)GO TO 743
      SOL(25,K)=3600.*1.44*SQRT(SL)
743   D1=DIF(TK1,TK2,TK3,R1,R2,1.44)
      IF(D1.EQ.(999.99))GO TO 747
      SOL(26,K)=D1
      IF(TM144(K1,K).LE.(0.0))GO TO 744
      R3=TP144(K1,K)/TM144(K1,K)
      IF(R3.LE.(0.0))GO TO 744
      IF(R3.LT.(0.1))R3=0.1
      SOL(27,K)=VS(D1,R3,1.44)
744   IF(TM144(K2,K).LE.(0.0))GO TO 745
      R4=TP144(K2,K)/TM144(K2,K)
      IF(R4.LE.(0.0))GO TO 745
      IF(R4.LT.(0.1))R4=0.1
      SOL(28,K)=VS(D1,R4,1.44)
745   IF(TM144(K3,K).LE.(0.0))GO TO 746
      R5=TP144(K3,K)/TM144(K3,K)
      IF(R5.LE.(0.0))GO TO 746
      IF(R5.LT.(0.1))R5=0.1
      SOL(29,K)=VS(D1,R5,1.44)
746   IF(TPK3(K).EQ.(999.99))GO TO 747
```

```
      IF(TPK3(K).LE.(0.0))GO TO 747
      HVP=VP(1.44,D1,TPK3(K))
      IF(HVP.LT.0.0)GO TO 748
      SOL(30,K)=3600.*SQRT(HVP)/TPK3(K)
748   SOL(31,K)=TPK3(K)
747   CONTINUE
80    CONTINUE
C     ROUTINE TO PRINT NUMERICALLY DERIVED HEAT
C     PULSE VELOCITIES.  THIS ROUTINE CALLS VARIOUS
C     PRINT ROUTINES FOR TABLES OF DIFFUSIVITY,
C     HPVS, HPVA OR HPVL.
      DO 83 I=1,KWR
      WRITE(6,602)TK1,TK2,TK3,CBARK,CSWD,CHWD
      K1 = 17*(I-1)+1
      K2=17*I
      IF(K2.GT.KR)K2=KR
      CALL VPRT(K1,K2)
83    CONTINUE
      K1=K2+1
      IF(K1.GE.KR)GO TO 81
      WRITE(6,602)TK1,TK2,TK3,CBARK,CSWD,CHWD
      CALL VPRT(K1,KR)
81    CONTINUE
50    CONTINUE
500   FORMAT(6F10.6)
501   FORMAT(19I4)
502   FORMAT(5I4)
503   FORMAT(11I4)
504   FORMAT(10F5.1)
600   FORMAT(1H1,'AT TIME=',I7)
601     FORMAT('1')
602   FORMAT(1H1,'SOLUTIONS FOR HPVA, HPVS, HPVM, HPVP. ',
     1'HPVT, AND DIFFUSIVITY DOWNSTREAM AT',/,'TIMES:'
     2 ,'T1=',F4.0,2X,'T2=',F4.0,2X,'T3=',F4.0,/,
     3 'IMPOSED DIFFUSIVITIES ARE: D BARK=',F7.4,2X,
     4 'D SAPWOOD=',F7.4,2X,'D HEARTWOOD=',F7.4)
603   FORMAT(1H1,'HPVA AND HPVT AND HPVP')
604   FORMAT(1H1,'HPVS AND HPVM1 AND HPVP')
605   FORMAT(1H1,'HPV IMPOSED AT EACH DEPTH FOR THIS RUN')
606   FORMAT(1H ,'VIMP',4X,17F7.2)
607   FORMAT(1H ,'DEPTH',3X,17F7.2)
608   FORMAT(1H1,'PROBE INDEX MATRIX USED FOR THE NEXT ',I3,2X,'HPVI')
609   FORMAT(1H ,'IDX @',I3,17I7)
610   FORMAT(1H ,7X,'ITC',7X,'IHC',7X,'IBC',7X,'MPT',7X,'MPC')
611   FORMAT(10I10)
612   FORMAT(2X,I3,2X,6F12.6)
613   FORMAT(1H1,'PROBE COEFFICIENT VALUES AT INDEX POINT',
     1 ' NUMBERS')
614   FORMAT(1H ,'INDEX',6X,'CAM',9X,'CAP',9X,'CTM',9X,'CTP',9X,
     1'PC',10X,'MISC')
```

```
 615   FORMAT(1H0,'TOP SENSOR SPACING =',F5.2,'CM',3X,
      1'BOTTOM SENSOR SPACING =',F5.2,'CM',3X,'KR=',I4)
 616   FORMAT(1H0,'HPV VALUES AT SOLUTION NODES'
      1,/,'NODE',7X,'HPVI',/)
 617   FORMAT(I5,5X,F7.2)
 618   FORMAT(1H0,'IT1=',I3,3X,'IT2=',I3,3X,'IT3=',I3,3X,
      1'ITF=',I4,3X,'NH1=',I3,3X,'NH2=',I3,3X,'NH3=',I3,3X,'NH4=',I3
      2,3X,'NH5=',I3,3X,'NH6=',I3,3X,'NH7=',I3,3X,'NH8=',I3)
 619   FORMAT(1H ,'DT1=',F4.1,3X,'DT2=',F4.1,3X,'DT3=',
      1F4.1,3X,'DT4=',F4.1,3X,'HT=',F10.0,3X,'HPL=',F5.2)
 620   FORMAT(1H0,'K IDX',3X,17I7)
 800   FORMAT(1H ,'I=',I3,' K=',I3,' LC=',I3,' LL=',I3,' CAM=',
      1F10.4,' CAP=',F10.4,' CRM=',F10.4,' CRP=',F10.4,
      2' CV=',F10.4,' PC=',F10.4)
 621   FORMAT(1H0,'SOLUTION RAN FROM T=0 TO T= ',F6.2)
 622   FORMAT(1H0,'VARIABLE HPV NODE ASSIGNMENTS ARE',/,
      1'NP1=',I3,3X,'NP2=',I3,3X,'NP3=',I3,3X,/,
      2'NV1=',I3,3X,'NV2=',I3,3X,'NV3=',I3,3X,'NV4=',I3)
       STOP
       END
       SUBROUTINE VPRT(J1,J2)
C      THIS ROUTINE PRINTS OUT A TABLE OF SOLUTIONS FOR
C      HPVA, HPVT, HPVM, HPVS, HPVP AND DIFFUSIVITY AT
C      THE SEVERAL TIME AND SPACE INTERVALS FOR WHICH
C      TEMPERATURE DATA ARE AVAILABLE IN THIS VERSION
C      OF THE NUMERICAL MODEL
       DIMENSION DEPTH(101),SOL(31,101),VIMP(101)
       COMMON/NOSOL/DEPTH,SOL,VIMP
       WRITE(6,32) (K,K=J1,J2)
       WRITE(6,33) (DEPTH(K),K=J1,J2)
       WRITE(6,30) (VIMP(K),K=J1,J2)
       WRITE(6,34)
       WRITE(6,1) (SOL(1,K),K=J1,J2)
       WRITE(6,2) (SOL(2,K),K=J1,J2)
       WRITE(6,3) (SOL(3,K),K=J1,J2)
       WRITE(6,4) (SOL(4,K),K=J1,J2)
       WRITE(6,5) (SOL(5,K),K=J1,J2)
       WRITE(6,35)
       WRITE(6,1) (SOL(6,K),K=J1,J2)
       WRITE(6,2) (SOL(7,K),K=J1,J2)
       WRITE(6,3) (SOL(8,K),K=J1,J2)
       WRITE(6,4) (SOL(9,K),K=J1,J2)
       WRITE(6,5) (SOL(10,K),K=J1,J2)
       WRITE(6,36)
       WRITE(6,6) (SOL(11,K),K=J1,J2)
       WRITE(6,7) (SOL(12,K),K=J1,J2)
       WRITE(6,8) (SOL(13,K),K=J1,J2)
       WRITE(6,9) (SOL(14,K),K=J1,J2)
       WRITE(6,10) (SOL(15,K),K=J1,J2)
       WRITE(6,11) (SOL(16,K),K=J1,J2)
```

```
      WRITE(6,13)(SOL(17,K),K=J1,J2)
      WRITE(6,37)
      WRITE(6,6)(SOL(18,K),K=J1,J2)
      WRITE(6,7)(SOL(19,K),K=J1,J2)
      WRITE(6,8)(SOL(20,K),K=J1,J2)
      WRITE(6,9)(SOL(21,K),K=J1,J2)
      WRITE(6,10)(SOL(22,K),K=J1,J2)
      WRITE(6,11)(SOL(23,K),K=J1,J2)
      WRITE(6,13)(SOL(24,K),K=J1,J2)
      WRITE(6,38)
      WRITE(6,6)(SOL(25,K),K=J1,J2)
      WRITE(6,7)(SOL(26,K),K=J1,J2)
      WRITE(6,8)(SOL(27,K),K=J1,J2)
      WRITE(6,9)(SOL(28,K),K=J1,J2)
      WRITE(6,10)(SOL(29,K),K=J1,J2)
      WRITE(6,11)(SOL(30,K),K=J1,J2)
      WRITE(6,13)(SOL(31,K),K=J1,J2)
1     FORMAT(1H0,'HPVA T1/T2',17F7.2)
2     FORMAT(1H ,'HPVA T1/T3',17F7.2)
3     FORMAT(1H ,'HPVA T2/T3',17F7.2)
4     FORMAT(1H ,'HPVT        ',17F7.2)
5     FORMAT(1H ,'T ZERO      ',17F7.2)
6     FORMAT(1H0,'HPVM T1,2,3',17F7.2)
7     FORMAT(1H ,'DIF T1,2,3 ',17F7.4)
8     FORMAT(1H ,'HPVS T1     ',17F7.2)
9     FORMAT(1H ,'HPVS T2     ',17F7.2)
10    FORMAT(1H ,'HPVS T3     ',17F7.2)
11    FORMAT(1H0,'HPVP        ',17F7.2)
13    FORMAT(1H ,'T MAX+      ',17F7.2)
30    FORMAT(1H0,'IMPOSED HPV',17F7.2)
33      FORMAT(1H0,'DEPTH',5X,17F7.2)
34    FORMAT(1H0,'ASYMMETRIC SOLUTIONS AT (-.48,0,+.96 CM)')
35    FORMAT(1H0,'ASYMMETRIC SOLUTIONS AT (-.96,0,+1.44 CM)')
36    FORMAT(1H0,'SYMMETRIC SOLUTIONS AT (-.96,0,+.96 CM)')
37    FORMAT(1H0,'SYMMETRIC SOLUTIONS AT (-1.20,0,+1.20 CM)')
38    FORMAT(1H0,'SYMMETRIC SOLUTIONS AT (-1.44,0,+1.44 CM)')
32    FORMAT(1H ,'K IDX',3X,17I7)
      RETURN
      END
      SUBROUTINE DPRT(J1,J2,J3)
C     THIS ROUTINE PRINTS OUT TEMPERATURE MATRIX
C     VALUES AT TIMES CALLED FOR BY MAIN PROGRAM
      DIMENSION TM48(10,101),TM96(10,101),TM120(10,101),
     1TM144(10,101),TP96(10,101),TP120(10,101),TP144(10,101),
     2DEPTH(101),TH(10,101),TZ1(101),TZ2(101),SOL(31,101),
     3TPK1(101),TPK2(101),TPK3(101),VIMP(101)
      COMMON/NOSOL/DEPTH,SOL,VIMP
      COMMON/REA4/TM48,TM96,TM120,TM144,TH,TP96,
     1 TP120,TP144,TZ1,TZ2,TPK1,TPK2,TPK3
      WRITE(6,620)(K,K=J1,J2)
```

```
      WRITE(6,500) (DEPTH(K),K=J1,J2)
      WRITE(6,501) (TP144(J3,K),K=J1,J2)
      WRITE(6,502) (TP120(J3,K),K=J1,J2)
      WRITE(6,503) (TP96(J3,K),K=J1,J2)
      WRITE(6,505) (TH(J3,K),K=J1,J2)
      WRITE(6,506) (TM48(J3,K),K=J1,J2)
      WRITE(6,507) (TM96(J3,K),K=J1,J2)
      WRITE(6,508) (TM120(J3,K),K=J1,J2)
      WRITE(6,509) (TM144(J3,K),K=J1,J2)
500   FORMAT(1H ,'DEPTH',6X,17F7.2)
501   FORMAT(1H ,'TP144',5X,17F7.1)
505   FORMAT(1H ,'THTR',6X,17F7.0)
502   FORMAT(1H ,'TP120',5X,17F7.1)
503   FORMAT(1H ,'TP096',5X,17F7.1)
506   FORMAT(1H ,'TM048',5X,17F7.1)
507   FORMAT(1H ,'TM096',5X,17F7.1)
508   FORMAT(1H ,'TM120',5X,17F7.1)
509   FORMAT(1H ,'TM144',5X,17F7.1)
620   FORMAT(1H0,'K IDX',3X,17I7)
      RETURN
      END


C     THIS PROGRAM, RLM+SOLVER, PRODUCES A FINITE DIFFERENCE
C     NUMERICAL SOLUTION IN THE LONGITUDINAL RADIAL PLANE
C     TO MARSHALL'S(1958) PARTIAL DIFFERENTIAL EQUATION
C     FOR HEAT TRANSPORT BY COUPLED CONDUCTION THROUGH
C     WOOD SUBSTANCE AND CONVECTION BY THE MOVING SAP.
C     PROBE THERMAL COEFFICIENTS AS WELL AS THOSE AT
C     VARIOUS EARLYWOOD/SAPWOOD OR LATEWOOD/HEARTWOOD
C     COMBINATIONS ARE CONTAINED IN MTS LINE FILE COEF.
C     AN INDEX TO WHICH COEFFICIENT IS TO BE USED AT EACH
C     NODE IS CONTAINED IN MTS LINE FILE PID(N).
C     CURRENT RUN PARAMETERS, I.E. WOOD MOISTURE, WOOD
C     DENSITY, SENSOR LOCATION, AND HPV'S TO RUN ARE
C     CONTAINED IN MTS LINE FILE RPAR(N).
C     FUNCTIONS ARE DEFINED BELOW TO SOLVE FOR HPVM,DIFFUSIVITY
C     HPVS, HPVA AND HPVP AT VARIOUS COMBINATIONS OF TIMES
C     FROM AMONG 15,20,30,40,45,60,80,90,120 AND 180 SECONDS,
C     AND AT VARIOUS SPACES RANGING FROM -1.20,-.96, .48 TO
C     +.96, +1.20, AND TO +1.44 CM.
      VM(TM1,TM2,TM3,R1,R2)=(TM1*ALOG(R1) -TM3*ALOG(R2))
     1 /(TM1*TM2*TM3*(ALOG(R1/R2)))
      DIF(TM1,TM2,TM3,R1,R2,XU)=(XU*XU*(-.5*(TM2-TM1)**2))
     1 /(TM1*TM2*TM3*(ALOG(R1/R2)))
      VS(DF,R3,XU)=3600.*(DF*ALOG(R3))/XU
      VA(XT,XB,TM1,TM2,S1,S2)=(XT+XB)*(TM1*ALOG(S1)
     1 -TM2*ALOG(S2))/(2.*TM1*TM2*(ALOG(S1/S2)))
      VP(XU,DF,TVP)=(XU*XU-2.*DF*TVP)
```

```
      SUBROUTINE SOLVER
      INTEGER LC(201),IPRB(19,101)
      INTEGER NT,IMAX,IMAX1,IMAX2,KR,KRM,KRP
      INTEGER IPRT,IT1,IT2,IT3,ITF,IT
      REAL A(201),B(201),C(201),D(201),G(201),BB(201)
      REAL SNA(201,101),SNR(201,101),T96(101),T120(101),T144(101)
      REAL TH(10,101),TM48(10,101),TM96(10,101),
     1TM120(10,101),TM144(10,101),TP96(10,101),TP120(10,101),
     2TP144(10,101),TZ1(101),TZ2(101),TPK1(101),TPK2(101),
     3TPK3(101)
      REAL CPRB1(200),CPRB2(200),CPRB3(200),CPRB4(200),CPRB5(200),
     X        CPRB6(200)
      COMMON /INT1/LC,IPRB
      COMMON /INT2/ IMAX,IMAX1,IMAX2,KR,KRM,KRP
      COMMON /INT3/ IT1,IT2,IT3,ITF,IT,ITC,IBC,IHC
      COMMON /INT4/ NH1,NH2,NH3,NH4,NH5,NH6,NH7,NH8
      COMMON /REA1/ SNA,SNR
      COMMON /REA2/ CPRB1,CPRB2,CPRB3,CPRB4,CPRB5,CPRB6
      COMMON /REA3/TIME,DT,HT,HHPL,HPL,DT1,DT2,DT3,DT4
      COMMON/REA4/TM48,TM96,TM120,TM144,TH,TP96,
     1 TP120,TP144,TZ1,TZ2,TPK1,TPK2,TPK3
C     IMPLICIT RADIAL FOLLOWED BY AXIAL BACKWARD DIFFERENCE
C     EQUATIONS.  MODIFIED THOMAS ALGORITHM AT SYMETRICAL
C     BORDER, WHICH IS CONSIDERED TO BE CENTRE OF TREE.
      DO 40 K=1,KR
      T96(K) = 0.0
      T120(K)=0.0
 40   T144(K) = 0.0
      ITZ=0
 41   TIME = TIME + DT
C     THIS IS START OF FIRST HALF STEP (IMPLICIT RADIAL).
      A(1)=0.0
      HTV = HT/(TIME**10.)
      IF(TIME.LE.HHPL)HTV=HT*TIME/HHPL
      IF(TIME.GT.HHPL.AND.TIME.LE.HPL)HTV=HT
      DO 170 I=2,IMAX1
      DO 160 KK=1,KRM
      K=KRP-KK
      KP1=K+1
      LL=IPRB(LC(I),K)
      LV=IPRB(1,K)
      CAM=CPRB1(LL)
      CAP=CPRB2(LL)
      CRM=CPRB3(LL)
      CRP=CPRB4(LL)
      CA=CAM+CAP
      CR=CRM+CRP
      PC=CPRB5(LL)
      CV=CPRB6(LV)*PC
      PC=PC/DT
```

```
      HTVS=0.0
      IF(LL.LE.2)GO TO 154
      IF(LL.EQ.NH1.OR.LL.EQ.NH2.OR.LL.EQ.NH3.OR.LL.EQ.NH4)HTVS=HTV
      IF(LL.EQ.NH5.OR.LL.EQ.NH6.OR.LL.EQ.NH7.OR.LL.EQ.NH8)HTVS=HTV
154   A(K) = -CRM
      B(K) = CR + PC
      C(K) = -CRP
      D(K) = (CV + CAM)*SNA(I-1,K) + (PC - CA)*
     1SNA(I,K) + (CAP -CV)*SNA(I+1,K) + HTVS
      IF(KRM-K)155,156,157
155   BB(KR)=B(KR)
      G(KR)=D(KR)
      GO TO 160
156   BB(K)=B(K)-2.0*A(KP1)*C(K)/BB(KP1)
      G(K)=D(K)-C(K)*G(KP1)/BB(KP1)
      GO TO 160
157   CB=C(K)/BB(KP1)
      BB(K)=B(K)-A(KP1)*CB
158   G(K)=D(K)-G(KP1)*CB
160   CONTINUE
      DO 171 K=2,KRM
171   SNR(I,K)=(G(K) - A(K)*SNR(I,K-1))/BB(K)
170   SNR(I,KR)=(G(KR)-2.0*A(KR)*SNR(I,KRM))/BB(KR)
C     END OF FIRST HALF-TIME STEP
C     START SECOND HALF-TIME STEP (IMPLICIT AXIAL)
      TIME = TIME + DT
      A(2) = 0.0
      C(IMAX1) = 0.0
      DO 270 K=2,KR
      KP1 = K+1
      IF(K.EQ.KR)KP1=K-1
      DO 260 I=2,IMAX1
      IM1=I-1
      LL=IPRB(LC(I),K)
      LV=IPRB(1,K)
      CAM=CPRB1(LL)
      CAP=CPRB2(LL)
      CRM=CPRB3(LL)
      CRP=CPRB4(LL)
      CA=CAM+CAP
      CR=CRM+CRP
      PC=CPRB5(LL)
      CV=CPRB6(LV)*PC
      PC=PC/DT
      HTVS=0.0
      IF(LL.LE.2)GO TO 254
      IF(LL.EQ.NH1.OR.LL.EQ.NH2.OR.LL.EQ.NH3.OR.LL.EQ.NH4)HTVS=HTV
      IF(LL.EQ.NH5.OR.LL.EQ.NH6.OR.LL.EQ.NH7.OR.LL.EQ.NH8)HTVS=HTV
254   A(I) = -CV - CAM
      B(I) = PC + CA
```

```
      C(I) = CV - CAP
      D(I) = CRM*SNR(I,K-1) + (PC - CR)*SNR(I,K)
     1+CRP*SNR(I,KP1) + HTVS
      IF(I.EQ.2)GO TO 280
      GO TO 257
280   BB(2)=B(2)
      G(2)=D(2)
      GO TO 260
257   CB=A(I)/BB(IM1)
      BB(I)=B(I)-C(IM1)*CB
      G(I)=D(I)-G(IM1)*CB
260   CONTINUE
      DO 270 II=1,IMAX2
      I = IMAX-II
270   SNA(I,K) = (G(I) - C(I)*SNA(I+1,K))/BB(I)
C     END OF SECOND HALF-TIME STEP
      IT=TIME +0.05
      IF(TIME.LE.10.0) GO TO 95
      DO 500 K=2,KR
      IF(T96(K).LT.SNA(125,K))GO TO 501
      IF(TPK1(K).EQ.(999.99))TPK1(K)=TIME
501   IF(T120(K).LT.SNA(131,K))GO TO 502
      IF(TPK2(K).EQ.(999.99))TPK2(K)=TIME
502   IF(T144(K).LT.SNA(137,K))GO TO 503
      IF(TPK3(K).EQ.(999.99))TPK3(K)=TIME
503   IF(SNA(125,K).LT.SNA(89,K))GO TO 504
      IF(TZ1(K).EQ.(999.99))TZ1(K)=TIME
504   IF(SNA(137,K).LT.SNA(77,K))GO TO 505
      IF(TZ2(K).EQ.(999.99))TZ2(K)=TIME
505   T96(K)=SNA(125,K)
      T120(K)=SNA(131,K)
      T144(K)=SNA(137,K)
500   CONTINUE
      IF(IT.EQ.15.OR.IT.EQ.20.OR.IT.EQ.30)GO TO 90
      IF(IT.EQ.40.OR.IT.EQ.45.OR.IT.EQ.80.OR.IT.EQ.90)GO TO 90
      IF(IT.EQ.60.OR.IT.EQ.120.OR.IT.EQ.180)GO TO 90
      GO TO 95
90    IF(IT.EQ.15)II=1
      IF(IT.EQ.20)II=2
      IF(IT.EQ.30)II=3
      IF(IT.EQ.40)II=4
      IF(IT.EQ.45)II=5
      IF(IT.EQ.60)II=6
      IF(IT.EQ.80)II=7
      IF(IT.EQ.90)II=8
      IF(IT.EQ.120)II=9
      IF(IT.EQ.180)II=10
      DO 91 K=1,KR
      TH(II,K)=SNA(101,K)
      TM48(II,K)=SNA(89,K)
```

```
      TM96(II,K)=SNA(77,K)
      TM120(II,K)=SNA(71,K)
      TM144(II,K)=SNA(65,K)
      TP96(II,K)=SNA(125,K)
      TP120(II,K)=SNA(131,K)
      TP144(II,K)=SNA(137,K)
91    CONTINUE
95    IF(IT.GE.IT1.AND.IT.LT.IT2)DT=DT2
      IF(IT.GE.IT2.AND.IT.LT.IT3)DT=DT3
      IF(IT.GE.IT3)DT=DT4
      IF(ITZ.EQ.1)GO TO 405
      DO 404 K=2,KR
      IF(TZ1(K).EQ.(999.99)) GO TO 406
      IF(TZ2(K).EQ.(999.99)) GO TO 406
      IF(TPK1(K).EQ.(999.99)) GO TO 406
      IF(TPK2(K).EQ.(999.99)) GO TO 406
      IF(TPK3(K).EQ.(999.99)) GO TO 406
404   CONTINUE
      ITZ=1
405   IF(IT.GE.180)GO TO 300
406   IF(IT.LT.ITF)GO TO 41
 300  CONTINUE
      RETURN
      END
```

Node coefficient file CPRB

INDEX	CAM	CAP	CTM	CTP	PC
1	0.000956	0.000956	0.000727	0.000727	0.532000
2	0.000795	0.000795	0.000490	0.000490	0.332000
3	0.030000	0.030000	0.030000	0.030000	0.594700
4	0.250000	0.250000	0.250000	0.250000	0.765000
5	0.030000	0.000956	0.015364	0.015364	0.563350
6	0.250000	0.000956	0.125364	0.125364	0.648499
7	0.030000	0.000795	0.015245	0.015245	0.463350
8	0.250000	0.000795	0.125245	0.125245	0.548500
9	0.000956	0.030000	0.015364	0.015364	0.563350
10	0.000956	0.250000	0.125364	0.125364	0.648499
11	0.000795	0.030000	0.015245	0.015245	0.463350
12	0.000795	0.250000	0.125245	0.125245	0.548500
13	0.015478	0.000956	0.015364	0.000727	0.547675
14	0.125478	0.000956	0.125364	0.000727	0.590250
15	0.015397	0.000795	0.015245	0.000490	0.397675
16	0.125397	0.000795	0.125245	0.000490	0.440250
17	0.000956	0.015478	0.015364	0.000727	0.547675
18	0.000956	0.125478	0.125364	0.000727	0.590250
19	0.000795	0.015397	0.015245	0.000490	0.397675
20	0.000795	0.125397	0.125245	0.000490	0.440250
21	0.030000	0.015478	0.030000	0.015364	0.579025
22	0.250000	0.125478	0.250000	0.125364	0.706750
23	0.030000	0.015397	0.030000	0.015245	0.529025
24	0.250000	0.125397	0.250000	0.125245	0.656750
25	0.015478	0.030000	0.030000	0.015364	0.579025
26	0.125478	0.250000	0.250000	0.125364	0.706750
27	0.015397	0.030000	0.030000	0.015245	0.529025
28	0.125397	0.250000	0.250000	0.125245	0.656750
29	0.015478	0.015478	0.030000	0.000727	0.563350
30	0.125478	0.125478	0.250000	0.000727	0.648499
31	0.015397	0.015397	0.030000	0.000490	0.463350
32	0.125397	0.125397	0.250000	0.000490	0.548500
33	0.030000	0.000876	0.015364	0.015245	0.513350
34	0.250000	0.000876	0.125364	0.125245	0.598500
35	0.000876	0.030000	0.015364	0.015245	0.513350
36	0.000876	0.250000	0.125364	0.125245	0.598500
37	0.000876	0.000876	0.000727	0.000490	0.432000
38	0.000876	0.000876	0.000490	0.000727	0.432000
39	0.000579	0.000579	0.000202	0.000727	0.332000
40	0.000956	0.000956	0.000727	0.000727	0.532000
41	0.000956	0.000956	0.000727	0.000727	0.532000
42	0.125478	0.000956	0.000727	0.125364	0.590250
43	0.015478	0.000956	0.000727	0.015364	0.547675
44	0.250000	0.125478	0.125364	0.250000	0.706750
45	0.030000	0.015478	0.015364	0.030000	0.579025
46	0.000956	0.125478	0.000727	0.125364	0.590250
47	0.000956	0.015478	0.000727	0.015364	0.547675
48	0.125478	0.250000	0.125364	0.250000	0.706750
49	0.015478	0.030000	0.015364	0.030000	0.579025
50	0.000956	0.000956	0.000727	0.000727	0.532000

File CPRB continued

INDEX	CAM	CAP	CTM	CTP	PC
51	0.000956	0.000956	0.000727	0.000727	0.532000
52	0.125478	0.125478	0.000727	0.250000	0.648499
53	0.015478	0.015478	0.000727	0.030000	0.563350
54	0.250000	0.000579	0.125101	0.125364	0.548500
55	0.030000	0.000579	0.015101	0.015364	0.463350
56	0.000579	0.250000	0.125101	0.125364	0.548500
57	0.000579	0.030000	0.015101	0.015364	0.463350
58	0.000956	0.000956	0.0	0.001455	0.532000
59	0.000956	0.000956	0.000727	0.000727	0.532000
60	0.000956	0.250000	0.125364	0.125364	0.648499
61	0.015101	0.000202	0.000202	0.015101	0.247675
62	0.125101	0.000202	0.000202	0.125101	0.290250
63	0.000202	0.015101	0.000202	0.015101	0.247675
64	0.000202	0.125101	0.000202	0.125101	0.290250
65	0.015101	0.015101	0.000202	0.030000	0.363350
66	0.125101	0.125101	0.000202	0.250000	0.448500
67	0.000202	0.000202	0.000202	0.000202	0.132000
68	0.250000	0.000202	0.125101	0.125101	0.448500
69	0.030000	0.000202	0.015101	0.015101	0.363350
70	0.000202	0.250000	0.125101	0.125101	0.448500
71	0.000202	0.030000	0.015101	0.015101	0.363350
72	0.250000	0.000202	0.000101	0.250101	0.448500
73	0.250000	0.250000	0.0	0.500000	0.765000
74	0.000202	0.250000	0.000101	0.250101	0.448500
75	0.015397	0.000876	0.015364	0.000490	0.447675
76	0.000876	0.015397	0.015364	0.000490	0.447675
77	0.030000	0.000876	0.015245	0.015364	0.513350
78	0.250000	0.000876	0.125245	0.125364	0.598500
79	0.000876	0.030000	0.015245	0.015364	0.513350
80	0.000876	0.250000	0.125245	0.125364	0.598500
81	0.015478	0.000876	0.015245	0.000727	0.497675
82	0.125478	0.000876	0.000245	0.000727	0.540250
83	0.000876	0.015478	0.015245	0.000727	0.497675
84	0.000876	0.125478	0.125245	0.000727	0.540250
85	0.000202	0.030000	0.000101	0.030101	0.363350
86	0.030000	0.030000	0.0	0.060000	0.594700
87	0.030000	0.000202	0.000101	0.030101	0.363350
88	0.000202	0.000202	0.0	0.000404	0.132000
89	0.000202	0.000202	0.000202	0.000202	0.132000
90	0.000579	0.000579	0.000202	0.000727	0.332000
91	0.000876	0.000876	0.000727	0.000490	0.432000
92	0.000795	0.000795	0.000490	0.000490	0.332000
93	0.030000	0.000956	0.000364	0.030364	0.563350

File IPRB, tangential-longitudinal model with sensor materials

K IDX	1	2	3	4	5	6	7	8	9	10	11
DEPTH, cm	0.0	0.04	0.08	0.12	0.16	0.20	0.24	0.28	0.32	0.36	0.40
IDX @ 19	1	1	1	1	1	1	1	1	1	1	1
IDX @ 18	1	1	1	1	1	1	1	1	1	1	1
IDX @ 17	1	1	1	1	1	1	1	1	1	1	1
IDX @ 16	1	1	1	1	1	1	1	1	1	1	1
IDX @ 15	1	1	1	1	1	1	1	1	1	1	1
IDX @ 14	1	1	1	1	1	1	1	1	1	1	1
IDX @ 13	1	1	1	1	1	1	1	1	1	1	1
IDX @ 12	1	1	1	1	1	1	1	1	1	1	1
IDX @ 11	1	1	1	1	1	1	1	1	1	1	1
IDX @ 10	1	1	1	1	1	1	1	1	1	1	1
IDX @ 9	1	1	1	1	1	1	1	1	1	1	1
IDX @ 8	1	1	1	1	1	1	1	1	1	1	1
IDX @ 7	1	1	1	1	1	1	1	1	1	1	1
IDX @ 6	1	1	1	1	1	1	1	1	1	1	1
IDX @ 5	1	1	1	1	1	1	1	1	1	1	1
IDX @ 4	1	1	1	1	1	1	1	1	1	1	1
IDX @ 3	1	1	1	1	1	1	1	1	1	1	1
IDX @ 2	1	1	1	1	1	1	1	1	1	1	1
IDX @ 1	1	1	1	1	1	1	1	1	1	1	1

K IDX	12	13	14	15	16	17	18	19	20	21	22
DEPTH, cm	0.44	0.48	0.52	0.56	0.60	0.64	0.68	0.72	0.76	0.80	0.84
IDX @ 19	1	1	1	1	1	1	1	1	1	1	1
IDX @ 18	1	1	1	1	1	1	1	1	1	1	1
IDX @ 17	1	1	1	1	1	1	1	1	1	1	1
IDX @ 16	1	1	1	1	1	1	1	1	1	1	1
IDX @ 15	1	1	1	1	1	1	1	1	1	1	1
IDX @ 14	1	1	1	1	1	1	1	1	1	1	1
IDX @ 13	1	1	1	1	1	1	1	1	1	1	1
IDX @ 12	1	1	1	1	1	1	1	1	1	1	1
IDX @ 11	1	1	1	1	1	1	1	1	1	1	1
IDX @ 10	1	1	1	1	1	1	1	1	1	1	1
IDX @ 9	1	1	1	1	1	1	1	1	1	1	1
IDX @ 8	1	1	1	1	1	1	1	1	1	1	1
IDX @ 7	1	1	1	1	1	1	1	1	1	1	1
IDX @ 6	1	1	1	1	1	1	1	1	1	1	1
IDX @ 5	1	1	1	1	1	1	1	1	1	1	1
IDX @ 4	1	1	1	1	1	1	1	1	1	1	1
IDX @ 3	1	1	1	1	1	1	1	1	1	1	1
IDX @ 2	1	1	1	1	1	1	1	1	1	1	1
IDX @ 1	1	1	1	1	1	1	1	1	1	1	1

File IPRB continued

K IDX	23	24	25	26	27	28	29	30	31	32	33
DEPTH, cm	0.88	0.92	0.96	1.00	1.04	1.08	1.12	1.16	1.20	1.24	1.28
IDX @ 19	1	1	1	1	1	1	1	1	1	1	1
IDX @ 18	1	1	1	1	1	1	1	1	1	1	1
IDX @ 17	1	1	1	1	1	1	1	1	1	1	1
IDX @ 16	1	1	1	1	1	1	1	1	1	1	1
IDX @ 15	1	1	1	1	1	1	1	1	1	1	1
IDX @ 14	1	1	1	1	1	1	1	1	1	1	1
IDX @ 13	1	1	1	1	1	1	1	1	1	1	1
IDX @ 12	1	1	1	1	1	1	1	1	1	1	1
IDX @ 11	1	1	1	1	1	1	1	1	1	1	1
IDX @ 10	1	1	1	1	1	1	1	1	1	1	1
IDX @ 9	1	1	1	1	1	1	1	1	1	1	1
IDX @ 8	1	1	1	1	1	1	1	1	1	1	1
IDX @ 7	1	1	1	1	1	1	1	1	1	1	1
IDX @ 6	1	1	1	1	1	1	1	1	1	1	1
IDX @ 5	1	1	1	1	1	1	1	1	1	1	1
IDX @ 4	1	1	1	1	1	1	1	1	1	1	1
IDX @ 3	1	1	1	1	1	1	1	1	1	1	1
IDX @ 2	1	1	1	1	1	1	1	1	1	1	1
IDX @ 1	1	1	1	1	1	1	1	1	1	1	1

K IDX	34	35	36	37	38	39	40	41
DEPTH, cm	1.32	1.36	1.40	1.44	1.48	1.52	1.56	1.60
IDX @ 19	1	1	1	1	51	50	50	50
IDX @ 18	1	1	1	1	51	50	50	50
IDX @ 17	1	1	1	1	51	50	42	6
IDX @ 16	1	1	1	1	51	42	44	4
IDX @ 15	1	1	1	1	51	52	4	4
IDX @ 14	1	1	1	1	51	46	48	4
IDX @ 13	1	1	1	1	51	50	46	10
IDX @ 12	1	1	1	1	51	50	50	50
IDX @ 11	1	1	1	1	51	50	50	50
IDX @ 10	1	1	1	1	51	50	50	50
IDX @ 9	1	1	1	1	51	50	50	50
IDX @ 8	1	1	1	1	51	50	43	5
IDX @ 7	1	1	1	1	51	43	45	3
IDX @ 6	1	1	1	1	51	53	3	3
IDX @ 5	1	1	1	1	51	47	49	3
IDX @ 4	1	1	1	1	51	50	47	9
IDX @ 3	1	1	1	1	51	50	50	50
IDX @ 2	1	1	1	1	51	50	50	50
IDX @ 1	1	1	1	1	51	50	50	50

File IPRB, radial-longitudinal model without sensor materials

K IDX	1	2	3	4	5	6	7	8	9	10	11
DEPTH, cm	0.0	0.04	0.08	0.12	0.16	0.20	0.24	0.28	0.32	0.36	0.40
IDX @ 19	1	93	1	1	1	1	1	1	1	1	1
IDX @ 18	1	93	1	1	1	1	1	1	1	1	1
IDX @ 17	1	93	1	1	1	1	1	1	1	1	1
IDX @ 16	1	93	1	1	1	1	1	1	1	1	1
IDX @ 15	59	73	59	59	59	59	59	59	59	59	59
IDX @ 14	1	93	1	1	1	1	1	1	1	1	1
IDX @ 13	1	93	1	1	1	1	1	1	1	1	1
IDX @ 12	1	93	1	1	1	1	1	1	1	1	1
IDX @ 11	1	93	1	1	1	1	1	1	1	1	1
IDX @ 10	1	93	1	1	1	1	1	1	1	1	1
IDX @ 9	1	93	1	1	1	1	1	1	1	1	1
IDX @ 8	1	93	1	1	1	1	1	1	1	1	1
IDX @ 7	1	93	1	1	1	1	1	1	1	1	1
IDX @ 6	1	93	1	1	1	1	1	1	1	1	1
IDX @ 5	1	93	1	1	1	1	1	1	1	1	1
IDX @ 4	1	93	1	1	1	1	1	1	1	1	1
IDX @ 3	1	93	1	1	1	1	1	1	1	1	1
IDX @ 2	1	93	1	1	1	1	1	1	1	1	1
IDX @ 1	1	93	1	1	1	1	1	1	1	1	1

K IDX	12	13	14	15	16	17	18	19	20	21	22
DEPTH, cm	0.44	0.48	0.52	0.56	0.60	0.64	0.68	0.72	0.76	0.80	0.84
IDX @ 19	1	1	1	1	1	1	1	1	1	1	1
IDX @ 18	1	1	1	1	1	1	1	1	1	1	1
IDX @ 17	1	1	1	1	1	1	1	1	1	1	1
IDX @ 16	1	1	1	1	1	1	1	1	1	1	1
IDX @ 15	59	59	59	59	59	59	59	59	59	59	59
IDX @ 14	1	1	1	1	1	1	1	1	1	1	1
IDX @ 13	1	1	1	1	1	1	1	1	1	1	1
IDX @ 12	1	1	1	1	1	1	1	1	1	1	1
IDX @ 11	1	1	1	1	1	1	1	1	1	1	1
IDX @ 10	1	1	1	1	1	1	1	1	1	1	1
IDX @ 9	1	1	1	1	1	1	1	1	1	1	1
IDX @ 8	1	1	1	1	1	1	1	1	1	1	1
IDX @ 7	1	1	1	1	1	1	1	1	1	1	1
IDX @ 6	1	1	1	1	1	1	1	1	1	1	1
IDX @ 5	1	1	1	1	1	1	1	1	1	1	1
IDX @ 4	1	1	1	1	1	1	1	1	1	1	1
IDX @ 3	1	1	1	1	1	1	1	1	1	1	1
IDX @ 2	1	1	1	1	1	1	1	1	1	1	1
IDX @ 1	1	1	1	1	1	1	1	1	1	1	1

File IPRB continued

K IDX	23	24	25	26	27	28	29	30	31	32	33
DEPTH, cm	0.88	0.92	0.96	1.00	1.04	1.08	1.12	1.16	1.20	1.24	1.28
IDX @ 19	1	1	1	37	2	2	2	2	2	2	2
IDX @ 18	1	1	1	37	2	2	2	2	2	2	2
IDX @ 17	1	1	1	37	2	2	2	2	2	2	2
IDX @ 16	1	1	1	37	2	2	2	2	2	2	2
IDX @ 15	59	59	59	91	92	92	92	92	92	92	92
IDX @ 14	1	1	1	37	2	2	2	2	2	2	2
IDX @ 13	1	1	1	37	2	2	2	2	2	2	2
IDX @ 12	1	1	1	37	2	2	2	2	2	2	2
IDX @ 11	1	1	1	37	2	2	2	2	2	2	2
IDX @ 10	1	1	1	37	2	2	2	2	2	2	2
IDX @ 9	1	1	1	37	2	2	2	2	2	2	2
IDX @ 8	1	1	1	37	2	2	2	2	2	2	2
IDX @ 7	1	1	1	37	2	2	2	2	2	2	2
IDX @ 6	1	1	1	37	2	2	2	2	2	2	2
IDX @ 5	1	1	1	37	2	2	2	2	2	2	2
IDX @ 4	1	1	1	37	2	2	2	2	2	2	2
IDX @ 3	1	1	1	37	2	2	2	2	2	2	2
IDX @ 2	1	1	1	37	2	2	2	2	2	2	2
IDX @ 1	1	1	1	37	2	2	2	2	2	2	2

K IDX	34	35	36	37	38	39	40	41
DEPTH, cm	1.32	1.36	1.40	1.44	1.48	1.52	1.56	1.60
IDX @ 19	2	2	2	2	2	2	2	2
IDX @ 18	2	2	2	2	2	2	2	2
IDX @ 17	2	2	2	2	2	2	2	2
IDX @ 16	2	2	2	2	2	2	2	2
IDX @ 15	92	92	92	92	92	92	92	92
IDX @ 14	2	2	2	2	2	2	2	2
IDX @ 13	2	2	2	2	2	2	2	2
IDX @ 12	2	2	2	2	2	2	2	2
IDX @ 11	2	2	2	2	2	2	2	2
IDX @ 10	2	2	2	2	2	2	2	2
IDX @ 9	2	2	2	2	2	2	2	2
IDX @ 8	2	2	2	2	2	2	2	2
IDX @ 7	2	2	2	2	2	2	2	2
IDX @ 6	2	2	2	2	2	2	2	2
IDX @ 5	2	2	2	2	2	2	2	2
IDX @ 4	2	2	2	2	2	2	2	2
IDX @ 3	2	2	2	2	2	2	2	2
IDX @ 2	2	2	2	2	2	2	2	2
IDX @ 1	2	2	2	2	2	2	2	2

HPV imposed at each depth for TLM run

K IDX	1	2	3	4	5	6	7	8	9	10	11
DEPTH, cm	0.0	0.04	0.08	0.12	0.16	0.20	0.24	0.28	0.32	0.36	0.40
HPVI	20.0	20.0	20.0	20.0	20.0	20.0	20.0	20.0	20.0	20.0	20.0

K IDX	12	13	14	15	16	17	18	19	20	21	22
DEPTH, cm	0.44	0.48	0.52	0.56	0.60	0.64	0.68	0.72	0.76	0.80	0.84
HPVI	20.0	20.0	20.0	20.0	20.0	20.0	20.0	20.0	20.0	20.0	20.0

K IDX	23	24	25	26	27	28	29	30	31	32	33
DEPTH, cm	0.88	0.92	0.96	1.00	1.04	1.08	1.12	1.16	1.20	1.24	1.28
HPVI	20.0	20.0	20.0	20.0	20.0	20.0	20.0	20.0	20.0	20.0	20.0

K IDX	34	35	36	37	38	39	40	41
DEPTH, cm	1.32	1.36	1.40	1.44	1.48	1.52	1.56	1.60
HPVI	20.0	20.0	20.0	20.0	10.0	0.0	0.0	0.0

Numerically derived temperature matrix at t=60 s.

K IDX	1	2	3	4	5	6	7	8	9	10	11
DEPTH	0.0	0.04	0.08	0.12	0.16	0.20	0.24	0.28	0.32	0.36	0.40
TP144	0.0	0.0	0.0	0.1	0.1	0.1	0.2	0.2	0.3	0.4	0.5
TP120	0.0	0.0	0.1	0.2	0.2	0.3	0.5	0.7	0.9	1.2	1.6
TP096	0.0	0.1	0.2	0.4	0.6	0.8	1.2	1.6	2.2	3.0	4.0
THTR	0	0	1	1	1	2	3	4	5	7	9
TM048	0.0	0.1	0.2	0.3	0.4	0.6	0.8	1.1	1.6	2.1	2.9
TM096	0.0	0.0	0.0	0.0	0.0	0.1	0.1	0.1	0.2	0.2	0.3
TM120	0.0	0.0	0.0	0.0	0.0	0.0	0.0	0.0	0.0	0.0	0.1
TM144	0.0	0.0	0.0	0.0	0.0	0.0	0.0	0.0	0.0	0.0	0.0

K IDX	12	13	14	15	16	17	18	19	20	21	22
DEPTH	0.44	0.48	0.52	0.56	0.60	0.64	0.68	0.72	0.76	0.80	0.84
TP144	0.7	0.9	1.2	1.5	1.9	2.4	3.0	3.7	4.5	5.4	6.5
TP120	2.2	2.8	3.7	4.7	6.0	7.6	9.5	11.7	14.3	17.3	20.8
TP096	5.3	6.9	9.0	11.6	14.8	18.6	23.3	28.8	35.3	42.8	51.4
THTR	13	17	22	28	37	47	59	74	91	112	136
TM048	3.9	5.2	6.8	8.9	11.4	14.7	18.6	23.4	29.2	36.0	44.1
TM096	0.4	0.5	0.7	0.9	1.2	1.6	2.0	2.5	3.2	4.0	4.9
TM120	0.1	0.1	0.2	0.2	0.3	0.3	0.4	0.6	0.7	0.9	1.1
TM144	0.0	0.0	0.0	0.0	0.0	0.1	0.1	0.1	0.1	0.2	0.2

K IDX	23	24	25	26	27	28	29	30	31	32	33
DEPTH	0.88	0.92	0.96	1.00	1.04	1.08	1.12	1.16	1.20	1.24	1.28
TP144	7.7	9.0	10.4	11.9	13.5	15.2	16.9	18.5	20.1	21.6	22.9
TP120	24.6	28.8	33.4	38.4	43.5	48.9	54.3	59.6	64.8	69.6	74.0
TP096	61.0	71.7	83.3	95.8	109.0	122.6	136.3	149.9	162.8	174.8	185.2
THTR	164	196	232	272	315	362	412	465	520	576	633
TM048	53.5	64.4	76.8	90.8	106.4	123.6	142.4	162.7	184.4	207.4	231.3
TM096	6.0	7.3	8.8	10.5	12.4	14.6	17.1	19.9	22.9	26.2	29.8
TM120	1.4	1.7	2.1	2.5	3.0	3.6	4.3	5.0	5.9	7.0	8.2
TM144	0.3	0.3	0.4	0.5	0.6	0.7	0.8	1.0	1.2	1.5	1.7

K IDX	34	35	36	37	38	39	40	41
DEPTH	1.32	1.36	1.40	1.44	1.48	1.52	1.56	1.60
TP144	24.0	24.7	25.2	25.2	24.6	24.0	23.6	23.5
TP120	77.9	81.2	83.8	85.5	86.1	86.5	87.1	87.4
TP096	193.8	200.0	203.6	204.3	202.5	201.0	201.0	201.0
THTR	688	742	792	839	881	914	914	914
TM048	256.0	281.2	306.7	332.1	357.2	378.2	391.0	395.4
TM096	33.7	38.0	42.5	47.4	52.7	58.1	58.3	58.3
TM120	9.6	11.2	13.0	15.1	17.4	19.5	21.0	21.5
TM144	2.0	2.4	2.8	3.2	3.6	4.1	4.3	4.4

Numerically derived temperature matrix at t=120 s.

K IDX	1	2	3	4	5	6	7	8	9	10	11
DEPTH	0.0	0.04	0.08	0.12	0.16	0.20	0.24	0.28	0.32	0.36	0.40
TP144	0.0	1.6	3.2	4.9	6.6	8.5	10.6	12.9	15.4	18.2	21.2
TP120	0.0	2.4	4.8	7.3	10.0	12.9	16.0	19.5	23.3	27.5	32.1
TP096	0.0	3.1	6.3	9.6	13.2	17.0	21.2	25.8	30.8	36.4	42.6
THTR	0	2	5	8	11	14	17	21	25	30	35
TM048	0.0	1.0	2.0	3.1	4.2	5.5	6.9	8.4	10.2	12.1	14.3
TM096	0.0	0.2	0.5	0.7	1.0	1.3	1.6	2.0	2.4	2.9	3.4
TM120	0.0	0.1	0.2	0.3	0.4	0.5	0.7	0.8	1.0	1.2	1.4
TM144	0.0	0.0	0.1	0.1	0.1	0.2	0.2	0.3	0.3	0.4	0.5

K IDX	12	13	14	15	16	17	18	19	20	21	22
DEPTH	0.44	0.48	0.52	0.56	0.60	0.64	0.68	0.72	0.76	0.80	0.84
TP144	24.5	28.2	32.2	36.5	41.1	46.1	51.4	57.0	62.9	69.0	75.2
TP120	37.2	42.8	48.9	55.5	62.6	70.3	78.5	87.2	96.3	105.8	115.6
TP096	49.4	56.9	65.1	74.1	83.8	94.2	105.4	117.2	129.7	142.8	156.3
THTR	41	48	55	63	72	81	92	103	115	128	142
TM048	16.7	19.5	22.5	25.9	29.7	33.8	38.3	43.3	48.6	54.4	60.6
TM096	4.0	4.7	5.5	6.3	7.3	8.3	9.5	10.8	12.2	13.8	15.4
TM120	1.6	1.9	2.2	2.6	3.0	3.4	3.9	4.5	5.1	5.8	6.5
TM144	0.6	0.7	0.8	0.9	1.1	1.2	1.4	1.6	1.9	2.1	2.4

K IDX	23	24	25	26	27	28	29	30	31	32	33
DEPTH	0.88	0.92	0.96	1.00	1.04	1.08	1.12	1.16	1.20	1.24	1.28
TP144	81.6	88.1	94.5	100.9	107.1	113.0	118.6	123.7	128.3	132.3	135.5
TP120	125.7	135.9	146.1	156.2	166.1	175.7	184.8	193.3	201.1	208.0	214.0
TP096	170.3	184.4	198.7	213.0	227.0	240.6	253.6	265.8	277.0	287.0	295.6
THTR	156	171	187	204	221	238	255	273	290	307	324
TM048	67.2	74.3	81.7	89.5	97.6	106.1	114.8	123.8	132.9	142.2	151.5
TM096	17.3	19.2	21.3	23.6	26.0	28.5	31.2	34.0	36.9	40.0	43.2
TM120	7.3	8.2	9.2	10.2	11.3	12.5	13.8	15.2	16.7	18.3	20.1
TM144	2.7	3.1	3.5	3.9	4.4	4.9	5.4	6.0	6.6	7.3	8.0

K IDX	34	35	36	37	38	39	40	41
DEPTH	1.32	1.36	1.40	1.44	1.48	1.52	1.56	1.60
TP144	137.9	139.4	139.9	139.3	137.5	135.5	134.3	134.0
TP120	219.0	222.8	225.5	226.9	226.8	226.2	226.2	226.2
TP096	302.6	307.9	311.4	313.0	312.8	311.9	311.9	311.9
THTR	340	356	371	385	397	408	408	408
TM048	160.9	170.3	179.6	188.8	197.9	205.4	210.0	211.5
TM096	46.5	49.9	53.4	57.1	60.8	64.4	64.4	64.5
TM120	22.0	24.0	26.1	28.5	30.9	33.2	34.6	35.1
TM144	8.8	9.6	10.5	11.4	12.4	13.2	13.7	13.9

Numerically derived temperature matrix at t=180 s.

K IDX	1	2	3	4	5	6	7	8	9	10	11
DEPTH	0.0	0.04	0.08	0.12	0.16	0.20	0.24	0.28	0.32	0.36	0.40
TP144	0.0	4.7	9.4	14.2	19.0	24.0	29.1	34.4	39.8	45.5	51.3
TP120	0.0	5.5	11.1	16.7	22.5	28.4	34.4	40.7	47.2	53.9	60.9
TP096	0.0	6.0	12.0	18.1	24.4	30.8	37.3	44.2	51.2	58.6	66.2
THTR	0	3	7	10	14	18	21	25	30	34	39
TM048	0.0	1.5	3.0	4.6	6.2	7.8	9.5	11.3	13.2	15.2	17.3
TM096	0.0	0.5	0.9	1.4	1.9	2.5	3.0	3.6	4.2	4.8	5.5
TM120	0.0	0.2	0.5	0.7	1.0	1.2	1.5	1.8	2.1	2.4	2.7
TM144	0.0	0.1	0.2	0.3	0.4	0.5	0.7	0.8	0.9	1.1	1.3

K IDX	12	13	14	15	16	17	18	19	20	21	22
DEPTH	0.44	0.48	0.52	0.56	0.60	0.64	0.68	0.72	0.76	0.80	0.84
TP144	57.4	63.7	70.1	76.8	83.7	90.7	97.9	105.1	112.5	119.8	127.2
TP120	68.2	75.7	83.5	91.5	99.8	108.3	117.1	125.9	134.9	144.0	153.0
TP096	74.2	82.5	91.1	100.0	109.2	118.7	128.5	138.4	148.5	158.8	169.1
THTR	43	49	54	60	66	72	78	85	92	99	107
TM048	19.6	22.0	24.5	27.1	30.0	32.9	36.1	39.4	42.8	46.4	50.2
TM096	6.2	7.0	7.9	8.8	9.7	10.7	11.8	13.0	14.2	15.5	16.8
TM120	3.1	3.5	3.9	4.4	4.9	5.4	6.0	6.6	7.2	7.9	8.6
TM144	1.4	1.6	1.8	2.0	2.3	2.5	2.8	3.1	3.4	3.7	4.1

K IDX	23	24	25	26	27	28	29	30	31	32	33
DEPTH	0.88	0.92	0.96	1.00	1.04	1.08	1.12	1.16	1.20	1.24	1.28
TP144	134.4	141.6	148.5	155.2	161.6	167.7	173.3	178.3	182.9	186.8	190.0
TP120	162.1	171.0	179.7	188.2	196.4	204.2	211.5	218.3	224.5	230.0	234.8
TP096	179.4	189.6	199.7	209.6	219.2	228.4	237.1	245.2	252.8	259.6	265.6
THTR	114	122	130	138	147	155	163	171	179	187	195
TM048	54.1	58.1	62.2	66.5	70.9	75.4	79.9	84.5	89.2	93.8	98.5
TM096	18.2	19.7	21.3	22.9	24.6	26.4	28.2	30.1	32.1	34.1	36.1
TM120	9.4	10.2	11.1	12.0	13.0	14.0	15.0	16.2	17.3	18.6	19.9
TM144	4.5	4.9	5.3	5.8	6.3	6.8	7.3	7.9	8.5	9.2	9.8

K IDX	34	35	36	37	38	39	40	41
DEPTH	1.32	1.36	1.40	1.44	1.48	1.52	1.56	1.60
TP144	192.4	194.1	194.9	194.9	193.9	192.6	191.9	191.6
TP120	238.8	242.0	244.4	245.9	246.3	246.4	246.5	246.5
TP096	270.8	275.1	278.4	280.7	282.0	282.7	282.7	282.7
THTR	203	210	217	224	231	236	236	236
TM048	103.2	107.9	112.5	117.1	121.7	125.5	127.8	128.6
TM096	38.2	40.4	42.6	44.8	47.1	49.2	49.3	49.3
TM120	21.3	22.7	24.3	25.9	27.6	29.2	30.1	30.5
TM144	10.5	11.3	12.0	12.8	13.6	14.3	14.8	14.9

Solutions for HPVA, HPVS, HPVM, HPVT and Diffusivity downstream at times 60, 120 and 180 s. Imposed Diffusivities: bark, 0.0015; sapwood, 0.0018; heartwood, 0.0026

K IDX	35	36	37	38	39	40	41
DEPTH	1.36	1.40	1.44	1.48	1.52	1.56	1.60
HPVI	20.00	20.00	20.00	10.00	0.00	0.00	0.00

Asymmetric solutions at (-0.48, 0, 0.96 cm)

HPVA t_1/t_2	11.77	11.33	10.87	10.42	10.17	9.89	9.83
HPVA t_1/t_3	11.84	11.41	10.97	10.53	10.20	10.02	9.87
HPVA t_2/t_3	11.34	10.92	10.49	10.07	9.75	9.59	9.54
HPVT	11.68	11.08	10.54	10.29	9.82	9.60	9.60
t zero	74	78	82	84	88	90	90

Asymmetric solutions at (-0.96, 0, 1.44 cm)

HPVA t_1/t_2	12.28	11.86	11.41	10.93	10.49	10.43	10.41
HPVA t_1/t_3	12.34	11.94	11.51	11.05	10.63	10.57	10.55
HPVA t_2/t_3	11.74	11.33	10.9[illegible]	10.46	10.08	10.02	10.00
HPVT	12.00	11.68	11.08	10.54	10.29	10.29	10.05
t zero	72	74	78	82	84	84	86

Symmetric solutions at (-0.96,0,0.96 cm)

HPVM $t_{1,2,3}$	12.81	12.65	12.44	12.20	11.91	11.90	11.90
D $t_{1,2,3}$	0.0015	0.0016	0.0016	0.0015	0.0016	0.0016	0.0016
HPVS t_1	9.58	9.11	8.52	7.82	7.22	7.20	7.20
HPVS t_2	10.49	10.25	9.92	9.51	9.18	9.17	9.17
HPVS t_3	11.07	10.92	10.69	10.40	10.16	10.16	10.16
HPVP	11.57	11.32	11.26	11.36	10.70	10.69	10.69
t max	124	124	124	124	126	126	126

Symmetric solutions at (-1.20, 0, 1.20 cm)

HPVM $t_{1,2,3}$	13.02	12.75	12.42	12.03	11.64	11.36	11.25
D $t_{1,2,3}$	0.0016	0.0017	0.0017	0.0017	0.0017	0.0017	0.0017
HPVS t_1	9.81	9.34	8.81	8.19	7.67	7.39	7.31
HPVS t_2	11.01	10.80	10.53	10.19	9.90	9.75	9.71
HPVS t_3	11.68	11.57	11.41	11.19	11.00	10.91	10.89
HPVP	12.77	12.48	12.22	12.03	11.45	11.27	11.20
t max	166	166	166	166	168	168	168

Symmetric solutions at (-1.44, 0, 1.44 cm)

HPVM $t_{1,2,3}$	12.51	12.08	11.59	11.10	10.66	10.37	10.26
D $t_{1,2,3}$	0.0017	0.0017	0.0017	0.0017	0.0017	0.0017	0.0017
HPVS t_1	10.03	9.54	8.96	8.27	7.67	7.34	7.23
HPVS t_2	11.43	11.17	10.84	10.43	10.07	9.86	9.79
HPVS t_3	12.16	12.01	11.79	11.49	11.22	11.07	11.02
HPVP	99.99	99.99	99.99	99.99	99.99	99.99	99.99
t max	99.99	99.99	99.99	99.99	99.99	99.99	99.99

Top sensor @ 0.96 cm (TP096), bottom sensor @ -0.96 cm (TM096)